



National Library
of Canada

Bibliothèque nationale
du Canada

Acquisitions and
Bibliographic Services Branch

Direction des acquisitions et
des services bibliographiques

395 Wellington Street
Ottawa, Ontario
K1A 0N4

395, rue Wellington
Ottawa (Ontario)
K1A 0N4

Your file *Votre référence*

Our file *Notre référence*

NOTICE

The quality of this microform is heavily dependent upon the quality of the original thesis submitted for microfilming. Every effort has been made to ensure the highest quality of reproduction possible.

If pages are missing, contact the university which granted the degree.

Some pages may have indistinct print especially if the original pages were typed with a poor typewriter ribbon or if the university sent us an inferior photocopy.

Reproduction in full or in part of this microform is governed by the Canadian Copyright Act, R.S.C. 1970, c. C-30, and subsequent amendments.

AVIS

La qualité de cette microforme dépend grandement de la qualité de la thèse soumise au microfilmage. Nous avons tout fait pour assurer une qualité supérieure de reproduction.

S'il manque des pages, veuillez communiquer avec l'université qui a conféré le grade.

La qualité d'impression de certaines pages peut laisser à désirer, surtout si les pages originales ont été dactylographiées à l'aide d'un ruban usé ou si l'université nous a fait parvenir une photocopie de qualité inférieure.

La reproduction, même partielle, de cette microforme est soumise à la Loi canadienne sur le droit d'auteur, SRC 1970, c. C-30, et ses amendements subséquents.

Canada

**HEAT TRANSFER AND KINETIC STUDIES OF PARTICULATES UNDER
ASEPTIC PROCESSING CONDITIONS**

by

George Brobbey Awuah

Department of Food Science and
Agricultural Chemistry,
Macdonald Campus,
McGill University,
Montreal, Canada.

July, 1994

A thesis submitted to the Faculty of Graduate Studies and Research in partial
fulfilment of the requirements for the degree of Doctor of Philosophy

© George Brobbey Awuah, 1994



National Library
of Canada

Acquisitions and
Bibliographic Services Branch

395 Wellington Street
Ottawa, Ontario
K1A 0N4

Bibliothèque nationale
du Canada

Direction des acquisitions et
des services bibliographiques

395, rue Wellington
Ottawa (Ontario)
K1A 0N4

Your file *Votre référence*

Our file *Notre référence*

THE AUTHOR HAS GRANTED AN
IRREVOCABLE NON-EXCLUSIVE
LICENCE ALLOWING THE NATIONAL
LIBRARY OF CANADA TO
REPRODUCE, LOAN, DISTRIBUTE OR
SELL COPIES OF HIS/HER THESIS BY
ANY MEANS AND IN ANY FORM OR
FORMAT, MAKING THIS THESIS
AVAILABLE TO INTERESTED
PERSONS.

L'AUTEUR A ACCORDE UNE LICENCE
IRREVOCABLE ET NON EXCLUSIVE
PERMETTANT A LA BIBLIOTHEQUE
NATIONALE DU CANADA DE
REPRODUIRE, PRETER, DISTRIBUER
OU VENDRE DES COPIES DE SA
THESE DE QUELQUE MANIERE ET
SOUS QUELQUE FORME QUE CE SOIT
POUR METTRE DES EXEMPLAIRES DE
CETTE THESE A LA DISPOSITION DES
PERSONNE INTERESSEES.

THE AUTHOR RETAINS OWNERSHIP
OF THE COPYRIGHT IN HIS/HER
THESIS. NEITHER THE THESIS NOR
SUBSTANTIAL EXTRACTS FROM IT
MAY BE PRINTED OR OTHERWISE
REPRODUCED WITHOUT HIS/HER
PERMISSION.

L'AUTEUR CONSERVE LA PROPRIETE
DU DROIT D'AUTEUR QUI PROTEGE
SA THESE. NI LA THESE NI DES
EXTRAITS SUBSTANTIELS DE CELLE-
CI NE DOIVENT ETRE IMPRIMES OU
AUTREMENT REPRODUITS SANS SON
AUTORISATION.

ISBN 0-612-00077-X

Canada

DEDICATED TO

My Wife Mary, my Son Kwabena Awuah Brobbey,
my Mother, Brothers and Sisters.

ABSTRACT

Fluid-to-particle heat transfer coefficients (h_{fp}) associated with food and model particles under simulated aseptic processing conditions were experimentally evaluated, and verified using measured inactivation kinetic parameters of the enzyme trypsin. Convective heat transfer coefficients were determined initially using two methods: a rate method based on evaluated heating/cooling rate indices (f_c/f_h) and a ratio method based on the ratio of temperature difference between the medium and particle locations. Inert materials including Teflon, polypropylene, Nylon, and Lucite in the form of infinite cylinders, slabs and spheres were used under different heating and cooling conditions. Values of h_{fp} ranged from 15 to 420 W/m²C, depending on the shape, size and ambient conditions. Although the two methods appeared sensitive to errors in parametric values when associated Biot numbers exceeded 20, the rate method generally gave more consistent results and hence was used in all subsequent work.

Carrot and potato tissue in the form of finite cylinders of different lengths (0.02-0.04 m) and diameters (0.016-0.023 m) were used for evaluating h_{fp} associated with aqueous CMC solutions (0-1.0% w/w) at temperatures ranging from 50 to 80°C and at relatively low fluid flow (0.2 to 0.7 × 10⁻³ m/s) conditions. Carrots generally gave higher h_{fp} values (100-550 W/m²C) compared to potatoes (80-450 W/m²C). With the exception of CMC concentration and temperature which had significant effects ($p < 0.05$), other process variables including sample size (length and diameter), flow rate and direction of fluid flow had no significant effects ($p > 0.05$) on h_{fp} . Laminar flow natural convection dominated the flow regime. Hence, the Nusselt number was modeled as a function of

Rayleigh's number which resulted in coefficients of determination (R^2) greater than 0.80.

A pilot scale holding tube simulator was designed and fabricated for routine/rapid gathering of heat penetration data which may be experienced in high temperature short time processing conditions. The simulator was calibrated to give fluid flow velocity as a function of pump rpm, fluid concentration, pipe diameter, and temperature. Medium temperature could be maintained in the range 80-110°C with small variation (± 0.2 C°).

Using the simulator under conditions comparable to industrial applications, and a full factorial experimental design, h_{fp} values were estimated using finite cylinders of Teflon and potato tissue of different sizes (length: 0.020- 0.0254 m; diameter: 0.0159- 0.0254 m), and spherical Teflon particles (diameter 0.0191 m) in food grade CMC solutions (0-1.0% w/w). Operating temperatures were 90, 100 and 110°C, and flow rate was varied from 1.0 - 1.9×10^{-4} m³/s. Average h_{fp} values ranged from 56 to 966 W/m²C depending on size, shape, fluid concentration, particle orientation, and tube diameter. Particle orientation and length had no significant effect ($p > 0.05$), whereas all the other factors had significant influences ($p < 0.05$) on associated h_{fp} values. Increasing particle diameter decreased the heat transfer coefficient. A similar trend was found with increasing pipe diameter. Both potato and Teflon particles exhibited different responses to temperature, concentration and fluid flow rates, with potatoes giving higher heat transfer coefficients compared to Teflon. Spherical particles gave higher h_{fp} values (between 7 to 29%) compared to finite cylinders of the same diameter. Differences caused by different particle materials were accounted for by introducing a thermal diffusivity ratio in developed dimensionless correlations for both mixed and forced convective heat transfer

to spherical and finite cylindrical particles under simulated aseptic processing conditions.

Thermal inactivation of trypsin (bovine pancreas type III) in low and high pH media was studied at temperatures ranging from 90 - 130°C. Comparative studies of its kinetic data with other bioindicators indicated the enzyme to be suitable for HTST verification/validation purposes. Further studies revealed, probably depending on pH, that trypsin was more susceptible to thermal inactivation at temperatures around 70°C. Values of h_{fp} evaluated using the pilot scale simulator were verified with established thermal inactivation kinetic data for trypsin and a finite difference program for finite cylinders. The enzyme was sealed in small stainless steel capsules and embedded at the centre of finite cylinders of potato which were pretested and found to be suitable for simulated aseptic studies. Predicted retention values were calculated using the mass average temperature of all nodal points occupied by the stainless steel capsule via the D-values corresponding to each temperature. An excellent agreement was found between predicted and measured percentage retentions, which indicated appropriateness of established kinetic data as well as heat transfer coefficients.

RÉSUMÉ

Les coefficients de transfert de chaleur (h_{fp}) fluide-particule associé aux systèmes alimentaires modèles sous des conditions simulées de procédé aseptique ont été évalués expérimentalement et vérifiés en mesurant la cinétique d'inactivation de l'enzyme trypsine. Les coefficients de transfert de chaleur convectifs ont été initialement déterminés en utilisant deux méthodes: la méthode des taux qui résulte de l'évaluation de l'indice du taux de chauffage/refroidissement (f_c/f_h) et la méthode des ratios qui est basée sur le ratio de la différence de température entre le médium et la particule à différentes localisation dans le système. Des matériaux inertes incluant le Teflon, le polypropylène, le Nylon et la lucite sous forme de cylindres infinis, de plaques infinies ou de sphères ont été soumis à plusieurs conditions de chauffage et de refroidissement. Les valeurs de h_{fp} obtenues variaient de 15 à 420 W/m²C dépendamment de la forme et de la grosseur des particules et des conditions du procédé. Même si les deux méthodes semblaient sensibles aux erreurs résultant de l'estimation des valeurs des paramètres lorsque les nombres de Biot excédaient 20, la méthode des taux a donné généralement des résultats plus consistants. Elle a donc été choisie pour les travaux subséquents.

Des particules de carotte et de pomme de terre sous forme de cylindres finis de différentes longueurs (0.02-0.04 m) et diamètres (0.016-0.023m), trempées dans des solutions aqueuses de CMC (0-1.0% w/w) de faibles débits (0.2 à 0.7 x 10⁻³ m/s) à des températures variant de 50 à 80°C ont été utilisées pour déterminer les h_{fp} . Les valeurs de h_{fp} pour les carottes étaient plus élevées (100-550 W/m²C) que pour les pommes de terre (80-450 W/m²C). A l'exception de l'effet des concentrations de CMC et de l'effet de la température, qui sont significatifs ($p < 0.05$), les autres variables incluant la grosseur des particules (longueur et diamètre), le débit et l'orientation des particules n'ont pas eu un effet significatif ($p > 0.05$) sur les valeurs de h_{fp} . Pour les écoulements laminaires, la

convection naturelle a dominé. Lorsque le nombre de Nusselt a été corrélié au nombre de Rayleigh, le coefficient de détermination (R^2) était plus de 0.80.

On a élaboré un concept de tube de retenue de type pilote et on l'a fabriqué pour générer rapidement des données de pénétration de chaleur durant des expériences conduites à hautes températures sur de courtes périodes de temps. Le simulateur a été calibré pour obtenir la vitesse du fluide en fonction de la vitesse de rotation de la pompe, de la concentration du fluide, du diamètre du tube et de la température. Il faut noter que les températures pouvaient être maintenues entre 80-100°C avec de petites variations ($\pm 0.2^\circ\text{C}$).

En utilisant le simulateur dans des conditions comparables aux applications industrielles du procédé aseptique et un plan statistique factoriel complet, on a déterminé des valeurs de h_{fp} pour des cylindres finis de pomme de terre de différentes grosseurs (longueurs: 0.02-0.025 m; diamètre: 0.0159-0.0254 m) et des sphères de Teflon (diamètre: 0.0191 m) dans des solutions de CMC (0-1.0% w/w). Les conditions de température étaient de 90, 100 et 110°C et les débits variaient de $1.0-1.9 \times 10^{-4} \text{ m}^3/\text{s}$. On a obtenu des valeurs moyennes de h_{fp} se situant entre 56 et 966 $\text{W}/\text{m}^2\text{C}$ dépendamment de la grosseur, de la forme et l'orientation de la particule, de la concentration du fluide et du diamètre du tube. L'orientation des particules et la longueur du tube n'ont pas eu un effet significatif ($p > 0.05$). Par ailleurs, tous les autres facteurs avaient une influence significative ($p < 0.05$) sur les valeurs de h_{fp} . En augmentant le diamètre des particules, le coefficient de transfert de chaleur diminue. La même tendance a été observée avec une augmentation du diamètre du tube. Des réponses différentes par rapport aux facteurs comme la température, la concentration et le débit de solution ont été observées pour les particules de pomme de terre et de Teflon. Des coefficients plus élevés ont été mesurés pour la pomme de terre. Des valeurs de h_{fp} entre 7 et 29% plus élevés ont été observées

pour les sphères par rapport aux cylindres finis de même diamètre.

On a tenu compte des différences causées par les matériaux utilisés en introduisant le ratio de diffusivité thermique dans les correlations sans dimensions pour les coefficients de transfert de chaleur en convection forcée et en écoulement mixte pour les sphères et les cylindres finis sous conditions de procédés aseptiques.

On a étudié l'inactivation thermique de trypsine (pancréas bovin type III) dans des conditions basses et élevées de pH et pour des températures variant de 90 à 130°C. Des études comparatives des données de cinétiques avec d'autres bioindicateurs ont indiqué que l'enzyme pourrait être utilisée pour la vérification/validation de procédés HSTS. Des études plus approfondies ont révélées que la trypsine était plus susceptible à l'inactivation thermique à des températures de 70°C et que ce phénomène était probablement dépendant du pH. Les valeurs h_{fp} , évaluées dans le simulateur pilote, ont été vérifiées avec des données de cinétique de destruction sur la trypsine et des simulations par ordinateur en utilisant la méthode des différences finies pour des cylindres finis. L'enzyme était encapsulée et les capsules d'acier inoxydable étaient implantées dans le centre d'un cylindre fini de pomme de terre. Certains échantillons étaient préalablement testés dans des conditions aseptiques. Les valeurs prédites des temps de rétention ont été calculées en utilisant la température moyenne de la masse de tous les noeuds de la capsule d'acier inoxydable via les valeurs de D correspondantes aux dites températures. Les valeurs prédites de pourcentage de rétention étaient comparables aux valeurs mesurées ce qui indique que les données de cinétique de destruction de la trypsine et l'évaluation des coefficients de transfert de chaleur donnaient des résultats comparables.

ACKNOWLEDGEMENTS

I would like to express my sincere gratitude to my supervisor Dr. H. S. Ramaswamy, and to Dr. B. Simpson for their guidance, patience, advice, invaluable criticism, encouragement and tremendous assistance throughout the study. I also wish to express my deepest appreciation to Dr. J. O. Darko and Mr. J. H. Oldham for having the trust in selecting me for the McGill/U.S.T project.

I would like to acknowledge the Canadian International Development Agency (CIDA) and the Natural Sciences and Engineering Research Council (NSERC) for providing the much needed financial assistance without which the author would not have been able to carry out the work. I also wish to thank Dr. F. R. van de Voort (Head, Food Science Department), Dr. J. P. Smith, Dr. I. Alli, Dr. V. J. Raghavan (Head, Agricultural Engineering Department) and all members of staff and students of the Food Science Department, who in diverse ways created a unique environment for studies.

I wish to express my sincere thanks to Mr. I. Ashie and Ms. Mary Kyei for proof reading drafts of the thesis, to Dr. S. Khanizadeh for his invaluable help with statistical analysis, to Mr. S. S. Sablani for the time spent together in writing the finite difference program for a finite cylinder, and to Ms. Michèle Marcotte for the French translation of the abstract. My heartfelt appreciation goes particularly to Dr. B. Simpson, Dr. M. V. Simpson, Mr. and Mrs. Ashie, Mr. and Mrs. Opoku Serebour, and Ms. Mary Kyei, whose friendship, concern, love, readiness to help, and advice meant a lot to my family. My sincere thanks go to my colleagues and most importantly, Dr. S. Grabowski and Dr. K. Abdelrahim for their constructive criticisms, Mr. A. Taherian, Ms. Carla Abbatemarco, Mrs. S. Basak, Mrs. D. Moussa, and Ms. S. Tajchakavit.

My deepest gratitude goes to my dear wife Mary for her support, encouragement and love, my son Kwabena Awuah Brobbey for his sacrifice, my mother Alice Awuah and my brothers and sisters; E. Awuah Boakye, Margaret Awuah, Ophelia Boafo, Benjamin Awuah, Andrew Awuah, and Christiana Awuah for their support and prayers. Finally, to all those whose names have unintentionally been left out, I wish to express my heartfelt apologies and thanks, and above all, my thanks to the Almighty Father for making all this possible.

CONTRIBUTION TO KNOWLEDGE

1. Mathematical simplification of relevant equations and comparative studies in relation to method sensitivity, of two analytical procedures for rapid estimation of heat transfer coefficients.
2. Studies involving the effect of mild flow conditions (temperature and flow rate) and product parameters on fluid-to-particle convective heat transfer coefficients for heating finite cylinders in viscous solutions, and the development of dimensionless correlations for such conditions. Fluid temperature and concentration were found to influence h_{fp} as a result of changes in fluid apparent viscosity.
3. The design and fabrication of a robust, yet, a cost effective pilot scale holding tube simulator for heat transfer studies, which with minor modifications, can be utilized for residence time distribution studies, at elevated temperatures and pressures.
4. A comprehensive study using full factorial experimental designs to establish the effects of both product and system parameters on associated fluid-to-particle convective heat transfer coefficients under simulated aseptic processing conditions. The type of particle material was found to affect the heat transfer coefficient. Heat transfer coefficients decrease with increasing particle diameter while sample length had no effect on h_{fp} associated with finite cylindrical particles.

5. The development of dimensionless correlations for forced and mixed convection heat transfer to finite cylinders and spherical particles under aseptic processing conditions. Natural convection contributions were accounted for even in situations where forced convection was suspected to dominate. A thermal diffusivity ratio, defined as the ratio of particle to fluid thermal diffusivities, was introduced to account for the effect of different particle properties.

6. The evaluation of thermal inactivation kinetics data for trypsin at temperatures ranging from 50 to 130°C. Trypsin in acidic media was highly stable to thermal inactivation. Stability decreased with increasing pH. Trypsin was found to be more susceptible to thermal inactivation at around 70°C than at other temperatures.

7. Using trypsin in tiny stainless steel capsules, centre point degradation was measured and compared with predicted data generated with a finite difference computer program to verify estimated heat transfer coefficients. The percentage retention was calculated as the cumulative effect (mass average) of all lethal temperatures in the capsule instead of using the centre point temperature history as the reference point.

PART OF THIS THESIS HAS BEEN PUBLISHED AS FOLLOWS:

2. Awuah, G. B., Ramaswamy, H. S., Simpson, B. K. and Smith, J. P. 1993. Thermal inactivation kinetics of trypsin at aseptic processing temperatures. *J. Food Proc. Eng.* 16:315-328.
1. Awuah, G. B., Ramaswamy, H. S. and Simpson, B. K. 1993. Surface heat transfer coefficients associated with heating of food particles in CMC solutions. *J. Food Proc. Eng.* 16:39-57.

PART OF THIS THESIS HAS BEEN SUBMITTED FOR PUBLICATION:

1. Awuah, G. B., Ramaswamy, H. S. and Simpson, B. K. 1994. Comparison of two methods for evaluating fluid-to-particle heat transfer coefficients. *Food Res. Int.* (*In press*)

PART OF THIS THESIS HAS BEEN PRESENTED AT SCIENTIFIC CONFERENCES :

5. Awuah, G. B., Ramaswamy, H. S., Simpson, B. K. and Smith, J. P. 1994. Fluid-to-particle heat transfer coefficient in a pilot-scale aseptic processing holding tube simulator. Northeast Agr./Bio. Engineering Conference. Univ. of Guelph, Ontario (July 24- 27).
4. Awuah, G. B., Ramaswamy, H. S., Simpson, B. K. and Smith, J. P. 1993. Thermal inactivation kinetics of trypsin in the high temperature range suitable for aseptic processing. CoFE 93: Conference of Food Engineering, American Institute of Chemical Engineers. Chicago (February 20-24).
3. Ramaswamy, H. S. and Awuah, G. B. 1993. Comparison of two techniques for the determination of fluid to particle surface heat transfer coefficients. CoFE 93: Conference of Food Engineering, American Institute of Chemical Engineers. Chicago (February 20-24).
2. Awuah, G. B., Ramaswamy, H. S., Simpson, B. K. and Smith, J. P. 1992. Fluid-particle heat transfer coefficients in CMC. Canadian Institute of Food Science and Technology (CIFST) 35th Annual Conference, Ottawa (May 31- June 3).
1. Awuah, G. B., Ramaswamy, H. S., Simpson, B. K., Pannu, K. and Smith, J. P. 1991. Fluid-to-particle heat transfer coefficients associated with carboxymethylcellulose solutions. American Society of Agricultural Engineers (ASAE) Winter meeting, Chicago (December 17-20).

NOMENCLATURE

a	Radius of a sphere or infinite cylinder
A	Cross sectional area (m ²)
A,B	Shape dependent functions of Biot number, or constants
A _c ,A _p	Characteristic functions of the Biot number
A _o ,A	Initial and transient enzyme activity
A _p	Cross sectional area of particle (m ²)
B _c ,B _p	Characteristic functions of the Biot number
Bi _c	Biot number associated with an infinite cylinder
Bi _p	Biot number associated with a plate
Bi _s	Biot number associated with a sphere
C,C _o	Nutrient concentration before and after processing
C(t)	Frequency ratio of particles which exist a test section between time t and t+Δt
C _p	Heat capacity (kJ/kg°C)
C _{ps}	Heat capacity of conduction heating material (kJ/kgC)
CV	Coefficient of variation (standard deviation/mean)
d	diameter (m)
D	Time required to reduce 90% of activity, or decimal reduction time(min)
d _{cd} ,L _c	Characteristic length of sample (m)
D _{co}	Decimal reduction time at reference temperature for nutrient (min)
D _{mo}	Decimal reduction time at reference temperature for microorganism (min)
D _o	Decimal reduction time at reference temperature (min)
D _p ,d _p	Diameter of particle (m)
D _t	Diameter of tube (m)
D _T	Decimal reduction time at temperature T (min)
E	Effectiveness fraction
E(t)	Exit age distribution function or RTD (min ⁻¹)
E _a	Activation energy (kJ/mole)
f _h	Negative reciprocal slope of the straight line portion of heating curve on semi-logarithmic coordinates (min)
f _c	Negative reciprocal slope of the straight line portion of the cooling curve on semi-logarithmic coordinates (min)
F(t)	Cummulative RTD function, dimensionless
F _o	Fourier number (αt/a ²)
F _o	Cummulative lethality (process lethality) (min)
F _{req}	Integrated lethality (required lethality) (min)
F _T	Equivalent heating time at a given temperature (min)
g	Acceleration due to gravity (m/s ²)
GGr	Generalized Grashof number
GPr	Generalized Prandtl number
GRe	Generalized Reynolds number
h _{fp}	Fluid-to-particle heat transfer coefficient (W/m ² C)

h_i	Heating medium to wall heat transfer coefficient (W/m^2C)
h_o	Wall to carrier fluid heat transfer coefficient (W/m^2C)
j	Lag factor $(T_{pi} - T_a)/(T_i - T_a)$
J_1	Bessel function of the first order.
J_o	Bessel function of the zeroth order
k	Reaction rate constant (min^{-1})
k_f	Thermal conductivity of fluid (W/mC)
k_o	Reaction rate constant at reference temperature
k_p	Thermal Conductivity of particle (W/mC)
L	Length of holding tube, half thickness of slab, or length of cylinder (m)
m	Consistency coefficient ($Pa.s^n$) or mass (kg)
m_f	Mass flow rate (kg/hr)
m_p	Mass of particle (kg)
n	Flow behaviour index
N, N_o	Microbial population before and after processing, or particles in an incremental length
Nu	Nusselt number
Pe	Peclet number
Pr	Prandtl number
R	Universal gas constant (kJ/mole K)
Re	Reynolds number
s	Frequency factor
t	Time (s), (min)
T	Temperature ($^{\circ}C$)
T_a, T_f	Ambient temperature or fluid medium temperature ($^{\circ}C$)
T_c, T_l	Temperature at centre and a distance labelled l from the centre of a sphere, slab or cylinder ($^{\circ}C$)
T_i	Initial temperature ($^{\circ}C$)
T_{ij}^n	Temperature at nodal point ij at previous time ($^{\circ}C$)
T_{ij}^{n+1}	Temperature at nodal point ij at present time ($^{\circ}C$)
T_{ip}	Initial temperature of particle ($^{\circ}C$)
t_m	Mean residence time (min)
T_o	Reference temperature ($^{\circ}C$)
T_{pi}	Pseudo-initial temperature ($^{\circ}C$)
T_{ps}	Particles surface Temperature ($^{\circ}C$)
T_s	Steam temperature ($^{\circ}C$)
U	Overall heat transfer coefficient (W/m^2C)
U	Dimensionless temperature ratio $((T_a - T)/(T_a - T_i))$
U_{ht}	Overall heat transfer coefficient associated with the holding tube (W/m^2C)
V	Volume (m^3) or velocity (m/s)
V_{max}	Fluid maximum velocity (m^2/s)
V_{mean}	Fluid mean velocity (m^2/s)
x	Thickness (m)

X	Distance from the coldest plane of a slab ($0 \leq X \leq L$) (m)
X_F	Mass fraction of fat (%)
X_m	Mass fraction of moisture (%)
X_s	Mass fraction of solids (%)
x, y, z	Cartesian co-ordinates
z	Temperature range required to change D by 90% ($^{\circ}\text{C}$)
Z	Constant
z_c	z-value for nutrient ($^{\circ}\text{C}$)
z_m	z-value for microorganism ($^{\circ}\text{C}$)
α	Thermal diffusivity (m^2/s)
α_f	Fluid thermal diffusivity (m^2/s)
α_p	Particle thermal diffusivity (m^2/s)
β	Root of characteristic equation, or volumetric thermal expansion coefficient ($^{\circ}\text{C}^{-1}$)
$\dot{\gamma}, \gamma$	Shear rate (s^{-1}) and Root of a characteristic equation respectively
δ	Root of characteristic equation
μ_{mean}	Mean apparent viscosity (Pa.s)
μ_w	Fluid apparent viscosity at wall temperature (Pa.s)
μ_{∞}	Fluid apparent viscosity at bulk fluid temperature (Pa.s)
ρ	Density (kg/m^3)
σ	Shear stress (Pa)

Abbreviations

CMC	Carboxymethylcellulose
CYL	Cylinder
EHT	Equivalent heating time (min)
FR	Flow rate
HTST	High temperature short time
LALD	Least absolute lethality difference
LSTD	Least sum of squared temperature difference
PAE	Percentage average error
PDM	Percentage deviation modulus
PSD	Percentage standard deviation
RA	Residual activity
RPM	Revolutions per minute
RT	Residence time
RTD	Residence time distribution
SAV	Surface area to volume ratio
SOR	Successive over relaxation
SPH	Sphere
SS	Sum of squares
SSHE	Scraped surface heat exchanger
UHT	Ultra high temperature

TABLE OF CONTENTS

	Page
ABSTRACT	iv
RESUMÉ	vii
ACKNOWLEDGEMENT	x
CONTRIBUTION TO KNOWLEDGE	xi
NOMENCLATURE	xiv
LISTS OF TABLES	xxii
LISTS OF FIGURES	xxiv
I. INTRODUCTION	1
II. LITERATURE REVIEW	7
Aseptic Processing in Retrospect	7
Theoretical Basis for Quality Improvement in Aseptic Processing	9
Advantages of Aseptic Processing	11
Limitations of Aseptic Processing	11
Unit Components for Sterilizing Particulate Products	12
Commercial System for Particulate Products	14
Principles of Process Calculations	15
Analytical Models for Process Evaluation	17
Numerical Models for Process Evaluation	19
Simulation approaches for Process Evaluation	22
Selection of Target F_0	24
Residence Time Distribution (RTD)	26
Heat Transfer	32
The Heat Exchanger	33
The Holding Tube	35
Temperature Distribution in Particulates	38
The Convective Heat Transfer Coefficient (h_{fp})	40
Analytical Models for Calculating h_{fp}	41
Numerical Models Calculating h_{fp}	44
Experimental Methods for Evaluating h_{fp}	45
Microbiological Method	45
Moving Thermocouple Method	47
Melting Point Method	48
Liquid Crystal Method	48
Relative Velocity Method	49
Liquid/Temperature Calorimetry Method	50
Transmitter Method	50
Stationary Particle Method	51
Predicting h_{fp} from Dimensionless Correlations	51

Factors affecting Heat Transfer Coefficients	55
Influence of Parameters associated with Particulates	58
Influence of Parameters associated with Carrier Fluids	60
Thermal Kinetics Data	62
Process Validation and Validation	67
Microbiological Indicators	67
Chemical and Enzymatic Markers	69
III. COMPARISON OF TWO METHODS FOR EVALUATING FLUID- TO-PARTICLE HEAT TRANSFER COEFFICIENT	72
Abstract	72
Introduction	72
Theoretical Considerations	75
The Rate Method	77
The Ratio Method	78
Materials and Methods	80
Sample Preparation	80
Experimental Conditions	81
Verification of Sample Thermal Diffusivity	81
Temperature Measurement and Data Analysis	82
Error Analysis	83
Results and Discussion	84
Thermal Diffusivity	84
The Rate Method	86
The Ratio Method	90
Comparison of Evaluated h_{fp} with Literature Values	93
Error Analysis	95
Conclusions	98
IV. FLUID-TO- PARTICLE HEAT TRANSFER COEFFICIENTS ASSOCIATED WITH HEATING FOOD PARTICLES IN CMC SOLUTIONS UNDER LOW FLOW AND MILD HEATING CONDITIONS	99
Abstract	99
Introduction	99
Theoretical Considerations	102
Materials and Methods	104
Raw Materials and CMC solution Preparation	104
Rheological Properties	104

	Experimental Setup and Procedure	107
	Experimental Factors	110
	Data Analysis	110
	Results and Discussion	113
	Conclusions	124
V.	DESIGN, CONSTRUCTION AND EVALUATION OF A PILOT SCALE ASEPTIC PROCESSING HOLDING TUBE SIMULATOR FOR HEAT TRANSFER STUDIES	125
	Abstract	125
	Introduction	126
	Design and Construction of Pilot Scale Simulator	128
	Design Features	128
	Construction of the Simulator	129
	Construction of the Test Compartment and Sample Holder	131
	Mode of Operation of the Simulator	131
	Data Acquisition System	134
	Results and Discussion	134
	Calibration of the Simulator	135
	Performance of the Simulator	138
	Conclusions	141
VI.	FLUID-TO-PARTICLE HEAT TRANSFER COEFFICIENT AS INFLUENCED BY PRODUCT AND SYSTEM PARAMETERS IN A PILOT SCALE HOLDING TUBE SIMULATOR	142
	Abstract	142
	Introduction	143
	Materials and Methods	146
	Theoretical Basis for Estimating the Fluid-to- Particle Heat Transfer Coefficient	146
	Test Materials and CMC Preparation	146
	Rheological and Thermal Properties	147
	Experimental Setup and Procedure	148
	Experimental Design	148
	Data Analysis	149
	Results and Discussion	150
	Effect of Particle Length	151
	Effect of Particle Orientation	151
	Effect of Particle Diameter and Particle-to-Tube Ratio	155
	Influence of Fluid Concentration, Temperature and Flow rate	161

	Heat Transfer Coefficients Associated with Cooling Heated Samples	172
	Influence of Particle Shape	174
	Conclusion	175
VII.	DIMENSIONLESS CORRELATIONS FOR MIXED AND FORCED CONVECTION HEAT TRANSFER TO SPHERICAL AND FINITE CYLINDRICAL PARTICLES IN A PILOT SCALE ASEPTIC HOLDING TUBE SIMULATOR	178
	Abstract	178
	Introduction	178
	Theoretical Considerations	181
	Materials and Methods	185
	Materials and experimental conditions	185
	Characteristic dimension	187
	Results and Discussion	189
	Characteristic dimension	189
	Limiting Nusselt number for finite cylinder	193
	Forced convection finite cylinders	193
	Mixed convection for finite cylinders	194
	Spherical particles	201
	Conclusions	203
VIII.	THERMAL INACTIVATION OF TRYPSIN AT ASEPTIC PROCESSING TEMPERATURES	204
	Abstract	204
	Introduction	204
	Materials and Method	206
	Enzyme and Chemicals	206
	Enzyme Assay	207
	Heat Treatment	207
	Kinetic Data Analysis	208
	Trypsin vs Microbial and Other Enzyme Kinetics	210
	Results and Discussion	211
	Conclusions	223
IX.	BIOLOGICAL VERIFICATION OF FLUID-TO-PARTICLE INTERFACIAL HEAT TRANSFER COEFFICIENT IN A PILOT SCALE HOLDING TUBE SIMULATOR	224
	Abstract	224

Introduction	224
Materials and Methods	228
Sample Preparation	228
Preparation and Immobilization of Bioindicator	228
Experimental Setup and Conditions	231
Enzyme Recovery and Assay	231
Mathematical Formulation of Heat Conduction to a Finite Cylinder	232
Data Analysis	235
Results and Discussion	236
Experimental and Simulated Temperature Profiles	236
Comparison of Kinetic Data obtained with Ampoule and Capsule Methods	236
Low Temperature Kinetics for Trypsin (pH=5.1)	238
Biological Verification of Heat Transfer Coefficients	242
Conclusions	244
X. GENERAL CONCLUSIONS	246
REFERENCES	251
APPENDICES	275

LISTS OF TABLES

Table	Page
2.1.	Empirical F_0 -values for low-acid canned food.	25
2.2.	Published data on fluid-to-particle heat transfer coefficients.	56
2.3.	Kinetic data for some foodstuff /microorganisms.....	63
3.1.	Thermophysical properties of test particles.	85
3.2.	Experimental data obtained by heating infinite Teflon cylinders in 1.0% w/w CMC solution (temperature = 100°C; flow rate = 11.1 L/min) in the holding tube of the aseptic unit	88
3.3.	Comparison of heat transfer coefficients determined with the two methods under different experimental conditions.....	89
3.4.	Percentage error associated with calculated heat transfer coefficient (h_{fp}) values as influenced by $\pm 5\%$ error in characteristic parametric values under various processing conditions using Teflon as a reference material.	96
4.1.	Power law parameters for CMC rheology at various temperatures and concentrations.....	106
4.2.	Physical properties of test materials	108
4.3.	Heat transfer coefficients for potato and carrot cylinders immersed in CMC solutions (0-1%).....	114
4.4.	Heat transfer coefficients for potato and carrot cylinders in 1.0% CMC as influenced by particle diameter	115
4.5.	Heat transfer coefficients for potato cylinders in 1.0% CMC as influenced by length.....	116
4.6.	Heat transfer coefficients in 1.0% CMC as influenced by temperature under stationary conditions.....	117

4.7.	Heat transfer coefficients for carrot cylinders as influenced by direction of fluid flow	118
4.8.	Average heat transfer coefficients at various linear velocities and temperatures and corresponding dimensionless parameters.....	119
5.1.	Analysis of variance of factors influencing fluid flow rate	137
6.1.	Heat transfer coefficients for Teflon cylinders as influenced by particle length and flow rate	152
6.2.	Heat transfer coefficient for Teflon cylinders as influenced by particle orientation.....	154
6.3.	Heat transfer coefficients for Teflon cylinders as influenced by particle diameter	157
6.4.	Analysis of variance for the 3x3x3 factorial design of factors influencing the fluid-to-particle convective heat transfer coefficient.....	163
6.5.	Comparison of heat transfer coefficients associated with heating and cooling potato samples in water at selected initial temperatures and flow rate	173
6.6.	Heat transfer coefficients as influenced by particle shape under selected conditions or flow rate, pipe diameter and fluid concentration at 100°C	176
7.1.	Power law parameters for CMC solution rheology at various temperatures and concentrations.....	186
7.2.	Errors associated with various characteristic dimensions.....	191
8.1.	Kinetic parameters for trypsin in dilute HCl and in citrate buffer.	215
8.2.	Activation energy (E_a), z values, D_0 , k_0 and their corresponding R^2 values for trypsin in dilute HCl or citrate buffer solutions.	218
9.1.	Low temperature kinetic data for trypsin in citrate buffer (pH=5.1).....	241
9.2.	A comparison of simulated and predicted percentage retention of immobilized trypsin at selected heating conditions.....	243

LISTS OF FIGURES

Figure	Page
2.1.	The aseptic processing system flow diagram.	13
3.1.	Typical semi-logarithmic plots of heat penetration curves under different heating/cooling conditions.	87
3.2.	Typical temperature ratio (Z) vs time curves for different heating/cooling conditions.	91
3.3	Graphical relationship between the rate and ratio methods.	94
4.1.	A schematic diagram of the test apparatus and setup.....	109
4.2.	A typical semi-logarithmic plot of the heat penetration curve for carrot.	111
4.3.	Nusselt number as a function of Rayleigh number (GGR.GPr) for carrot and potato cylinders heated in CMC solutions.	120
5.1.	A schematic diagram of the pilot scale simulator.	130
5.2.	A schematic diagram of the sample holder.	132
5.3.	Heat penetration curves for heating a 25.4 mm diameter and 25.4 mm long Teflon particle at 110°C.....	136
5.4.	Plot of observed vs predicted flow rate as a function of temperature, concentration and pump rpm.	139
6.1.	Plot of heat transfer coefficients (h_{fp}) as influenced by particle diameter and fluid flow rate for heating 25.4 mm Teflon particle at 100°C.	158
6.2.	Plots of heat transfer coefficients (h_{fp}) as influenced by particle-to-tube diameter and fluid flow rate for heating 25.4 mm length Teflon in 0.5%CMC at 100°C.	160

6.3.	Heat transfer coefficients (h_{fp}) as influenced by flow rate for heating Teflon and potato particles.	165
6.4.	Heat Transfer coefficients (h_{fp}) as influenced by temperature for heating Teflon and potato particle.....	166
6.5.	Heat transfer coefficients (h_{fp}) as influenced by fluid concentration for heating Teflon and potato particles.....	167
6.6.	Heat transfer coefficients (h_{fp}) as influenced by fluid concentration and flow rate for heating Teflon and potato samples.	168
6.7.	Heat transfer coefficient (h_{fp}) as influenced by fluid temperature and concentration for heating Teflon and potato particles.	169
6.8.	Heat transfer coefficient (h_{fp}) as influenced by fluid flow rate and temperature for heating Teflon and potato particles.	170
7.1.	Correlation between predicted and observed Nusselt number (Eq.7.19).....	195
7.2.	Correlation between predicted and observed Nusselt number for cylindrical particles satisfying GGr/GRe^2 ratio between 2.0 and 3.1 (Eq.7.20).....	197
7.3.	Correlation for observed and predicted Nusselt numbers after introducing the diffusivity in Eq. (7.21) for GGr/GRe^2 between 0.88 and 2.0.	200
7.4.	Correlation for observed and predicted Nusselt numbers after introducing the diffusivity ratio for GGr/GRe^2 ratio between 2.0 and 3.1 (Eq. 7.22).	201
8.1.	Residual activity as a function of heating time at various temperatures for trypsin in dilute (pH = 3.8).	212
8.2.	Residual activity as a function of heating time at various temperatures for trypsin in citrate buffer solution (pH = 5.1).....	213
8.3.	Residual activity as a function of heating time at various temperatures for trypsin in citrate buffer solution (pH = 6.0).....	214

8.4.	Thermal inactivation time curves for trypsin in relation to pH.....	217
8.5.	Process lethality (F_0) achieved by a decimal reduction in activity of trypsin and selected bio-indicators at various temperatures.....	220
8.6.	Residual activity (%) of trypsin and selected bio-indicators as a function of temperature resulting in F_0 of 10 min.....	222
9.1.	A schematic diagram of sample preparation for verification studies.	229
9.2.	A schematic representation of grid size for test sample with embedded capsule.....	234
9.3.	Measured and predicted heat penetration curves for heating potato in water at 90°C.....	237
9.4.	Residual activity as a function of heating time at temperatures (50 - 80°C) for trypsin in citrate buffer (pH = 5.1).	240

CHAPTER I

INTRODUCTION

Food preservation has been a major concern and continues to occupy an important position in the economies of nations the world over. With its recognition as a way of extending the useful shelf life of food and feedstuffs, research efforts have focussed on consolidating the fundamental principles and behaviour of foodstuffs in conjunction with deteriorating agents such as microorganisms and chemicals which have the potency of producing carcinogenic compounds in stored products. Evidently, there has been a subtle improvement in both preservation principles and practices which has gone a long way to alleviate safety concerns raised by the consumer. Until recently, energy costs of food preservation operations was regarded as inevitable and recognized as a fixed cost. With increasing global concern on environmental imbalances, reduction in energy consumption has become vital to the financial well-being of the food industry.

Thermal processing of foods has generally been viewed as an energy-intensive preservation technique, but persists as the most widely used method of food preservation (Teixeira, 1992). Today, there is an ever increasing consumer awareness and request for flavourful, colourful, inexpensive, conveniently packaged, high quality, readily available, clearly and informatively labelled, and above all safe products. These demands require innovative processing techniques having safety and quality as primary priorities. Aseptic processing (Lopez, 1987) is one of the processing techniques with tremendous potential for high quality and reduction in overall energy input when compared with other conventional processing operations such as retorting, flame sterilization and hydrostatic

pressure cooking.

The evolution of aseptic processing (Heldman, 1989) had been sporadic for the past 40 years due primarily to the rapid development of new packaging materials such as plastics and polymer-coated paper containers. The concept of aseptic processing, as opposed to conventional canning, involve heating, holding and cooling of a food product in meticulously designed unit operations, but mechanically synchronized to work in perfect unison. Theoretically, all food systems can be processed aseptically provided unit operations are so chosen to impact the desired lethality within stipulated time limits, as well as maintain product characteristics and integrity.

Successes realized with milk-based beverages and fruit juices gave considerable impetus to the concept resulting in over 420 aseptic processing lines in the United States alone (Jairus, 1992). According to the author, the number of retail packages rose from 40 million in 1981 to 5 billion packages at a retail cost of \$1.5 billion, and an annual growth rate of 12%. In recent years, there has been a widespread growth and industrial concern to process low-acid ($\text{pH} > 4.6$), high-viscosity foods containing discrete particles. The ultimate challenge with these products include microbiological assurance and quality maintenance through proper establishment of critical control factors which conform to regulatory requirements (Heldman, 1989).

In thermal process evaluation, the temperature response of processed foods are critical especially with foods which heat up by conduction. With traditional processing methods, the food temperature can be monitored during heating and simultaneously documented. With discrete particles suspended in a continuously moving fluid, however,

particle temperature cannot be easily measured since current thermometry techniques are inapplicable. Solution to this problem requires the development of techniques to measure and/or predict microbial lethality at the coldest spot of the continuously flowing particle in complex two-phase systems. Adequate control of such complex systems becomes questionable and probably impossible. Consequently, the need to ensure microbiological safety may result in gross over-processing of the product. Although considerable thought and effort in terms of mathematical modelling and simulations (Dial, 1985; Sastry, 1986; Chandarana and Gavin, 1989a,b; Chandarana *et al.*, 1989; Larkin, 1989) have gone into finding suitable techniques for estimating lethality of low-acid foods containing particulates, such products are yet to penetrate the American market.

There is a school of thought that the renewed interest to process low-acid particulate foods can not be possible from both quality and microbiological standpoints, since the liquid portion need to be held at much higher temperatures for longer periods (over-processed) in a traditional heat-hold-cool system. This has resulted in the consideration of other alternatives such as batch sterilizing particulates followed by packaging with sterile liquid phase. This notion probably led to the installation of the APV Jupiter system on the European scenes. Although the Jupiter system sounds promising, it somewhat deviates from the aseptic tradition and concept of having a product processed in a continuous fashion.

Several predictive models and or simulations have been published (Sastry, 1986; Chandarana *et al.*, 1989) which highlight critical factors; these models require verification with data obtained under real processing conditions. Although microbiological verification

is the pre-requisite for establishing thermal processes, it may not be the active constraint for high-temperature short time processing (Saguy *et al.*, 1992), rather heat resistant enzymes may present severe problems and might be used as processing criterion. Another major obstacle in modelling particle temperature history in an aseptic processing unit is the unavailability of several important input parameters. Heldman (1989), classified all factors needed for verification and establishment of particulate products into two broad groups: heat transfer factors and residence time distribution (RTD) factors. Process lethality (Dignan *et al.*, 1989) should be calculated by either biological evaluation of delivered lethality or the time-temperature relationship at the coldest spot. The latter approach, although relatively easier in term of the volume of work, time and resources when compared to the former, requires a knowledge of the convective heat transfer coefficient at the fluid/particle interface. Apparently, the fluid-to-particle heat transfer coefficient (h_{fp}) represents the most important (Heldman, 1989) of all critical parameters needed to establish a sound thermal process for particulates.

Evaluating the fluid-to-particle heat transfer coefficient under aseptic processing conditions will provide the much needed information concerning heat transfer characteristics, and bridge the current gap in the quest to process low-acid particulate foods which meet both sterility and nutritional requirements. Again it will provide the much needed engineering data necessary for proper process/equipment design. Optimum processing conditions can not be established without proper assessment of heat transfer in relation to particle/fluid relative velocities, shape and size of particles, pipe diameter, temperature and concentration of carrier fluid. The overall optimum processing condition

can only be obtained by integrating heat transfer characteristics and residence time distribution, with the destruction kinetics of enzymes/nutrients and heat resistant micro-organisms.

Recognizing consumer demands and the keen interest demonstrated by the food industry and academia to get low-acid particulate foods cleared by the appropriate regulatory agencies, the primary challenge will be to ensure product quality, yet, satisfying the microbiological constraint within the framework federal by-laws.

The objectives of this research were to:

1. Identify and establish, in relation to sensitivity, an appropriate analytical method for routine evaluation of fluid-to-particle heat transfer coefficients,
2. Estimate the fluid-to-particle heat transfer coefficient under low flow and mild heating conditions using *finite cylindrical* particles,
3. Design and fabricate a pilot scale aseptic holding tube simulator for heat transfer studies,
4. Evaluate fluid-to-particle heat transfer coefficient in relation to both product and system parameters under simulated aseptic processing conditions,
5. Develop dimensionless correlations for estimating heat transfer coefficients associated with food and model particles under conditions suitable for industrial applications,
6. Identify and establish kinetic data for a thermally stable bioindicator for rapid

verification/validation of thermal processes, and

7. Verify heat transfer coefficients determined under simulated aseptic processing conditions using the established kinetic data for the bioindicator.

CHAPTER II

LITERATURE REVIEW

Aseptic Processing in Retrospect

In 1860, Louis Pasteur explained the principle of heat preservation after carrying out experiments which related heat sterilization and microbial inactivation to re-contamination of foods in hermetically sealed containers. The credit for successful canning however goes to the French inventor Nicholas Appert who published the first book on canning in 1810. The concept of canning had been an "art" until Bigelow and Ball developed the first scientific-based method (now referred to as the Graphical method) for calculating safe sterilization processes. Within the same decade Ball (1923) formulated the classical Formula method. In spite of more advanced mathematical methods (Stumbo 1953; Patashnik, 1953; Hayakawa, 1968; Teixeira *et al.*, 1969) which led to the use of computers for rapid, accurate and routine process calculations, the Formula method persists as the most favoured method by the canning industry.

An important landmark in the history of food processing/preservation was achieved when aseptic concepts were conceived during the early parts of 1948. Aseptic technology differs markedly from in-container processing where non-sterile products are hermetically sealed in non-sterile containers and subsequently subjected to thermal treatment. The original intent and application (Heldman, 1992) was to replace traditional retort processing of liquid foods in storage containers. Although the process of heat-cool-fill (HCF) was initiated by Ball in 1927, aseptic processing technology has gained momentum only in the

past four to five decades (Stevenson and Ito, 1991).

Modern aseptic processing has two historic roots (Lopez, 1987). The first root which had the priority of providing better quality product than obtained with conventional systems, was the development of the Martin-Dole system in the United States in 1948. The other root is due to two Swiss pioneers Loelinger and Regez who in 1960 developed a system which utilized hydrogen peroxide to sterilize flexible packaging materials. The antimicrobial action of hydrogen peroxide is believed to be due to its reduction to highly reactive hydroxyl radicals which react with membranes, lipids and nucleic acids (Singleton and Sainbury, 1987). The primary focus of the Swiss system was to extend the useful shelf life of fresh milk without refrigeration. The filling of milk was done in a modified Tetra Pak machine which produced tetrahedron packs from paperboard and polyethylene (Buchner, 1993). These developments gave considerable impetus to aseptic processing/packaging and most importantly in February 1981 when the US Food and Drug Administration (FDA) approved hydrogen peroxide as a sterilant for polyethylene, after critical re-evaluation of the Japanese findings (Buchner, 1993). Recently, ultraviolet light and gamma radiation have been accepted by the FDA as packaging sterilants (Stevenson and Ito, 1991). Due to its poor penetrative power, ultraviolet is normally used in combination with hydrogen peroxide (Joyce, 1993). In the mid of the 70's, extensive work was performed on the filling of fruit purees and particulates in drums and bag-in-bag packs (Loire, 1976), and in 1984/85, the first Combibloc pack containing aseptically processed soup appeared on the British market.

Among other challenging processes such as extruded food technology, freeze

drying, controlled atmosphere packaging, and microwave, aseptic processing and packaging was rated the most significant innovation in food science developed during the 50-year history of the Institute of food Technologists (IFT Staff Report, 1989). The potential, growth and development achieved with aseptic processing, probably led the IFT to naming aseptic processing and packaging as the top invention.

Needless to say, aseptic processing technology has been instrumental in providing consumers with high quality liquid and acid food products. Current Industrial endeavour is to process low-acid particulate foods. The food technologist is therefore faced with the problem of providing a microbiologically safe product within the framework of proven quality assurance and particulate integrity.

Theoretical basis for Quality Improvement in Aseptic Processing

The definition of aseptic processing depends on which sector the concept is employed. The dairy industry for instance, uses the term "high-temperature short-time (HTST)" to describe pasteurization processes with time-temperature combination in the neighbourhood of 72 °C for 15 seconds. Sterilization at temperatures between 135 to 150°C for holding times between 3 to 5 s is referred to as ultra high temperature (UHT) processing by the same industry (Lopez, 1987). Generally, HTST refers to the sterilization of food products from times ranging from a few seconds to a minute (Ball and Olson, 1957). The HTST approach is based on differential temperature sensitivity of microorganisms and quality factors with the gap between these factors widening in favour of a reduced nutrient degradation at temperatures greater than 120 °C. From a food quality

standpoint (Ohlsson, 1989), there is no need going to temperatures above 130-132°C. The effect of temperature was demonstrated by Hersom and Shore (1981) who described a batch aseptic system for sterilizing 2 cm maximum-sized carrot cubes. The maximum upper limit temperature, which was selected on the basis of excessive tissue softening, sloughing and damage on the outside of the vegetable pieces, as well as enzyme survival and regeneration was about 132 °C. Apparently, the selection of optimum processing conditions depend on several factors, the most important being quality attributes in relation to anticipated microbiological load. Although modern processing equipments allow processing to be done at high temperatures, the introduction of particle/liquid suspensions complicate design requirements needed to maintain particle integrity, prompting the need for quality optimization as a function of operating temperatures.

Evidently, the aseptic promise is based on the relative response of microorganisms and nutrients to temperature since thermal inactivation of microorganisms are much more temperature dependent than destruction of quality attributes (Lund, 1977). This forms the basis for high-temperature short-time processing and rotatory sterilization of low-viscosity food products (Mansfield, 1962). Toledo and Chang (1990) presented a mathematical relationship which relates the extent of nutrient degradation to microbial inactivation at any given processing temperature as follows:

$$\log(C/C_o) = \pm [(D_{mo}/D_{co}) \log(N_o/N)] [10^{(T_o-T)(1/z_m-1/z_c)}] \quad (2.1)$$

where C and C_o, N and N_o are nutrient concentration and microbial count before and after

processing respectively. D_{co} and D_{mo} are the decimal reduction times at a reference temperature T_o and z is the temperature range required to change D by a log cycle. The constraint to Eq. (2.1) is that medium temperature should be reached instantaneously (Toledo and Chang, 1990). This constraint limits its application to mostly liquid products, however, it proves the advantages gained from processing at elevated temperatures.

Advantages of Aseptic Processing

Lopez (1987), listed major advantages of aseptic processing as: (1) minimal destruction of food components responsible for typical organoleptic attributes (2) better retention of heat sensitive nutrients resulting from shorter processing times at elevated temperatures (3) possible utilization of a wider variety of packaging materials of different shapes and sizes (4) continuous sterilization and packaging which avoids possible re-contamination of sterilized foods (5) efficient use of energy due to rapid heat transfer rates and (6) adaptability of the aseptic system to automatic controls with fewer operators compared to traditional systems. It is important to note that, of all the advantages listed, the primary motivation for aseptic processing is the achievement of higher quality products with similar level of microbiological safety as achieved in traditional canning processes.

Limitations of Aseptic Processing

Notwithstanding the potentials outlined above with regards to overall quality assurance, HTST adoption is challenged by: (1) the apparent difficulty in destroying heat

resistant enzymes (2) higher initial capital investment (3) limitations to specific product types and (4) the sophisticated instrumentation needed to initiate the process (Lund, 1977; Lopez, 1987). However, such apparent limitations are outweighed by long-term economic returns. Silva *et al.* (1992) indicated that HTST principles may not be readily applicable to solids and highly viscous foods. The authors reasoned that slow heat penetration to cold spots would increase the time required to achieve commercial sterility, thereby causing severe surface burns as suggested by Teixeira *et al.* (1969).

Unit Components for Sterilizing Particulate Products

Figure 2.1 illustrates some processing and packaging alternatives, and shows in particular, various sterilization options. Although the ultimate goal is to achieve commercial sterility irrespective of the processing path chosen, specialized equipments may be needed for specific products. Recent advancements in packaging technology allow various forms of packaging materials to be adopted for specific needs. Evidently, the selection of a particular processing/packaging path is product dependent.

Conventionally the aseptic processing system consists of one or more heat exchangers for heating, a holding tube, and one or more heat exchangers for cooling. Lund and Singh (1993) divided the aseptic processing system into six elements including the product, flow controls, product heating, holding tube, product cooling and packaging. Elevating product to the desired temperature in the heater is very essential, especially with conduction-heating products where considerable temperature lag exists between different sublayers of the same food system. Although direct steam heating and tubular heat exchangers

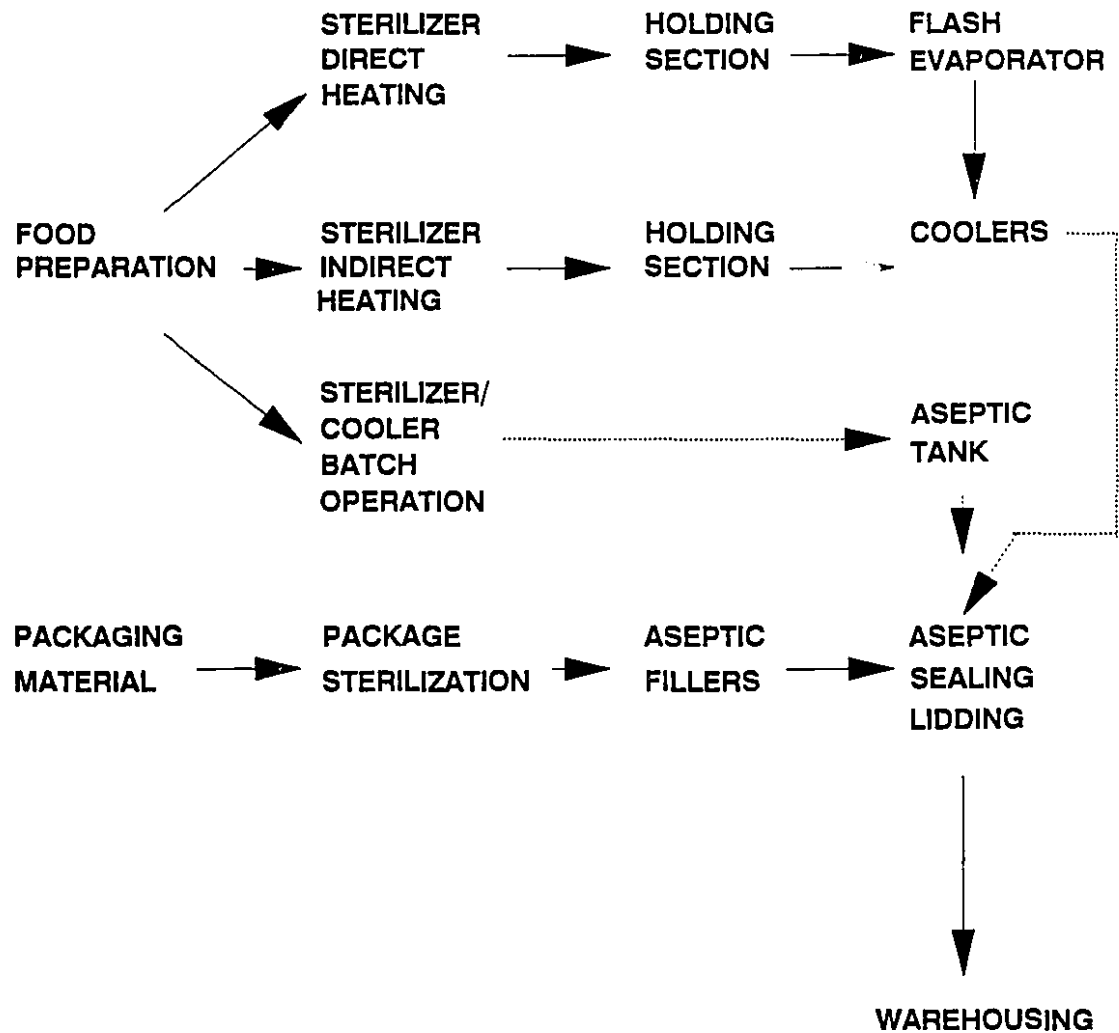


Figure 2.1 The aseptic processing system flow diagram

provide the shortest processing times, the scraped surfaced heat exchanger has been the choice for particulate/viscous liquid mixtures. The benefits gained is that slow heating coupled with agitation allows adequate heat penetration to particles, thereby producing uniform flavour (Lopez, 1987). According to Warrick (1990), the scraped surfaced heat exchanger is unsuitable for low-acid food products with particle diameters greater than 15 mm, and Heldman (1989) emphasized the need to redesign specialized exchangers to handle such products. According to Buchner (1993), tests performed on specially designed and optimized SSHE indicates that such systems can handle particulates up to 37 mm.

Commercial Systems For Particulate Products

Currently, there are two commercial processing systems offered by manufacturers for processing liquid-particle mixtures (Dennis, 1990). These are the Steripart and the Jupiter systems. The steripart equipment aims at increasing the retention time of particulates in conventional tubular heat exchangers coupled to a "Rota Hold" holding device with built-in sieves purposed to hold particles while the hot carrier fluid flows. The Rota-hold device originally developed by Stork in 1985 consists of a cylindrical vessel equipped with infeed and discharged ports, and a set of fork-blades mounted on a rotatable central shaft to effect different residence times. Thus, the heat load needed by product could be adjusted to give the required quality. The steripart is reported to have been tested for a variety of products ranging from 15 mm meat particles in tomato sauce to 18 mm mushroom particles in cream style soups (Buchner, 1993). The quality and integrity of the particles were reported to be satisfactory (Hermans, 1988; Holdsworth,

1992; Buchner, 1993).

The Jupiter system originally developed in Europe, has been described in detail by Hersom and Shore (1981). It operates such that particles are heated in steam-jacketed double-cone-shaped vessels into which steam is admitted under pressure and rotated about its central axis. Cooling is done in the same vessel but with steam replaced by water. The condensate from processed particles is either retained for subsequent batches or reconstituted with the sauce which is processed in a standard HTST equipment. Although the Jupiter system is reported to be capable of handling, heating and cooling large particulate without the liquid, it is a batch system which is very expensive to run aside from a number of product transfers which has to be done under sterile conditions. According to Singh and Heldman (1993) the APV Jupiter system has not achieved commercial acceptance in North America.

Principles of Process Calculations

The severity of any thermal process depends on the physical characteristics of the food material being processed, its pH, the size, heating conditions and most importantly, the target enzyme or microorganism present in the food (Fellows, 1988). Traditionally, thermal processes focus on reducing a hypothetical population of a target microorganism capable of growing in the product at the intended distribution temperature to some small yet finite value. Estimation of a parameter called the sterilizing value (F_p) or otherwise "process lethality", is the basis for mathematical determination of a proper heat process (Hayakawa, 1977):

$$F_p = \int_0^t 10^{(T-T_{ref})/z} dt \quad (2.2)$$

The integrant of Eq. (2.2) is referred to as the lethal rate, while F_p represents the cumulative lethal effect resulting from impacted lethal temperatures. T_{ref} is the reference processing temperature while z represents the temperature sensitivity of the organism of concern. Two approaches can generally be used to express the impact of lethal temperatures on foods in relation to process lethality: (1) an integrated lethality (F_s) value which represents the volume average survival of microorganisms or (2) target lethality (F_c) at the coldest spot of the product (Stumbo, 1973). For integrated lethality in a particle, F_s can be evaluated as follows:

$$F_s = D_{ref} \log(TMV) \quad (2.3)$$

where

$$TMV = \frac{1}{V} \int_0^V 10^{\left[-\frac{1}{D_{ref}} \int_0^t 10^{(T-T_{ref})/z} dt \right]} dV \quad (2.4)$$

TMV is the target mass average survival of microorganisms and V is the volume in m^3 . For a "safe" heating process, process lethality (F_p) calculated with either Eq. (2.2) or (2.3) must compare with the thermal death time (required lethality) needed to reduce an initial microbial population from A to a target value B (Stumbo, 1965; Teixeira *et al.*, 1969):

$$F_{req} = D_{ref}(\log A - \log B) \quad (2.5)$$

where F_{req} , and D_{ref} are the integrated lethality and decimal reduction time at the reference temperature respectively. Obviously, lethality factor, defined as the ratio of F_p to F_{req} must at least be equal to unity for commercial sterility to be achieved (Merson *et al.*, 1978). For commercial sterility therefore, process calculations should involve either: (1) the determination of the process time t for a given heating and cooling cycle which produces $F_{req} = F_p$ or (2) determination of the F value for a process of given duration. These two procedures, are referred to as the General and Formula methods.

Analytical Models for Aseptic Process Evaluation

Dial (1985), suggested the adoption of Ball's formula method (Ball and Olson, 1957) for estimating holding times for low-acid foods containing particulates but failed to justify his claim. Merson *et al.* (1978) presented detailed discussions and limitations associated with Ball's formula method which included: (1) an infinite fluid-to-particle heat transfer coefficient (2) the necessity for long process times required to satisfy the first term approximation of the infinite series solution and (3) the need for a constant medium temperature. According to Sastry (1986), the straight-line curve obtained for conduction heated canned foods will never exist for particulate products in continuous flow systems. The reason given was that particles continue heating in the holding tube at the expense of the fluid temperature hence, resulting in a decrease in fluid temperature. Quite recently, Larkin (1989) modified Ball's formula by introducing a hyperbolic function to determine

process lethality for particulate products. Using computer simulations which accommodated a finite heat transfer coefficient, the author illustrated that Ball's formula method can over-estimate lethality by 241% of the actual value for heating and holding alone, if heat penetration parameters f_h and j_h are estimated from the linear portion of the semilogarithmic plot. According to Rao (1992) the modified Ball's formula developed by Larkin (1989) has the potential for particulate foods but needs further exploration.

Swartzel (1982), developed the Equivalent Point Method (EPM) for comparing different thermal treatments. Provided an accurate time-temperature history of the process exist, the EPM method yields an isothermal treatment which characterizes the entire process using an equivalent time and temperature.

Using the EPM approach, Yang *et al.* (1992) studied lethality distribution in the holding tube of a model aseptic system containing particulates. Individual particle lethalties were calculated with Eq. (2.2), and the overall sterilizing value by the weighted average of individual particle. Using a least square regression model for time-temperature profiles at both the centre and surface of a particle to estimate the equivalent temperature and time, Yang *et al.* (1992) simulated particulate lethalties as a function of particle density, flow rate, and the heat transfer coefficient (h_{fp}). The authors concluded that F_0 values achieved at the centre of particles followed a quadratic function of the particle-to-fluid ratio. The particle-to-fluid ratio was also found to have similar trends as residence time distributions, with the distribution of F_0 values at particle centres increasing as the fluid-to-particle heat transfer coefficient (h_{fp}) values increased.

Numerical Models for Process Evaluation

With the advent and rapid development of powerful high-memory computers, the possibility of using computer simulations have increased in both the academic field and food industry. These programmes are useful in establishing critical control points in the design and development of food products.

Sastry (1986) perhaps, was the first to present a comprehensive model for particulate laden products flowing in the aseptic unit. The following assumptions were considered in his model: (1) the calculation of fluid temperature profiles over the heat exchanger and holding tube length (2) determination of temperature and lethality at the coldest location of individual particles using a finite heat transfer coefficient (3) the fluid medium was well mixed in the radial direction of the heat exchanger and holding tube, and at all times was in contact with a population of particles of uniform sizes moving at the same average velocity and (4) negligible viscous dissipation in the scraped surface heat exchanger. Sastry (1986) used an energy balanced equation involving energy input from steam and energy loss from a population of average-sized particles to calculate the temperature profile of the carrier fluid. The calculated fluid temperature profile and a conservative heat transfer coefficient estimated from Nusselt number ($Nu = 2.0$) for spherical particles were used as input data for simulating temperature profiles within individual particles using the Galerkin-Crank-Nicolson finite difference algorithm.

Sastry's results demonstrated that the sizing of the holding tube should be based on (1) the slowest heating particle (2) the most rapidly moving particle in both the heat exchanger and holding tube and (3) the lowest heat transfer coefficient. According to the

author, particle size and residence time distribution within the scraped surfaced heat exchanger and the holding tube influenced the minimum holding tube required to attain commercial sterility while the effect of the convective heat transfer coefficient levelled off for convective coefficient factors (CCF) above 0.5. Below a CCF value of 0.5 which usually occurs with viscous carrier fluids, the required residence time increased significantly.

Lee *et al.* (1990a) developed a finite difference model to simulate an aseptic processing system containing either beef, carrot, chicken, pea, or potato particles in either water or starch solutions using the product flow rate as control parameter instead of the external medium temperature. This assumption holds for specified fluid exit temperature and length of the scraped surface heat exchanger (SSHE). Lee *et al.* (1990a) solved using an implicit Crank-Nicolson finite difference algorithm, the energy balanced equations for a plate, infinite cylinder and spherical particles in relation to various product and system parameters. Their simulation results indicated that the size, shape, thermal properties of particles and residence time distributions within the SSHE and the holding tube, influenced the minimum time required to achieve 6D for *Clostridium sp* (PA 3679) and 12D for peroxidase and hence the minimum required processing time. In addition, no lethality accumulated at the centre of the largest particle in the SSHE regardless of the simulation approach used.

Chandarana *et al.* (1989) developed an explicit finite difference model based on energy balanced equations to study an aseptic system containing particulates. They concluded that the thermal, physical and rheological properties of products, their residence

time distributions within the aseptic system, and the fluid-to-particle convective heat transfer coefficient were vital in process evaluations. Using an explicit finite difference model for cube shaped particles to simulate various heating and cooling situations, Chang and Toledo (1989) demonstrated that the choice of the fluid-to-particle heat transfer coefficient had severe implications on product sterility. The temperature profile of the product was found to depend on the liquid to solid ratio at various sections of the aseptic unit.

Recently, Skjoldebrand and Ohlsson (1993a,b) reported the development of a computer simulation program for particulate products at the Swedish Institute for Food Research (SIK) in Sweden. The program among others, facilitates simulations on the influence of process variables on product quality expressed in terms of the volume average cook value *via* a first order kinetic assumption. Simulation variables included product flow rate, residence time distribution, particle size and geometry, equipment specification, particle load and thermal properties. Critical assumptions made in the programme were similar to those suggested by Sastry (1986), but with accommodation for several heat exchangers for both heating and cooling. The accuracy of numerical routines depend extensively on how accurate input data are. This necessitates biological validation of derived F_0 values if simulated time-temperature data are used, and sufficient justification of (1) assumed residence times (2) applicability of empirically-estimated heat transfer coefficients and other thermophysical properties and (3) limitations and experimental validation of mathematical models in relation to assumption made.

Simulation Approaches for Process Evaluation

For continuous sterilization of liquid foods, it is sufficient for process evaluation to consider only lethal effects achieved while the product is resident in the holding tube (Teixeira and Manson, 1983). Charm (1966) suggested that integrating lethality across the holding tube could account for different residence times of streamlines from the centre to the wall. According to Teixeira and Manson (1983), this consideration simplifies heat transfer models by allowing the assumption of isothermal conditions in an insulated holding tube. Using a computer model, the authors examined differences between single-point (F_0) and integrated (F_s) lethality in the holding tube with fluids ranging from pure non-Newtonian pseudoplastics to dilatants. The influence of the holding tube temperature, the z and D values, the holding tube diameter, and flow rate were studied. They concluded that with the exception of the flow behaviour index and D which had significant impact, other parameters had insignificant effects on differences between F_0 and F_s .

Chandarana and Gavin (1989b) suggested three approaches for scheduling heterogeneous foods as follow: (1) the " F_0 hold" approach which adds thermal credit in the SSHE to the thermal and lethality credits in the holding tube. With this approach, lethality in the SSHE is assumed to be zero, although, particles temperature rises (2) the "Hold only" approach which excludes thermal and lethality contributed in the SSHE and recognizes that achieved in the holding tube alone and (3) the "Total system" approach where accumulated thermal and lethality credits are accounted for in both the SSHE and holding tube.

Computer simulations by Chandarana and Gavin (1989b) demonstrated that, neglecting thermal contributions from the SSHE while scheduling a process for a particle centre F_0 of 6.0 min could result in an effective F_0 as high as 78 min. Hersom (1984), however attributed only 10% of the total microbial inactivation to the heating section of a sterilization process. Lee *et al.* (1990b) performed sensitivity analysis on the three approaches suggested by Chandarana and Gavin (1989b). The holding tube length required to achieve 6D of *Clostridium sporogenes* (PA3679), the destruction of thiamine and peroxidase after processing were used as reference points for evaluation. They found no significant differences between the "Total system" and " F_0 Hold" approaches. The "Hold only" approach resulted in overprocessing of the product. For lack of comprehensive data on the effect of rheological properties on the convective heat transfer coefficient and residence time distribution of particulates, the authors failed to conduct sensitivity simulations on h_{tp} under aseptic conditions.

According to Stevenson and Ito (1991) and Pflug *et al.* (1990), US food regulations require that processes for low acid foods be sufficient to protect the public from health hazards. For example, a product should be filed in accordance with Title 21 Part 108 of the *Code of Federal Regulations* (21 CFR 108), "Emergency Permit Control" (Bernard *et al.*, 1990), if it is regulated by the FDA to have a pH and water activity (a_w) greater than 4.6 and 0.85 respectively. In this regard, issues to be addressed in relation to establishing a continuous heat-hold-cool sterilization for low-acid particulate foods (Dignan *et al.*, 1989) must include: (1) identification and selection of the appropriate sterilizing value (2) development of conservative models to predict sterilizing value

achieved at the slowest heating spot in a particle when it reaches the end of the holding tube (3) microbiological validation of lethality delivered and (4) specifications with regards to critical factors and methods to be used for controlling them.

Selection of a Target F_0

To ensure commercial sterility, foods must experience 12D cycle reduction at the coldest spot based on the kinetic data for *Clostridium botulinum*. In conventional canning therefore, the minimum "bot cook" which refers to a process lethality (F_0) of 3 min at 121°C is used for low acid foods (Brown, 1991). In real processing however, F_0 values in excess of 3 min are employed to destroy the most heat resistant thermophiles capable of causing storage problems and other unknowns. Pflug *et al.* (1990) outlined the need to consider three organisms in designing low-acid canned foods. The authors presented empirical (F_0) values (Table 2.1) as a general guideline to be used in the absence of actual data for process design. Apparently, the target F_0 may be different for the solid and liquid phases of a product. For vegetable products, the time needed at 121.1°C. range from 1 to 4.4 min to reach acceptable overall cook quality (Mansfield, 1974). It should be recognized that selecting a conservative F_0 value may result in significant overprocessing of the product. According to Pflug *et al.* (1990) sterilization values calculated from time-temperature data using a z value of 10C° and a reference temperature of 121.1°C are acceptable validations since a specified F_0 will have similar microbiological killing power whether it is calculated from physically-measured data or proven biological methods. According to Dignan *et al.* (1989) lethality credited to particulates in the holding tube

Table 2.1 Empirical F_0 -values for low-acid canned food*.

Hazard	Endpoint probability	F_0 (min)
Public health concern	10^{-9}	3
(a) Mesophilic spores	10^{-6}	5-7
(b) Thermophilic spores at distribution temperature below 30°C	10^{-3}	5-7
(c) Thermophilic spores at distribution temperature above 30°C	10^{-6}	15-21

*Pflug *et al.* (1990).

should be treated in a non-dynamic sense. This means that lethality should be calculated on the basis of the coldest temperature for the fastest moving particle in the holding tube. Alternatively, lethality credited to particles should be that associated with the largest particle having the least residence time (RT).

Residence Time Distribution (RTD)

One essential processing parameter is the time needed to achieve commercial sterility. In conventional canning, every container is adequately exposed to the heating medium. Due to shear stresses in continuous HTST processes, food products develop a velocity distribution. The instantaneous velocity will therefore depend on the location of the product in the heat-hold-cool system. Therefore aseptic processing of particulate products require the residence times at various components of the aseptic system to be accounted for. Factors affecting the residence time include the particle size and its distribution, the characteristics and flow properties of the fluid medium, the velocity profile within the holding tube and heat exchanger, heating characteristics of the product and the configuration of the holding tube (Heldman, 1989; Sastry, 1989a,b). The utility of particle residence time if measured between two points becomes more evident by converting it to particle velocity for estimating required holding tube length (Yang and Swartzel, 1991).

Discussing the relevance of residence time in thermal process evaluation, Bateson (1969) stressed that the RTD in a scraped surface heat exchanger (SSHE) exhibits physical characteristics between a perfectly stirred tank and that of pflug flow in a pipe.

According to Cuevas *et al.* (1982) residence time distribution in the SSHE lies closer to pflug flow. With the exception of ideal pflug flow in continuous systems (Singh and Lee, 1993), each fluid element spends different lengths of time to flow through the heat exchanger or holding tube. Evidently, predicting accurate product lethality would require the residence time distribution.

Singh and Lee (1992) listed commonly used techniques in characterizing RTD as follows: (1) a step function change where input concentration is changed from one level to another (2) a sinusoidal input where frequency of a sinusoidal variation is changed and the steady state response of the exit stream at different input levels are used to generate a frequency response plot and (3) a pulse input where a small amount of tracer is injected into the feed stream (effluent) at the shortest possible time. The step function and pulse input methods are relatively easy to implement compared to the sinusoidal method which requires special equipments.

Normally, the RTD of fluid elements are determined with the pulse input method with the effluent time-concentration curve being referred to as the C curve (Yang and Swartzel, 1991). Implementing a pulse input function in real systems containing discrete particulates is complicated by differences in particle-to-tube diameter ratio as well a different radial locations exhibited by the particles as they enter the holding tube. However, for replicated data with overall number of runs given by N_o , the frequency ratio of particles which exit a test section between times t and $t + \Delta t$ can be estimated (Yang and Swartzel, 1991) as:

$$C(t) = \frac{\Delta N}{N_0} \quad (2.6)$$

where ΔN is the number of particles encountered in each residence time category. The $E(t)$ function, commonly referred to as the exit-age distribution function, describes quantitatively, the different times spent by particles in a reactor in discrete terms and expressed mathematically (Brown and Fogler, 1986; Levenspiel, 1972) as:

$$E(t) = \frac{C(t)}{\Delta t} \quad (2.7)$$

Since the $E(t)$ curve gives the fraction of volume element leaving a reactor at a particular time (Singh and Lee, 1992), a graphical plot of $E(t)$ against time gives the E curve (a normalized distribution) which means that the total area beneath the curve is unity. Thus a cumulative function, $F(t)$, which represents the fraction of particles in exit stream that has spent time t or less in a reactor is expressed mathematically as:

$$F(t) = \sum_{i=0}^n E(t_i) \Delta t_i \quad (2.8)$$

To characterize and compare residence time distributions, the mean value (t_m) serves as a useful indicator (Yang and Swartzel, 1991; Singh and Lee, 1992) expressed mathematically in the form of Eq. (2.9):

$$t_m = \frac{\sum_{i=0}^n t_i E(t_i)}{\sum_{i=0}^n E(t_i)} \quad (2.9)$$

Establishing residence time of the fastest moving particle in the aseptic unit is a necessity from a food safety point of view (Dignan *et al.*, 1989). But to predict quality changes without overprocessing significant portions, the average (mean) and maximum residence times and their distribution characteristics should be well established (Singh and Lee, 1992).

Using calcium alginate beads in water, Taeymans *et al.* (1985) evaluated the mean residence time as a function of axial Reynolds number, rotational Reynolds number, and centrifugal Archimedes numbers. The authors observed that increasing scraper rotational speed, increased the mean residence time of the dispersed phase. However, increasing the fluid flow rate or axial Reynolds number caused a decrease in particle mean residence time which finally approached the mean residence time of the liquid phase. Defining Heat Exchanger Residence Time Ratio (HXRTR) as the ratio of particle residence time to the mean particle residence within the SSHE, Sastry (1986) simulated a process for particles which travel unusually fast as well as slow in the SSHE by varying the HXRTR value between 0.2 and 2.5. The author remarked that the effect of heat exchanger residence time distribution was significant because the fastest moving particles greatly increased the required process time. For product homogeneity in the SSHE, ideal pplug flow is preferable. With pplug flow however, heat and mass transfer rate are quite slow due to

lack of radial and axial mixing (Lee and Singh, 1991,1993). Although heat and mass transfers are enhanced in perfectly mixed flow with adequate agitation, residence time distributions are broadened.

Utilizing an RTD function in conjunction with thermal inactivation kinetics of microorganisms, Lin (1980) presented an analytical routine for calculating the length of a tubular sterilizer for processing non-Newtonian liquid food products. The author indicated that longer sterilizers were needed for higher pseudoplastic foods with higher pH values but with lower operating temperatures. Sastry (1986), using a situation where particles moved faster than the fluid demonstrated that the holding tube has to be over 300 m long to achieve sterility, which would result in an unacceptable product.

Using modelled food particles in a 6.1 m long, 38 mm internal diameter glass holding tube, Berry (1989) found that no particle residence time ratio fell below 0.5. This indicated that no particle travelled faster than twice the bulk fluid velocity. His finding on residence time ratio was confirmed by Dutta and Sastry (1990b). According to McCoy *et al.* (1987), particles travel by as much as 85% higher than the average velocity of the fluid. According to the authors, particle behaviour becomes highly unstable at bends with RTD increasing with decreasing particle size. They conducted their studies with polystyrene spheres of density 1.04 g/mL in a non-Newtonian fluid flowing in a holding tube. Chandarana *et al.* (1991) embedded 2-3 mm wide flexible magnets into diced potato and chicken alginate mixtures for residence time distribution studies. The magnets were detected as they entered and exited the SSHE, the holding tube and a SSHE cooler. By introducing one particle at a time, the authors found no particle to travel with velocity that

equalled or exceeded twice the average product velocity in the SSHE heater. They also found the residence time distribution to be skewed such that majority of particles had residence times which exceeded the mean product residence time.

Berry (1989) characterized the RTD of 13 mm rubber cubes in carboxymethyl-cellulose at 25°C by a normal distribution whereas smaller particles of sizes between 6 and 10 mm followed a bimodal distribution with two distinct peaks which illustrated particle flow closer to the wall of the tube and those which travelled at the centre. Dutta and Sastry (1990b) investigated velocity distribution of food particles in a holding tube. They reported that the mean normalized particle velocities were significantly influenced by particle Froude number and a dimensionless velocity. Particle flow distributions were best described by log-normal models with fluid viscosity having the largest impact on velocity distribution. Sastry and Zuritz (1987) and Sastry *et al.* (1989) modelled single particle trajectories and velocities during pipe flow in relation to the Saffman lift, Magnus lift, drag, and buoyancy forces resulting from liquid motion. Simultaneous solution to equations involving the above forces yielded particle velocity as a function of time. Particle velocities were reported to be greater at the axis as compared to those closer to the wall.

Quite recently, Abdelrahim (1994) studied residence time distributions of meat and carrot cubes with sizes ranging from 6 to 20 mm in a pilot scale aseptic processing system containing between 6 to 10% w/w starch concentrations. Important conclusions drawn by the author were as follows: (1) carrot and meat particles on the average travelled at about 1.4 and 1.6 times faster than the carrier fluid respectively (2) larger

particles on the average travelled faster than smaller ones in the holding tube as opposed to a reverse trend for the SSHE and (3) the RTD of carrot and meat particles in the aseptic system followed a logistic growth model. The author presented a detailed study on the influence of both system and product parameters on RTD and derived dimensionless correlations for low-acid particulates as a function of fluid hydrodynamic properties for temperatures up to 100°C. The author correlated particle Froude and Reynolds numbers to carrier fluid Reynolds, Froude, and Archimedes numbers, thus making it possible to predict particle maximum velocity as a function of properties associated with carrier fluids.

Apparently, thermal processes based on the fastest moving particle would likely result in significant overprocessing of particles at low viscosities and flow rates where most particles lag the fluid (Sastry, 1989a,b; Sastry *et al.* 1989). Presently, the conservative approach is to assume a particle residence time ratio of 0.5 for the holding tube (Singh and Lee, 1992). According to the authors, deviations from this criterion would demand detailed studies on particle residence time and the basis for achieving it.

Heat Transfer

When solid particles are present in a liquid, a very complex heat transfer system results. The particles in the liquid would need to be sterilized besides the liquid itself. Since the particles heat up by a slow conduction process, sterilization of the food system will be limited by the size and population of particles in the food matrix (Simpson and Williams, 1974; Chandarana, 1992; Mwangi *et al.*, 1992). Therefore particle distribution

at any given location with time becomes essential.

Heat transfer to cold spots within particles will be restricted by the thermal resistance within the product and the total thermal resistance at the surface. The thermal resistance of the product is a function of its thermophysical (density, specific heat, and thermal conductivity), its geometry and dimensions (Hendrickx *et al.*, 1992b). Practically, the carrier fluid will exhibit a decrease in temperature while in the holding tube (Larkin, 1989). This drop in temperature will depend, but not limited to, the population of particle in the holding tube. Therefore, using the holding tube exit temperature for process designing is probably the best, because if the number of particles should increase in the holding tube the heater exit/holding tube inlet temperature can be increased to compensate for the drop in temperature. Again, for viscous fluids with particulates, the scraped-surface heat exchanger (SSHE) which by their nature, keeps the product well mixed and evenly distributed (Chandarana, 1992; Lund and Singh, 1993) is preferred.

The Heat Exchanger

The SSHE has the ability to process at very high temperature with low pressure drops, however, fragile particles can disintegrate (Lopez, 1987; Lund and Singh, 1993). Three mechanisms are involved with the heating of products within the SSHE. Firstly, heat is transferred from a source to the inside wall of the exchanger. The liquid portion is then heated by convection caused by blades paring the product away (Hayes, 1988). The rate of temperature change of the liquid portion needed to arrive at a pre-selected outlet temperature can be modelled exponentially (Adams *et al.*, 1984; Holman, 1986) as:

$$T = T_s + (T_i - T_s) \exp\left(\frac{-UAt}{V\rho C_p}\right) \quad (2.10)$$

where T_s , T_i , ρ , C_p , U , A , t , and V represents steam temperature, initial temperature, density, specific heat, overall heat transfer coefficient, surface area, process time and volume respectively. Using Eq. (2.10) to predict fluid medium temperature assumes the following: (1) a uniform fluid temperature in the radial direction at each section (2) constant fluid thermophysical properties (3) no phase change is associated with the fluid and (4) no heat exchange between the fluid and particles. Generally, the overall heat transfer coefficient (U) is estimated from an equation which incorporates the resistance to heat transfer on the product side, the heating medium side, and the interface between the fluid and the wall:

$$\frac{1}{U} = \frac{1}{h_o} + \left(\frac{x}{k}\right)_w + \frac{1}{h_i} \quad (2.11)$$

where h_o and h_i are the medium and product heat transfer coefficients respectively and $(x/k)_w$ is the thickness of the SSHE wall divided by its thermal conductivity. In order to determine the total heat supplied to fluid/particle mixtures however, the resistance occurring at the particle fluid interface for the total mass has to be incorporated in the above model.

The Holding Tube

Since required lethality cannot be achieved during heating alone, the holding tube forms one of the most important components of the aseptic system. Irrespective of contributions made towards cumulative lethality by both heating and cooling, the FDA will acknowledge lethality achieved in the holding tube alone (Dignan *et al.*, 1989; Singh and Heldman, 1993). Singh and Heldman (1993) listed some design requirements to be met in designing the holding tube as follows: (1) it must slope upward at a minimum of 2.1 cm per meter (1.194°) upwards in order to eliminate air pockets and promote adequate drainage after cleaning (2) no heating should be carried out along the holding tube (3) the tube should not be exposed to condensate or draft air (4) the interior surface of the holding tube should be smooth (5) the pressure in the holding tube must be higher than the vapour pressure of the liquid to prevent boiling of product and (6) appropriate temperature sensors and controller devices must be installed at the inlet and exit of the holding tube. For liquid/particle suspension, heat transfer in the holding tube can be calculated by conducting an energy balance over an incremental area, assuming negligible viscous dissipation of energy and perfect mixing in all radial directions. The resulting mathematical relationship (Sastry, 1986; Chandarana and Gavin, 1989b) is as follows:

$$U_{ht} A_{ht} (T_f - T_a) = m_f C_{pf} (T_f^{n+1} - T_f) - h_{fp} A_p N (T_f - T_{ps}) \quad (2.12)$$

where T_f is the fluid temperature at time t , T_f^{n+1} is the fluid temperature at time $t+1$, T_f is the temperature at time t , T_{ps} is the mean particle surface temperature, and N is the

number of particles. A_{ht} and A_p are the incremental surface area of the holding tube and the surface area of the particle respectively. Particulate population will cause the fluid portion to exhibit a decrease in temperature at the holding section (Lee *et al.*, 1990a), because sensible heat will be lost to both the particles and surroundings. Larkin (1989) modelled changes in temperature within the holding tube as either exponential or linear. For the linear model, a straight line equation with a variable slope, chosen to represent up to 13°C drop in temperature was used. The use of exit fluid temperature of the holding tube eliminates the problem of accounting for heat losses along the tube (Teixeira, 1992). The wall-to-fluid convective heat transfer coefficient for a horizontal tube (Singh and Heldman, 1993) can be estimated from the relationship:

$$Nu = 0.023 Re^{0.8} Pr^{0.4} \quad (2.13)$$

The holding tube to environment convective heat transfer coefficient will depend on the Rayleigh (GrPr) number (Geankoplis, 1978) giving the relationship for GrPr greater than 10^9 :

$$h_e = 1.32 \left(\frac{T_s - T_a}{d} \right)^{1/4} \quad (2.14)$$

and for GrPr greater than 10^9 the heat transfer coefficient is :

$$h_e = 1.24 (T_s - T_a)^{1/3} \quad (2.15)$$

where T_w , T_a and d are the tube wall temperature, ambient temperature, and holding tube diameter. The minimum safe holding tube length should provide adequate residence time to render all portions of the product commercially sterile. For fully developed laminar flow under constant pressure gradient (Gavin, 1985; Sastry, 1989a), the solution to the Navier Stokes equation in one dimension gives a relationship between maximum and mean velocities. The nature of the relationship depends on the rheological properties of the fluid and the flow regime which could be laminar, transitional or turbulent. For laminar flow, the relationship between mean and maximum velocity is:

$$V_{\max} = 2 V_{\text{mean}} \quad (2.16)$$

and for Newtonian fluids in turbulent flow:

$$V_{\max} = 1.2 V_{\text{mean}} \quad (2.17)$$

For power law fluids in laminar flow, the fluid momentum equation yields:

$$V_{\max} = \left(\frac{3n+1}{n+1} \right) V_{\text{mean}} \quad (2.18)$$

where n is the flow index behaviour. Since $n < 1$ for pseudoplastic fluids, $V_{\max} < 2V_{\text{mean}}$ while $V_{\max} > 2V_{\text{mean}}$ for dilatants. Since the fluid at the centre of the tube moves with the maximum velocity and possess the shortest residence time at processing temperature, calculating the holding tube length (Sastry, 1989a) must be based on sterilizing that

component. Therefore, the minimum holding tube length (L) may be calculated as follows (Dickerson et al., 1968; Sastry, 1989a):

$$L = t V_{\max} \quad (2.19)$$

Knowing the death rate of a target microorganism in a product, it is possible to determine the time (t) which the product should be kept in the holding tube at the processing temperature.

Temperature Distribution in Particulates

In HTST processing of solid-liquid mixtures the particles experience a time-dependent medium temperature which should be known as a function of time or of location within the system. Two methods can be used to measure the temperature profile of the carrier fluid (Sastry, 1989a). The first approach, is to perform energy balance on both the fluid and particle, assuming a constant medium temperature for a well mixed fluid. The second method is by measuring the temperature at various locations within the system. With both methods, the medium temperature can be expected to follow an exponential growth (Sastry, 1989a). The time-temperature distribution in a particle with constant thermophysical properties is obtained by solving the transient heat transfer equation for conduction, which in cartesian coordinates is given as follows:

$$\frac{\partial T}{\partial t} = \alpha \left(\frac{\partial^2 T}{\partial x^2} + \frac{\partial^2 T}{\partial y^2} + \frac{\partial^2 T}{\partial z^2} \right) \quad (2.20)$$

with the time dependent convective boundary condition:

$$k_p \frac{\partial T}{\partial x}; k_p \frac{\partial T}{\partial y}; k_p \frac{\partial T}{\partial z} = -h_{fp} (T_p - T_f) \quad (2.21)$$

The convective boundary condition defined by Eq. (2.21) is obtained by equating at the surface, the fluxes given by Newton's law defined as:

$$q = h_{fp} A_p (T_p - T_f) \quad (2.22)$$

to Fourier's Equation:

$$q = -k_p A_p \frac{\partial T}{\partial x} \quad (2.23)$$

where A_p , k_p and α , are area, thermal conductivity and thermal diffusivity respectively of the particle. h_{fp} and T_f are the heat transfer coefficient at the fluid-to-particle interface, and the temperature of the fluid respectively. Relevant assumptions made in solving the partial differential equations (Incropera and deWitt 1985; Chapman, 1989; Lee *et al.*, 1990a; Weng *et al.*, 1992) are: (1) constant thermal and physical properties (2) homogeneous and isotropic particle (3) pure conduction heating within particles (4) no phase change in the fluid and particle during processing and (5) uniform initial temperatures for both liquid and particle. There are a number of published literature on thermophysical properties (Polley *et al.*, 1980; Singh, 1982; Murakami *et al.*, 1985; Murakami and Okos, 1987). But, a point worth noting is that thermophysical parameters are most likely to be temperature

dependent. However, there is paucity of data on temperature dependence of thermophysical parameters. Utilizing a temperature dependent data would require solving the transient heat transfer equation by a numerical approach.

The Convective Heat Transfer Coefficient (h_p)

The term "convection" applies to the heat transfer mechanism which takes place in a fluid as a result of conduction within the fluid and energy transport due to the fluid motion produced either by artificial means or by density differences (Chapman, 1989). The introduction of particulates into a mobile fluid complicates the dynamics of the flow phenomenon. Therefore the rate of heat penetration into suspended particles becomes a function of the boundary layer surrounding the particle. This boundary layer causes a thermal lag between the particle surface temperature and the ambient fluid temperature.

The complexities introduced by heat conduction, fluid dynamics and boundary layer may be lumped together in a single parameter by introducing Newton's Law of cooling defined by Eq. (2.22). The quantity h_p known as *heat transfer coefficient*, *film coefficient*, or *unit thermal conductance* represents the proportionality factor between heat transferred by convection to a body immersed in a fluid and the temperature difference between the particle and fluid.

The convective heat transfer coefficient is not a material property such as thermal conductivity or specific heat but rather a complex function of the composition of the fluid, the geometry of the particle surface, and the hydrodynamics of the fluid motion past the surface (Chapman, 1989). Heat transfer associated with immersed flow depends on the

geometry of the object, its position, the proximity of other bodies, flow rate and fluid properties (Gunn and Narayanan, 1986; Burfoot and James, 1988). This dependence indicates that the convective heat transfer coefficient varies over an immersed object (Geankoplis, 1978).

The temperature distribution within suspended solid particles will therefore strongly depend on the convective heat transfer coefficient (h_{fp}) which characterizes conditions occurring at the fluid particle interface. However, h_{fp} poses one of the most difficult parameters to evaluate under practical aseptic conditions (Heldman, 1989) due to the dynamic nature of the particles. Information on the above factors are currently lacking in the literature (Mwangi *et al.*, 1992) in relation to both product and system parameter. The significance of the heat transfer coefficient lies in the fact that the temperature history of suspended particles has to be predicted in order to calculate product sterility. Again, it is needed in determining equipment, process design and optimization (Lund and Singh, 1993). According to the authors, the interaction between particles suspended in a dynamic fluid introduce complications in predicting the heat transfer coefficient. Furthermore, no mathematical correlation has generally been recognized to be capable of predicting the liquid-to-particle heat transfer coefficient in both the SSHE and the holding tube under aseptic conditions.

Analytical Models for Calculating h_{fp}

Analytical solutions in the form of Fourier infinite series equations have been presented by Carslaw and Jaeger (1959) and Luikov (1968) for transient heat conduction

into an infinite slab, infinite cylinder and spheres. The series solutions for the above shapes are complex and require the Biot number which in turn depends on the heat transfer coefficient as well as thermal conductivity. Employing these equations would require the time-temperature data gathered from either the surface or within the particle to back-calculate the heat transfer coefficient iteratively. Chang and Toledo (1989) used the first four terms of the exact series solution for an infinite slab to calculate the heat transfer coefficient to cubes immersed in an isothermal fluid. The multiplicative technique was employed in simplifying the infinite series solution for the finite cube. The authors calculated the time-temperature data iteratively at three locations until the h_p value which gave the best fit between experimental and predicted data was found. Stoforos and Merson (1990) presented a mathematical procedure for estimating h_p for particles using liquid temperature as the only input parameter. In arriving at the expression for the heat transfer coefficient, the authors solved the energy balanced equation for a can and the partial differential equation for temperature distribution in a spherical particle. They used a multiple regression scheme in the Laplace transform plane and the liquid portion temperature alone to estimate both the fluid-to-particle and overall heat transfer coefficients. This approach appears inadequate because two unknown parameters are estimated from one input parameter, and a number of combinations of these two parameters can yield the same solution.

When the resistance to conduction within a solid particle is negligible (i.e. Biot number < 0.1) compared to the resistance to convection across the fluid boundary layer, the exact location of thermocouple becomes unimportant because particle temperature

distribution becomes homogeneous and equilibrates instantaneously (Deniston *et al.*, 1987). Under such situations the 'lump capacity' approach (Maesmans *et al.*, 1992) becomes readily applicable for evaluating the convective heat transfer coefficient:

$$\ln(T_p - T_f) = \ln(T_{ip} - T_f) - \left(\frac{h_{fp} A_p}{m_p C_p}\right) t \quad (2.24)$$

The lumped capacity method assumes that the material is cooled or heated uniformly. This indicates that the temperature at any location and the mass average temperature are the same as the centre temperature (Ramaswamy *et al.*, 1982,83). A semilogarithmic plot of $(T-T_f)$ against time gives a straight line asymptote from which the convective heat transfer coefficient (h_{fp}) is determined from the slope. Using this approach, Lenz and Lund (1978) evaluated heat transfer coefficient to lead spheres surrounded by spherical food particles in water and 60% starch solutions. Sastry *et al.* (1989), Alhamdan *et al.* (1990), Alhamdan and Sastry (1990) and Zuritz *et al.* (1990) used mushroom-shaped aluminium particles to measure either the average or time-dependent heat transfer coefficients with either Newtonian or non-Newtonian fluids. They verified their data by re-calculating the Biot number from estimated heat transfer coefficients. According to Ramaswamy *et al.* (1982) and Ramaswamy *et al.* (1983), the lumped capacity method predicts lower heat transfer coefficients compared to that obtained from the solutions to the transient conduction equation. According to the authors, errors ranging from 5 to 25% may result as the heat transfer coefficient increases from 1000 to 10,000 W/m²C. Concerns about thermocouple placement in particles have been raised and Stoforos (1988) advocated it be placed at the

surface of particles. Hassan (1984) reported a 10% drop in h_p for errors in the placement of thermocouples at the surface of the particle.

Apparently, errors associated with thermocouple placement appear to depend on the mathematical simplifications and assumptions employed in solving relevant equations. There is lack of a comprehensive verification on analytical methods for routine calculations for the fluid-to-particle convective heat transfer coefficient with special emphasis on thermocouple placement.

Numerical Models for Calculating h_p

Numerical solutions to the governing partial differential equation enables evaluation of temperature distribution at various points within particles, and makes possible, the calculation of centre point and integrated lethalties with higher accuracies. Furthermore, numerical techniques can accommodate temperature dependent thermophysical properties. Sastry (1986), Chandarana *et al.* (1989), Chang and Toledo (1989), Larkin (1990), Lee *et al.* (1990a,b), Weng *et al.* (1992) and Mwangi *et al.* (1993), used finite difference approximations to solve the governing partial differential equations to particles, and verified their solutions with analytical solutions under isothermal conditions.

Although numerical approximations are versatile in terms of accommodating complex geometries and processing conditions, precision will depend on how accurate thermocouples are placed in the particle if predicted data are to be compared with experimental values for h_p estimations. Exact location of thermocouple and heat

conduction within the particle assumes importance when lethality has to be predicted, thus demanding for safe aseptic process, accurate data on the heat transfer coefficient between the liquid and particle throughout the aseptic system.

Experimental Methods for Evaluating h_{fp}

Accurate prediction of particulate response to lethal temperatures through mathematical models depend on how accurate associate h_{fp} data are estimated, especially under aseptic conditions where both product and system parameters are expected to have significant influence. h_{fp} is traditionally determined from physical measurement of the temperature history within a particle under well defined initial and boundary conditions. In real processing situations such as rotational retorting and aseptic processing however, the particles are dynamic, due to gravitational, centrifugal, drag, and buoyancy forces in rotating cans (Deniston *et al.*, 1987; Maesmans *et al.*, 1992) and to drag, buoyancy forces, Magnus lift and Saffman lift under dynamic flow conditions (Dutta and Sastry 1990a). Several experimental techniques have been developed for evaluating h_{fp} associated with liquid-solid mixtures (Sastry, 1992a). These methods, which depend on either direct or indirect temperature measurements include, microbiological history indicators, moving thermocouple, melting point, liquid crystal method, relative velocity, liquid temperature/calorimetry, transmitter, and stationary particle methods.

Microbiological Method: Hunter (1972) and Heppel (1985) were the first to pioneer and use microorganisms suspended in beads to back-calculate the convective heat

transfer coefficient using a mathematical model. This approach prompted further research with the use of chemical indicators. In place of microorganisms, Weng *et al.* (1992) used a time-temperature integrator in the form of immobilized peroxidase to determine heat transfer coefficients at pasteurization temperatures. A polyacetal sphere loaded with the indicator at the centre, was hooked onto a thermocouple and placed at the geometric centre of a can. Heating and cooling time-temperature data were gathered for estimating process lethality with the general method. The indicator was recovered after heat treatment and its activity determined for estimating the actual accumulated lethality. The authors developed a method called the Least Absolute Lethality Difference (LALD), defined as the absolute value of the difference in lethalties realized from a mathematical model and that obtained experimentally to calculate the heat transfer coefficient. An estimated heat transfer coefficient and known thermophysical properties were substituted into an explicit finite difference program to predict the time-temperature history and associate integrated lethality at the centre of the particle. The heat transfer coefficient was modified and lethality re-calculated till the difference between the predicted and actual lethalties fell within a tolerant limit. The authors compared their results with the Least Sum of Squared Temperature Differences (LSTD) approach introduced by Lenz and Lund (1977), and found their model to predict accurate results than the LSTD method. The LSTD approach is based on selecting the heat transfer coefficient which gives the least sum of squared deviations between measured and predicted data. Differences between the two approaches can be attributed to the different contributions of the entire time-dependent temperature profile adopted by both approaches. With the LALD approach the weight of lethal

temperatures is more pronounced than the weight of lower temperatures, whereas in the LSTD approach each registered temperature is considered in minimizing the difference between experimental and predicted temperatures. Both methods appear adequate and should be used to compliment each other for h_{fp} evaluations.

Generally, the microbiological method predicts average h_{fp} over the entire aseptic unit rather than individual components. Again, the infusion/immobilization process may alter particle characteristics due to differences in materials used in holding the microorganisms or indicator in place. Although the microbiological method is noninvasive in relation to particle trajectory as well as suitable to high temperature applications, sample-to-sample variation in microbial population for instance can cause major problems and discrepancies in replicated data.

Moving Thermocouple Method: In an attempt to measure the effect of particle motion on h_{fp} , Sastry *et al.* (1989) developed the moving thermocouple method which involved the withdrawal of a thermocouple-hooked-transducer from a tube using a motor at pre-determined speeds. The heat transfer coefficient was calculated from the gathered time-temperature data using the lumped capacity approach. Major advantages associated with this procedure include (1) recording the exact temperature of a mobile particle and (2) the possibility of using an opaque carrier fluid. However, particle motion is somewhat restricted, resulting in considerable interference with the carrier fluid. According to Sastry (1990), such situations can enhance heat transfer considerably. In a recent review, Sastry (1992) indicated that the moving thermocouple method predicts conservative values.

However, replicating experimental data with this method is impossible since particle trajectories cannot be controlled or restricted to a definite path within the aseptic system. In addition, the moving thermocouple approach is not readily adaptable to high temperatures and pressures due to difficulties in equipment design. Again this method constraints fluid motion and profiles when particles are withdrawn.

Melting Point Method: The melting point method utilizes polymers which change colour at specific temperatures. The heat transfer coefficient is back-calculated after careful calibration of colour with temperature. Mwangi *et al.* (1993) mobilized a melting point indicator with temperatures ranging from 51 to 80°C at the centre of transparent polymethylmethacrylate spheres with diameters ranging from 8 to 12.7 mm. The particles were introduced through a venturi device into the holding tube of an aseptic simulator containing glycerin/water mixtures. As the melting point was reached, the surface of the indicator changes colour, and the time lapse for the colour change was recorded in addition to the time-temperature data of the fluid. The temperature at the surface of the indicator within the particle was predicted with a finite difference program for transient heat conduction to the spherical particle using an assumed value for the convective heat transfer coefficient. The h_{fp} value which minimizes predicted and observed temperature profiles is adopted. Since colour change is irreversible (Mwangi *et al.*, 1993), particles are not re-useable. This method is non-invasive but limited to transparent tubes.

Liquid Crystal Method: Moffat (1990) provided detailed discussion on the use of

the liquid crystal method for estimating h_{fp} , and Stoforos *et al.* (1989) were the first to employ the method to determine heat transfer to particulates in a continuous system. It involves coating the surface of a particle with temperature-sensitive colour-changing crystals and video-taping colour changes. Surface temperature is obtained by comparison with a standard colour after proper calibration. The method is non-invasive, rapid and provides a surface-temperature measurement which is sensitive to variations in h_{fp} . The accuracy of measured temperatures with this method is however limited by: (1) the range of temperatures over which colour changes (2) the resolution of the video image and (3) the necessity to visualize surface changes in colour. Therefore the liquid crystal method falls short of high temperature/pressure applications involving opaque carrier fluids.

Relative Velocity Method: The relative velocity method utilizes established empirical correlations associated with fluid flow over objects of known geometry. Examples of such correlations include those presented Kramers (1946), Ranz and Marshall (1952) and Whitaker (1972) which relates flow properties, flow characteristic and particle geometry to the Nusselt number. The relative velocity method requires measuring the velocity of both the fluid and particle with a video camera. The carrier fluid velocity is essentially monitored by introducing a tracer particle into the fluid stream and the relative velocity is determined by recording the time elapsed for a given tracer particle to pass over a test particle. The accuracy of data estimated with this method depends on the reliability of adopted correlations. This technique, according to Sastry (1992), can be used to characterize radial variations in h_{fp} .

Liquid/Temperature Calorimetry Method: The liquid temperature/calorimetry method although simple in principle is inappropriate for evaluating individual variations in heat transfer coefficients. With this method the convective heat transfer coefficient is determined by adding a number of relatively low-temperature particles to a hot liquid and monitoring the temperature of the fluid as time progresses. Knowing the thermophysical properties of both the particles and fluid, h_{fp} can be estimated by performing energy balance on the product. Although the method provides h_{fp} for bulk particles even in opaque carrier fluids, individual changes in h_{fp} cannot be distinguished. In addition, the method is not readily adaptable to high temperature/pressure treatments.

Transmitter Method: Although the transmitter method sounds practical and promising for evaluating the heat transfer coefficient non-invasively, it may cause considerable variation in the density of the particle in which it is embedded. In principle, the technique involves the placement of a miniature sensor at the coldest spot of concern in order to relay time-temperature data to a logging system. The present sensor in its compact form, is far denser than real foods (Sastry, 1992). In a recent study with this method, Balasubramaniam and Sastry (1994) used a quartz crystal which transmitted magnetic signals to an external receiver, which converted the magnetic signals to temperature readings. The crystal was placed in a hollow cylindrical capsule made of boron nitride. Heat transfer coefficients were back-calculated from the time-temperature history data using a finite difference program. Although the method is envisaged to have all the potentials for aseptic studies, little information has been reported in the

literature.

Stationary Particle Method: Generally, the stationary method involves the placement of a transducer particle in a flowing stream such that direct temperature measurement of both fluid and particle can be gathered simultaneously. Since actual time-temperature data is gathered the solutions for transient heat conduction in the form of either numerical or analytical routines become readily applicable for estimating the convective heat transfer coefficient. Due to particle restriction to both translational and rotational motions, the stationary methods may not reflect conditions in real situations, which in turn can lead to deviations from real situations (Maesmans *et al.*, 1992). However, since fluid/particle relative velocities are low for non-Newtonian fluids in particular (Zuritz *et al.*, 1990), and laminar regime probably dominates in most practical/industrial applications, the stationary method may be adopted for conservative estimation of h_{fp} . Again, the relative differences between fluid and particle velocities can be simulated for sensitivity of h_{fp} to different processing parameters and conditions relevant to industrial applications.

Predicting h_{fp} from Dimensionless Correlations

When the surface of an object is brought in contact with a fluid whose bulk temperature is significantly different from the temperature of the particle, a non-uniform temperature field is generated in the fluid. The temperature field, which are acted upon by local gravitational and centrifugal forces, causes changes in density which may,

through buoyant forces, cause the fluid to move relative to the surface. As might be expected, associated velocities are small hence inertial forces are marginal. Heat transfer under such a phenomenon is referred to as free or natural convection heat transfer as opposed to forced convection heat transfer where fluid motion is induced with pumps.

In all forced convection situations (Fand and Keswani, 1973), natural convection mechanisms still operate since density gradients and for that matter, buoyant forces exist. Therefore, natural convection effects are present in all heat transfer processes. The Reynolds number which represents the ratio of inertia to viscous forces, and the Grashof number which represents the ratio of buoyant to viscous forces, play important roles in the establishment and evaluation of heat transfer by both mechanisms. In situations where one must take into consideration the simultaneous exchange of momentum through viscosity and heat transfer through conduction, the ratio of kinematic viscosity to thermal diffusivity (i.e. Prandtl number), has to be taken into consideration. Generally therefore, the dimensionless heat transfer coefficient (Nusselt number) is described as a function of the dimensionless quantities in the following relationship:

$$Nu = f(Re, Gr, Pr) \quad (2.25)$$

Although the convective heat transfer coefficient varies over a given body during heating/cooling, dimensionless/empirical correlations serve as a useful tool in providing average values, particularly, in situations where processing conditions are complex and parameters are difficult to estimate with conventional techniques. Again the influence of fluid thermophysical properties and relative velocities on the convective heat transfer

coefficient (Incropera and deWitt, 1985) may be evaluated by comparing experimental data with published correlations such as those presented by Kramers (1946), Ranz and Marshall (1952), , and Whitaker (1972) for spherical particles.

The most conservative approach (Sastry *et al.*, 1989) is to assume that the particle and fluid travel at identical velocities through the aseptic system, so that the Reynolds number becomes zero, yielding a relationship:

$$Nu = 2.0 \quad (2.26)$$

For a freely rotating particle in shear flow at high Peclet numbers (Simpson and William, 1974), the Nusselt number becomes independent of the magnitude of the impressed shear, yielding an Nu value of 9. Studies by Chang and Toledo (1989) however indicated that the Nusselt number may range from 10 to 20 at zero fluid velocity. The above values were arrived at by pumping fluid through a packed bed of carrot cubes at a fluid flow rate of 1.58 cm/s. The pump was shut off after the bed was full. According to Hunter (1972) a process designed on the basis of $Nu = 2.0$ may result in over-heating of the carrier fluid. Results obtained by Simpson and William (1974) differs from other correlations for flow past a stationary particle. The explanation offered by Mwangi *et al.* (1992) to the above discrepancies in the Nusselt number was that at high Peclet numbers, a freely rotating sphere is surrounded by a region of effective isothermal streamlines, across which heat is transferred by conduction alone.

For stationary particles with flow past it (Mwangi *et al.*, 1992), heat transfer takes place by both conduction and convection across a convectioal thermal boundary layer

of thickness identified by a Peclet number in the order $Pe^{1/3}$. Johnson *et al.* (1942) proposed for Reynolds number (Re) greater than 500, the relationship:

$$Nu = 0.714 Re^{0.5} Pr^{0.5} \quad (2.27)$$

and for $Re > 200$ Williams (1942) proposed:

$$Nu = 0.37 Re^{0.6} Pr^{0.33} \quad (2.28)$$

When the Peclet number (Pe) is smaller than unity, conductive effects predominate over convection resulting in $Nu = 2.0$ for pure conduction to spherical particles (Mwangi *et al.*, 1992). According to the authors, the additional rate of heat transfer due to convection can be considered as a function of the Peclet number as follows:

$$Nu = 2.0 + 0.5 Pe + 0.25 Pe^2 \ln(Pe) + 0.334 Pe^2 + (1/16) Pe^3 \ln(Pe) \quad (2.29)$$

Conduction effects become negligibly small and can be ignored as Pe approaches infinity.

Chang and Toledo (1989) compared their experimental data with published correlations. At $Re < 700$ their experimental results deviated from the trend predicted with published correlations. The explanation offered was that free convection dominates before relative velocities become zero. For a mushroom-shaped aluminium particle suspended in a non-Newtonian fluid at 70°C, Zuritz *et al.* (1990) obtained the correlation, valid for flow rates ranging from 0.06 to 0.287 kg/s:

$$Nu = 2.0 + 28.37 Re^{0.233} Pr^{0.143} \left(\frac{D_p}{D_{tube}} \right)^{1.787} \quad (2.30)$$

where D_p/D_{tube} represent the particle-to-tube diameter. According to Chandarana *et al.* (1989), decreasing particle dimension increases the surface area to volume ratio of the particle (SAV) thus increasing the heat transfer coefficient. The authors related the convective heat transfer coefficients to particle dimensions and the Reynolds number as follows:

$$h_{fp} = 1.14 \times 10^{-4} (SAV)^{1.94} Re^{0.07} \quad (2.31)$$

Several dimensionless correlations have been presented in the literature (Chandarana *et al.*, 1988; Alhamdan and Sastry, 1990; Alhamdan *et al.*, 1990a,b; Chandarana *et al.*, 1990; Sastry *et al.*, 1990; Mwangi *et al.*, 1993; Astrom and Bark, 1994) however, most were derived for either forced or natural convection alone.

Factors affecting Heat Transfer Coefficients

The convective heat transfer coefficient is most likely to be influenced by factors including: (1) particle size and shape (2) particle and fluid thermophysical properties (3) particle location (4) fluid-particle relative velocity (5) the diameter of the particle in relation to that of the tube (6) fluid viscosity and temperature. Table 2.2 shows a summary of published data on h_{fp} in relation to some of the above factors and their limitations. These factors are discussed in two broad sections: those related to particle and

Table 2.2 Published data on fluid-to-particle heat transfer coefficients.

Particle material	Shape and size	Type of fluid	Flow conditions	h_{fp} (W/m ² C)	Reference
Potato	Cube 1-2 cm	Water	0.36-0.86 cm/s	239-303	Chang and Toledo (1989)
Potato	Cube 1-2 cm	35% sucrose solution	-	146	Chang and Toledo (1989)
Silicone Rubber	Cube 2.54 cm	Water	Static	51-63	Chandarana (1988)
Silicone Rubber	Cube 2.54 cm	Water	0.26-0.88 cm/s	65-107	Chandarana <i>et al.</i> (1988)
Silicone Rubber	Cube 2.54 cm	Starch dispersion	Static	8-36	Chandarana <i>et al.</i> (1989)
Silicone Rubber	Cube 2.54 cm	Starch dispersion	0.26-0.88 cm/s	56-90	Chandarana <i>et al.</i> (1988)
Aluminium	Sphere 23.9 mm	Water	4.3-11 gal/min	2039-2507	Sastry <i>et al.</i> (1989)
Aluminium	Mushroom shaped 3 sizes	CMC solution	0.08-0.29 kg/s	548-1175	Zuritz <i>et al.</i> (1990)
Aluminium	Sphere 1.33-2.39 cm	Water	2.1-12.7 gal/min	688-3005	Sastry <i>et al.</i> (1990)
Alginate Gel	Sphere 3.4 mm	Water	Re=5250- 50,000	2180- 7870	Heppel (1985)
Alginate Gel	Sphere 3.4 mm	Starch dispersion	Re=30	930	Heppel (1985)

Table 2.2. Continuation.

Particle material	Shape and size	Type of fluid	Flow conditions	h_{fp} (W/m ² C)	Reference
Aluminium	Mushroom shaped	Water	Static(heating)	652-850	Alhamdan <i>et al.</i> (1990)
Aluminium	Mushroom shaped	Water	Static(cooling)	384-616	Alhamdan <i>et al.</i> (1990)
Aluminium	Mushroom shaped	CMC solution	0.05-0.9 (heating)	75-310	Alhamdan and Sastry (1990)
Aluminium	Mushroom shaped	CMC solution	0.05-0.9 (cooling)	22-153	Alhamdan and Sastry (1990)
Boron nitride	Cylinder	CMC solution	2.0-5.0 gal/min	134-669	Balasubramaniam and Sastry (1994)
Gellan Gel	Cubes 0.96 cm	Water	1.3-3.8 $\times 10^{-4}$ m ³ /s	2000-4500	Gratzek and Toledo (1994)
Polymethyl methacrylate	Sphere 8-12.7 mm	Glycerine/ Water	Re=73.1-369	58-1301	Mwangi <i>et al.</i> (1993)
Lead	Sphere 8 mm	Silicone oil	Static	287-448	Astrom and Bark (1994)
Alginate Gel	Sphere 8 mm	Silicone oil	Static	231-360	Astrom and Bark (1994)
Turnip	Sphere 17 mm	Starch dispersion	Static	156-177	Astrom and Bark (1994)

fluid respectively.

Influence of Parameters Associated with Particulates

Particle size and shape are the first factors to consider because the larger the particle the more difficult it takes to sterilize (Heldman, 1989). Berry (1989) suggested that the largest particle may not necessarily be the fastest moving particle and hence not the most difficult to sterilize. Using a conventional canning process for lead particles of diameters 0.95, 2.065, and 3.015 cm immersed in water, Lenz and Lund (1978) found the heat transfer coefficient to increase with increasing particle dimensions. With a 60% aqueous sucrose solution however, a straightforward relationship could not be found. In a similar process but with potato particles, Deniston *et al.* (1987) found particle size to have insignificant effect on the heat transfer coefficient. Hassan (1984) reported a reverse trend to that of Deniston *et al.* (1987): the heat transfer coefficient was higher for smaller potato particles processed in water as compared to bigger particles. The effect of particle size on the heat transfer coefficient in continuous flow systems appears remote since various authors have reported conflicting trends (Chandarana *et al.*, 1988; Zuritz *et al.*, 1990). Zuritz *et al.* (1990) reported an increase in heat transfer coefficient with increasing spherical particle size, while Chandarana *et al.* (1988) found the heat transfer coefficient to increase with decreasing cube size. Although particle shape is known to affect fluid flow profiles and hence h_{fp} , limited information has been presented on the magnitude and sensitivity of different shapes to h_{fp} under similar experimental conditions.

Since different geometrical shapes give different fluid profiles, the heat transfer

coefficient will reflect such variations in addition to surface characteristic of the particle. Using spherical as well as cube-shaped lead particles in a rotating fluid, Astrom and Bark (1994) found insignificant differences in heat transfer coefficients obtained for the two geometries of the same volumes. So far as particle properties such as density and surface roughness does not affect particle-fluid motion (Maesmans *et al.*, 1992) the type of particle material will not influence the magnitude of the convective heat transfer coefficient. However a freely moving particle would definitely distort the fluid profile and probably enhance heat transfer.

Chandarana and Gavin (1989a) using computer simulations, found for the same percentage of particles in the holding tube that, the length required to achieve sterility for cube shaped particles was greater than cylindrical particles followed by spherical particles of the same dimension. According to Mwangi *et al.* (1993) heat transfer is enhanced between 80 and 200% with increase in solid fraction and flow rate. The enhancement was attributed to disturbances in the fluid field caused by the presence of other particles. Recent simulation studies by Larkin (1990) indicated that increasing particle size from 1.27 to 1.91 cm required 142% increase in the holding tube length, while a decrease from 1.27 to 0.64 cm required 79% reduction in the holding tube length required to achieve a specified lethality. Another key finding by the author was that, assumed thermophysical properties have significant impact on the holding tube length.

Aside from particle size, the magnitude of the fluid-to-particle relative velocity would affect the heat transfer coefficient (Maesmans *et al.*, 1992). According to the authors an increase in fluid-to-particle relative velocity will increase h_p with particle size.

Dutta and Sastry (1990a,b) studied particle-particle interaction and their velocity distributions in a holding tube and found in certain situations that a number of particles moved slowly over the bottom wall of the tube, thereby causing channelling of fluid through the free portion of the tube. The heat transfer coefficient can be expected to be affected by such phenomenon probably in a decreasing fashion.

Influence of Parameters Associated with Carrier Fluids

Depending on fluid characteristics and shearing conditions, fluids can be classified as either Newtonian or non-Newtonian. These differences are quantitatively characterised for engineering purposes by the power law model (Rha, 1978):

$$\sigma = m (\dot{\gamma})^n \quad (2.32)$$

where σ is the shear stress, $\dot{\gamma}$ the shear rate, m is the consistency coefficient and n the flow behaviour index. Other models which have successfully been applied to foods in general includes Casson's model, the linear model, Herschel-Bulkley's model, the logarithmic model and the classical Arrhenius model for temperature dependence of apparent viscosity. With Newtonian fluids, the shear stress is directly proportional to the shear rate. The constant of proportionality called viscosity is independent of shear rate within the laminar flow range (Bourne, 1982).

Most liquid foods used in industry are semi-solid, viscous in nature and fall into several classes of non-Newtonian fluids, classified as either dilatant, pseudoplastic, Bingham plastic or non-Bingham. These fluids do not bear directly, a linear relationship

between shear rate and stress. Examples of such foods include colloidal systems such as emulsions, paste and suspension, and macromolecules like starch, pectin, gums and hydrocolloids (Charm, 1962; Holdsworth, 1971; Rao, 1977; Bourne, 1982).

According to Sastry (1988), the power law model breaks down in regions of low shear giving an infinite apparent viscosity. A better descriptor may be the Ellis model (Tadmor and Klein, 1970; Sastry, 1988). Pseudoplastic characteristics is the most observed of non-Newtonian fluids. Pseudoplastic behaviour (Rha, 1978) indicates a continuous breakdown or rear-arrangement of the molecular structure, resulting in less resistance to flow. Such behaviour according to Rha (1978) is due to the presence of (1) the interaction between particles which causes aggregation or association by secondary bonding such as van der Waal forces, and (2) non-rigid or flexible particles which can undergo geometrical or conformational changes.

Heat transfer to particulates depend on the rheological attributes of the carrier fluid, most often characterised by the apparent viscosity. Chandarana *et al.* (1990b) found the heat transfer coefficient for silicone cube immersed in water to be higher than for starch solutions under the same experimental condition. Upon varying fluid temperature between 133 to 145°C, the heat transfer coefficient values changed. At a relatively low temperature compared to that used by Chandarana *et al.* (1990b), Zuritz *et al.* (1990) found higher heat transfer coefficients with decreasing mean apparent viscosity of carboxymethylcellulose solutions used.

Higher fluid apparent viscosity retards heat transfer when decreased turbulences lowers the effective relative particle-to-fluid velocity (Maesmans *et al.*, 1992). Apparently,

the combined effect of carrier fluid attributes and other parametric data on the fluid-to-particle heat transfer coefficient under aseptic conditions are lacking in the open literature. It is desirable to determine the rheological properties under actual processing conditions, since the apparent viscosity is generally expected to be affected by ultra high temperature processing (Sastry, 1988). The effectiveness of heat transfer from a carrier fluid to suspended particles is reflected in the convective heat transfer coefficient h_{fp} .

Thermal Process Kinetics Data

Since aseptic processing utilizes the same principles for conventional in-container processing (Lund and Singh, 1993), quality factor (texture, colour, flavour, and nutrients) retention with simultaneous destruction of microorganism/enzymes forms the primary goal (Witter, 1983). Generally, thermal inactivation of microorganisms proceed rapidly compared to other biological materials as indicated by the lower z -values and higher activation energies (Table 2.3). The mechanism of destruction of various nutritional, quality factor attributes as well as microorganisms have been characteristic extensively to follow first order reaction kinetics (Lund, 1975; Mulley *et al.*, 1975a,b; Saguy and Karel, 1979). Rodriguez *et al.* (1988) suggested an integrated procedure to be used for modelling non-isothermal processes as temperature varies as a function of time. Taking population dynamics and system analysis into consideration, Rodriguez *et al.* (1987) developed a sophisticated model for spore death kinetics. Holdsworth (1985), pointed out that great caution should be exercised in making the assumption that most thermal

Table 2.3 Kinetic data for some foodstuff/microorganisms¹

	z (C°)	Ea (kJ/mol)	D ₁₂₁ (min)
Chemical changes			
Non-enzymatic browning	17-39	100-250	0.4-4.0
Denaturation of protein	5-10	250-800	5.0
Vitamin destruction			
In general	20-30	80-125	100-1000
Thiamine	20-30	90-125	38-380
Ascorbic acid	51	65-160	245
Enzyme inactivation			
In general	7.55	40-125	1-10
Peroxidase	26-37	67-85	2-3
Lipase(from <i>Pseudomonas</i>)	25-37	(75-110)	1.2-1.7 ^a
Microorganisms			
<i>B. stercorophilus</i>	7-13	225-425	3.5-6.8
<i>B. subtilis</i>	6.8-13	230-400	0.4-0.76
<i>C. botulinum</i>	8-12	265-340	0.1-0.3
<i>C. sporogenes</i>	9-13	230	0.15-2.6
<i>C. sporogenes</i> (PA 3679)	10.6	1340-1780	3-22
Cooking value- overall quality estimation			
Peas	17-28	80-95	12.5
Whole corn	36	65-80	2.4
Carrots	15	160	1.4
Potatoes	21	115	1.2
Green beans	14-29	90-170	1.4
Colour			
Chlorophyll(spinach, pea puree)	38-80	30-90	14-350
Carotenoids (paprika)	19	140	0.038

^a Evaluated at 150°C

¹Hallstrom *et al.* (1988).

processes follow first order kinetics. According to Labuza (1982a,b) nutritional losses during processing have been generally established to follow a zero or first order kinetics expressed mathematically as:

$$\frac{dC}{dt} = -kC^n \quad (2.33)$$

where dC/dt = the time rate of change of concentration (C), k is the reaction rate constant, n is the order of reaction. Rearranging Eq.2.33 and integrating over time range $t_1 = 0$ and $t_2 = t$, with the corresponding concentrations C_0 and C respectively, and converting natural logarithm to base 10, gives:

$$\log C = \log C_0 - \frac{kt}{2.303} \quad (2.34)$$

On a semilogarithmic plot, Eq. (2.34) gives a straight line with slope = $-k/2.303$. The decimal reduction time (D-value) which represents the time required to reduce the concentration by 90% is related to k as $D = 2.303/k$. Although Eq. (2.34) represents the destruction of microbes/nutrients under specific temperatures, it bears no direct relationship with temperature.

Two principal methods which describe the temperature dependence of the reaction rate constant are the Arrhenius model which is based on a thermodynamic approach, and the Thermal Death Time (TDT) approach which is based on empirical considerations

introduced by Bigelow (Lund, 1975). The Arrhenius model relates the reaction rate constant to temperature as follows:

$$k = S \exp\left(\frac{-E_a}{RT}\right) \quad (2.35)$$

where E_a is the activation energy, R = universal gas constant, and S is the frequency factor. For two temperatures T_1 and T_2 with their corresponding reaction rate constants k_1 and k_2 Eq. 2.35 becomes:

$$\log \frac{k_1}{k_2} = \frac{-E_a}{2.303 R} \left[\frac{1}{T_1} - \frac{1}{T_2} \right] \quad (2.36)$$

With the TDT concept, the D -values relate proportionally with temperature as follows:

$$\log \frac{D_1}{D_2} = \frac{T_2 - T_1}{z} \quad (2.37)$$

According to Lund (1975) and Mauri *et al.* (1989), the z and reference D values for a given nutrient or quality indicator are dependent on intrinsic factors which include food composition, pH, water activity, oxidation-reduction potential as well as extrinsic factors such as gas composition and their interactions. The two concepts (TDT and Arrhenius) contradict each other since kinetic parameters relates inversely to temperature with the Arrhenius model. According to Lund (1975), the two concepts are reconcilable at small temperature ranges. Combining the two models gives the relationship between z and E_a ,

as:

$$z = 2.303 \frac{R T T_1}{E_a} \quad (2.38)$$

The z-value makes possible, interconversion of F-values at any temperature to an F value at a reference temperature of 121.1 °C, and to sum the lethal rates of a product subjected to a transient temperature environment.

Ramaswamy *et al.* (1989) indicated that the two concepts are suitable for studying degradation kinetics but cautioned that converting parameters from one concept to the other could lead to erroneous results. The authors demonstrated that converting parameters from one concept to the other depend on associated reference temperature and the temperature range employed. They recommended the use of the lower and upper limits of the experimental temperature range instead of the approach suggested by Lund (1975) where temperature T is assumed to be proportional to 1/T for small temperature ranges.

Although the two concepts appear to give similar results (Holdsworth and Richardson, 1989a,b), most workers maintain the Arrhenius model is best in relation to a wide temperature range. Jairus and Merson (1990) studied the thermal inactivation of *Bacillus stercorophilus* at temperatures between 115 to 145°C in a computer controlled reactor and compared the two kinetic models. They concluded that the TDT concept predicted accurate data than the Arrhenius model in terms of extrapolating data to UHT regions. According to Hallstrom *et al.* (1988) and Ramaswamy *et al.* (1989) the TDT concept has a widespread application and recommendation in terms of validating

product sterility.

Process Verification and Validation

The selection of a process indicator becomes questionable especially at aseptic processing conditions although process validation has to be proven microbiologically. While processes designed to tenderise meat products are adequately stable in terms of their microbial load (Brown, 1991), pasteurising products like pickles would require the destruction of enzymes rather than microorganisms in order to ensure a shelf-stable product. The activation energy associated with microorganism are high (50-100 kcal/mol), intermediate (15-30 kcal/mol) for quality factor (colour, flavour, texture and nutritional properties) degradation, and relatively low (2-15 kcal/mol) for enzyme catalysis, diffusion-controlled and oxidative reactions (Sadler, 1987). From a biochemical viewpoint, the differences in activation energies reflect the relative changes during processing with higher values responding readily to temperature increases. Although needed for product sterilization, the rapid destruction of microorganisms is done at the expense of heat resistant enzymes which survive HTST processes and regenerate during storage. For shelf stable products it may be necessary to use heat resistant enzymes for verification and validation purposes.

Microbiological Indicators

Several researchers have utilized the thermophilic bacterium, *Bacillus stercorophilus* to validate particulate sterility in various model foods under aseptic

conditions (Brown *et al.*, 1984; Sastry *et al.*, 1988; Hilton *et al.*, 1989; Ronner, 1990). Hilton *et al.* (1989) for instance immobilized *Bacillus stercorophilus* at the centre of beef particles and found no survivors after 52.2 sec heating at 131°C. Centrepoint lethality obtained was 25D, which far exceeds the traditional minimum value of 12 decimal reductions.

The alginate particle technique developed to mimic conditions in food particles, opened an important avenue for biological validation of particulate products under continuous aseptic conditions. With this method, microorganisms are mixed with the food product and immobilised with sodium alginate. The mixture allows the formulation of various shapes and sizes comparable to the real product. One advantage of this technique is the achievement of similar environment in relation to product pH, water activity and protection to microbes from food components such as proteins and fat (Joyce, 1993). Since complete destruction of immobilized microorganisms is possible in demonstrating process severity, the need arises for proper calibration of model foods. Sastry *et al.* (1988) mobilized spores of *Bacillus stercorophilus* within mushroom particles and tested it in relation to the following: (1) leakages during reconstitution, blanching and thermal processing (2) successful infusion of spores at the coldest spot and background information on concentration of the same strain present in the raw product (3) verification of the heating characteristics of the model particle in relation to real particles and (4) microbial concentration as influenced by processing conditions of time-temperature combinations. In addition to the above tests, model particles should demonstrate enough strength to withstand stresses without disintegrating. These tests are time consuming and

cumbersome to perform but vital for proper evaluation of particulate sterility.

Since the z-value curve of *Bacillus stercophilus* spores concaves downwards and decreases from 10C° at 116°C to 6 C° at 127°C, its use as an indicator would require some form of correction for temperatures above 116°C if results are to be presented in equivalent F_o-values (Pflug *et al.*, 1990). According to the authors, needed corrections could be calculated from time-temperature data using the General Method or equations developed by Pflug and Christensen (1980). Although Pflug *et al.* (1990) did not specify the strain of *Bacillus stercophilus* in their presentation, reported z-values appeared different from those obtained by Jairus and Merson (1990) who reported for strain TH24(NCDO 1096), z values of 9.3C° for temperatures between 115 and 145°C and 16.9C° for temperatures greater than 145°C respectively. These discrepancies require extensive experimental data on particular strains if their kinetic data are to be adopted for process evaluation. Pflug *et al.* (1990) strongly recommended the adoption of data on *Clostridium botulinum* for engineering design of low acid foods. For validation purposes therefore, strains having same kinetic data could be used.

Chemical and Enzymatic Markers

Although microbiological validation gives a direct proof of product sterility, its use under varying process conditions such as flow rate, temperature, holding tube length and different foods has limited value. Monitoring chemical changes in foods offer potential alternative for assessing integrated time-temperature exposition of particulates to lethal temperatures (Kim and Taub, 1993).

Traditionally, one would look out for known compounds with established methodology for evaluation of losses in processed foods. These methods should be simple to perform, reproducible, and sensitive to experimental conditions. Mulley *et al.* (1975a) used thiamine hydrochloride in canned model food products to predict sterilization efficiency. Adams (1978) studied peroxidase inactivation and regeneration in relation to HTST processing of vegetables, and Rao *et al.* (1981) used vitamin C in canned peas to measure product quality in terms of nutrient retention.

Weng *et al.* (1991a,b) found the z-value of immobilized peroxidase in an organic solvent (dodecane) to correspond favourably with that on *Clostridium botulinum*. However their study was limited to pasteurization temperatures. Berry *et al.* (1989a) recommended methylmethionine sulfonium (MMS) for indexing microbial lethality at high-temperature low-pH combination compared to low-temperature high-pH combination. Quite recently, Kim and Taub (1993) studied the formation of chemical indicators formed during processing of various food products. Products investigated included broccoli, chicken meat, ham, potato, green beans, pea and carrot. Two formed compounds, 2,3-dihydro-3,5-dihydroxy-6-methyl-(4H)-pyran-4-one and 5-hydroxymethylfurfural were identified as precursors of D-fructose. In a typical experiment, the formation of the markers were approximately 70% higher at the surface than the centre due to time-temperature lag between the two locations. The authors strongly recommended markers for HTST process verifications.

Heat treatments capable of destroying bacterial spores are often regarded as adequate to destroy enzymes, however studies have shown that some enzymes are

extremely resistant (Adam, 1978; Scott, 1985). Schwartz (1992) explained that the mechanism for enzyme inactivation may involve partial denaturation of proteins and the possibility also exists for re-folding and regeneration of native structure and activity. Therefore, enzymes deserve special attention during high temperature short time processing. To eliminate residual peroxidase activity, a 3D deduction is employed for peroxidase under practical situations (Saguy, 1988). Adam (1978), using HTST processing of vegetables found that peroxidase was inactivated during the process but regenerated.

Food processors in general, have accepted that if peroxidase is completely destroyed then all quality deteriorating enzymes are destroyed during the blanching of vegetables (Schwartz, 1992). Whereas peroxidase is accused of causing off-flavour and colour changes in some products, some studies (Lu and Whitaker, 1974) found no evidence attributable to peroxidase for quality changes. Although several markers have been characterised as suitable for bio-verification and validation purposes, the choice of a particular indicator should involve: (1) simple but effective instrumentation for evaluation (2) sensitive to changing environmental conditions and readily implemented for routine evaluation of input parametric values and (3) a clear cut demonstration of thermal stability at aseptic conditions to merit its adoption.

CHAPTER III

COMPARISON OF TWO METHODS FOR EVALUATING FLUID-TO-PARTICLE HEAT TRANSFER COEFFICIENTS

ABSTRACT

Fluid to particle heat transfer coefficients (h_{fp}) were evaluated based on two methods using transient time-temperature data obtained from regular objects. The first (rate method) was based on heating rate at any given location while the second (ratio method) was based on the ratio of temperature gradients at two locations. Regular shape objects made from four test materials (Teflon, Lucite, polypropylene and Nylon) were used in the study under different experimental conditions. Depending on the ambient condition, test particle type, size and shape, h_{fp} values ranged between 15 and 420 W/m²C. The two methods generally compared well especially in situations where the associated Biot numbers were low (< 10). However, larger variations were associated with the ratio method which in most cases also predicted higher h_{fp} than the rate method. An error analysis indicated that both methods were sensitive to variations in parametric values when the associated h_{fp} values were high ($Bi > 20$). Overall, the rate method gave more consistent and conservative h_{fp} values.

INTRODUCTION

Over the past few decades, research efforts have focussed on diversified thermal processing alternatives: thin profile, rotational as well as continuous aseptic processing,

and use of non-conventional heating techniques such as microwave and ohmic heating. The increased consumer demand for high quality, nutritious and safe products at affordable prices has resulted in a need to minimize the severity of heat treatments without compromising safety. Several researchers (Gillespy, 1953; Ball and Olson, 1957; Stumbo, 1973; Flambert and Deltour, 1972b; Hayakawa, 1974a,b) have utilized theoretical formulae for estimating heat transfer in foods and developed methods for evaluating thermal processes. In conventional canning, the assumption of negligible surface resistance holds valid only when pure steam is used to heat food in metal containers. To accurately model the temperature distribution during overpressure processing with water or steam/air mixture, it is important to consider a finite heat transfer coefficient (Ramaswamy *et al.*, 1983; Shin and Bhowmik, 1990; Tucker and Clark, 1990). Since the relevance of time-temperature distribution becomes readily apparent when process lethality has to be evaluated, a good estimate of heat transfer coefficient is an important pre-requisite to be satisfied.

For continuous processing of low acid particulate foods under aseptic conditions, several simulation models have been developed for predicting the temperature history of both liquid and solid phases (Sastry, 1986; Chandarana *et al.*, 1989; Chang and Toledo, 1989; Larkin, 1989; Larkin, 1990; Lee *et al.*, 1990ab; Stoforos and Merson, 1990). Most of these models are based on numerical solution to the transient heat conduction under finite surface convection. Larkin (1990), using numerical simulations for low-acid particulate foods, indicated that one of the most influential parameters affecting accumulated lethality is the fluid-to-particle surface heat transfer coefficient (h_{fp}) in the

holding tube. Earlier workers (Pflug *et al.*, 1965; Manson and Cullen, 1974) assumed an infinite heat transfer coefficient (h_p) and Gaffney *et al.* (1980) proposed techniques for reducing errors associated with such assumptions.

Experimental evaluation of thermal diffusivities also depend on accurate estimates of heat transfer coefficients (Gordon and Thorne, 1990). Pflug *et al.* (1965), Kopelman and Pflug (1968), Hayakawa and Bakal (1973), Lenz and Lund (1973), Bhowmik and Hayakawa (1979), Olivares *et al.* (1986), Rice *et al.* (1988), and Tong *et al.* (1993), used analytical formulae for estimating transient state heat transfer in infinite slab or cylinder to investigate heat transfer and thermophysical properties of foods. Larkin and Steffe (1983) indicated that thermal diffusivity determined from heat penetration data would be affected by errors associated with temperature measurements rather than thermocouple location while, Gordon and Thorne (1990) reported that thermocouple placement can lead up to 33% error in thermal diffusivity. Evidently, accurate prediction of the temperature history curves in conductive products depend on product geometry and thermophysical properties of both the heating medium and food as well as conditions occurring at the boundary of the food and the heating medium. Furthermore, thermophysical and surface conductance values are needed in predicting heat transfer processes and performance of processing equipments through computer modelling.

Heat transfer coefficients are commonly evaluated from time-temperature data obtained from test objects of known shape, size and thermal properties. Of the two methods commonly used, both based on analytical solution to transient heat conduction equation, the first one (rate method) is based on relating h_p to the rate of heating at a

given location in the product. The second method (ratio method) is based on relating h_{fp} to the temperature lag between two locations in the test object. Both methods require accurate thermophysical properties as input parameters.

The objective of this investigation was to compare the two analytical techniques for calculating h_{fp} under various heating/cooling situations and to establish the appropriate approach in relation to method sensitivity and accuracy in predicting h_{fp} . To broaden the scope of application and understanding of the mathematical simplification of the transient heat conduction equation, three sample shapes were studied.

THEORETICAL CONSIDERATIONS

The unsteady state heat conduction differential equation governing heat transfer to isotropic objects, suddenly transferred into a constant temperature medium is generally expressed as (Grigull and Sandner, 1984):

$$\frac{\partial U}{\partial t} = \alpha \left(\frac{\partial^2 U}{\partial r^2} + \frac{n}{r} \frac{\partial U}{\partial r} \right) \quad (3.1)$$

with $n = 0, 1,$ and 2 corresponding to slab, cylinder, and sphere respectively.

The analytical solution to Eq. (3.1) under convective boundary conditions as outlined in Carslaw and Jaeger (1959) and Luikov (1968) are as follows:

For an infinite slab:

$$U_p = \sum_{n=1}^{\infty} \frac{2 \sin \beta_n \cos(\beta_n X/L)}{(\beta_n + \sin \beta_n \cos \beta_n)} \exp(-\beta^2 Fo_p) \quad (3.2)$$

where β_n is the nth positive root of

$$\beta \tan \beta = Bi_p \quad (3.3)$$

For an infinite cylinder:

$$U_c = 2 Bi_c \sum_{n=1}^{\infty} \frac{J_o(\gamma_n r/a)}{(Bi_c^2 + \gamma_n^2) J_o(\gamma_n)} \exp(-\gamma_n^2 Fo_c) \quad (3.4)$$

where γ_n is the nth positive root of

$$\frac{\gamma J_1(\gamma)}{J_o(\gamma)} = Bi_c \quad (3.5)$$

and for a sphere:

$$U_s = 2 Bi_s \sum_{n=1}^{\infty} \frac{[\delta_n^2 + (Bi_s - 1)^2] \sin(\delta_n)}{\delta_n^2 (\delta_n^2 + Bi_s (Bi_s - 1))} \frac{\sin(\delta_n r/a)}{(r/a)} \exp(-\delta_n^2 Fo_s) \quad (3.6)$$

where δ_n is the nth positive root of

$$1 - \delta \cot(\delta) = Bi_s \quad (3.7)$$

The series solutions, Eq. (3.2), (3.4), and (3.6) converge rapidly to the first term beyond an Fo value of 0.2 (Heisler, 1947; Grigull and Sandner, 1984). Equations (3.2), (3.4), and

(3.6) can be generalized for the first root situation and written as:

$$U = A \exp(-BFo) \quad (3.8)$$

where A and B are shape dependent functions of Biot number based on the first root of characteristic functions (Eqs. 3.3, 3.5 or 3.7).

for an infinite slab:

$$A_p = \frac{2 \sin \beta_1 \cos(\beta_1 X/L)}{(\beta_1 + \sin \beta_1 \cos \beta_1)} \quad (3.9)$$

for an infinite cylinder:

$$A_c = \frac{2 Bi_c J_0(\gamma_1 r/a)}{(Bi_c^2 + \gamma_1^2) J_0(\gamma_1)} \quad (3.10)$$

and for a sphere:

$$A_s = \frac{2 Bi_s \sin(\delta_1) [\delta_1^2 + (Bi_s - 1)^2]}{\delta_1^2 [\delta_1^2 + Bi_s (Bi_s - 1)]} \frac{\sin(\delta_1 r/a)}{(r/a)} \quad (3.11)$$

and also $B_p = \beta_1^2$; $B_c = \gamma_1^2$; and $B_s = \delta_1^2$.

The Rate Method

The rate method requires time-temperature data gathered from any one location

within the object. By taking the logarithm on both sides and rearranging, Eq. (3.8) can be transformed to Eq. (3.12):

$$\log U = \log A - \left(\frac{B \alpha t}{2.303 a^2} \right) \quad (3.12)$$

Eq. (3.12) represents the straight line portion of a heating or cooling curve obtained by a plot of $\log(U)$ vs t . The slope index f_h (also called heating rate index) is related to B in the form of Eq. (3.13):

$$f_h = \frac{2.303 a^2}{\alpha B} \quad (3.13)$$

An examination of Eqs. (3.12) and (3.13) indicates that the slope (and hence f_h) is dependent on the Biot number function (B) and thermal diffusivity (α) but independent of the location. It is, therefore, apparent that the exact location within the sample need not be known. Knowing f_h (or f_c) [determined from experimental heating (or cooling) data respectively], B can be calculated and substituted into the transcendental Eq. (3.3), (3.5), or (3.7), to determine the Biot number and hence the heat transfer coefficient.

The Ratio Method

The ratio method involves gathering time-temperature data from two locations within the object, and simultaneously solving the heat conduction equations for the two locations. The following illustrates the procedure for an infinite cylinder using the first

term approximation of the infinite series. For any location r within the object, Eq. (3.4) becomes:

$$\frac{T_a - T_l}{T_a - T_i} = \frac{2Bi_c J_o(\gamma_1 r/a)}{(Bi_c^2 + \gamma_1^2) J_o(\gamma_1)} \exp(-\gamma_1^2 Fo_c) \quad (3.14)$$

At centre of the infinite cylinder, $r = 0$ and therefore,

$$\frac{T_a - T_c}{T_a - T_i} = \frac{2Bi_c}{(Bi_c^2 + \gamma_1^2) J_o(\gamma_1)} \exp(-\gamma_1^2 Fo_c) \quad (3.15)$$

Taking the ratio of Eq. (3.14) to (3.15), we get:

$$Z_c = \frac{T_a - T_l}{T_a - T_c} = J_o(\gamma_1 r/a) \quad (3.16)$$

The root (γ_1) can iteratively be obtained from Eq (3.16) after graphical determination of Z_c from the plot of $(T_a - T_l)/(T_a - T_c)$ vs time. γ_1 is back-substituted into Eq (3.5) to get Bi . Using a similar approach, expressions can be written for infinite slab and sphere as follows:

infinite slab:

$$Z_p = \frac{T_a - T_l}{T_a - T_c} = \cos(\beta_1 X/L) \quad (3.17)$$

sphere:

$$Z_s = \frac{T_a - T_l}{T_a - T_c} = \frac{\sin(\delta_1 r/a)}{(\delta_1 r/a)} \quad (3.18)$$

It is important to note that, in both methods, all thermal and physical properties of the solid and heating medium are assumed to be constant with respect to temperature.

MATERIALS AND METHODS

Sample Preparation

The validity of the transient heat conduction equation and verification of the two methods previously described require accurate preparation of sample in relation to shape, size and thermocouple location. All three regular shapes were used with different test materials: spheres of Nylon, polypropylene, polymethylmethacrylate (Lucite), and Teflon (Small Part Inc., Miami Lakes, FL) as well as end insulated plates and cylinders of Teflon. Two holes were drilled at pre-determined locations in each sample using a drilling machine. Teflon-insulated 30 AWG copper-constantan thermocouples, calibrated against an ASTM mercury-in-glass thermometer, were inserted into the holes and secured with epoxy glue. The thermocouple positioning procedure was first verified with the transparent Lucite samples before extending to other samples. A Teflon slab, 2 x 10 x 15.2 cm, was used to simulate an infinite plate configuration as detailed in Ramaswamy *et al.* (1983). For an infinite cylinder, an end insulated technique was employed (Bhowmik and Hayakawa, 1979). A 25.5 mm length was first cut from a 25.4 mm diameter Teflon rod.

A 12.7 mm thick hard rubber discs having the same diameter were screwed onto the ends of the Teflon piece. Two "O" rings were then glued onto the rubber disc at both ends followed by another layer of 6.35 mm thick rubber. With this method, the entrapped air and the two rubber ends permitted efficient end insulation to simulate an infinite cylinder configuration.

Experimental Conditions

The two methods were compared under the following experimental conditions: (1) Steam Heating: Test samples were heated in a steam cabinet at $100 \pm 0.5^\circ\text{C}$; (2) Aseptic Processing Unit: Test samples in two sample shapes (infinite cylinder, and sphere) were positioned as stationary particles in the holding tube (diameter = 7.62 cm) of an aseptic unit (Ramaswamy *et al.*, 1992) using food grade 1% w/w carboxymethylcellulose (Pre-hydrated CMC PH-2500, TIC Gum Inc, Belcamp, MD) as a carrier fluid at 100°C and a volumetric flow rate of 11.1 L/min. The preparation of CMC solution and its rheological parameters are detailed elsewhere (Awuah *et al.*, 1993); (3) Cold Room: Samples were cooled from ambient conditions (20°C) in a frozen storage room with fan circulated air at -18°C ; (4) Water Cooling: Steam-heated samples were cooled in a tank (43 x 60 x 90 cm) filled with water at 20°C , and (5) Air Cooling: Steam-heated samples were cooled in still air at approximately 20°C .

Verification of Sample Thermal Diffusivity

Although literature values were available for some test samples, it was found

necessary to gather thermophysical properties for some others. When the associated surface heat transfer coefficients are very large, the heating rate of a solid material would depend primarily on its thermal diffusivity, shape and size (Ball and Olson, 1957). Under such conditions, the B value in Eq. (3.13) is a constant: 3.14, 5.783, 9.80, respectively, for an infinite slab, infinite cylinder and a sphere. Thermal diffusivity of samples heated under such situations could be obtained from evaluated f_h values. Reported h_{fp} values for steam exceed 10,000 W/m²C (Ramaswamy *et al.*, 1983; Ozisik, 1985); therefore steam heating of test samples provide conditions for experimental verification of sample thermal diffusivity. Heat capacity of test samples were determined calorimetrically using a thermos flask and density was evaluated from mass and volume. Thermal conductivity values were calculated from thermal diffusivity, density and heat capacity.

Temperature Measurement and Data Analysis

The time-temperature history of test particles and medium were continuously recorded at 5 s intervals with a Metra-Byte Dash-8 (Metra-Byte Corp., Tauton, MA) data logger coupled to a personal computer. Since small errors in monitored temperatures can cause significant variation in temperature differences, all data points were normalized to the appropriate medium and initial sample temperatures using the method suggested by Stumbo (1973). The logarithm of the unaccomplished temperature difference ($T_s - T$) was plotted against time for the two locations in each sample. The heating or cooling rate index (f_h or f_c) was calculated from the linear regression of the straight-line portions of the curves. The calculated rate index was substituted into Eq. (3.13) to determine the root

B. The Biot number (Bi) was calculated from the transcendental Eq. (3.3), (3.5), or (3.7) for the two locations for comparison.

For the temperature ratio method, $(T_s - T_1)/(T_s - T_c)$ was plotted against time. After sufficient time has elapsed, the equilibrium value of temperature ratio Z was calculated as the average of data points within the range when $(T_s - T_1)/(T_s - T_c)$ remained constant. From the experimental Z values, the characteristic roots γ_1 , β_1 , δ_1 were determined using Eq. (3.16), (3.17), or (3.18) depending on sample shape and from these their respective Bi's were obtained. Knowing Bi, k and the significant dimension, h_{fp} was calculated from $h_{fp} = Bi k/a$.

Error Analysis

Several uncertainties, due to variations in thermophysical properties, temperature measurement techniques, product dimensions and system operational conditions have been reported to be associated with the heating rate index (Ramaswamy and Tung, 1986) and hence the evaluated h_{fp} . According to the authors, a 5% error in estimated f_h is conservative. Three other potential error contributing parameters associated with the rate method (Eq. 3.13) were thermal diffusivity, sample size, and f_h . From Eq. (3.16), (3.17), and (3.18) it is evident that three error contributing parameters affect the ratio method: sample size, thermocouple location (r or X) and the ratio Z . Errors contributed by thermal conductivity values will influence the results from both methods by the same margin since h_{fp} values were obtained from Bi as $h_{fp} = Bi k/a$.

To test the sensitivity of both methods, individual parameters were tested at $\pm 5\%$

error levels for all the three shapes using property values of Teflon. Selected values for the convective heat transfer coefficient $h_{fp(ref)}$ were chosen to represent various experimental conditions. Using all other property values at a base level the base f_h for the rate method and the base Z for the ratio method were calculated. Then each property value was varied between the error limits, one at a time, and the resulting $h_{fp(cal)}$ was obtained by back-calculation. The percentage deviation of calculated heat transfer coefficient $h_{fp(cal)}$ from the reference $h_{fp(ref)}$ was computed as the predicted error due to a $\pm 5\%$ deviation from the base level:

$$Predicted\ error = \left(\frac{h_{fp(cal)} - h_{fp(ref)}}{h_{fp(ref)}} \right) \times 100 \quad (3.19)$$

Hence, a positive value in predicted error represents an overestimation of the convective heat transfer coefficient while a negative value represents the opposite.

RESULTS AND DISCUSSION

Thermal Diffusivity

Experimentally determined thermal diffusivity for Teflon and Lucite compared well with data presented by Burfoot and Self (1988) and Mwangi *et al.*(1993) while they differed for Nylon and polypropylene from the values reported in Ramaswamy and Tung (1986) and Frank (1968), respectively. The discrepancies were considered to be due to differences in the type of materials tested. Property values employed for the studies are summarized in Table 3.1.

Table 3.1. Thermophysical properties of test particles.

Parameter	Tefion ^a	Nylon	Polyp ¹	Lucite ^f
Density (kg/m ³)	2195	1128 ^b	829 ^b	1340
Thermal conductivity (W/mC)	0.29	0.37 ^c	0.33 ^c	0.31
Specific heat (kJ/kgC)	0.98	2.143 ^d	1.842 ^d	1.660
Thermal Diffusivity (x10 ⁻⁷ m ² /s)	1.35	1.518 ^c	2.145 ^c	1.39

¹Polypropylene

^aBurfoot and Self (1988).

^bDetermined from the ratio of sample mass to volume.

^cDetermined from $k = \alpha \rho C_p$.

^dDetermined calorimetrically with a thermos flask.

^eDetermined experimentally with a steam cabinet.

^fMwangi *et al.* (1993).

The Rate Method

Typical semi-logarithmic temperature-time curves for the end insulated Teflon cylinder (simulated infinite geometry) and spherical Lucite particles are shown in Figure 3.1 for various heating/cooling conditions. Figure 3.1A for example, shows the temperature history curves for the cylinder heated in the aseptic unit. Curve 1 represents the temperature response at the geometric centre while curve 2 describes the temperature response at a location 3.39 mm radial distance below the sample surface. Theoretically shown to be valid (Ramaswamy and Tung, 1986), the nearly parallel nature of linear portions of the curves demonstrates that f_h is independent of thermocouple location within the sample whereas the intercept varies with location. The consistency of experimental f_h values obtained from two different locations within the same sample is demonstrated in Table 3.2. For a given replicate, a maximum deviation of 4.6% was found whereas the cumulative deviation between replicates was below 2.0% (Table 3.2). These values fall within the conservative range (5%) of variability for experimental f_h values reported by Ramaswamy and Tung (1986). The overall coefficient of variation for h_{fp} values calculated by the rate method under the condition described in Table 3.2 was 5.5%. The coefficient of variation for calculated h_{fp} ranged from 2.7 to 8.6% taking into account different samples under different experimental conditions (Table 3.3). Irrespective of the sample type used, the rate method gave consistent results for calculated h_{fp} values under the same experimental condition. This is evident especially from data obtained from air cooling, water cooling and cold storage room. These results emphasize the fact that the convective heat transfer coefficient is a "system" property and depend on the conditions

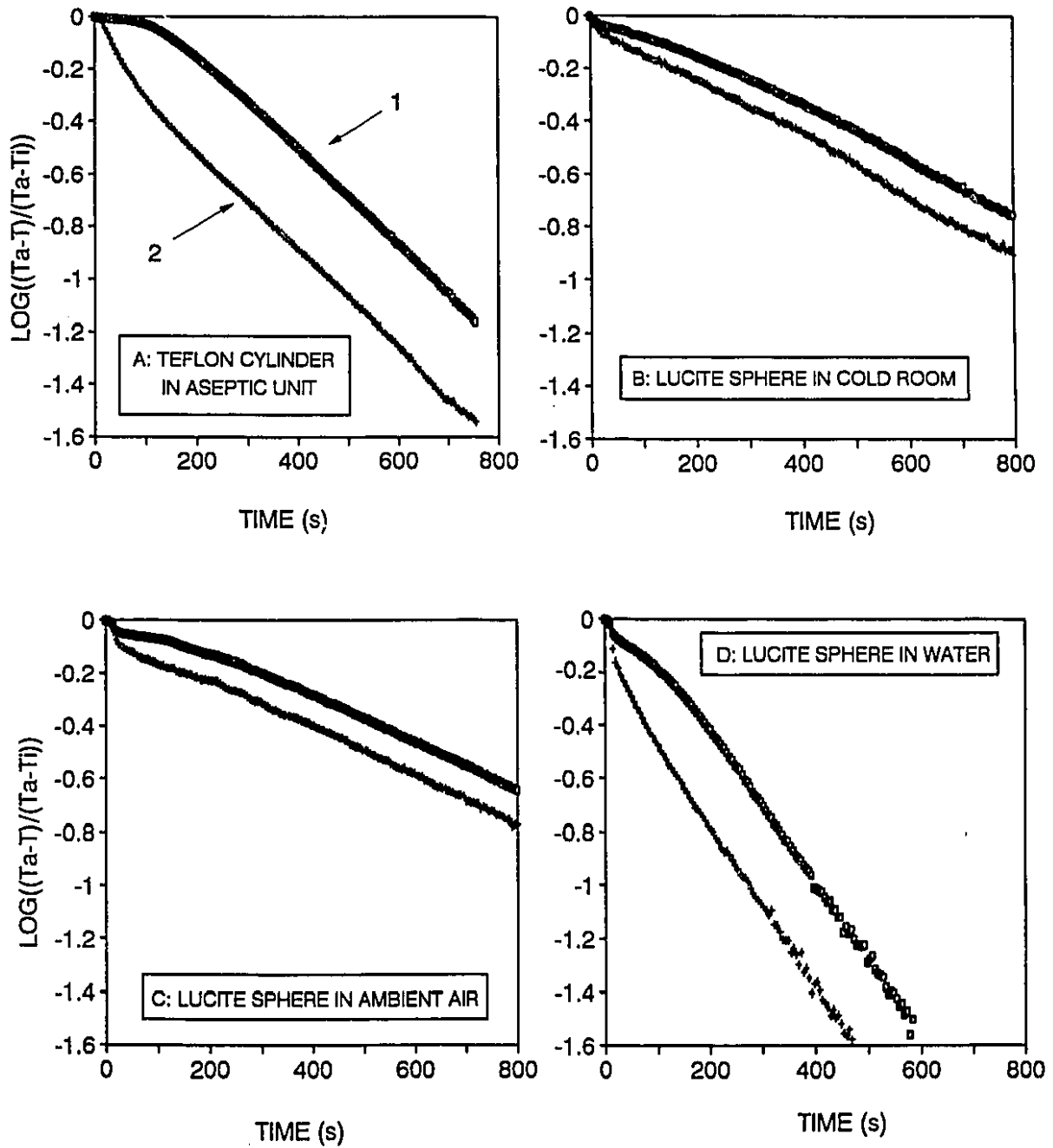


Figure 3.1. Typical semi-logarithmic plots of heat penetration curves under different heating/cooling conditions.

TABLE 3.2. Experimental data obtained by heating infinite Teflon cylinders in 1.0% w/w CMC solution (temperature = 100°C; flow rate = 11.1 L/min) in the holding tube of the aseptic unit.

Run No.	f_h' (min)	f_h'' (min)	h'_{fp} (w/m ² c)	h''_{fp} (w/m ² c)	Z	γ_1^a	γ_1^b	h_{fp}		
								Rate ^c Method (w/m ² c)	Ratio Method (w/m ² c)	
1	9.33	9.17	278	311	0.410	2.227	2.290	294	466	
2	9.04	9.16	347	314	0.411	2.245	2.288	331	456	
3	9.46	9.05	255	343	0.419	2.226	2.271	299	396	
4	9.07	9.12	338	325	0.419	2.246	2.271	331	396	
5	9.08	9.17	333	312	0.417	2.242	2.274	322	407	
6	9.10	9.09	328	332	0.423	2.245	2.260	330	366	
7	8.91	9.19	389	307	0.411	2.251	2.289	348	459	
								Mean	322	421
								CV	5.5	8.6

f_h' and f_h'' are the heating rate indices at the centre and 3.39 mm below the surface of the sample.

h'_{fp} and h''_{fp} are the corresponding heat transfer coefficients based on f_h' and f_h'' .

γ_1^a is the average root obtained with f_h' and f_h'' .

γ_1^b is the root obtained with the ratio method.

^cMean of h'_{fp} and h''_{fp} .

Table 3.3 Comparison of heat transfer coefficients determined with the two methods under different experimental conditions.

Material	D ^a (mm)	Experimental Condition	Number of Experiments	h' _{fp} (W/m ² C)	h'' _{fp} (W/m ² C)	CV' %	CV'' %
Teflon ^c	25.40	aseptic unit	7	322	421	5.5	8.6
Polyp ^s	25.40	"	5	276	247	3.2	7.5
			Mean ^k	303	358	9.0	24.7
Teflon ^c	25.40	air cooled	4	15	18	4.6	6.5
Teflon ^{sl}	"	"	6	14	15	7.6	5.8
Teflon ^s	19.05	"	4	19	27	5.8	7.7
Polyp ^s	25.4	"	3	19	20	4.7	4.8
Lucite ^s	"	"	4	22	26	8.6	11.0
			Mean	18	20	17.9	24.2
Nylon ^s	19.05	cold room	4	45	51	6.8	16.0
Polyp ^s	25.40	"	4	41	22	6.7	6.6
Lucite ^s	"	"	3	55	41	3.5	27.4
			Mean	47	39	14	37.3
Teflon ^{sl}	25.40	water tank	4	198	207	2.7	2.7
Teflon ^s	19.05	"	5	210	296	4.5	3.2
Lucite ^s	25.40	"	4	212	162	6.7	5.3
			Mean	206	216	5.9	25.1

^aDiameter of sample; ^cInfinite cylinder; ^sSphere; ^{sl}Slab; h'_{fp} & CV' are heat transfer coefficient and coefficient of variation determined with the f_h or f_c method respectively; h''_{fp} & CV'' are heat transfer coefficient and coefficient of variation determined with the temperature ratio method respectively; ^kMean heat transfer coefficient and the corresponding coefficient of variation, Polyp represents polypropylene.

occurring at the boundary of a given transducer. Based on the overall variability, it was considered that reliable estimates of h_{rp} could be obtained using the rate method.

The Ratio Method

Examples of temperature ratio curves for end insulated Teflon cylinder (simulated infinite geometry) are shown in Figure 3.2 for the same heating/cooling conditions shown in Figure 3.1. Although mathematical computations are simplified (especially with infinite cylinders which involve Bessel functions), the advantage of installing thermocouples within the sample rather than at the surface is demonstrated by the smooth temperature profile depicted by the temperature ratio curves Figure 3.2. Early attempts at gathering data with installed surface thermocouples showed considerable scatter in the temperature data making it difficult to get good estimates of the Z ratio. As the temperature difference between the heating/cooling medium and the sample diminished, the computed ratio showed considerable scatter and tend to deviate from the equilibrium value. The deviations become more evident when the medium temperature fluctuated widely. This was observed from graphs plotted with data from the cold storage room where the temperature distribution in the room varied somewhat due to intermittent nature of the circulating fans (Figure 3.2B), and air cooling (Figure 3.2C) where minor air movement/temperature changes are readily responded to by thermocouple located closer to the surface. Similar observations have been noted by Bhowmik and Hayakawa (1979) with semi-solid products. The first term approximation of the infinite series solution on which both methods are based was valid for heating time beyond $Fo > 0.2$. This translates

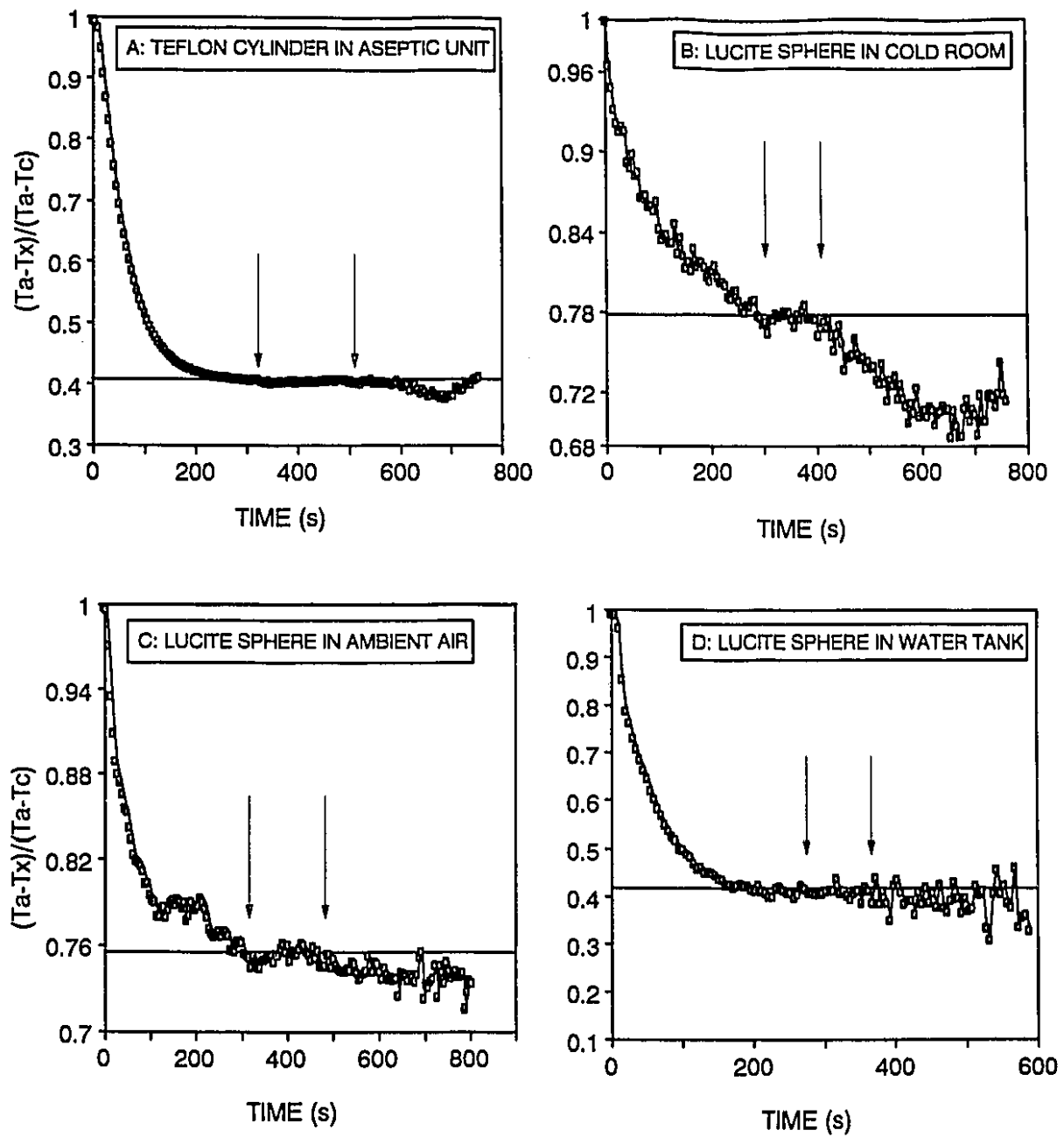


Figure 3.2. Typical temperature ratio (Z) vs time curves for different heating/cooling conditions.

to a heating time of about 200-250 s depending on the material. The plots of temperature ratio vs time curve (Figure 3.2) appeared to stabilize after about 200 s and generally remained constant up to about 500 s. Averaging the temperature ratio values were generally done between 260 and 500 s depending on the shape and type of sample.

If all input parametric data (determined experimentally or chosen from the literature) are correct, then the two methods should theoretically predict the same h_{fp} value. However, several discrepancies were observed especially with the ratio method which in most cases predicted somewhat more inconsistent results. To predict equal heat transfer coefficients, the root B calculated with both methods should be the same. In order to match these roots, a correction factor for the relative location of the two thermocouples had to be introduced. This correction factor was essentially the correct value of r/a or X/L (depending on the shape of the object) to be used in either Eq. (3.16), (3.17) or (3.18) which would give the same value for the root B by the ratio method as with the rate method. Steam heating condition was used for this purpose since data from steam heating conditions were primarily used for thermal diffusivity calibration purposes. Once a correction was found with real experimental data, the same value was used for other testing conditions. Corrected location factors were 0.730, 0.720, 0.872, 0.726, 0.720, and 0.777 for infinite Teflon cylinder, Teflon slab, polypropylene, Teflon, Nylon and Lucite spheres respectively which were slightly different from the intended values.

The coefficient of variation associated with h_{fp} under the same heating condition (Table 3.2) with the ratio method was 8.6% compared with 5.5% for the rate method. With different test samples the resulting CV ranged from 2.7 to 27.5% (Table 3.3).

Inconsistencies associated with the ratio method become apparent from variations in data observed especially with reference to different test materials cooled under the same condition, for example cold storage room (Table 3.3). The calculated values using Nylon and Lucite were different from those calculated using polypropylene spheres of comparable size. Based on the overall variability, the ratio method was considered less consistent than the rate method. Evaluating h_p values from the two methods are compared in Figure 3.3, which showed a somewhat linear relationship with an R^2 value of 0.91. The ratio method predicted higher values on the average compared to the rate method.

Comparison of Evaluated h_p with Literature Values

Although the primary focus of this research was to compare the two analytical techniques for calculating heat transfer coefficients, an attempt was made to compare the results (irrespective of method used for analysis) with those reported in the literature. Heat transfer coefficients (Ozisik, 1985) vary with the type of fluid flow and passage area, its physical properties and temperature, the geometry and position of the conducting body, and the mechanism of heat transfer (e.g., forced or natural convection). Typical heat transfer coefficients for free convection of air over a 0.25 m vertical plate, a 0.02 m diameter cylinder, and a 0.02 m diameter sphere were reported to be 5, 8, and 9 W/m^2C respectively and for forced convection (at 25°C) of air flowing at 10 and 5 m/s over a flat plate and cylinder, the values were 39 and 85 W/m^2C , respectively (Ozisik, 1985). The data for air cooled samples fall within the range specified above, but slightly higher than reported data for free convection. Stoforos and Merson (1990) reported experimental as

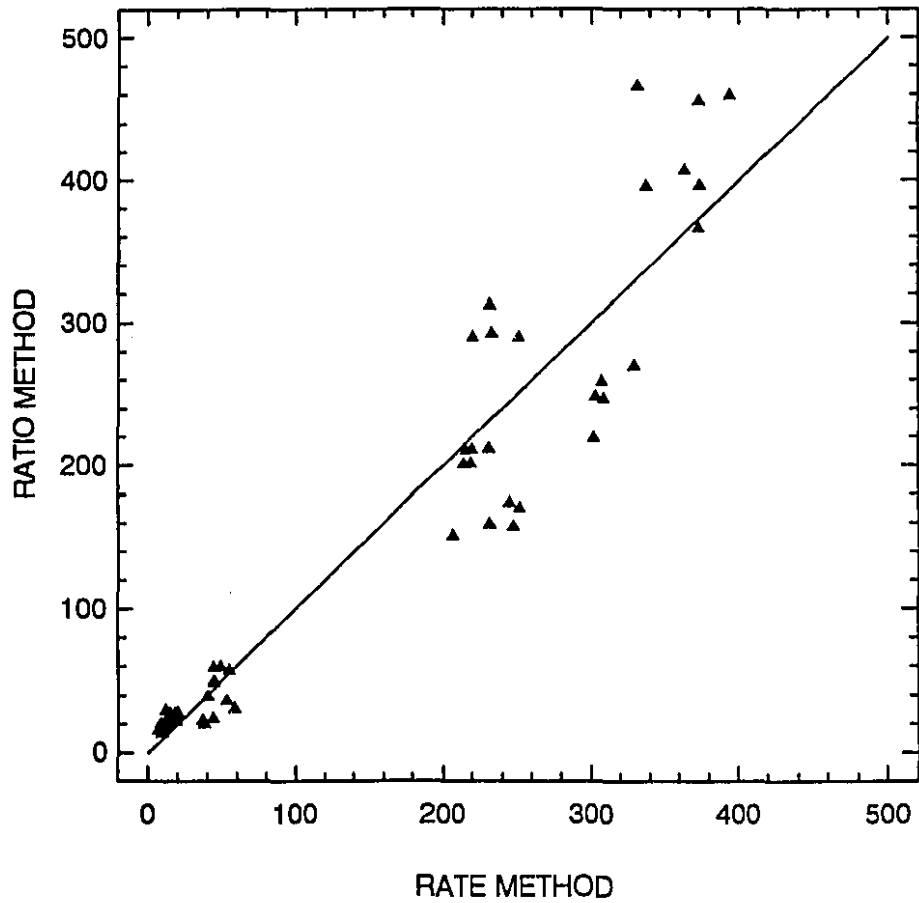


Figure 3.3 Graphical relationship between the rate and ratio methods.

well as predicted h_{fp} values for heating Teflon spheres in deionized water to range from 75 to 700 W/m²C. Using Teflon cubes with sizes ranging from 15 to 30 mm, Burfoot and Self (1988) found h_{fp} between 830 to 1550 W/m²C for heating in a water bath (64 to 94°C). Smith *et al.* (1967) reported a value of 568 W/m²C for anomalous shapes in a circulating ice water bath. In general, our data falls in the range reported by Stoforos and Merson (1990) but deviates widely from those obtained by Smith *et al.* (1967) and Burfoot and Self (1988). Higher values obtained by the other authors suggest the significance and contribution from turbulent motion resulting from bath agitation/circulation employed in their studies.

Error Analysis

Table 3.4 shows error associated with calculated heat transfer coefficients as affected by $\pm 5\%$ error in parametric values under various processing conditions. Since the heating rate index is inversely proportional to the thermal diffusivity (Eq. 3.13), they present similar levels and trends in errors should one be kept constant and the other varied. Only analysis related to error in f_h is included in the table. It was recognized that the effect of sample radius or half thickness (r or L) and thermal conductivity were the same for both methods. A 5% variability in thermal conductivity would result in an identical 5% variability in h_{fp} by both methods (hence not listed in Table 3.4). Errors due to wrong estimates of sample size escalates in situations where the associated h_{fp} were higher (> 250 W/m²C; $Bi > 20$). For example, a 5% error on the positive side results in underestimation of h_{fp} by 25 - 35% while a 5% error on the negative side (assumed

Table 3.4. Percentage error associated with calculated heat transfer coefficient (h_{fp}) values as influenced by $\pm 5\%$ error in characteristic parametric values under various processing conditions using Teflon as a reference material.

Condition	Shape ^a	h_{fp} ^b	Parameter				
			Rate method		Ratio method		Both methods
			f_i	f_c	Ratio	Location	Radius ^c
Aseptic Unit	Cy	250	+40 to -22	+37 to -22	+134 to -36	-34 to +109	
"	Sp	"	+26 to -17	+25 to -18	+70 to -29	-26 to +56	
"	Sl	"	+31 to -19	+39 to -24	+87 to -32	-30 to +71	
Water-cooled	Cy	190	+29 to -18	+30 to -20	+80 to -31	-28 to +65	
"	Sp	"	+19 to -14	+22 to -16	+47 to -24	-22 to +37	
"	Sl	"	+23 to -16	+33 to -22	+59 to -28	-25 to +47	
Air-cooled	Cy	20	+6 to -7	+31 to -28	+13 to -12	-8 to +7	
"	Sp	"	+5 to -6	+37 to -34	+12 to -11	-7 to +6	
"	Sl	"	+6 to -7	+44 to -38	+13 to -12	-8 to +7	
Cold storage	Cy	50	+9 to -8	+20 to -18	+20 to -15	-11 to +13	
	Sp	"	+7 to -7	+13 to -15	+16 to -13	-9 to +9	
	Sl	"	+9 to -8	+28 to -23	+19 to -15	-11 to +12	

^aCy, Sp, and Sl represents cylinder, sphere and slab, respectively.

^bCharacteristic heat transfer coefficients for given conditions.

^cRadius of sphere or cylinder or half thickness of a slab.

shorter dimension as compared to actual) will cause 50 - 100% over-estimation of h_{fp} . It should be noted that this error will tend towards infinity as the associated Bi number increases. With the exception of sample size (r or L) and thermal conductivity, a 5% underestimation of parametric values overestimate predicted h_{fp} (Table 3.4). These errors are prominent and higher with Z and the relative location associated with the ratio method as compared to f_h for the rate method. In addition, predicted h_{fp} resulting from a 5% error in f_h were consistently lower and conservative for h_{fp} from 20 to 50 W/m²C (Bi between 0.9 and 2.2). An important limitation to the use of the ratio method is that if for example the surface thermocouple is placed 5% closer to the centre, an error as high as 134% in calculated h_{fp} (Table 3.4) may result. In this regard, the rate method would obviously be more advantageous since f_h is independent of thermocouple placement and only one thermocouple is required to monitor temperature changes. Aside from practical limitations to installing thermocouples within smaller-sized samples, the ratio method can have a major effect on calculated lethality if temperature response/distribution is to be predicted with estimated values. Process lethality overestimated with the ratio method can raise safety concerns. In general both f_h and Z values (determined experimentally) become very sensitive to minor errors in parametric values when higher Biot numbers (Bi) in excess of 22 has to be predicted. Under such situations, high conductive material such as aluminium should be used (Ramaswamy *et al.*, 1983) although such transducers may not reflect the heating behaviour as well as surface characteristics exhibited by real foods. Apparently, both methods will provide good estimates in situations where h_{fp} values are expected to be low. Recognizing the relative sensitivity of the temperature ratio method,

chances of having errors in predicted heat transfer coefficients are higher.

CONCLUSIONS

Two analytical routines for evaluating heat transfer coefficient has been studied using inert materials with properties similar to that of food under different processing conditions. Mathematical analysis shows that the two methods should predict the same heat transfer coefficient. The two methods generally compared well given a coefficient of determination (R^2) of 0.91. Although the two methods compared very well especially in situations where low heat transfer coefficient or $Bi < 10$ had to be predicted, several anomalies were observed with the ratio method. Average heat transfer coefficients ranged between 15 to 420 W/m^2C depending on method used, the type of sample, shape, and experimental conditions. In general the ratio method overestimated h_{fp} values. Error analysis indicated the ratio method to be very sensitive to the relative distance between located thermocouples and Z even at low Bi numbers, whereas the rate method maintained consistent and relatively lower errors resulting from $\pm 5\%$ deviation in f_h at low Biot numbers. Modelling temperature profiles with data obtained from the temperature ratio method may result in overestimation of process lethality thus raising safety concerns. It was observed that both methods are sensitive to minor errors in parametric values when higher heat transfer coefficients has to be estimated. In such situations, the use of a highly conductive material would be beneficial. Since the f_h method gave consistent data as well as conservative values for calculated heat transfer coefficients, it is highly favoured compared to the temperature ratio method.

CHAPTER IV

FLUID-TO-PARTICLE HEAT TRANSFER COEFFICIENTS ASSOCIATED WITH HEATING FOOD PARTICLES IN CMC SOLUTIONS UNDER LOW FLOW AND MILD HEATING CONDITIONS

ABSTRACT

The fluid-to-particle heat transfer coefficients (h_{fp}) associated with heating cylindrical specimens of potato and carrot were evaluated in carboxymethylcellulose (CMC) solutions (0 - 1.0% w/w) at 50 - 80°C. Average h_{fp} values ranged from 80 to 450 W/m²C for potatoes and 100 to 550 W/m²C for carrot. Temperature, fluid velocity (0.2 to 0.7 x 10⁻³ m/s) and concentration of CMC influenced its power law parameters and hence, h_{fp} values while sample size (0.016 - 0.023 m diameter, 0.02 - 0.04 m length) and flow direction (upward and downward) had marginal effects. Natural convection dominated the flow regime, giving good correlations between Nusselt and Rayleigh numbers.

INTRODUCTION

Data on thermal properties and boundary values are required in the design of thermal processing equipment and process schedule, especially for predicting the time-temperature response of a food undergoing heat processing. Successful temperature prediction for particulate foods in viscous fluids requires data on the convective heat

transfer coefficient (h_{fp}) at the fluid-particle interface. In most conventional canning applications employing steam, the surface heat transfer coefficient is assumed to be infinite (Ball and Olson, 1957), although lower values have been recognized for steam/air heating media (Pflug and Borrero, 1967; Ramaswamy *et al.*, 1983; Tung *et al.*, 1984). For continuous sterilization of food particulates, de Ruyter and Brunet (1973), and Manson and Cullen (1974) assumed the heat transfer coefficient to be infinite. But, the existence of finite convective heat transfer coefficient at the fluid-particle interface has been demonstrated by several researchers (Sastry, 1986; Deniston *et al.*, 1987; Chandarana and Gavin, 1989a,b; Chang and Telodo, 1989; Chandarana *et al.*, 1990b).

The majority of carrier fluids used in the food industry are viscous and non-Newtonian. Higher viscosities associated with such fluids prevent turbulence under practical situations and laminar regimes generally prevail. The heat transfer mechanism associated with non-Newtonian fluids is more complicated as a result of the combination of natural and forced convection (Alhamdan and Sastry, 1990). Irrespective of the mechanism, heat transfer rate from these fluids have been recognized to be lower than from water.

Zuritz *et al.* (1990) obtained h_{fp} values between 548 and 1175 W/m²C for a mushroom-shaped aluminium particle immersed in carboxymethylcellulose (CMC) with mean apparent viscosity between 2.08 to 17.70 Pas. They reported that h_{fp} values increased with particle size and fluid flow rate and decreased with apparent viscosity at a temperature of 71°C. Under similar conditions, Alhamdan and Sastry (1990) found h_{fp} values of 75 - 310 W/m²C for natural convection at 20 - 80°C, while for water the h_{fp}

values were 652 - 850 W/m²C. The authors also observed that h_{fp} values increased with the initial temperature difference and decreased with the apparent fluid viscosity. Chandarana *et al.* (1989) found h_{fp} values between 8.1 and 35.9 W/m²C for a 25.4 mm silicone rubber cube held stationary at 135°C in starch, decreasing with consistency coefficient between 3.0×10^{-3} and 3.17 Pasⁿ. In water, the h_{fp} value was 51.1 W/m²C. For water and starch (2 - 3%) at 129.4 °C, Chandarana *et al.* (1990b) found h_{fp} of 65.7 - 107.1 W/m²C and 55.6 - 86.5 W/m²C, respectively. By recording the surface temperature of spherical potatoes in rotating cans containing water, Deniston *et al.* (1987) reported average value of h_{fp} to be 160 ± 30 W/m²C. Chang and Toledo (1989) found h_{fp} values for potatoes cubes in water to be 239 and 303 W/m²C at 0 and 0.86 cm/s while in stationary 35% sucrose solution it was 146 W/m²C. Chang and Toledo (1990) found the average h_{fp} at ~135°C to range from 600 - 1533 W/m²C and 359 - 735 W/m²C at 0 and 1.58 cm/s fluid velocity in a packed bed of carrot cubes (1 and 2 cm) assuming a carrot thermal diffusivity value of 1.94×10^{-7} m²/s. Lamberg and Hallstrom (1986) simulated temperature profiles and heat transfer coefficients during blanching of carrots, and found good correlation between the theoretical and experimental data when the heat transfer coefficient was 750W/m²C.

The objectives of this study were to: (1) determine the magnitude of the fluid-to-particle heat transfer coefficient for heating finite cylindrical samples of carrots and potatoes in CMC solutions, (2) study the effect of CMC concentration on h_{fp} , and (3) study the effect of fluid flow rate, direction of fluid flow, and particle size (diameter and length) on h_{fp} . Cylindrical test samples and related equations were employed in these

studies in order to broaden the scope and validity of heat transfer concepts since the majority of previous studies employed spherical or cube-shaped particles.

THEORETICAL CONSIDERATIONS

A finite cylinder is formed at the intersection of an infinite slab and an infinite cylinder (Charm, 1978; Heldman and Singh, 1981). Therefore, the solution with respect to finite cylindrical objects under surface convection will involve heat transfer equations governing an infinite slab and an infinite cylinder. The solution for the temperature history of an infinite cylinder and infinite plate with uniform initial temperature when plunged into a constant temperature environment are detailed in Carslaw and Jaeger (1959) and Luikov (1968) and presented in Chapter III. After sufficient time has elapsed ($Fo > 0.2$), the terms in the infinite series converge rapidly (to the first term) due to the presence of the exponential term (Heisler, 1947). Therefore, in most cases, the series solutions can be approximated by the first term and represented as follows for an infinite cylinder:

$$U_c = A_c \exp(-B_c Fo) \quad (4.1)$$

and an infinite slab:

$$U_p = A_p \exp(-B_p Fo) \quad (4.2)$$

where A_c , A_p , B_c , and B_p are characteristic functions of the Biot number defined in Chapter III. Solutions for the characteristic functions generally involve graphical methods

or computer work. Simplified forms of the characteristic functions have been published (Ramaswamy *et al.*, 1982), valid for $Fo > 0.2$, and $0.02 < Bi < 200$. For a finite cylinder, Eq. 4.1 and 4.2 are combined to give

$$U_{fc} = U_p U_c = A_p A_c \exp[-(B_p Fo_p + B_c Fo_c)] \quad (4.3)$$

Or

$$U_{fc} = U_p U_c = A_p A_c \exp\left[-\left(\frac{B_p}{L^2} + \frac{B_c}{a^2}\right) \alpha t\right] \quad (4.4)$$

Ball and Olson (1957), introduced an equation for calculating the thermal process time as follows:

$$t = f_h \left[\log j + \log \left(\frac{T_a - T_i}{T_a - T} \right) \right] \quad (4.5)$$

This represents an equation of the straight line portion of the curve on a semi-logarithmic plot of temperature ratio versus time. Eq. 4.5 can be rearranged for a finite cylinder as:

$$\frac{T_a - T}{T_a - T_i} = U_{fc} = j \exp\left(-\frac{2.303 t}{f_h}\right) \quad (4.6)$$

Comparing Eq. 4.4 and 4.6, it is evident that $j = A_c A_p$ and that the exponential terms can be equated and written as:

$$f_h = \frac{2.303}{\left(\frac{B_p}{L^2} + \frac{B_c}{a^2}\right) \alpha} \quad (4.7)$$

It is important to note that a finite cylinder has two finite dimensions, and will therefore have one set of Bi and Fo related to an infinite slab and another set related to an infinite cylinder. Eq. 4.7 therefore needs to be solved iteratively for h_p .

MATERIALS AND METHODS

Raw Material and CMC Solution Preparation

Carrots and potatoes were purchased from a local market and stored in a refrigerator at 5°C. Cylindrical specimens were punched out using a cork borer of known diameter, and the required length was cut using a knife. Two concentrations (0.5 and 1.0% w/w) of commercial CMC (Sigma; St. Louis, Mo) were used. CMC solutions were prepared by adding a known amount of CMC powder to water and thoroughly mixing to break undispersed lumps. The solution was left for 24 h to ensure total dispersion of the powder. Final hand-mixing was done to obtain a homogeneous solution. The solution was heated to the desired temperature in a steam kettle and transferred to a constant temperature water bath.

Rheological Properties

Rheological properties of CMC were determined before and after each

experimental run with a Haake rotational viscometer Model Rotovisco RV3 (Haake Mess-Technik GmbH, Co., Karlsruhe, Germany). In order to maintain the same rheological properties it was found necessary to add some fresh CMC solution to the bath at the end of each run. Needed rheological data were obtained from previous studies (Abdelrahim *et al.*, 1991) in the form of coefficients for the power law model (Table 4.1):

$$\sigma = m (\dot{\gamma})^n \quad (4.8)$$

Thermal properties

The thermal conductivity and specific heat of CMC solutions were estimated at bath temperatures using the following equations (Heldman and Singh, 1981):

$$k_f = [326.575 + 1.0412 T - 0.00337 T^2][0.796 + 0.009346(\% W)] \times 10^{-3} \quad (4.9)$$

$$C_{pf} = 1.675 + 0.025(\% W) \quad (4.10)$$

The specific heat of carrots (moisture content, 84%; negligible fat content) was determined by the relationship in British units (Charm, 1978):

$$C_{ps} = 0.5X_F + 0.3X_S + 1.0X_m \quad (4.11)$$

The thermal conductivity was back calculated from reported thermal diffusivity (Kostaropoulos *et al.*, 1975) and measured density ($\rho = m/V$): $k = \alpha\rho C_{ps}$. Other property

Table 4.1. Power law parameters^a for CMC rheology at various temperatures and concentrations.

Concentration (%)	Temperature (°C)	Consistency coefficient (Pas ⁿ)	Flow behaviour index
0.5	80	0.02	1.00
1.0	50	2.88	0.52
	60	2.23	0.55
	70	1.84	0.57
	80	1.03	0.70

^aAbdelrahim *et al.* (1991).

values obtained from literature have been summarized in Table 4.2.

Experimental Setup and Procedure

The experimental arrangement (Figure 4.1) consisted of a water bath equipped with a heater and a pump, a Dash-8 data acquisition system (MetraByte Corporation, Tauton, MA), a test chamber (8.6 cm diameter and 20 cm long), and a personal computer. The bath and test chamber were insulated to reduce heat losses, and the bath was filled to about three quarters full with test fluid. The average linear velocity of the fluid was obtained from the measured volumetric through flow rate and the cross-sectional area of the chamber. Test fluid was introduced from either the bottom (upward flow) or from the top (downward flow). A perforated plate was used to distribute the medium, which was returned to the water bath and recirculated. Two needle type copper-constantan thermocouples (Ecklund-Harrison Technologies Inc., Cape Coral, FL) calibrated against an ASTM mercury-in-glass thermometer were used to gather time-temperature data. One was attached to the particle with its tip at the geometric center, while the other was suspended in the fluid. A known distance was marked on the thermocouple to coincide with the geometric center of the test cylinder in the central direction, and the thermocouple was carefully inserted up to the mark. A combination of a special industrial adhesive (Loctite Canada Inc., Mississauga, ON) and epoxy resin was used to hold the test sample to the probe and prevent possible flow of fluid along the thermocouple probe. Temperatures were continuously recorded in a spreadsheet format at 5 s intervals.

Table 4.2. Physical properties of test materials.

Material	Temp (°C)	Density heat (kg/m ³)	Specific conductivity (kJ/kg°C)	Thermal diffusivity (W/m ² C)	Thermal (x 10 ⁻⁷ m ² /s)
Carrot	-	1035	3.738 ^a	0.657 ^b	1.70 ^c
Potato ^d	-	1070	3.270	0.556	1.59
Water ^e	82	970	4.195	0.673	1.65
1% CMC	80	1003 ^f	4.15 ^g	0.668 ^h	
0.5% CMC	80	1003 ^f	4.16 ^g	0.670 ^h	

^a From Charm (1978)

^b Calculated from $k = \alpha\rho C_{ps}$

^c Kostaropoulos *et al.* (1975)

^d Yamada (1970)

^e Holman (1976)

^f Determined with pycnometer at 20°C

^{g,h} From Heldman and Singh (1981)

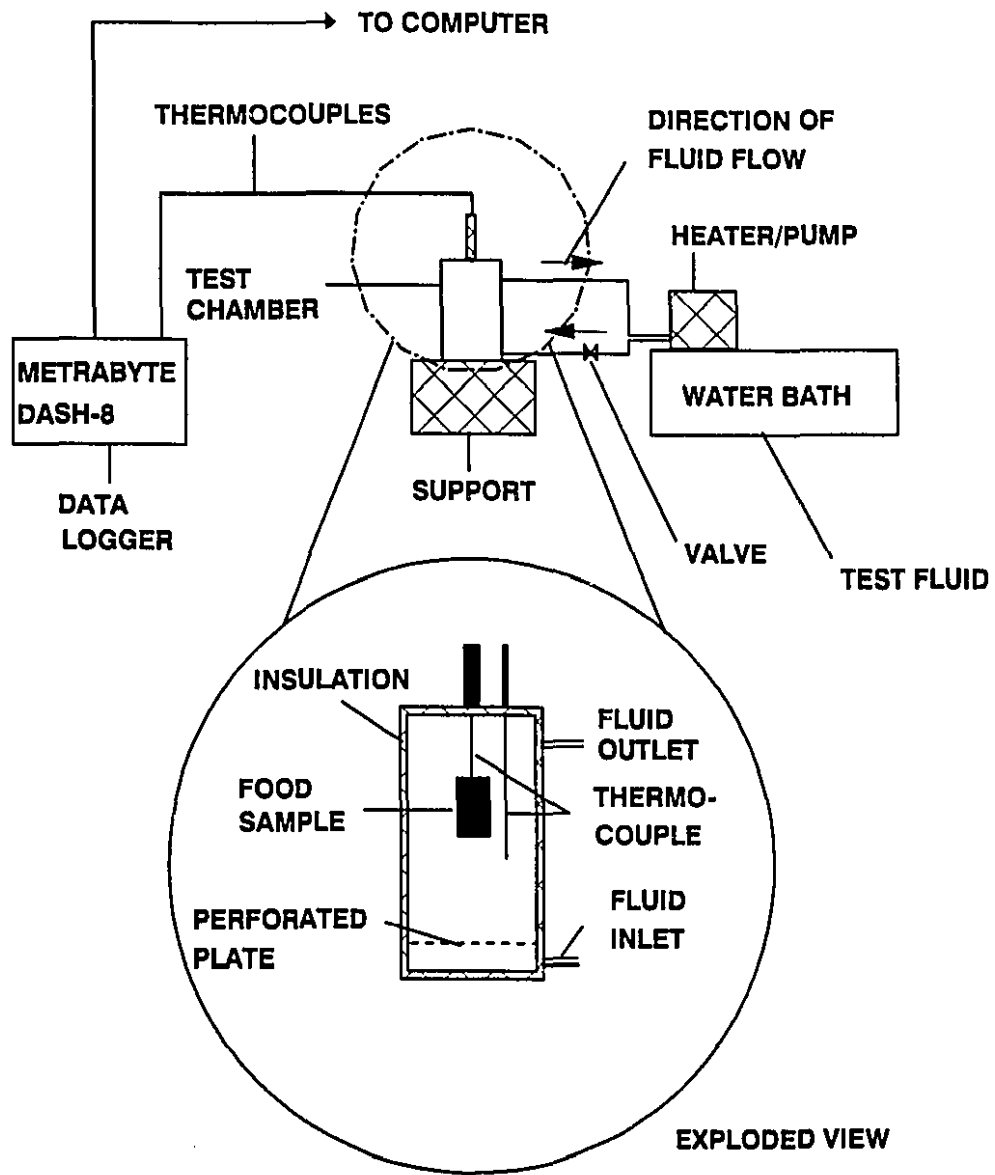


Figure 4.1 A schematic diagram of the test apparatus and setup.

Experimental Factors

Experiments were carried out to test the effect of various parameters on the convective heat transfer coefficient. The influence of CMC concentration was tested at three levels (0, 0.5, and 1.0% w/w) using 0.023m diameter, 0.04 m long cylinders of potatoes and carrots. Effects of sample size (diameters 0.016, 0.019, and 0.023 m with length kept at 0.04 m; sample lengths of 0.02, 0.03, 0.04 m with diameter at 0.023 m) was studied with potatoes and carrots in 1.0 % CMC solution at 80 °C and a flow rate of 4.2 mL/s. Effect of flow rate (2.3 and 4.2 mL/s) was evaluated at 80°C, while the effect of temperature (50 - 80°C) was evaluated at 0, and 2.3 mL/s using 0.04 m length and 0.023 m diameter samples. The combined effects of flow rate and temperature were also studied at selected levels (1.4 mL/s at 50°C, 2.6 mL/s at 60°C, 3.3 mL/s at 70°C, and 4.2 mL/s at 80°C). All the factors mentioned above were evaluated with the CMC solution flowing upward. The effect of the direction of fluid flow on h_{fp} was evaluated at 50 and 70°C with flow rates of 1.4 and 2.3 mL/s, respectively for carrots in 1.0 % CMC solution. A minimum of five runs was performed for each experimental variation.

Data Analysis

The logarithm of the temperature ratio ($T_s - T$)/($T_s - T_i$) was plotted against linear time as shown in Figure 4.2, and the heating rate index f_h was evaluated by linear regression of the straight-line portion of the curve. An iterative computer programme (Appendix 1) based on Eq. 4.7 was developed for the purpose of computing the convective heat transfer coefficient (h_{fp}). An estimate of h_{fp} was first made using the

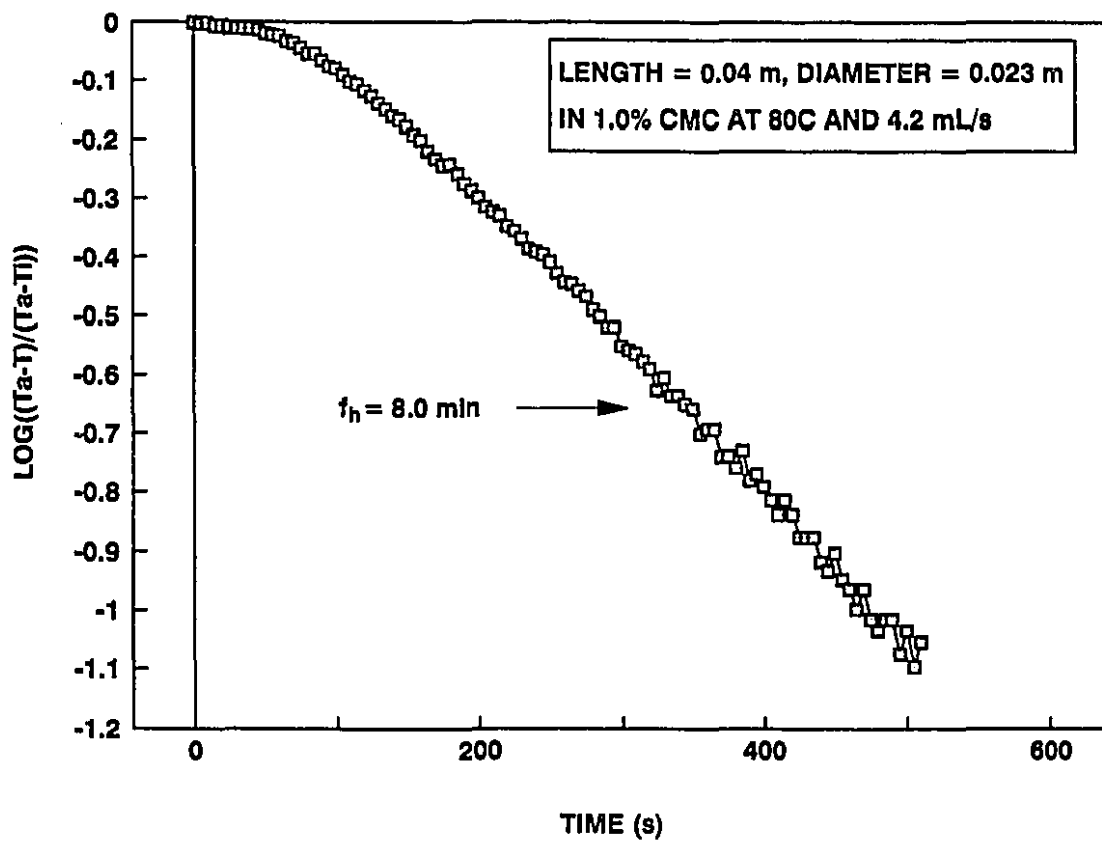


Figure 4.2 A typical semi-logarithmic plot of the heat penetration curve for carrot.

lumped capacity method [$h_{fp} = 2.303d_{cd} k_s / (\alpha f_h)$] assuming the Biot number to be less than 0.1 (Kreith, 1973). Individual Biot numbers (Bi_c and Bi_p) and characteristic functions (B_c and B_p) for the two finite dimensions were computed from the h_{fp} value. The heating rate index was calculated using Eq. 4.7 and compared with the experimental f_h . The h_{fp} value was changed in a stepwise fashion until the difference between the experimental and calculated values of f_h was equal to or less than 0.01% of the experimental value. This method is based on back-calculating the h_{fp} value from f_h , which is independent of the thermocouple location and hence is not sensitive to errors in the placement of the thermocouple.

Dimensionless parameters were evaluated for further data analysis. The forced convection heat transfer coefficient for immersed bodies was predicted by the relationship (Heldman and Singh, 1981):

$$Nu = h_{fp} \frac{d_{cd}}{k_f} = A_1 (Re)^b (Pr)^{1/3} \quad (4.12)$$

For natural convection, the general relationship used was :

$$Nu = h_{fp} \frac{d_{cd}}{k_f} = A_2 (PrGr)^c \quad (4.13)$$

where A_1 , A_2 , b and c are system constants with Re , Pr , and Gr representing Reynold, Prandtl, and Grashof numbers respectively. For non-Newtonian fluids, Re , Pr , and Gr are replaced by their generalized forms GRe , GPr , and GGr (Skelland, 1967; Zuritz *et al.*,

1990):

$$GRe = \frac{d_{cd}^n V^{2-n} \rho}{[8^{n-1} m [(3n+1)/4n]^n]} \quad (4.14)$$

$$GPr = \frac{C_{pf} m [(3n+1)/n]^n 2^{n-3}}{k_f (d_{cd}/V)^{n-1}} \quad (4.15)$$

$$GGr = \frac{g \beta \rho^2 (T_a - T_i) d_{cd}^3}{[m ((3n+1)/n)^n 2^{n-1} / (4 V^{1-n} d_{cd}^{n-1})]^2} \quad (4.16)$$

Dimensionless parameters were calculated using the length of the cylinder as the characteristic length. This is justified by an analogy between the particle's configuration in the test chamber and fluid flow in vertical pipes. In order to evaluate the effects of sample length and diameter on h_{fp} , however, the volume to area ratios were adopted.

RESULTS AND DISCUSSION

Tables 4.3 - 4.8 summarize average h_{fp} values for potato and carrot cylinders. Correlations between dimensionless numbers (Nusselt, Grashof and Prandtl) are plotted in Figure 4.3 for potatoes and carrots, respectively. Depending on the experimental variation, the average h_{fp} ranged between 76 to 456 W/m²C and 96 to 556 W/m²C for

Table 4.3 Heat transfer coefficients for potato and carrot cylinders immersed in CMC solutions (0-1%).

Food	Concentration (%)	h_{fp} (W/m ² C)	Coefficient of variation (%)
Potato	0	456 ^a	7.7
	0.5	199 ^b	11.1
	1.0	143 ^c	4.2
Carrot	0	556 ^d	4.7
	0.5	233 ^e	11.2
	1.0	172 ^f	2.9

^{a,b,c,d,e,f} Mean h_{fp} values sharing the same superscript are not significantly different ($p > 0.05$)
 Particle length 40 mm, diameter 23 mm; medium at 80°C and a linear velocity of 0.7×10^{-3} m/s.

Table 4.4 Heat transfer coefficients for potato and carrot cylinders in 1.0% CMC as influenced by particle diameter.

Food	Diameter (mm)	Volume/area ($\times 10^{-3}$ m)	h_{fp} (W/m ² C)	Coefficient of variation (%)
Potato	23	4.5	143 ^a	4.2
	19	3.8	143 ^a	5.6
	16	3.3	175 ^b	6.9
Carrot	23	4.5	172 ^b	2.9
	19	3.8	173 ^b	8.9
	16	3.3	182 ^b	2.7

^{a,b} Mean h_{fp} values sharing the same superscript are not significantly different ($p > 0.05$)
Particle length 40 mm; CMC at 80°C and a linear velocity of 0.7×10^{-3} m/s

Table 4.5. Heat transfer coefficients for potato and carrot cylinders in 1.0% CMC as influenced by length.

Food	Length (mm)	Volume/area (x 10 ⁻³ m)	h _{fp} (W/m ² C)	Coefficient of variation (%)
Potato	40	4.5	143 ^a	4.2
	30	4.2	156 ^a	8.3
	20	3.7	157 ^a	5.7
Carrot	40	4.5	172 ^b	2.9
	30	4.2	188 ^b	6.9
	20	3.7	195 ^b	14.4

^{a,b} Mean h_{fp} values sharing the same superscript are not significantly different (p > 0.05)
Particle diameter 23 mm; CMC at 80°C and a linear velocity of 0.4 x 10⁻³ m/s.

Table 4.6. Heat transfer coefficients in 1.0% CMC as influenced by temperature under stationary conditions.

Food	Temperature (°C)	h_{fp} (W/m ² C)	Coefficient of variation (%)
Potato	80	120 ^a	2.5
	70	118 ^a	5.1
	60	93 ^b	4.3
	50	76 ^c	5.3
Carrot	80	145 ^d	2.8
	70	133 ^c	2.3
	60	115 ^a	4.4
	50	96 ^b	8.3

^{a,b,c,d,e} Mean h_{fp} values sharing the same superscript are not significantly different ($p > 0.05$).

Particle length 40 mm, diameter 23 mm.

Table 4.7 Heat transfer coefficients for carrot cylinders as influenced by direction of fluid flow

Direction	Flow rate (mL/s)	Temperature (°C)	h_{fp} (W/m ² C)	Coefficient of variation (%)
Downward	2.3	70	151 ^a	5.3
Upward	2.3	70	147 ^a	6.1
Downward	1.4	50	103 ^a	8.7
Upward	1.4	50	97 ^a	6.2

^{a,b} Mean h_{fp} values sharing the same superscript are not significantly different ($p > 0.05$). Particle diameter 23 mm, length 40 mm in 1.0% CMC solution.

Table 4.8 Average heat transfer coefficients at various linear velocities and temperatures, and corresponding dimensionless parameters.

Food	Velocity $\times 10^{-3}$ (m/s)	Temperature (°C)	h_{fp} (W/m ² C)	GRe $\times 10^{-3}$	GPr	GGr $\times 10^4$	Nu
Potato	0.7	80	143 ^a	14.7	12.3	10.96	8.56
	0.4	80	128 ^b	6.80	1.50	6.79	7.67
	0.4	70	122 ^b	2.70	3.79	0.66	7.30
	0.4	60	109 ^c	2.10	4.93	0.31	6.53
	0.4	50	85 ^d	1.49	7.02	0.10	5.10
Carrot	0.7	80	172 ^e	14.7	1.23	11.1	10.3
	0.4	80	155 ^f	6.80	1.50	7.79	9.30
	0.4	70	146 ^f	2.70	3.79	0.57	8.74
	0.4	60	131 ^b	2.10	4.93	0.37	7.84
	0.4	50	103 ^c	1.49	7.02	0.11	6.17

^{a,b,c,d,e,f} Mean values for carrots and potatoes sharing the same letter are not significantly different ($p > 0.01$).

Particle length 40 mm, diameter 23 mm, fluid 1.0% CMC.

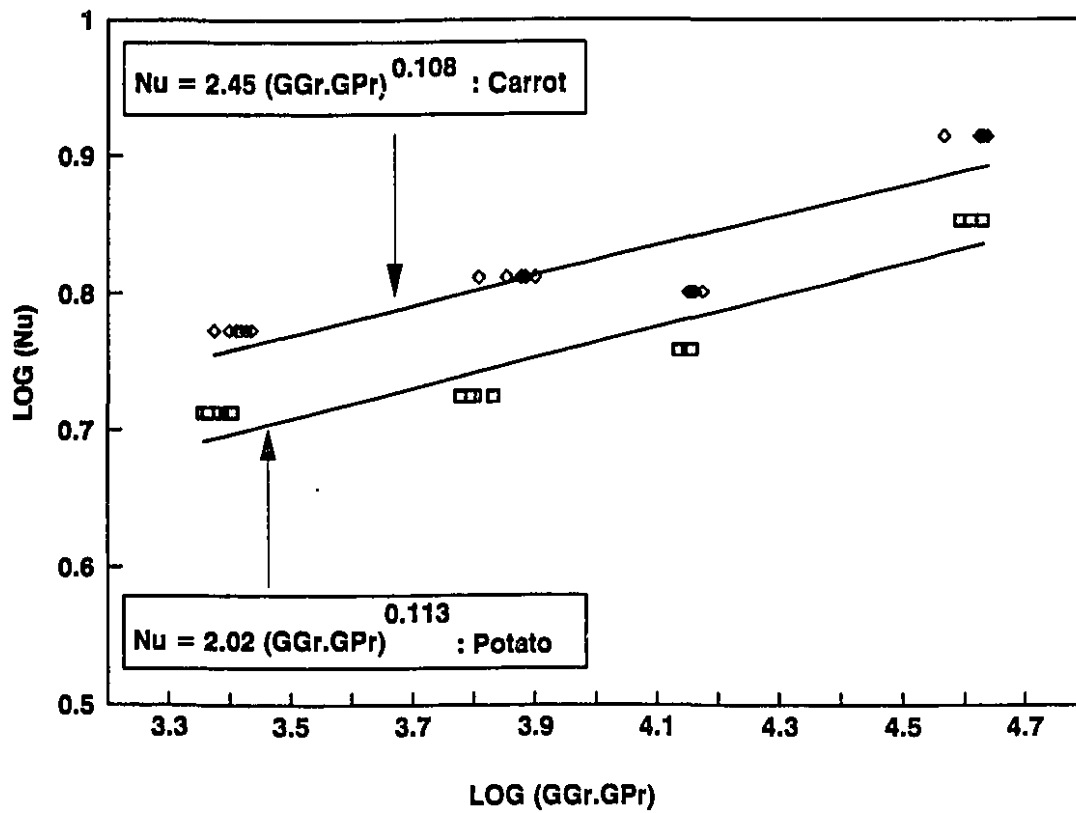


Figure 4.3. Nusselt number as a function of Rayleigh number (GGr.GPr) for carrot and potato cylinders heated in CMC solutions.

potatoes and carrots, respectively. In general, carrots had higher associated h_{fp} values than potatoes under similar experimental conditions, possibly due to structural and textural differences. Results obtained compared well with published values (Deniston *et al.*, 1987; Chang and Toledo, 1989; Alhamdan and Sastry, 1990; Zuritz *et al.*, 1990). Chandarana *et al.* (1989) obtained h_{fp} values lower than found in this study, while Lamberg and Hallstrom (1986) found higher values. Results for carrot and potatoes in water (0% CMC) also compared favourably with the minimum h_{fp} values reported by Alhamdan *et al.* (1990). The differences in results as compared to those published can be attributed to differences in experimental conditions and methodology adopted for h_{fp} evaluation.

The concentration of CMC had a significant ($p < 0.01$) effect on h_{fp} , with h_{fp} values decreasing with increasing CMC concentration (Table 4.3), possibly due to the increased apparent viscosity at higher concentrations (Table 4.1). An increase in CMC concentration from 0 to 1.0% decreased h_{fp} values by about 70%, which is in agreement with the findings of Alhamdan and Sastry (1990). Tables 4.4 and 4.5 illustrate a small increase in h_{fp} values with a decrease in the associated volume to surface area ratio of the test samples. This suggests possible effects of sample size (length and diameter) on the convective heat transfer coefficient. However, except with 16 mm-diameter, 40 mm-length potatoes (Table 4.4), the observed changes were not statistically significant ($p > 0.05$). Notwithstanding the above observation, it was suspected that the influence of sample dimensions on h_{fp} might have been masked by the relatively high apparent viscosity of the fluid. Zuritz *et al.* (1990) reported the contrary: an increase in h_{fp} with particle size. They reasoned that as the particle size increased, the available cross section for fluid flow

decreased. This resulted in an apparent increase in fluid velocity and enhanced localized turbulence, both contributing to higher h_{fp} . In this study, however, the chamber diameter was 86 mm, corresponding to approximately four times the maximum sample diameter. Furthermore, the flow rates used were very low, minimizing the chances for localized forced convection.

Table 4.6 shows the effect of temperature on h_{fp} under stationary fluid conditions. With the exception of potato with h_{fp} values in the range 118 and 120 W/m²C at 70 and 80°C, there was a significant ($p < 0.01$) decrease of h_{fp} values with temperature. The test fluid flowing in the downward direction had generally higher h_{fp} values than in the upward direction (Table 4.7); however, the difference between downward and upward flow on h_{fp} was not significant ($p > 0.05$). Table 4.8 shows the effects of temperature and flow rate on the convective heat transfer coefficient. There was a significant decrease in h_{fp} for both carrots and potatoes when the flow rate was lowered from 0.7×10^{-3} m/s. Temperature had a similar decreasing effect on h_{fp} values, except for potatoes between 80 and 70°C.

Mixed convection (forced-on-free convection) usually occurs when there is a small amount of forced fluid along with significant temperature difference between the convecting body and surrounding fluid. As the Reynolds number increases, mixed convection gives way to a pure forced convection regime (ASHRAE, 1981; Johnson *et al.*, 1988). To analyze the effects on convective heat transfer coefficients of fluid velocity and temperature of viscous fluids, the generalized dimensionless parameters defined by Eqs. 4.14, 4.15, and 4.16 were evaluated. Furthermore, in order to establish which regime

reigned with regard to natural, forced or mixed convection, Nusselt numbers based on equations 4.12 and 4.13 were evaluated. Data used for the latter were those obtained from simultaneous variation of temperature and flow rate.

The results obtained did not follow the trend indicated by the generalized relationship relating Nusselt (Nu) to Reynolds (GRe) and Prandtl (GPr) numbers under forced convection (Eq. 4.12), probably due to the prevailing low flow rates (Table 4.8). This indicated the possibility of existence of natural convection (Eq. 4.13) as opposed to forced convection. According to ASHRAE (1981) data, the laminar region of natural convection is characterized by Rayleigh number ($GPr.GGr$) in the range 10^4 - 10^8 while turbulent flow will have a range 10^8 - 10^{12} . The product $GPr.GGr$ ranged between 10^3 and 10^4 , indicating the possibility of laminar flow natural convection. Dimensionless correlations were developed to relate Nu to Rayleigh number ($GPr.GGr$). The logarithm of Nu was plotted against the logarithm of GGr and GPr combinations as shown in Figures 4.3 for potatoes and carrots, respectively. Regression analysis yielded the following equations for carrot and potato respectively as follows:

$$Nu = 2.45(GGr.GPr)^{0.108} \quad (4.17)$$

$$Nu = 2.02(GGr.GPr)^{0.113} \quad (4.18)$$

with coefficient of determination (R^2) of 0.80, and 0.88 for carrot and potato respectively. Eq 4.17 and 4.18 are valid for $3 \times 10^3 < GGr.GPr < 6 \times 10^4$. The regression output gave

standard errors for Nu as 0.025 and 0.019 for carrot and potato, respectively. Figure 4.3 shows good correlations between the experimental and predicted values, and demonstrates increasing Rayleigh (GGr.GPr) number with Nu. This clearly depicts the contribution of temperature to heat transfer at low flow rates.

CONCLUSIONS

Heat transfer coefficients associated with food samples heated in low velocity viscous fluid flow ranged from 80 to 450 W/m²C for potato cylinders and 100 to 550 W/m²C for carrot cylinders. Fluid concentration, flow rate (0.2 to 0.7 x 10⁻³ m/s) and temperature had large impact on the convective heat transfer coefficient, with higher fluid concentrations and lower temperatures decreasing the h_p . Sample size (0.016-0.023) m diameter, 0.02-0.04 m length) and flow direction (upward and downward) had only small effects on h_p . Good correlations were obtained between Nusselt and Rayleigh numbers, indicating strong natural convection.

The study indicates the dominance of natural convection while heating food particles in viscous fluids. From a safety viewpoint, it might be conservative to assume natural convection as the mechanism of heat transfer associated with the processing of real foods at low relative flow rates. However, the sensitivity and response of fluid viscosity to higher temperatures may shift the above trends from natural to mixed or forced convective heat transfer. Further exploration at elevated temperatures is in order.

CHAPTER V

DESIGN, CONSTRUCTION AND EVALUATION OF A PILOT SCALE ASEPTIC PROCESSING HOLDING TUBE SIMULATOR FOR HEAT TRANSFER STUDIES

ABSTRACT

A pilot scale aseptic processing holding tube simulator was designed and fabricated for evaluating fluid-to-particle convective heat transfer coefficients at temperatures up to 110°C. A constant operating temperature could be obtained with minimal heat losses to the environment. The simulator was calibrated to give the desired fluid flow rate as a function of fluid concentration, temperature, pump speed and pipe diameter. Statistical analysis indicated that all the above factors and their interactions were significant ($p < 0.005$) in influencing the fluid flow. Based on a stepwise multiple regression, empirical relationships were obtained relating the required pump rpm as a function of fluid concentration, temperature, flow rate and pipe diameter, or the desired fluid flow rate as a function of fluid concentration, temperature, pump rpm and pipe diameter. Good correlations were obtained between observed and predicted values ($R^2 \geq 0.90$). Medium temperature could be established either in time dependent (M1) or time independent (M2) fashions for studying the temperature histories of both liquid and suspended particle. The simulator made possible, rapid gathering of time-temperature responses of both suspended particles and carrier fluid as a function of both product and system parameters.

INTRODUCTION

The complex interaction between fluid and particles in continuous processing systems makes gathering of particle temperatures extremely difficult because current technology appear inadequate for such situations. In addition, traditional liquid based systems used for aseptic processing do not provide adequate control over particle residence times (RT), resulting in significant overprocessing of the product (Heldman, 1992). Uncertainties associated with RT prompted active research into batch-sterilizing particulates followed by mixing with the sauce to achieve the required recipe. This approach, however, leads to significant equipment complexity and costs (Heldman, 1992). An example is the APV Jupiter system presented by Horsom and Shore (1981). A major drawback with batch systems is possible recontamination during the transfer of product from one unit to the other. Heldman (1992) pointed out that an ideal design will be one which allows the liquid phase to flow freely while particles are controlled or somewhat restricted.

Predicting temperature/lethality distribution of suspended particles in a dynamic system with either analytical or numerical models become difficult due to lack of required data at real processing conditions. Presently, the fluid-to-particle interface heat transfer coefficient (h_{fp}) remain one of the unknown parameters for predicting temperature histories of suspended particles. This parameter has to be evaluated for the entire aseptic unit but most importantly, for the holding tube where the required lethality has to be achieved as per FDA standards (Chandarana and Gavin, 1989a,b; Dignan *et al.*, 1989). Within the holding tube, the product is held at a minimum temperature often dictated by temperature

controllers at the exit of both the heat exchanger and the holding tube, and for times dictated by (1) the length of the holding tube and (2) the flow and heating characteristic of the product. Commercial sterility (Dignan *et al.*, 1989) is however determined on the basis of the temperature at the exit of the holding tube. Sastry (1986) demonstrated that because of heat transfer from the liquid medium to suspended particles, there will be a drop in temperature of the medium. The magnitude of temperature drop depends on the particle to fluid ratio, their heat capacities and heat losses to the surrounding atmosphere. At present, the cooling section is considered less important from lethality point of view due to regulatory limitations which prohibit addition of lethality contributed during cooling to the overall process establishment (Dignan *et al.*, 1989; Heldman, 1992). From a product quality standpoint however, cooling should be accomplished as rapidly as possible. This constraint, aside from microbiological sterility, would require a knowledge of product characteristics such as particle size and their distribution, heat transfer coefficient as well as residence time distribution (RTD) during cooling.

Most model simulation systems reported in the literature focus primarily on the holding tubes for heat transfer studies (Sastry *et al.*, 1989; Alhamdan *et al.*, 1990; Alhamdan and Sastry, 1990; Sastry *et al.*, 1990; Zuritz *et al.*, 1990) but limited to lower temperatures. Evaluating fluid-to-particle heat transfer coefficients at elevated temperatures will in addition to presenting real situations, reflect fluid and particle sensitivity to such temperatures; a factor not accommodated by several researchers. Designing an appropriate heat transfer unit to study changes in both system and product parameters on the heat transfer coefficient at elevated temperatures was considered the primary objective of this

study. Specifically, the objectives were (1) to design and fabricate a robust, yet, a cost effective pilot-scale system capable of simulating aseptic processing conditions for heat transfer studies and (2) to evaluate the performance of the simulator in relation to gathering heat penetration data for routine estimation of fluid-to-particle convective heat transfer coefficients.

DESIGN AND CONSTRUCTION OF THE PILOT SCALE SIMULATOR

Design Features

One important requirement for solving the transient heat transfer equation analytically is an instantaneous exposure of a heat conducting material to a constant cold or hot temperature environment. The simulator was constructed to meet this primary constraint with the following salient features: (1) a heat exchanger and a reservoir, (2) steam inlet controls for temperature regulation, (3) a positive displacement pump, (4) a holding tube equipped with a by-pass mechanism for carrier fluid temperature stabilization, (5) a mechanism for rapid cooling of heated samples, (6) a readily accessible compartment for mounting model/food particles, (7) a device for holding the particle along the geometric centre of the holding tube in either parallel or perpendicular direction with respect to fluid flow, (8) a flow meter for measuring fluid flow rates and (9) a safety valve to release excess pressure from the system. Copper pipes and brass plates were chosen for construction of most parts on the basis of strength, workability and cost.

Construction of the Simulator

Figure 5.1 shows a schematic diagram of the simulator which consisted mainly of either a 5.08 or 7.62 cm nominal diameter copper piping equipped with a by-pass and mounted on a metal framework (not shown in diagram). The piping network was insulated to reduce heat losses to the surrounding, and inclined upward at an angle of 1.194° as per FDA requirement. A standard steam jacketed kettle was used to heat the fluid which was recirculated back into the kettle using a variable-speed sine pump (Model SPS 20, Systron Proquip, Pointe Claire, PQ) through the system. A special lid having two openings was secured onto the steam kettle with G-clamps. One of the openings facilitated the filling of the system with cold fluid, while the other served as a return port for the fluid to be reheated. Aside from heating the cold fluid to a pre-determined temperature, the steam kettle served as an on-line reservoir for the 90 L capacity unit. The steam kettle was shielded from other components of the simulator with plexiglass for safety reasons.

A minimum length of 24 times the tube diameter was provided before and after the test compartment to minimize fluid distortions. A flow meter (Model FTB-5005, Omega Engineering Inc, Stamford, CT) located on the return path measured the volumetric through flow rate. Five Teflon-insulated 30 AWG copper-constantan thermocouples were installed at several locations on the piping network with brass thermocouple receptacles (Type C-5.2, Ecklund-Harrison Technologies Inc, Cape Coral, FL). The temperature of the fluid leaving the steam kettle and that 0.61 m to the test compartment were visually observed with thermocouples connected to two T-type

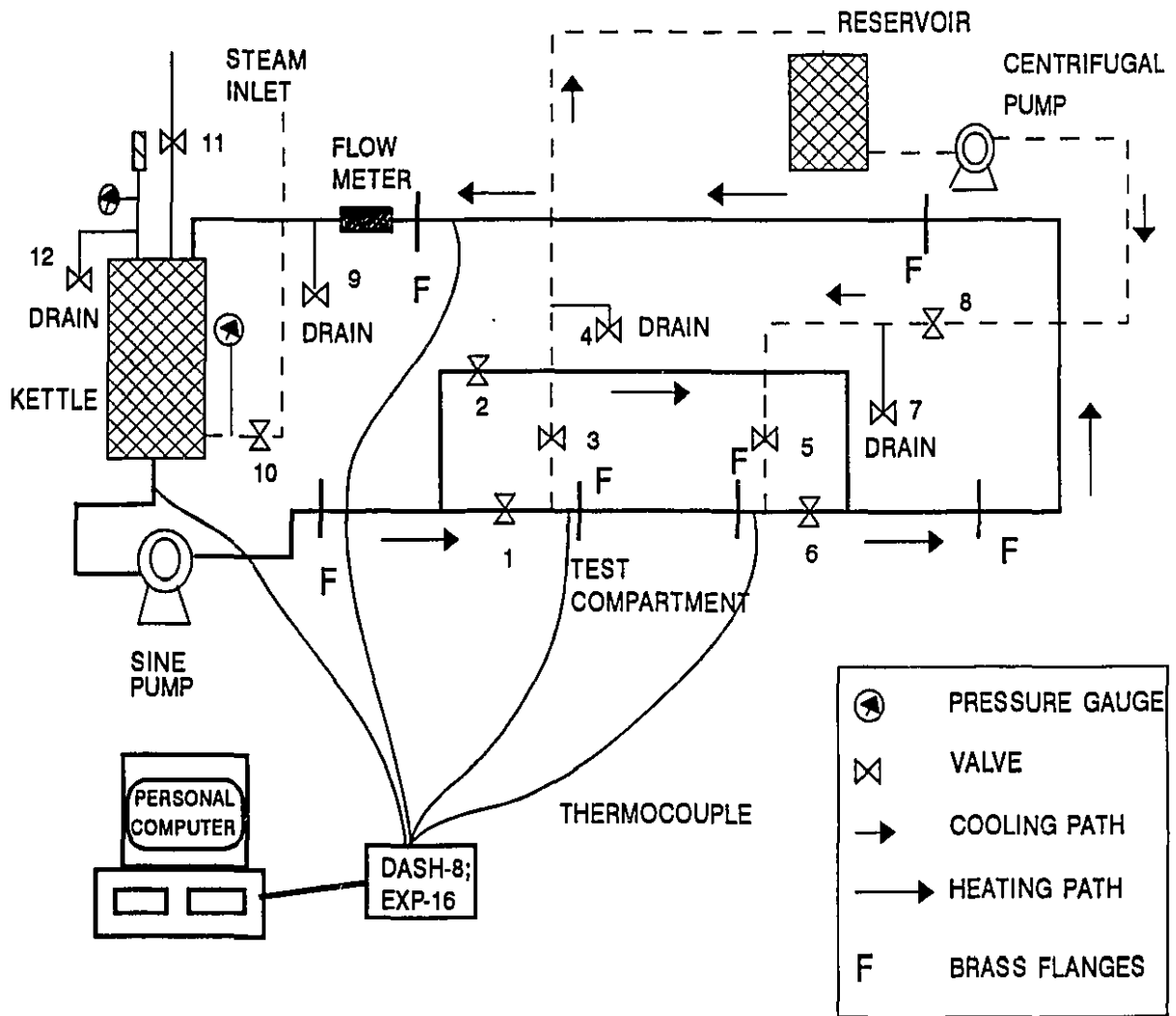


Figure 5.1 A schematic diagram of the pilot scale simulator (not drawn to scale)

thermocouple thermometers (Model 650, Omega Engineering Inc, Stamford, CT). In addition to the heating network, a "cooling loop" including a cold water reservoir, valves and a variable-speed centrifugal pump (Micropump, Cole Parmer Instrument Co. Chicago, IL) enabled heated samples to be cooled *in-situ*.

Construction of the Test Compartment and Sample Holder

The test compartment (Figure 5.1) consisted of approximately 30.5 cm long copper pipe welded onto brass plates (flanges). Four holes were drilled on each flange for coupling the test compartment to the holding tube. A hole was punched at the exit of the test compartment and sealed off with a miniature (approximately 1.27 cm long) brass rod which protruded into the compartment, purposely, to support the sample holder from sliding out during fluid flow. Two Teflon-insulated 36 AWG copper-constantan thermocouples were attached to the entrance and exit of the test compartment to monitor fluid temperature. The sample holder consisted of (1) a perforated cylindrical cup (Figure 5.2A) which was carefully dimensioned and slotted to fit the test compartment by sliding along the miniature brass rod and turning to lock and (2) approximately 15 cm long brass rod with copper rings (Figure 5.2B) welded at its tip to hold a test sample. The brass rod was threaded at the other end and connected to the perforated cup by means of a miniature nut.

Mode of Operation of the Simulator

During pre-heating, the test compartment was isolated by diverting the fluid

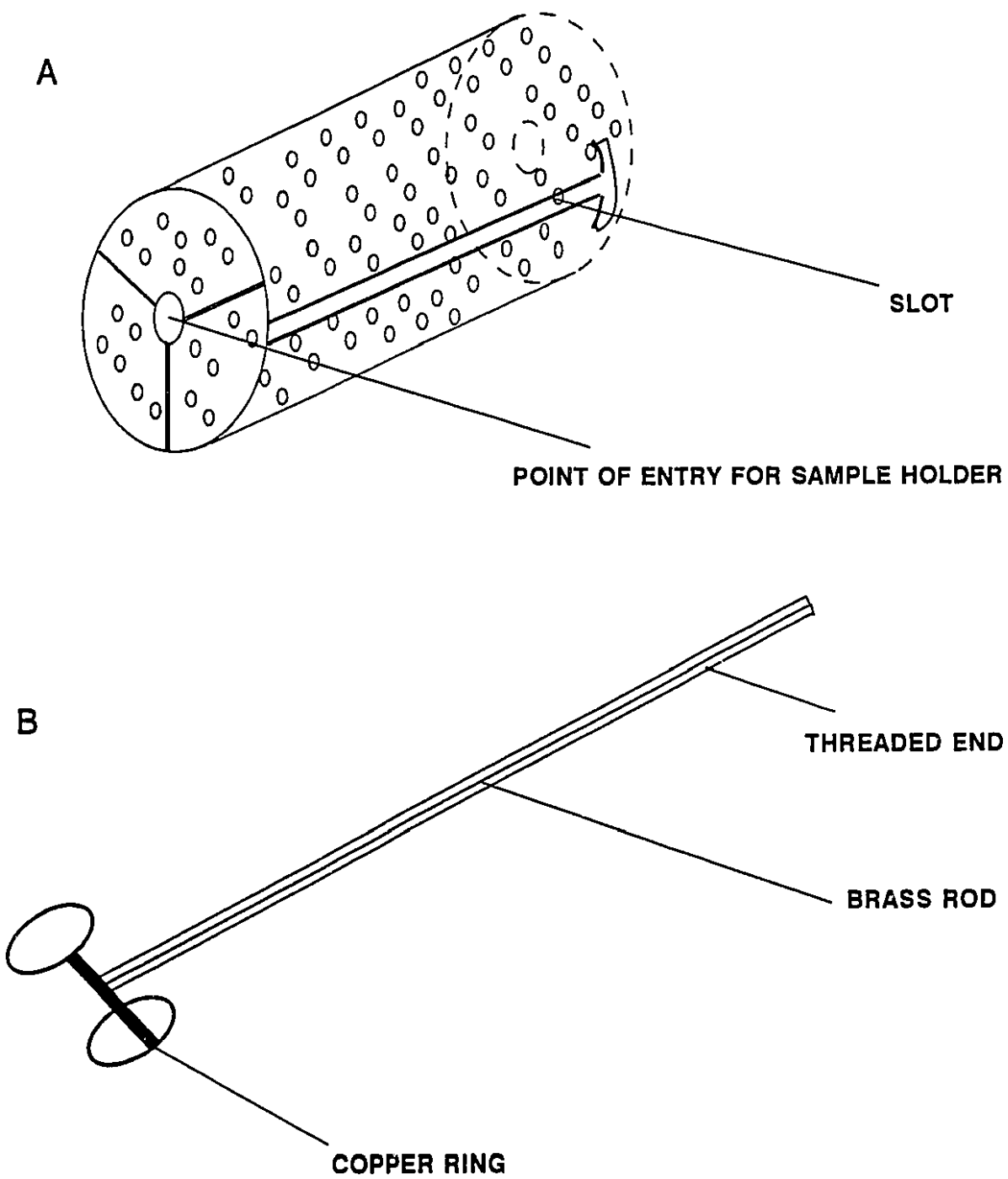


Figure 5.2 A schematic diagram of the sample holder.

through the by-pass and back into the kettle. This was achieved with all ball valves closed except 2 (Figure 5.1). The system was stabilized with recirculating fluid until the desired temperature was obtained. The temperature of the fluid was thereafter adjusted by manual regulation of the steam inlet valve. Prior to each experimental run, the test compartment was taken out of the system and fitted with the perforated-cup sample-holder combination which ensured flexibility and proper positioning of test samples along the central axis of the tube. On achieving the desired system temperature, the test compartment was attached and secured in place. Valves 1 and 2 were simultaneously opened and closed respectively to allow fluid into the test compartment. All valves except 1, 5 and 7 remained opened as the test compartment was filled up with the hot fluid. This procedure drove any resident fluid out of the compartment through valve 7. Once the test compartment was full, valves 6 and 5 were simultaneously opened and closed and the fluid flowed back into the kettle to be reheated. Time-temperature data was continuously gathered at pre-determined time intervals and simultaneously stored on the personal computer. Once heating was completed, valve 2 was opened while valves 1 and 6 were closed, hence, allowing the fluid to be diverted back into the kettle. Valves 3 and 5 were gradually opened to release excess pressure from the system through the drains. Cooling was initiated by opening and closing valves 8 and 7 respectively and pumping cold fluid into the test chamber using the variable-speed centrifugal pump (Micropump, Cole Parmer Instrument Co. Chicago, IL).

Data Acquisition System

All thermocouples were connected to a data acquisition system which consisted of (1) a personal computer (2) a Dash-8, 8 analog input channels featuring a high-speed, 12-bit, successive-approximation A/D converter with 35 μ s maximum conversion time and data throughput rate of approximately 30 kHz, and (3) an EXP-16 expansion multiplexer and amplification board with cold-junction sensing and compensation circuitry with a 24.4 mV/ $^{\circ}$ C scaling. The multiplexer provided 16 different analog input channels for attachment of thermocouples while the amplifier provided user-selectable switch gains.

RESULTS AND DISCUSSION

Since uniform fluid flow profiles were essential in heat transfer studies, adequate pipe lengths were provided before and after the test compartment to reduce disturbances due to pipe bends. The clamping mechanism allowed the system to take pressures and temperatures up to 15 psig and 115 $^{\circ}$ C, respectively. This constraint was imposed by the "soft" components (especially the scraper gate) of the positive displacement sine pump. The location of the thermocouples and visual observation of the fluid temperatures allowed excellent control of system temperature manually. In general, a 2 $^{\circ}$ C drop in temperature was found between the exit of the jacketed steam kettle via the holding tube back to the steam kettle, covering a total pipe length of approximately 5 m. This indicated that pipe insulation was very effective in reducing heat losses to the surrounding. Stabilizing the simulator to the desired operating temperature took between 30 to 50 min depending on fluid concentration and data collection was initiated prior to exposing the

compartment to the hot fluid. Figure 5.3 shows a time-temperature plots of data gathered from a stationary particle in a typical experiment. A constant fluid temperature could be maintained over the heating period and heating was carried out till the particle centre temperature approached that of the fluid.

Calibration of the Simulator

It was observed that for a given pump speed (rpm), the volumetric through flow rate measured with the flow meter varied for different fluid concentrations and temperatures. This observation could be attributed to slip between the pump's rotor, scrapper gate, and housing resulting in a reduced fluid output for less viscous fluids. This observation indicated qualitatively that fluid concentration was temperature dependent, with fluid apparent viscosity decreasing with increasing temperature. Therefore, fluid flow rates were recorded for three (3) concentrations (0, 0.5 and 1.0% w/w CMC, three (3) temperatures (90, 100 and 110°C), and three (3) pump speeds (120, 160 and 190 rpm) for two (2) pipe diameters (5.08 and 7.62 cm nominal diameter). The influence of the above factors and their interactions was assessed with a General Linear Model (GLM) procedure of the Statistical Analysis System (SAS) on McGill University Computer Network. As indicated in Table 5.1, pump speed (RPM), fluid concentration, temperature, pipe diameter and their interactions had significant influence ($p < 0.005$) on measured flow rate. Using stepwise multiple regression, the required flow rate (FR) for predetermined levels of concentration (C), temperature (T), pump rpm (RPM) and pipe diameter (D) was obtained as:

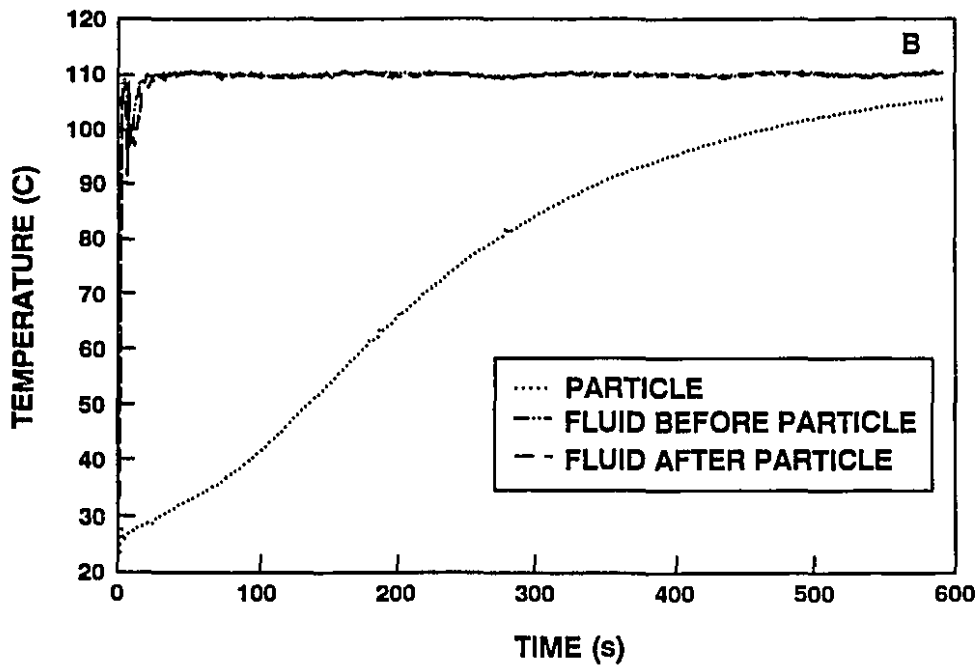
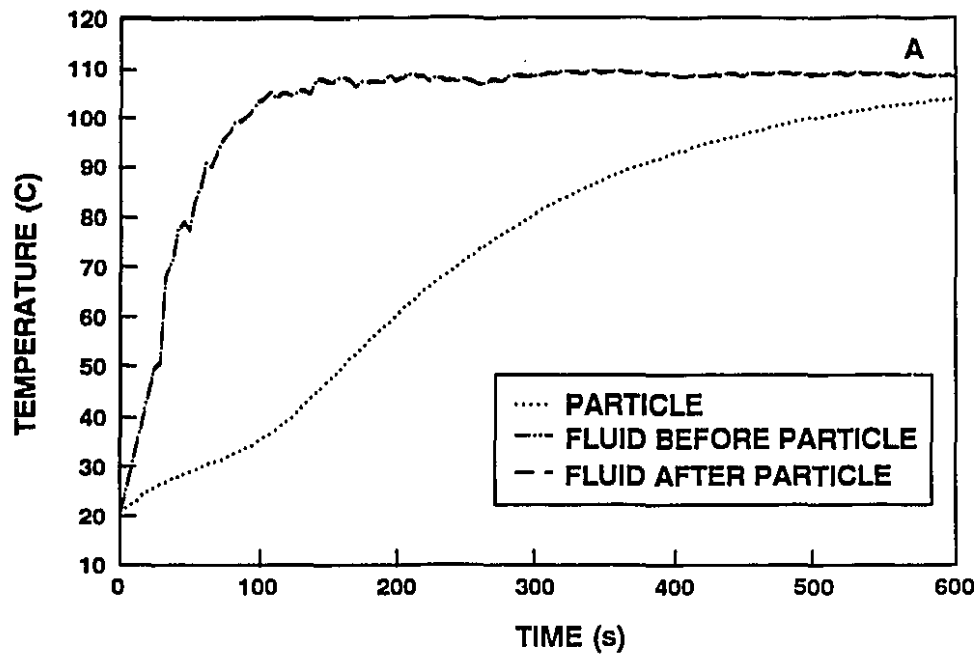


Figure 5.3 Heat penetration curves for heating a 25.4 mm diameter and 25.4 mm long Teflon particle at 110 °C.

Table 5.1 Analysis of variance of factors influencing fluid flow rate.

Source	dF	Sum of squares	Mean Square	F
Model	25	45.33	1.81	267.27*
Main effects				
Concentration (C)	2	3.16	1.58	233.14*
Temperature (T)	2	1.27	0.63	93.36*
Pump speed (RPM)	2	24.35	12.18	1795 *
Diameter (D)	1	2.31	2.31	340.16*
Interactions				
C*T	4	0.705	0.176	25.97*
C*RPM	4	0.148	0.0371	5.46**
C*D	2	0.59	0.30	43.63*
T*RPM	4	0.36	0.09	13.33*
T*D	2	0.213	0.106	15.69*
RPM*D	2	0.18	0.09	13.01*
Residual (error)	118	0.801	0.007	
Total	143	46.13		
R ^{2b}		0.98		

^b Coefficient of determination; Level of significance * p< 0.005; Level of significance

** p< 0.01

$$FR = 0.22D + 0.134CT + 0.023RPM - 0.4CD - 0.0022DRPM - 0.97 \quad (5.1)$$

A good correlation ($R^2 = 0.92$) was obtained between observed and predicted values (Figure 5.4). Thus, the pump speed (RPM) needed to output a given fluid flow was generally found to be higher for less viscous fluids compared to more viscous fluids at all temperatures. Alternatively, the pump speed (RPM) required for predetermined levels of concentration (C), temperature (T), flow rate (FR) and pipe diameter (D) could be correlated as

$$RPM = 39.4 + 3.7FRD + 18.3CD + 42.5FR - 0.63CT \quad (5.2)$$

giving $R^2 = 0.90$

Performance of the Simulator

The simulator could be operated under one or two modes for gathering heat penetration data from test samples. In the first mode of operation (referred to as M1), the test compartment was initially filled with cold fluid. The hot recirculating fluid was then let in, forcing the cold fluid out of the compartment within 120 to 150 s depending on operating temperature and fluid flow rate (Figure 5.3A). Higher pressures associated with elevated temperatures contributed to reducing the "come-up" time in the compartment. Although, the test compartment goes through a transient phase prior to establishing the

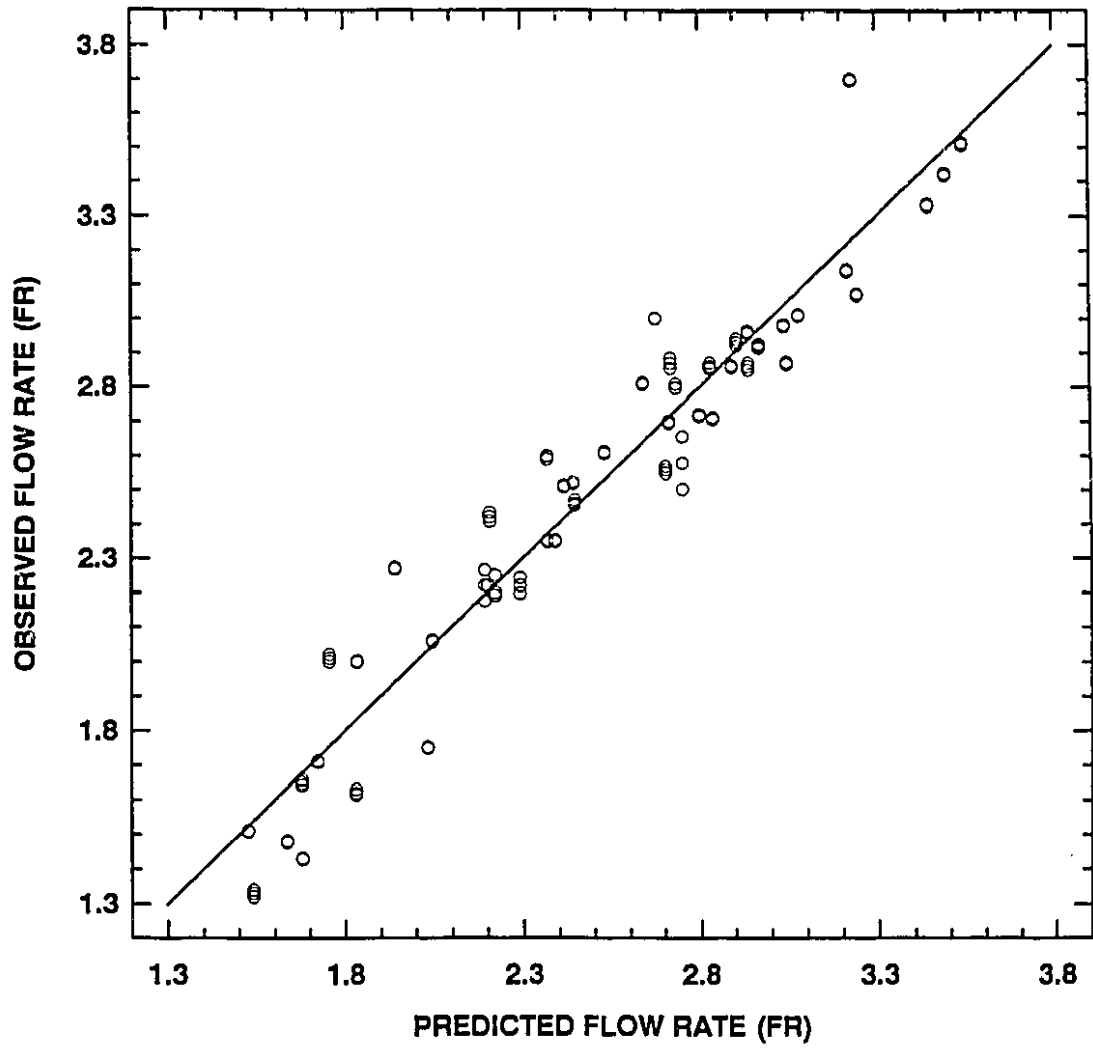


Figure 5.4. Plot of observed vs predicted flow rate as a function of temperature, concentration, and pump rpm.

desired operating temperature (Figure 5.3A), this mode of operation was found suitable for both low and highly conductive materials. However, the use of analytical routines for calculating heat penetration and other parametric values become limiting especially for highly conductive materials which may follow almost the same temperature profile as that of the fluid. Calculating the convective heat transfer coefficient under such situations will require numerical techniques which accommodate transient changes in medium temperatures.

In the second mode of operation (referred to as M2), the test compartment was left empty prior to exposure to the hot fluid. Filling and heating of the test compartment to operating condition was achieved much more rapidly (Figure 5.3B). The fundamental requirement (i.e. a constant temperature medium) for implementing analytical routines was satisfied with the rapid exposure of test particles to the medium temperature. The fluid, however, goes through a momentary temperature drop (Figure 5.3B) especially for conditions in excess of 100 °C due to both heat losses to the test compartment and sudden exposure to atmospheric conditions which was found necessary to evacuate entrapped air. After approximately 50 s of heating (Figure 5.3B), the fluid temperature appears to stabilize and remain constant over the rest of heating period, with an average standard deviation of $\pm 0.2^{\circ}\text{C}$. It should be emphasized that achieving constant fluid temperature was easily effected with the strategic location of the visual thermometer thermocouples and manual regulation of the steam inlet valve. To stimulate the effect of relative velocities on heat transfer coefficients, turbulent eddies had to be minimized from the onset of data gathering. Hence, the use of highly conductive materials in conjunction with

the mode of operation M2 appear inappropriate for estimating heat transfer coefficients.

Based on the heating characteristics of the test compartment in relation to the mode of operation, M2 was found more adequate and convenient for routine estimation of heat transfer coefficients as a function of system parameters using low conductive products.

CONCLUSIONS

A versatile holding tube simulator was designed and fabricated for carrying out heat transfer studies using stationary particles at temperatures up to 110°C, although the system could go up to 115°C. The sample holder allowed exact location of different diameter particles along the central axis of the holding tube. The simulator was calibrated to output the desired flow rate as a function of fluid concentration, temperature, pump speed, and pipe diameters. Statistical analyses indicated the above factors to significantly influence fluid discharged from the pump. Higher pump speeds were needed to maintain a given flow for less viscous fluids. Good correlations ($R^2 \geq 0.90$) were obtained between predicted and observed fluid flow rate and pump RPM. The equipment could be operated in two modes for studying heat transfer to suspended particles. Heat losses to the surrounding was generally found to be small and a constant operating temperature could be obtained without any specialized skills of the operator.

CHAPTER VI

FLUID-TO-PARTICLE HEAT TRANSFER COEFFICIENT AS INFLUENCED BY PRODUCT AND SYSTEM PARAMETERS IN A PILOT SCALE HOLDING TUBE SIMULATOR

ABSTRACT

Fluid-to-particle heat transfer coefficients (h_{fp}) were estimated with real and model food particles in a pilot scale aseptic holding tube simulator at temperatures between 90 and 110°C. Data were gathered under various conditions: fluid concentration (0 - 1.0% w/w CMC), flow rate ($1.0 - 1.9 \times 10^{-4} \text{ m}^3/\text{s}$), particle diameter (15.9 - 25.4 mm), shape (sphere and cylinder) and particle orientation (parallel and perpendicular to fluid flow). Average h_{fp} ranged from 56 to 966 W/m²C with Biot numbers ranging from 5 to 42. CMC mean apparent viscosity ranged from 0.02 to 0.21 Pa.s. With the exception of particle length and orientation all other parameters and their interactions had significant ($p < 0.05$) influence on h_{fp} . Increasing particle size from 19.1 to 25.4 mm, for instance, caused between 36 to 72% drop in the heat transfer coefficient. Changing particle-to-tube diameter ratio caused up to 74% change in h_{fp} values. The effect of temperature was more pronounced with real food samples compared to model food. h_{fp} associated with a cylindrical particle having approximately same diameter and length gave lower values (between 7 to 29%) compared with spherical particles of the same diameter.

INTRODUCTION

High temperature short time (HTST) sterilization has long been demonstrated to be effective in minimizing nutrient and quality factor degradation and therefore highly favoured over traditional processing of heterogeneous foods in metal, glass and plastic containers. Such a concept has resulted in commercialization of aseptic processing of liquid foods. However, commercialization of low-acid ($\text{pH} > 4.6$) foods containing discrete particles greater than 3.2 mm in major dimension (Chandarana and Gavin, 1989a,b) still remain to be accomplished, particularly in North America where stringent Federal regulations require absolute proof of process adequacy through microbiological verification in accordance with *Code of Federal Regulations* (CFR 21:108).

In aseptic processing of heterogeneous foods, particle trajectories depend on the Saffman lift, Magnus lift, drag, buoyancy and centrifugal forces (Sastry *et al.*, 1989; Dutta and Sastry, 1990a). The complex interaction between these forces in a dynamic two-phase food system makes residence times as well as temperature histories of the suspended particles extremely difficult to predict. Implementing traditional routines for process calculations become questionable under such situations (Weng *et al.*, 1992). To obtain commercial sterility for such systems, process calculations have to be based on biological measurement of the F_0 -value delivered to the centre of the particle (Dignan *et al.*, 1989).

Mathematical modelling serves as an important tool in reducing the number and cost of experiments required in designing, validating, and optimizing processing systems (Clark, 1978; Maesmans *et al.*, 1992). Several researchers (Manson and Cullen, 1974; Sastry, 1986; Astrom *et al.*, 1988; Larkin, 1989; Chandarana and Gavin, 1989a,b;

Mckenna and Tucker, 1990; Skjoldebrand and Ohlsson, 1993a,b) have proposed mathematical procedures for predicting heat transfer to particles and computer simulation programmes for process evaluation. The effectiveness of these models and programs in predicting adequate processes depend on the accuracy of input thermophysical and boundary value parameters.

Dignan *et al.* (1989) listed critical factors needed in modelling heat transfer and lethality distribution in continuously processed low-acid particulate foods as: particle size/distribution, the convective heat transfer coefficient and residence time distribution both in the heat exchanger and holding tube. According to Larkin (1990), examining critical control factors depend not only on whether the parameters influence the process, but the extent to which these factors affect the process. Using an implicit Crank-Nicolson finite difference method to simulate an aseptic unit, Lee *et al.* (1990a) demonstrated that particle size, shape, particle thermal properties and residence time distribution within the SSHE and the holding tube influenced the minimum process time required to achieve a 6D for *Clostridium sporogenes* PA3679. The authors found that the effect on the minimum process time was significant when the fluid-to-particle heat transfer coefficient (h_{fp}) ranged between 50 to 500 W/m²C, but levelled out beyond 500 W/m²C. The physical significance is that minor changes in h_{fp} beyond 500 W/m²C does not greatly affect the holding tube length/processing time required to achieve a given F_0 . Larkin (1990) also demonstrated that a change in h_{fp} from 175 to 181 W/m²C in the holding tube could result in more than 5% increase in predicted F_0 . Since the Biot number of real foods are most likely to fall between 0.1 and 40 (Heldman and Singh, 1981), the convective

heat transfer coefficient may present one of the rate limiting parameters in process design. Proven to be highly influential and significant in process evaluation through simulations, the fluid-to-particle heat transfer coefficients in both the heat exchanger and holding tube probably are the most important but difficult parameters to be determined experimentally (Dignan *et al.*, 1989; Heldman, 1989).

Two approaches can be identified with estimating h_{fp} at elevated temperatures; the "indirect method" which utilizes time-temperature integrators (TTI) such as immobilized enzymes or microorganisms (Hunter, 1972; Heppel, 1985), and the "direct method" which uses time-temperature data gathered directly from a stationary particle (Alhamdan *et al.*, 1990; Alhamdan and Sastry, 1990; Chandarana *et al.*, 1990b; Chang and Toledo, 1990; Zuritz *et al.*, 1990). Aside from the fact that TTIs depend on the reliability and reproducibility of systems whose kinetics are accurately established, locating it in high Biot number particles ill-conditions the particle, thus making the particle respond readily to thermal diffusivity rather than h_{fp} (Maesmans *et al.*, 1992).

A survey of the literature shows that most of the studies on h_{fp} were carried out under atmospheric conditions which ignores changes in apparent fluid viscosity by temperatures in excess of 100°C. Under such conditions the relative velocity between the particle and the carrier fluid may vary depending on the characteristics of both the fluid and system. The objectives of this study were to (1) simulate different yet practical relative velocities and estimate their influences on the convective heat transfer coefficient (2) study the individual and combined effects of fluid apparent viscosity, temperature and flow rate on h_{fp} (3) study the type, size, and shape of particle on h_{fp} (4) study the effect

of particle orientation on h_{fp} (5) study the effect of particle-to-tube diameter ratios on h_{fp} and (6) study h_{fp} associated with cooling heat treated food particle in relation to heating of raw samples. Carboxymethylcellulose (CMC) solution was used for the studies due to its wide industrial applications, particularly in the preparation of viscous sauces. The studies were conducted with spherical and *finite cylindrical* particles due to paucity of experimental data and correlations associated with such particles in the open literature.

MATERIALS AND METHODS

Theoretical Basis for Estimating the Fluid-to-Particle Heat Transfer Coefficient

Given the temperature history at one or more locations inside a heat-conducting body of defined geometry, the convective heat transfer coefficient can be estimated by the "Inverse Problem" technique (Chen and Thompson, 1975). The theoretical background involved with calculating the heat transfer coefficient is detailed in Chapters III and IV. The rate (f_h) method was chosen on the basis of appropriateness and its non restrictive nature with respect to thermocouple placement in the test materials. A computer program, coded in Fortran 77 (Appendix 1) was used for estimating the convective heat transfer coefficient from the heating rate index (f_h).

Test Materials and CMC Preparation

Cylindrical test samples of potatoes (purchased from a local market and stored in a refrigerator at 5°C) and Teflon (Small Parts Inc., Miami Lakes, FL) were prepared as described in Chapter IV. However, the thermocouple installation was a little different for

potato tissues. A pinhole was made along the axis of the particle to coincide with the central plane. A Teflon-insulated 30 AWG copper-constantan thermocouple was attached to a toothpick and pushed along the pinhole till it travelled an equivalent distance made with the pin. The point of entry was then sealed off with epoxy glue and left to dry within 5 min. This approach reduced chances of water leaking into the sample along the thermocouple wire. For cylindrical Teflon particles, appropriate lengths were cut from a Teflon rod and a hole was drilled along its axis to predetermined depths using a drilling machine. A lathe was used in drilling the hole in spherical Teflon particles. Teflon-insulated 30 AWG copper-constantan thermocouple was inserted into the holes and secured with epoxy glue. All thermocouples were calibrated against an ASTM mercury-in-glass thermometer prior to installation. The technique used to install test samples in the aseptic processing simulator is detailed in Chapter V.

Two concentrations (0.5 and 1.0 % w/w) of food grade CMC (Pre-hydrated CMC PH-2500, TIC Gum Inc, Belcamp, MD) were prepared by adding water to a known quantity of CMC powder in a variable speed mixer (Hobart Model D-300, Hobart Canada Inc, Mississauga, ON). Thorough mixing was carried out to complete the dissolution of CMC. The solution was adjusted to the desired concentration in a 90 L plastic container and left overnight till use.

Rheological and Thermal Properties

High temperature rheological data were obtained using a rotational viscometer Model RV20 (Haake Mess-Technik, Karlsruhe, Germany) coupled to an M-5 OSC

measuring head and a D100/300 sensor and modelled with the classical power law equation for the downward linear-ramp shearing curve (Abdelrahim, 1994). Other property values of CMC, potato and Teflon are defined in Chapters III and IV. Effective mean CMC apparent viscosity values were obtained as defined in Skelland (1967) and Zuritz *et al.* (1990):

$$\mu_{mean} = [2^{n-2} m [(3n+1)/n]^n (\frac{D}{V})^{1-n}] / (3n-1) \quad (6.1)$$

Experimental Setup and Procedure

All experiments were carried out using either a 5.08 or 7.62 cm internal diameter pipe as detailed in Chapter V. Since relatively low conductive materials (both real and simulated food particles) were used, mode of operation M2 (Chapter V) was adopted. Temperature history of test samples were continuously gathered at 5 s intervals.

Experimental Design

A 2 x 2 x 2 fully randomized factorial design involving flow rate (1.26 and 1.8 x 10⁻⁴ m³/s), sample length (20 and 25.4 mm) and diameter (19.05 and 25.4 mm) for Teflon particles heated with 0.5% CMC at 100°C in a 7.62 cm diameter pipe was used to study the effect of sample length on the heat transfer coefficient. The effect of particle orientation (i.e. cylindrical axis either parallel (axial-flow) or perpendicular (cross-flow) to the direction of fluid flow) was studied for two levels of flow rates (1.26 and 1.8 x 10⁻⁴ m³/s), and two levels of sample diameters (19.05 and 25.4 mm) with 0.5% CMC solution

at 100°C flowing through a 7.62 cm diameter pipe. A 2 x 3 x 3 x 2 fully randomized factorial design involving CMC concentration (0.5 and 1.0%), flow rate (1.0, 1.5 and 1.9 m³/s), sample diameter (15.9, 19.05 and 25.4 mm), and pipe diameter (5.08 and 7.62 cm) was carried out to study the influence of particle diameter and particle-to-tube diameter ratio on the heat transfer coefficient. To study the influence of both system and product parameters, a 3 x 3 x 3 full factorial design involving fluid concentration (0, 0.5 and 1.0% CMC), flow rate (1.0, 1.5, and 1.9 m³/s), and temperature (90, 100, and 110°C) was conducted with 25.4 mm diameter by 25.4 mm length Teflon and 21 mm diameter by 24 mm length potato samples in 5.08 cm diameter pipe. Similar experiments were conducted in the 7.62 cm diameter pipe for both Teflon and potato but at selected levels of temperature, concentration and flow rate. With the exception of studies involving sample orientation, all experiments were conducted with particle axis perpendicular to the direction of fluid flow. Heat transfer coefficients associated with cooling heated potato particles were also estimated at selected conditions: initial temperatures (90, 100 and 110°C), and flow rate (1.0, 1.53, 1.61, 1.62, and 1.71 m³/s). Cooling medium was water at 20°C. Finally, the effect of sample shape (spherical and cylindrical Teflon particle of the same diameter) on h_{fp} was studied at selected conditions of flow rate, concentration, and pipe diameter at 100°C. All experiments were replicated at least five (5) times resulting in over 900 heat penetration tests.

Data Analysis

In order to facilitate data handling and visual comparison of temperature profiles,

all time-temperature data were normalized with respect to initial and medium temperatures as detailed in Stumbo (1973). As follows from theory, such normalization does not influence the evaluated f_h which is the basis of the present studies for h_{fp} determination. Due to unequal number of observations within the same treatment, mean values of the heat transfer coefficient as affected by various processing conditions were analyzed using Least Significance Difference (LSD) multiple comparison procedure (Steel and Torrie, 1960). Since a finite cylinder has two Biot numbers (related to cylindrical and cross sectional surfaces), a *characteristic* dimension (l_c) estimated as the radius of a sphere having the same volume-to-surface area ratio was used in calculating the representative Biot number ($Bi = h_{fp}l_c/k_p$).

RESULTS AND DISCUSSION

Depending on experimental conditions, the fluid-to-particle heat transfer coefficient ranged from 56 to 966 W/m²C and 176 to 724 W/m²C with corresponding Biot number (Bi) ranging from 4.0 to 42.0 and 5 to 21 for Teflon and potato samples, respectively. The range of Biot numbers found in the present study fall within the range 0.1 to 40 specified by Heldman and Singh (1981) for conditions involving both internal and external resistances to heat transfer. With the exception of relatively small particles subjected to high fluid flow rates, the associated convective heat transfer coefficients were below the 500 W/m²C (upper limit for aseptic processing reported by Lee *et al.*, 1990a) indicating h_{fp} to be a significant factor in determining process time/holding tube length required to achieve the desirable sterility. CMC effective mean apparent viscosity varied from 0.02

to 0.21 Pa.s. The range of h_{fp} values for the present study compared well with published data (Chandarana *et al.*, 1988; Chang and Toledo, 1989; Alhamdan and Sastry, 1990; Alhamdan *et al.*, 1990; Chandarana *et al.*, 1990a,b; Zuritz *et al.*, 1990; Mwangi *et al.*, 1993; Astrom and Bark, 1994).

Effect of Particle Length

In the previous Chapter (IV), it was reported that decreasing volume to area ratio had marginal effect on h_{fp} for heating both carrot and potato samples in 1.0% CMC solution. The reason given was that higher fluid apparent viscosity masked the influence of both sample length and diameter on h_{fp} . This warranted further exploration with a less viscous fluid at relatively higher rates. Table 6.1 shows the effect of sample length on h_{fp} for two different diameters. Smaller particles had a significantly higher h_{fp} value than larger particles at medium flow rate ($1.26 \times 10^{-4} \text{ m}^3/\text{s}$). At higher flow rates, h_{fp} values associated with 20 mm length particles were statistically no different ($p > 0.05$) from those associated with 25.4 mm particles. This indicates the dominant effect of radial heat flow to overall heat transfer to particle.

Effect of Particle Orientation

The dynamics of fluid flow around a cylinder is complicated by the combined effect of Reynolds number, free stream turbulence and other factors including particle shape and configuration with respect to fluid flow. For a cylinder in cross-flow (i.e. axis perpendicular to the direction of fluid flow), a laminar boundary layer is formed on the

Table 6.1. Heat transfer coefficients for Teflon cylinders as influenced by particle length and flow rate.

Flow rate $\times 10^{-4}$ (m^3/s)	Length (mm)	Diameter (mm)	Volume/area $\times 10^{-3}$ (m)	h_{fp} ($\text{W}/\text{m}^2\text{C}$)	Coefficient of variation (%)
1.80	20	19.05	3.2	268 ^a	17.2
1.80	25.4	19.05	3.5	262 ^a	16.4
1.26	20	19.05	3.2	208 ^b	15.4
1.26	25.4	19.05	3.5	160 ^c	6.9
1.80	25.4	25.4	4.2	129 ^d	6.9
1.80	20	25.4	3.9	125 ^d	7.2
1.26	20	25.4	3.9	112 ^{de}	15.2
1.26	25.4	25.4	4.2	105 ^e	5.7

^{a,b,c,d,e}Mean h_{fp} values sharing the same superscript are not significantly different ($p > 0.05$). Particles were heated in 0.5% CMC at 100°C.

front part as a result of dominant viscous forces. At low Reynolds number ($Re=1$) a cylinder is completely enveloped all around by the laminar boundary layer, which separates from the surface only at the rear stagnation point (Žukauskas and Žiugžda, 1985). Since inertial forces increase as the Reynolds number increases, the laminar boundary separates from the surface at a particular distance from the rear stagnation point, causing a complex vortex structure to be formed in the wake (Churchill, 1983; Žukauskas and Žiugžda, 1985). The boundary layer is distorted with the onset of turbulence at higher Reynolds numbers, shifting the rear stagnation point further upstream. For a cylinder in axial flow (i.e. axis parallel to the direction of fluid flow) with its "blunt surface" facing the direction of flow, the boundary layer detaches, separating from the surface at the upstream end resulting in a wake (Pitts and Sissom, 1977). This phenomenal behaviour becomes even more complex for particles in restricted enclosures, causing a shift in boundary layer as a result of changes in the velocity distribution. Therefore, fluid velocity within the void volume can be expected to increase in favour of particle in axial flow due to localized turbulence. Differences in fluid profiles for both configurations will be reflected in estimated h_{fp} values, with higher rates probably associated with particle axial flow.

Table 6.2 summarizes average heat transfer coefficients for heating Teflon particles in a 7.62 cm diameter tube. Statistically, heat transfer coefficients associated with particle in crossflow were no different than those for axial flow ($p > 0.05$). It was anticipated that lower apparent viscosities associated with higher temperatures would introduce localised turbulence between the axially located particle and the tube, thereby enhancing heat

Table 6.2 Heat transfer coefficients for Teflon cylinders as influenced by particle orientation.

Flow rate $\times 10^{-4}$ (m^3/s)	Orient ¹ .	Diameter (mm)	Volume/area $\times 10^{-3}$ (m)	h_{fp} ($\text{W}/\text{m}^2\text{C}$)	Coefficient of variation (%)
1.80	PER	19.05	3.5	262 ^a	16.4
1.80	PAR	19.05	3.5	236 ^a	22.5
1.26	PER	19.05	3.5	160 ^c	6.9
1.26	PAR	19.05	3.5	159 ^c	7.6
1.80	PER	25.4	4.2	129 ^d	6.9
1.80	PAR	25.4	4.2	116 ^{dc}	5.2
1.26	PER	25.4	4.2	105 ^c	5.7
1.26	PAR	25.4	4.2	104 ^c	10.6

^{a,b,c,d,c}Mean h_{fp} values sharing the same superscript are not significantly different ($p > 0.05$)

¹Particle located in either parallel (PAR) or perpendicular (PER) respectively in the holding tube for heating 25.4 mm length samples in 0.5% CMC at 100°C.

transfer. The data obtained shows such phenomena did not occur although the flow rate enhanced h_{fp} by a percentage difference ranging between 10 to 39% (Table 6.2) for the same particle size and orientation. The insignificance of differences between particle orientation could possibly be due to the use of 7.62 cm diameter pipe, which might have provided nonrestrictive flow or the fluid flow rates used were probably too low to reflect such mechanisms.

Effect of Particle Diameter and Particle-to-Tube Ratio

Contrary to Zuritz *et al.*(1990) observation of increasing h_{fp} with increasing equivalent particle diameter for a mushroom shaped aluminium particle, Chandarana *et al.*(1988) found h_{fp} to increase with decreasing particle (cube) dimension. Using an 8.6 cm tube for heating food particles in 1.0% CMC at 80°C (Chapter IV), it was found that increasing particle diameter had no significant effects on estimated heat transfer coefficients. Studying particle-particle interaction and particle velocity in a holding tube, Dutta and Sastry (1990a,b) found under certain conditions that particles moved slowly at the bottom of the holding tube. The effective cross-section available for fluid flow reduces, resulting in channelling of fluid through the void fraction of the tube. Increasing the fluid-to-particle relative velocity according to the authors, caused an increase in the heat transfer coefficient with increasing particle size. They further indicated that h_{fp} does not depend on particle size alone but also on their position and fluid flow conditions. Using the moving thermocouple approach, Sastry *et al.* (1990) found h_{fp} to increase with increasing particle-to-tube diameter ratio and fluid flow rate. The authors performed

experiments in a 3.8 and 5.0 cm diameter pipes. Mwangi *et al.* (1993) found a similar trend for heating polymethylmethacrylate spheres imbedded with a melting point indicator. With the exception of Chandarana *et al.* (1988) whose work was done with cubes at aseptic temperatures, most of the studies were conducted at atmospheric conditions with spherical particles in restricted enclosures. Hence, the present studies associated with particle size and particle-to-tube diameter ratio were purposely conducted to determine which trend particle size followed especially for finite cylindrical particles carefully located at the centre axis of the tube.

Table 6.3 shows the influence of sample diameter on the heat transfer coefficient for heating Teflon in 0.5 and 1.0% CMC solutions at 110°C. Figure 6.1 is included to illustrate the behaviour of particle diameter on the convective heat transfer coefficient for heating 25.4 mm long Teflon particles of three (3) different diameters (15.9, 19.05, and 25.4 mm) using both the 5.08 and 7.62 cm diameter pipes containing either 0.5 or 1.0% CMC solutions at 100°C. Table 6.3 indicates that sample diameter has a significant ($p < 0.05$) influence on estimated heat transfer coefficients, with h_{fp} values increasing with decreasing volume to area ratio, contrary to reported trends for spherical particles. For example an increase in particle diameter from 19.05 to 25.4 mm caused a 36% drop in the heat transfer coefficient for the same flow rate ($1.9 \times 10^{-4} \text{ m}^3/\text{s}$) and concentration (0.5% CMC). For the same particle size, temperature and flow rate but different concentration (1.0% CMC), the change was 52%. Higher percentage differences up to approximately 72% (Table 6.3) occurred as the flow rate decreased with increasing fluid apparent viscosity. These effects which were not clear cut in the preliminary studies

Table 6.3. Heat transfer coefficients for Teflon cylinders as influenced by particle diameter.

Flow rate $\times 10^{-4}$ (m ³ /s)	Conc (%)	Diameter (mm)	Volume/area $\times 10^{-3}$ (m)	h_{fp} (W/m ² C)	Coefficient of variation (%)
1.9	0.5	15.88	3.0	893 ^a	4.3
1.9	0.5	19.05	3.5	554 ^{f,g,h}	8.1
1.9	0.5	25.40	4.2	354 ^{u,s,r,t,q}	4.0
1.5	0.5	15.88	3.0	761 ^{bc}	6.6
1.5	0.5	19.05	3.5	526 ^{hij}	2.5
1.5	0.5	25.40	4.2	138 ^{x,y,z}	1.5
1.0	0.5	15.88	3.0	596 ^{e,f}	0.7
1.0	0.5	19.05	3.5	380 ^{g,p,r,s}	19.7
1.0	0.5	25.40	4.2	129 ^{y,z}	1.55
1.9	1.0	15.88	3.0	888 ^a	7.2
1.9	1.0	19.05	3.5	632 ^{d,e}	4.9
1.9	1.0	25.40	4.2	303 ^{u,v}	5.0
1.5	1.0	15.88	3.0	812 ^b	5.4
1.5	1.0	19.05	3.5	457 ^{k,l,m}	3.5
1.5	1.0	25.40	4.2	132 ^{y,z}	1.5
1.0	1.0	15.88	3.0	569 ^{f,g,h}	0.9
1.0	1.0	19.05	3.5	380 ^{q,p,r,s}	5.5
1.0	1.0	25.40	4.2	123 ^z	1.6

^{a-z}Mean h_{fp} values sharing the same superscript are not significantly different ($p > 0.05$).
25.4 mm long samples heated in 5.08 cm diameter pipe with CMC at 110°C.

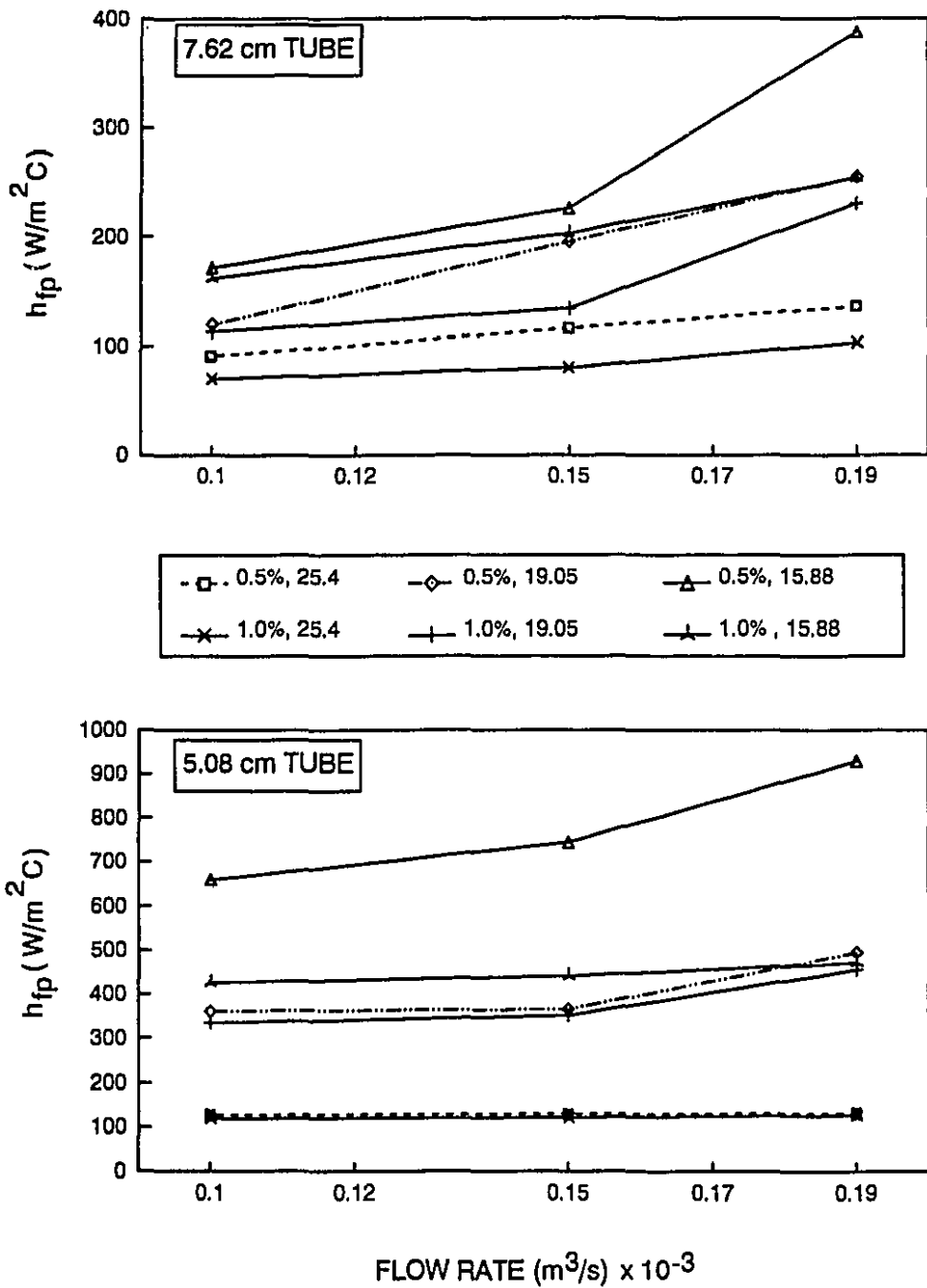


Figure 6.1 Plots of heat transfer coefficients (h_{fp}) as influenced by particle diameter, and fluid flow rate for heating 25.4 mm Teflon particle at 100°C.

(Chapter IV) shows that temperature plays an important role in reducing fluid apparent viscosity, and in conjunction with higher fluid flow rates, manifest itself in revealing the impact of sample diameter on the fluid-to-particle heat transfer coefficient. Again, the observed trend demonstrates that particle diameter plays an important role in establishing critical control points and may represent a limiting factor for highly viscous products. It may be prudent to use higher operating temperatures in simulating aseptic conditions involving larger particles suspended in viscous fluids. It was consistently found for all experimental conditions that h_{fp} values decreased as the particle-to-tube diameter increased (Figure 6.2): d_s , d_m and d_l , representing small (15.9 mm) medium (19.05 mm) and large (25.4 mm) diameter particles respectively in either a 5.08 cm (D2) or 7.62 cm (D3) internal diameter tube. Changing the particle-to-tube diameter ratio from $d_s/D3 = 0.25$ to $d_l/D3 = 0.33$ caused a decrease in h_{fp} by 55% for 1.0% CMC solution flowing at $1.9 \times 10^{-4} \text{ m}^3/\text{s}$ (Figure 6.2). For similar experimental conditions but with 0.5% CMC solution, the change was 47%. Furthermore, changing the tube diameter from 5.08 to 7.62 cm for a 15.88 mm particle in 0.5% CMC caused a decrease in h_{fp} by 74%. However, with a 25.4 mm particle under the same condition, the change was insignificant (Figure 6.2). Changing the tube diameter for a given particle diameter caused a percentage difference up to 75%, the difference, increasing with decreasing flow rate but increasing fluid apparent viscosity. These trends agree with the observation made by Chandarana *et al.* (1988) for cube shaped particles, but contradicts that observed by Zuritz *et al.* (1990), Sastry *et al.* (1990) and Mwangi *et al.* (1993) for spherical particles. Results obtained in the present studies supports that of Chau and Snyder (1988) who found higher heating

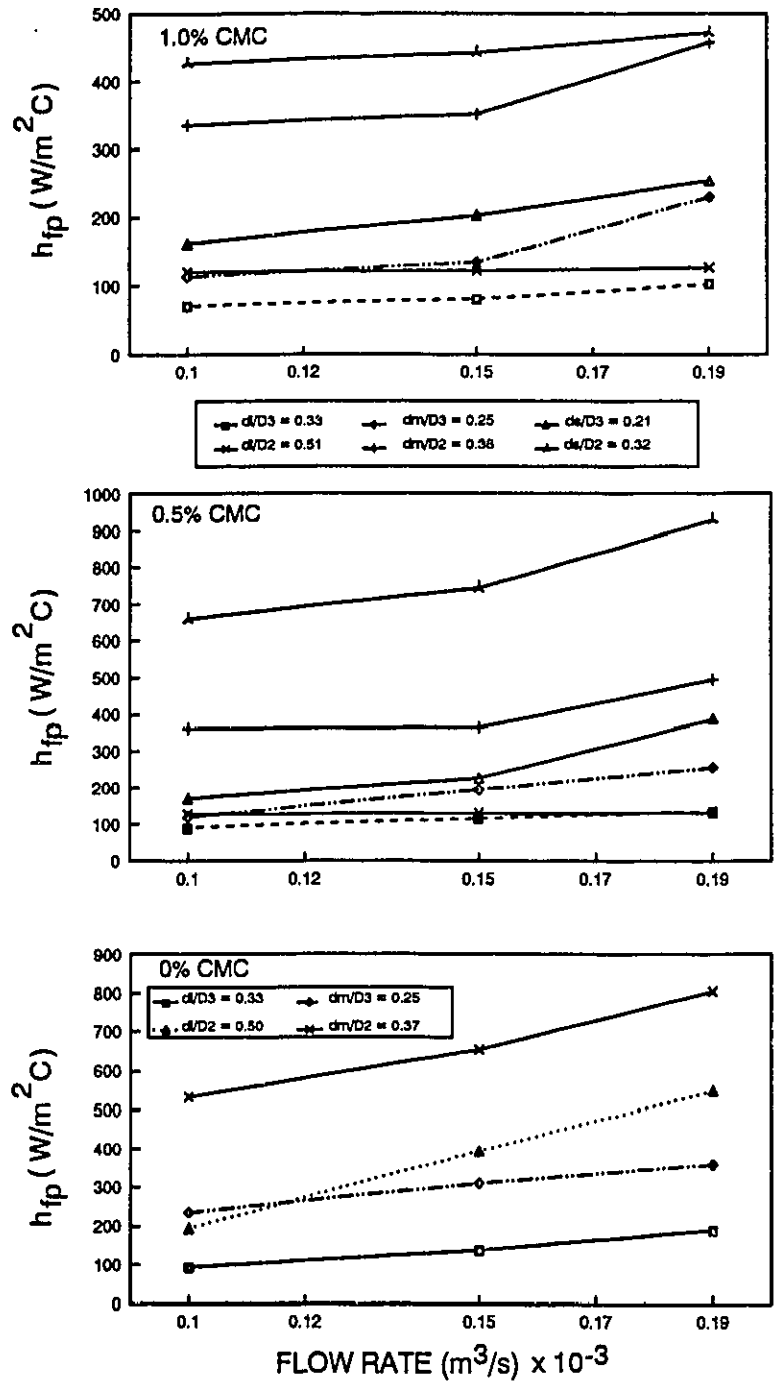


Figure 6.2 Plots of heat transfer coefficients (h_{fp}) as influenced by particle-to-tube diameter and fluid flow rate for heating 25.4 mm length Teflon in 0.5% CMC at 100°C.

rates to be associated with smaller shrimps compared to larger ones. The shape of the shrimp was modelled as a short cylinder followed by a circular cone. Apparently, decreasing volume to area ratio enhances heat transfer. Conversely, decreasing sample diameter increases the surface area to volume ratio. Decreasing volume to area ratio enhances heat transfer and explains the observed trends for finite cylindrical particles in a restricted environment. Although increasing fluid flow rate caused an increase in h_{fp} values for all particle sizes, the reverse trend, ie larger sized particles having higher h_{fp} values than smaller ones under the same flow conditions were generally not encountered. Figures 6.1 and 6.2 show that a linear relationship probably exists between fluid flow rate and particle diameter.

Influence of Fluid Concentration, Temperature and Flow Rate

Dutta and Sastry (1990b) pointed out that one critical factor affecting particle velocity and therefore the heat transfer coefficient is fluid apparent viscosity. Higher viscosities associated with viscous fluids, retard heat transfer rates, especially when the associated turbulences decrease the effective relative fluid-to-particle velocity at the interface. The impact of fluid viscosity and flow rate on h_{fp} has been reported in several studies (Chandarana *et al.*, 1988; Chang and Toledo, 1989; Alhamdan and Sastry, 1990; Alhamdan *et al.*, 1990; Sastry *et al.*, 1990; Zuritz *et al.*, 1990; Gaze *et al.*, 1990; Awuah *et al.*, 1993; Mwangi *et al.*, 1993; Astrom and Bark, 1994). Most of the studies were conducted at low temperatures. Such conditions ignore the combined influence of temperature and concentration on h_{fp} . Studying heat transfer to particulates under free

convection situations, Awuah *et al.* (1993) highlighted the fact that the sensitivity and response of fluid viscosity to higher temperatures may shift natural to mixed or forced convective heat transfer mode. According to Astrom and Bark (1994), aseptic simulations should be carried out with liquids of relevant apparent viscosity at the operating temperature. One major limitation to the use of higher temperatures in studying aseptic processes is the lack of data on rheological properties of carrier fluid at aseptic conditions (Abdelrahim, 1994). In a recent review on modelling continuous sterilization of particulate foods, Sastry (1992b) stressed the fact that food tissues permit free transport of mass across its boundary, and may be considered to possess higher effective thermal conductivities. The author also highlighted the possibility of starch leaching out of starchy particles into the fluid, thus increasing fluid viscosity. These phenomena are most often considered to have negligible effects and therefore ignored in heat transfer studies. A survey of the literature shows a paucity of data to confirm the hypothetical behaviour of real foods. A probable solution will be the use of real food materials as test samples, or a model particle with similar themophysical properties. A material with a very different heat capacity may influence natural convection (Astrom and Bark, 1994). The 3 x 3 x 3 full factorial design experiments involving concentration, flow rate and temperature for two sample (real and model food particle) in a 50.8 cm diameter pipe was carried out in this study to explore the above scenarios although mass transfer aspects were not verified experimentally.

Table 6.4 shows the single and combined influence of the above factors on both potato and Teflon particles of approximately same volume to surface area ratio. The

Table 6.4 Analysis of variance for the 3x3x3 factorial design of factors influencing the fluid-to-particle convective heat transfer coefficient.

Source	dF	SS ^T	F ^T	SS ^P	F ^P
Model	26	2419537	261***	2260081	123***
Main effects					
Temperature (T)	2	334615	469***	996623	702***
Concentration (C)	2	1039027	1458***	707589	499***
Flow rate (F)	2	412391	578***	307638	216***
interactions					
T x C	4	169673	119***	89501	31***
T x F	4	147482	104***	51288	18***
C x F	4	124060	87***	68857	24***
T x F x C	8	192287	67***	38586	7***
Residual (error)	97 ^T (120 ^P)	34573		85083	
Total	123 ^T (146 ^P)	2454109		2345164	
R^{2b}			0.99 ^T		(0.96 ^P)

^TTeflon; ^PPotato

***Level of significance (p < 0.0001)

^b Coefficient of determination

analysis of variance using the General Linear Model (GLM) procedure indicated the model was highly significant ($p < 0.0001$) with an R^2 value greater than 0.95 for both samples. Examination of the data (Table 6.4) shows that all main factors, i.e., temperature (T), concentration (C), and flow rate (F) significantly influenced the convective heat transfer coefficient. Furthermore, the two factor interactions, Temperature*Concentration (T*C), Temperature*Flow rate (T*F), and Concentration*Flow rate (C*F) and the three factor interaction significantly influenced estimated h_{fp} . Based on the highly positive correlation coefficients of the main effects and their higher order interactions, estimated heat transfer coefficient can be said to be affected as the level of each factor changes. Conversely, a decrease in the level of each factor except for concentration will result in a decrease in estimated h_{fp} . However, the trends for each level and their interaction for both materials looked somewhat different.

The effect plots of the influence of various parameters and some of their interactions on h_{fp} are presented in Figures 6.3-6.8. The flow rate effect was generally linear in the range studied (Figure 6.3) especially with Teflon particles. h_{fp} values increased by 50% (potato) and 100% (Teflon) as the flow rate changed from 1.0×10^{-4} to $1.9 \times 10^{-4} \text{ m}^3/\text{s}$. The effect of temperature, however, was found to be more pronounced for heating potatoes than Teflon (Figure 6.4). A 6% increase resulted when the temperature increased from 100 to 110°C for Teflon. Within the same temperature margin, a 40% increase was found for heating potato. This suggests that temperature probably ruptured/altered the interfacial/boundary layer characteristics which enhanced heat transfer. The release of gases as suggested by Sastry (1992b) may have caused a thermal boundary

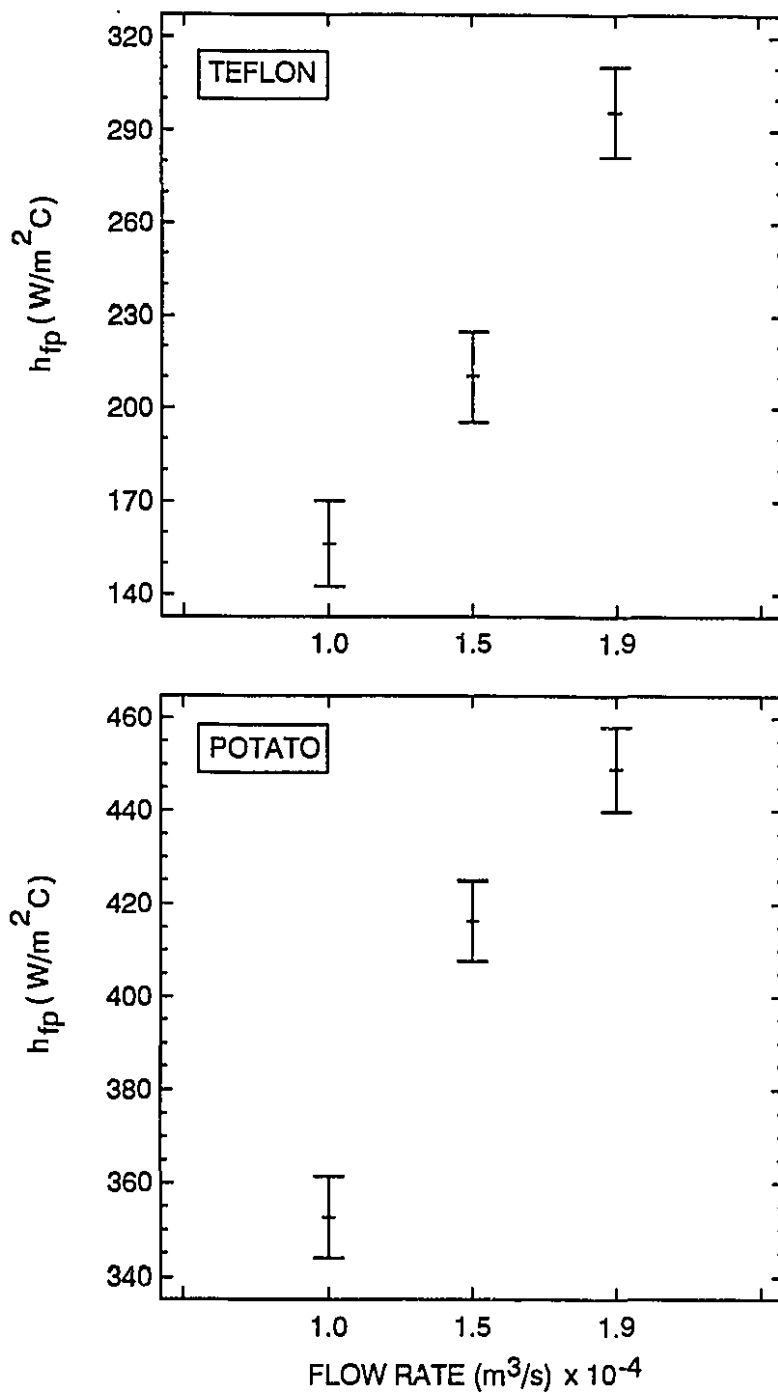


Figure 6.3. Heat transfer coefficients (h_{fp}) as influenced by flow rate for heating Teflon and potato particles.

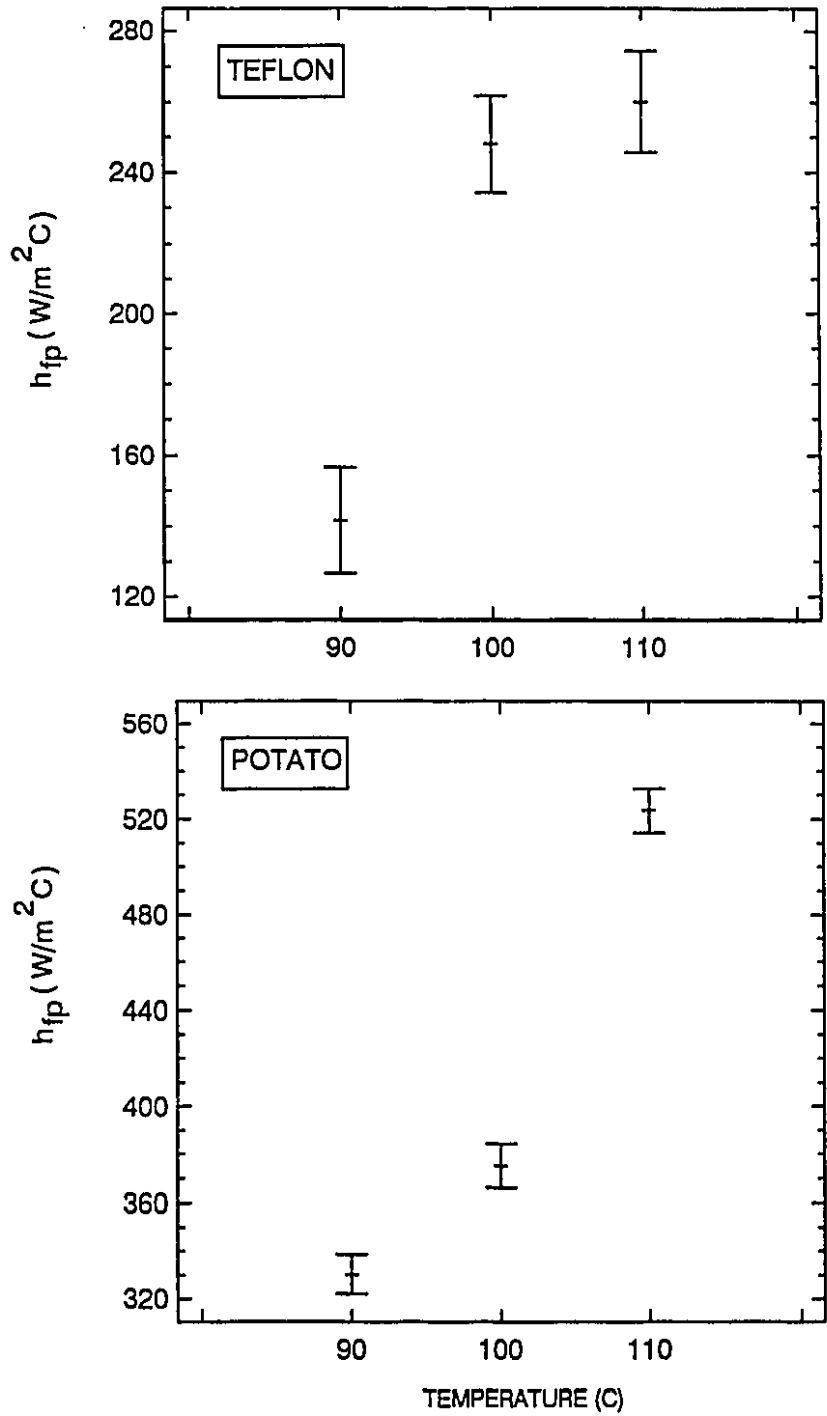


Figure 6.4. Heat transfer coefficients (h_{fp}) as influenced by temperature for heating Teflon and potato particle.

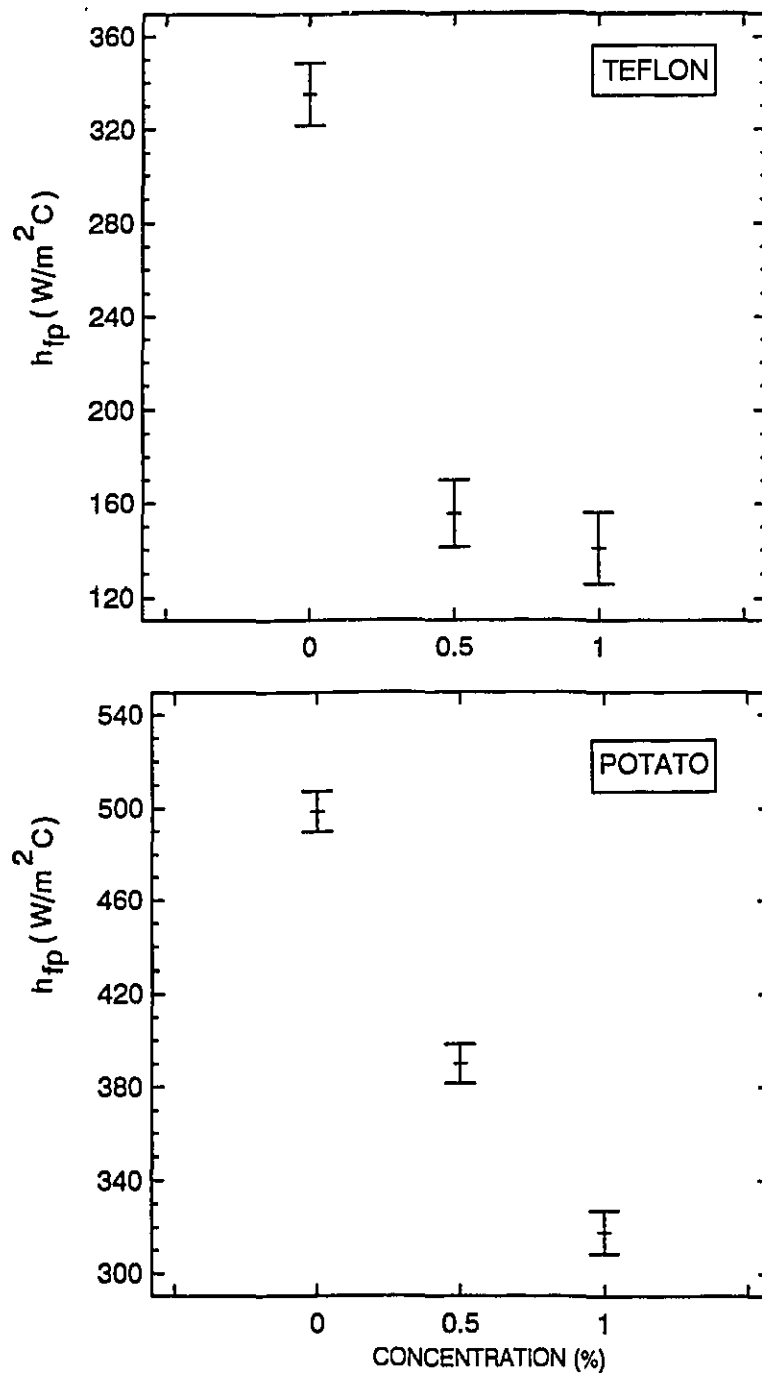


Figure 6.5. Heat transfer coefficients (h_{fp}) as influenced by fluid concentration for heating Teflon and potato particles.

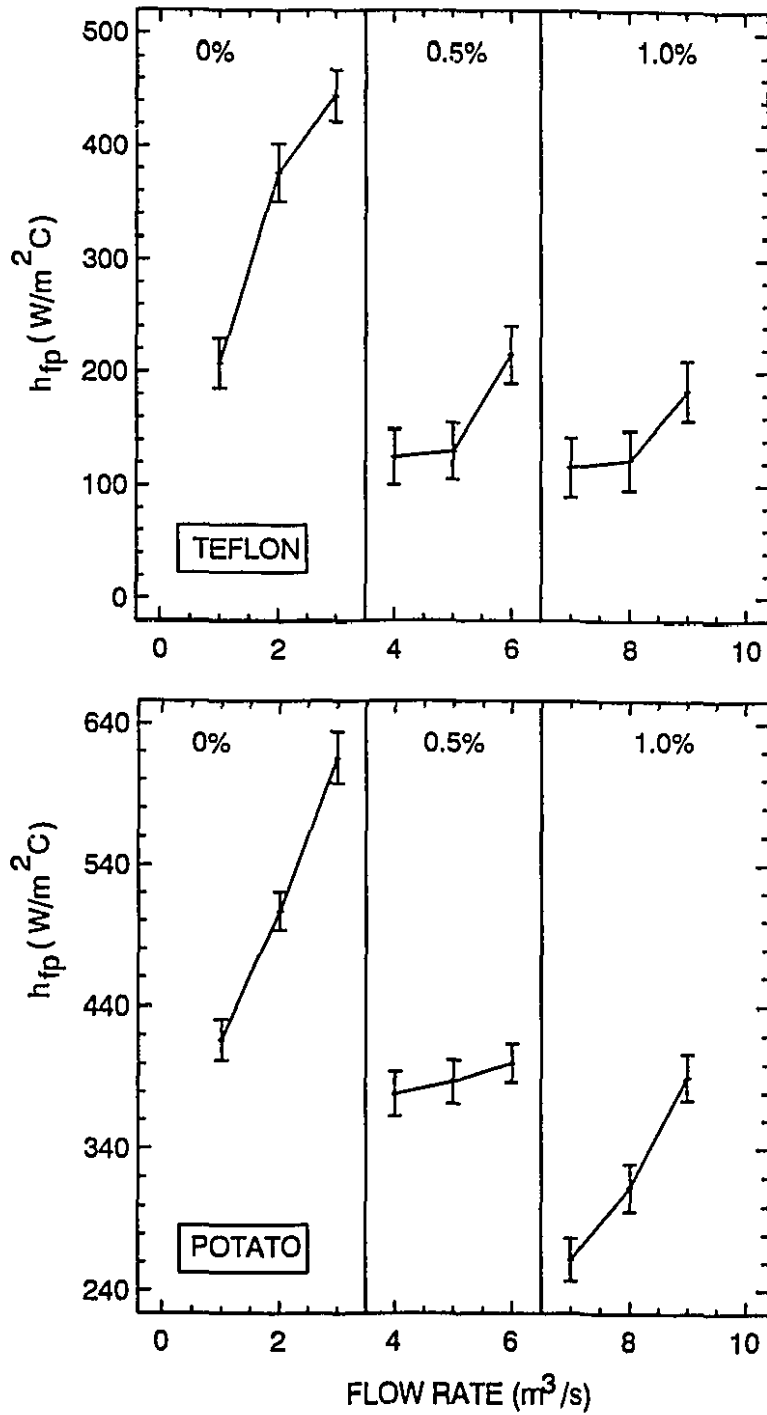


Figure 6.6. Heat transfer coefficients (h_{fp}) as influenced by fluid concentration and flow rate for heating Teflon and potato samples.

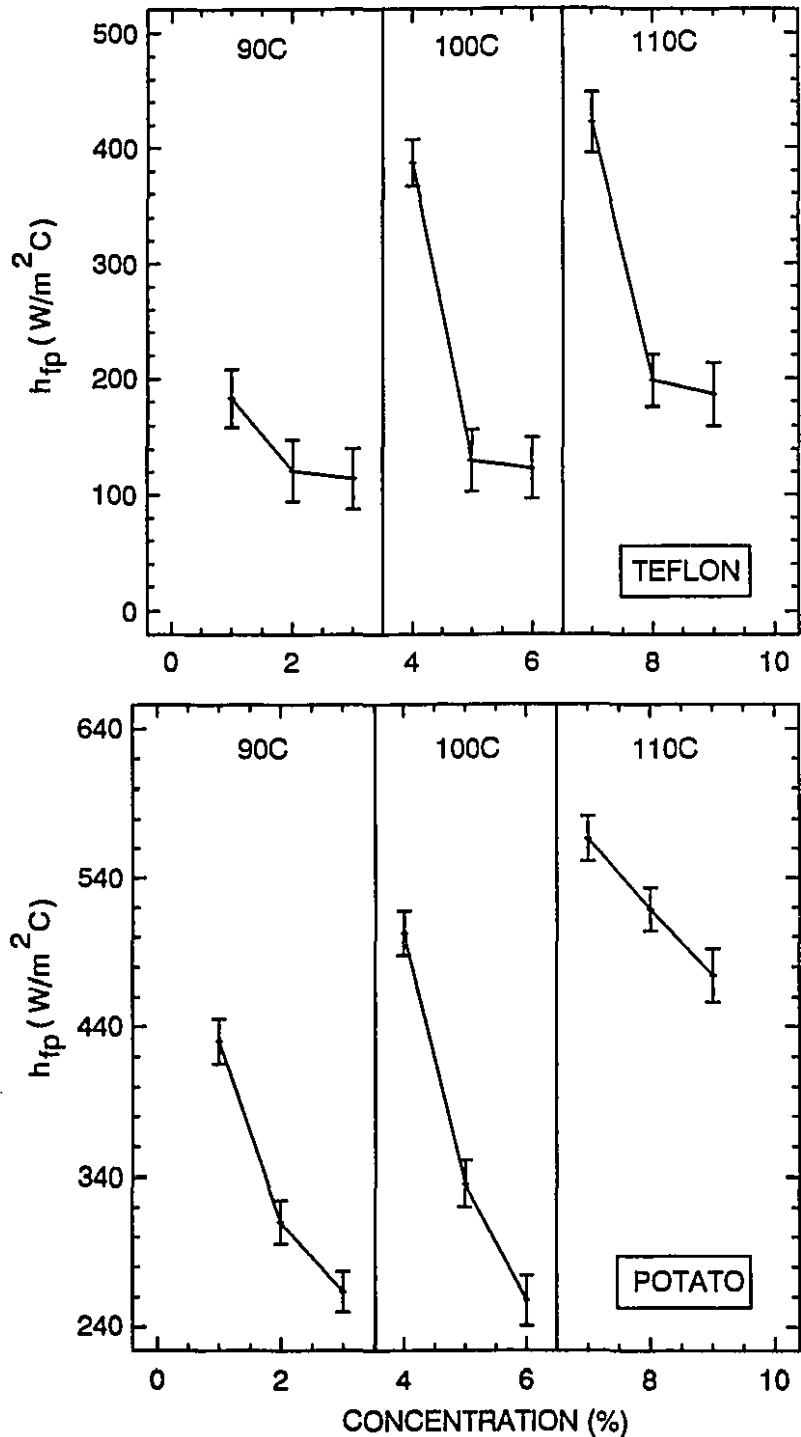


Figure 6.7 Heat transfer coefficients (h_{fp}) as influenced by fluid temperature and concentration for heating Teflon and potato particles.

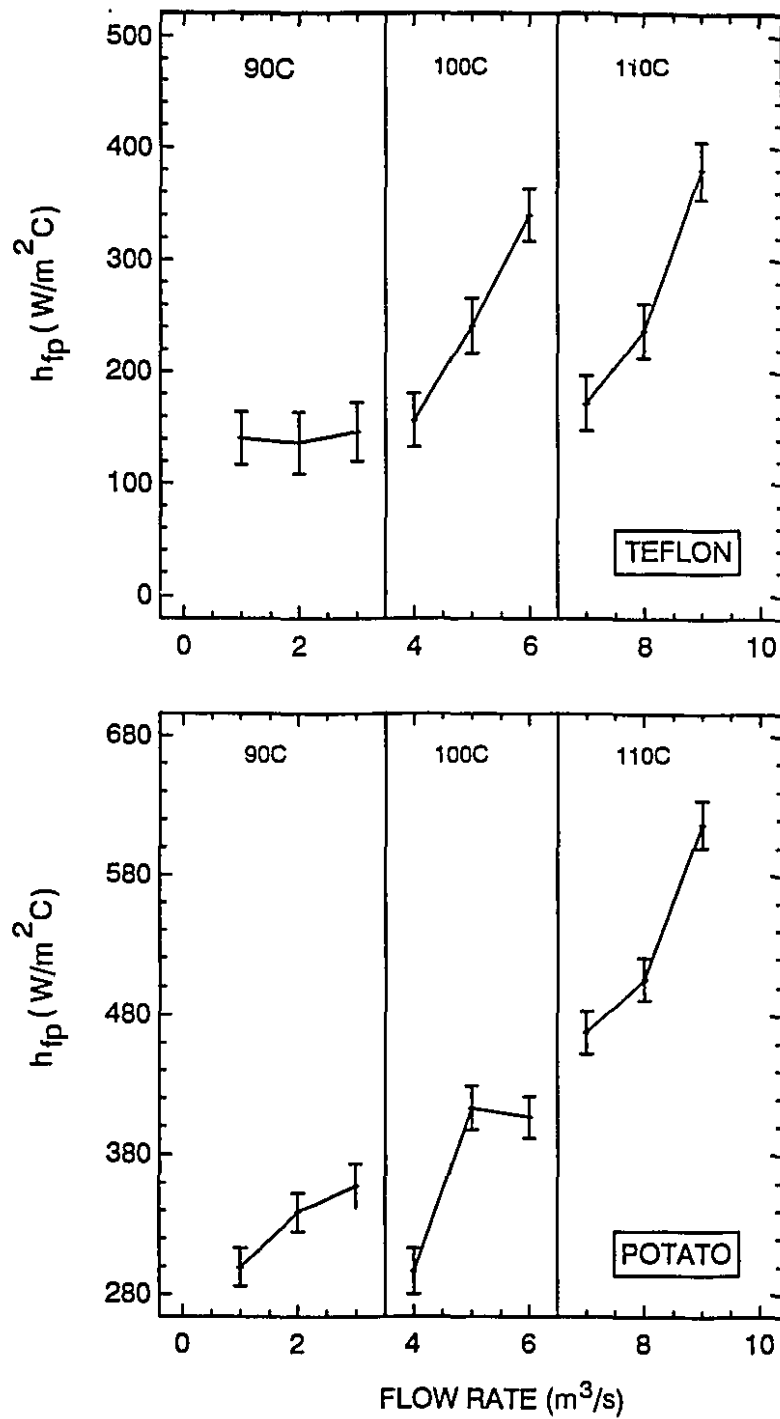


Figure 6.8. Heat transfer coefficient (h_{fp}) as influenced by fluid flow rate and temperature for heating Teflon and potato particles.

layer disruption, resulting in the enhancement of the fluid-to-particle interface heat transfer coefficient. One surprising trend is that of concentration on the two samples. The impact of concentration on h_{fp} for Teflon was much more drastic between 0 and 0.5% CMC (54% drop) but levelled off between 0.5 and 1.0% CMC (Figure 6.5), giving a marginal 9% drop from 0.5 to 1.0% CMC concentration. Within the same range for potato, approximately 20% drop occurred in a linear fashion. Figures 6.6, 6.7, and 6.8 show graphically, the two way interaction effects of fluid temperature, concentration and flow rate on both Teflon and potato. With the exception of potato treated at 100°C for flow rates between 1.5 and 1.9 x 10⁻⁴ m³/s which had no significant differences (Figure 6.8), all figures show definite trends of the combined effects on h_{fp} , supporting the above trends for the main effects.

Figure 6.7 shows a linear decrease in h_{fp} with decreasing concentration for a given temperature for potato, while with Teflon, the h_{fp} values dropped quickly between 0 and 0.5% concentrations and changed somewhat moderately thereafter. The impact of fluid concentration at 90°C on Teflon was less pronounced as compared to other conditions for potato. These trends suggest significant interaction between system and product parameters. Heat transfer coefficients determined by Hassan (1984) were higher for potato than for Teflon processed in a can containing water. During heating in silicone fluids, the author found higher values to be associated with Teflon than aluminium particles of the same size. Stoforos (1988) observed similar trends: Teflon particle exhibited higher h_{fp} values than aluminium in an axially rotated can. So far as properties such as specific heat, and surface roughness density (in the case of mobile particle) does not affect particle-

fluid flow profiles, the material/nature of the particle should theoretically not be reflected on estimated heat transfer coefficients since h_{fp} is a boundary layer property. The response of food particles to temperature and concentration demonstrated in this study illustrates that mass transfer does occur between the particle and fluid, and proves the need to utilize real food particle in heat transfer studies, since natural convective contributions become inevitable as a result of differences in specific heat capacities.

Heat Transfer Coefficients Associated with Cooling Heated Samples

Irrespective of contributions made toward overall lethality during cooling and heating, the FDA recognizes that achieved in the holding tube alone. Contribution realized during cooling serves as a safety factor (Dignan *et al.*, 1989). On achieving the required lethality, quality becomes the primary goal. As such cooling should be carried out as quickly as possible to prevent overprocessing, because suspended particles cool slowly compared to the carrier fluid. Under natural convection situations, test material assumes greater importance (Astrom and Bark, 1994). Since starch gelatinizes on heating beyond 70°C, structural changes occur and probably would affect the heat transfer coefficient. Table 6.5 shows that heat transfer coefficients associated with heating are significantly higher than cooling ($p < 0.05$). For example, a 36% difference occurred between heating raw potato sample from 20 to 90 °C and cooling heated samples from 90 to 20 °C. The reason for the differences can be related to difference in (1) the interfacial characteristics resulting from textural differences between cooked and raw potatoes, (2) lower fluid apparent viscosity associated with higher temperatures and (3) moisture transfer occurs

Table 6.5. Comparison of heat transfer coefficients associated with heating and cooling potato samples in water at selected initial temperatures and flow rate.

Flow rate ($\times 10^{-4}$ m ³ /s)	MTemp ¹ (°C)	PTemp ² (°C)	h_{ip} (W/m ² C)	Coefficient of variation (%)
1.61	20	100	190 ^d	3.7
1.53	20	100	183 ^{de}	2.7
1.01	20	100	177 ^{ef}	4.0
1.61	20	90	189 ^d	2.7
1.53	20	90	170 ^f	2.9
1.61	20	110	189 ^d	5.3
1.61	90	20	294 ^c	5.4
1.62	100	20	343 ^b	2.6
1.71	110	20	360 ^a	2.2

^{a-b}Mean values sharing different superscript are significantly different (p<0.05)

¹Heating medium temperature in 7.62 cm internal diameter pipe.

²Initial temperature of the particle.

Particle length and diameter are 24 and 21 mm respectively.

at a faster pace with raw potato. Alhamdan *et al.* (1990) found that the average heat transfer coefficient for heating was 140 to 200% higher than for cooling. The authors used an aluminium-shaped particle under natural convection conditions. The initial particle temperature prior to cooling had no significant effect ($p > 0.05$) on estimated heat transfer coefficients. Changing fluid flow rate followed the trend discussed earlier but had insignificant effect on the heat transfer coefficient.

Influence of Particle Shape

Particle shape is generally known to have an influence on h_{fp} as a result of differences in fluid flow profiles for different geometries. Using mathematical simulations, Lee *et al.* (1990a) found the temperature at the centre of a spherical particle to increase faster than an infinite cylinder, which in turn increased faster than an infinite slab. For the same percentage of particulate matter according to Chandarana and Gavin (1989b), the holding tube length required for cube-shaped particles was greater than cylindrical particles which in turn was greater than spherical particles of the same maximum dimensions. Although the volume to surface area for a cube is identical to that of a cylinder whose height and diameter are equal to the linear dimension of a cube, the above trend was observed by the author. Contrary to that, Astrom and Bark (1994) found no differences in heat transfer coefficients estimated with a lead cube and sphere of the same volume. The authors conducted their experiments in a rotating fluid, i.e., a stationary particle placed in a rotating cylinder. They reasoned that the ability to transfer hot fluid to particle surfaces is limited when a sphere or cube is exposed to a fluid in pure rotation.

Apparently very little information has been presented in the open literature on the effect of particle shape on h_{fp} .

Table 6.6 shows differences in h_{fp} associated with different shapes (sphere and finite cylinder) of equal diameters. Spherical shaped particles gave higher h_{fp} values compared with finite cylinders of the same diameter. Higher values associated with spherical particle can be attributed to the smaller volume to surface area ratio or larger area to volume ratio. Again, flow rate had significant influence while the effect of concentration levelled off between 0.5 and 1.0% CMC solution for spherical particles. Between 7 to 29% difference (Table 7.6) occurred between a spherical particle and a finite cylinder with a length-to-diameter ratio of one.

CONCLUSIONS

A detailed study has been made describing the magnitude, influence, and variation in critical processing parameters including particle size, shape, flow rate, concentration, temperature, pipe diameter, and particle orientation on the fluid-to-particle heat transfer coefficient. System temperature ranged from 90 to 110°C for 0 to 1.0% CMC concentration travelling between 1.0 to 1.9×10^{-4} m³/s. Depending on experimental conditions, the h_{fp} value ranged from 56 to 966 W/m²C for heating Teflon and potato samples, with Biot numbers ranging from 5 to 42. Particle length and its orientation in the holding tube had no significant ($p > 0.05$) effect on h_{fp} , indicating that sample length may not play a leading role in the establishment of critical control parameters especially for viscous fluids under low to moderate flow conditions. Sample diameter (15.9 -25.4

Table 6.6. Heat transfer coefficients as influenced by particle shape under selected conditions for flow rate, pipe diameter and fluid concentration at 100°C.

Shape ¹	Tube ² cm	Flow rate ($\times 10^{-4}$ m ³ /s)	Conc %	Length mm	Volume/area ² ($\times 10^{-3}$ m)	h_{fp} W/m ² C
Sph	7.62	1.9	0.0	-	3.18	475 ^a
Sph	7.62	1.5	0.0	-	3.18	395 ^{bc}
Sph	7.62	1.0	0.0	-	3.18	280 ^{efg}
Sph	7.62	1.9	0.5	-	3.18	300 ^{ef}
Sph	7.62	1.5	0.5	-	3.18	271 ^{fg}
Sph	7.62	1.0	0.5	-	3.18	254 ^{gh}
Sph	7.62	1.9	1.0	-	3.18	300 ^{ef}
Sph	7.62	1.5	1.0	-	3.18	270 ^{fg}
Sph	7.62	1.0	1.0	-	3.18	249 ^{gh}
Sph	5.08	1.9	0.5	-	3.18	502 ^a
Sph	5.08	1.5	0.5	-	3.18	418 ^b
Sph	5.08	1.0	0.5	-	3.18	376 ^{cd}
Cyl	7.62	1.9	0.5	20	3.23	279 ^{gh}
Cyl	7.62	1.5	0.5	20	3.23	235 ^h
Cyl	7.62	1.0	0.5	20	3.23	180 ⁱ
Cyl	5.08	1.9	0.5	25.4	3.46	496 ^a
Cyl	5.08	1.5	0.5	25.4	3.46	365 ^{cd}
Cyl	5.08	1.0	0.5	25.4	3.46	361 ^d
Cyl	7.62	1.9	0.5	25.4	3.46	255 ^{gh}
Cyl	7.62	1.5	0.5	25.4	3.46	195 ⁱ
Cyl	7.62	1.0	0.5	25.4	3.46	120 ^j
Cyl	7.62	1.9	1.0	25.4	3.46	230 ^h
Cyl	7.62	1.5	1.0	25.4	3.46	134 ^j
Cyl	7.62	1.0	1.0	25.4	3.46	114 ^j
Cyl	7.62	1.9	0.0	25.4	3.46	360 ^d
Cyl	7.62	1.5	0.0	25.4	3.46	311 ^c
Cyl	7.62	1.0	0.0	25.4	3.46	235 ^h

¹Sph and cyl represents 19.05 mm diameter sphere and cylinder respectively .

²Diameter of the tube.

^{a-j}Mean values of h_{fp} sharing the same superscript are not significantly different ($p > 0.05$).
Least Significance Difference (LSD) = 31.5.

mm), flow rate and temperature had significant ($p < 0.05$) influence on the convective heat transfer coefficient. As opposed to reported trends of h_{fp} increasing with particle diameter resulting from localized turbulence, smaller sized particle were generally found to have higher h_{fp} values compared to larger ones for all experimental conditions. Increasing particle diameter from 19.05 to 25.4 mm decreased h_{fp} between 36 to 72% depending on fluid flow rate and concentration. Changing particle-to-tube diameter ratio between 0.21 to 0.50 caused up to 74% change in the heat transfer coefficient. Higher percentage differences were found to be associated with viscous fluids at lower flow rates.

For a given tube diameter the heat transfer coefficient increased with decreasing sample diameter, suggesting higher h_{fp} values to be associated with smaller volume to surface area ratios. Although temperature, concentration, flow rate and their interactions had significant influence on estimated h_{fp} , the impact was found to depends on the type of material used due to differences in specific heat capacities which plays a significant role under natural convection situations. Increasing temperature from 100 to 110°C increased h_{fp} by 6% for Teflon and 40% for potato. Spherical particles were generally found to have higher h_{fp} compared to cylindrical particles of the same diameter. A 7 to 29% difference was observed between a sphere and a finite cylinder having similar dimensions. A 36% difference was also found between values of h_{fp} estimated from heating and cooling.

CHAPTER VII

DIMENSIONLESS CORRELATIONS FOR MIXED AND FORCED CONVECTION HEAT TRANSFER TO SPHERICAL AND FINITE CYLINDRICAL PARTICLES IN A PILOT SCALE ASEPTIC HOLDING TUBE SIMULATOR

ABSTRACT

Dimensionless correlations for estimating heat transfer coefficients for spherical and finite cylinders under mixed and forced convection heat transfer regimes were individually investigated using multiple regression of significant dimensionless groups. Real and model food particles were heated in both Newtonian and non-Newtonian fluids flowing in tubes at processing conditions comparable to commercial aseptic processing situations. The type of test material was found to have significant impact on the Nusselt number, and hence developed correlations. Introducing a diffusivity ratio defined as the ratio of particle-to-fluid thermal diffusivities was consistently found to improve developed models. Excellent correlations ($R^2 \geq 0.97$) were obtained between the Nusselt number and dimensionless groups for all models. Natural convection in heat transfer correlations in situations where forced convection is expected to be the dominant mechanism was accommodated.

INTRODUCTION

Aside from residence time distribution of particulates travelling in continuous heat-hold-cool systems, interfacial fluid-to-particle convective heat transfer coefficients (h_p)

play a key role in establishing proper processing schedules from both quality and safety standpoints (Dignan *et al.*, 1989; Pflug *et al.*, 1990). However, h_p values present one of the most difficult parameters to estimate under practical aseptic conditions (Sastry, 1989a,b; Larkin, 1990).

Aseptic processing systems generally require a pump for feeding raw materials to the heat exchanger and the holding tube. Since carrier fluids associated with such products are generally viscous and non-Newtonian in nature, heat treatment times become complex as a result of the dependence of residence times on particle size and density, shape, concentration of the carrier fluid and system parameters such as temperature, pressure, fluid flow rate and system configuration. Therefore, lethalties achieved by individual particles will depend on such factors as well as the relative velocities between the fluid and the particle.

The pumping mechanism associated with particulate laden products suggest forced convection as the dominant mechanism of heat transfer between the fluid and particles. However, since fluid flow rates are usually low, the mechanisms involved are complex combinations of natural and forced convection; the predominant mechanism depending on system design and operational conditions (Alhamdan and Sastry, 1990). In all forced convection situations (Fand and Keswani, 1973), natural convection operates since buoyant forces resulting from density gradients persist. Since mixed convection occurs whenever there is a temperature difference between the convecting body and the fluid along with the slightest amount of forced fluid, buoyant as well as inertial forces operate simultaneously within the fluid, and in some situations, may have the same order of

magnitude (Ozisik, 1985, Chapman, 1989). In such circumstances, heat losses should be related to a combined effect rather than either natural or forced convection alone (Fand and Keswani, 1973).

Studies related to natural and forced convection about submerged particles include those by Yuge (1960), Klyachko (1963) and Johnson *et al.*(1988) for spheres in air; Chandarana *et al.* (1990b), Chang and Toledo (1989), Alhamdan *et al.* (1990), Alhamdan and Sastry (1990), Sastry *et al.* (1990), Zuritz *et al.* (1990), Mwangi *et al.* (1993) and Astrom and Bark (1994) for either spherical, cube shaped, or irregular shaped particles in Newtonian or non-Newtonian fluids. In most of the above studies especially those involving non-Newtonian fluids, proposed dimensionless correlations describe the dominance of either natural or forced convection alone at relatively lower operating temperatures. The conservative approach has generally been to assume zero velocity between the fluid and particle, resulting in a Nusselt number of 2.0 for spherical particles (Geankoplis, 1978) and 0.3 for an infinite cylinder (Gnielinski, 1983) respectively. Although several predictive models and computer softwares (Sastry, 1986; Larkin, 1989, Chandarana *et al.*, 1989, Skjoldebrand and Ohlsson, 1993a,b) have been presented for estimating product sterility and quality optimization, good estimates of the fluid-to-particle heat transfer coefficient is an important prerequisite for successful implementation of such models.

In real dynamic flow conditions, dimensionless correlations are hard to use since the relative particle-to-fluid velocity is unknown (Maesmans *et al.*, 1992). Although the Nusselt number depends primarily on fluid properties, the heat capacity and thermal

conductivity of the particle material (Astrom and Bark, 1994) can be expected to influence the rate of heat transfer to the fluid and to some extent enhance free convection. The open literatures shows lack of information on the combined effect of forced and natural convection to the overall transfer of heat under aseptic conditions.

The objective of this study was to develop dimensionless correlations for mixed and forced convection heat transfer to spherical and cylindrical particles processed in a pilot scale holding tube simulator operated at temperatures between 90 and 110°C.

THEORETICAL CONSIDERATIONS

Analytical solution to heat transfer problems involve simultaneous solution of Navier-Stokes equations of motion and continuity, and the energy equation for four dependent variables including two-dimensional velocity components, pressure, and temperature (Sucec, 1985; Burmeister, 1983; Chapman, 1989). The equations involved are sufficiently complex that analytical solutions can be obtained for simple boundary conditions and geometry (Chapman, 1989). From dimensional analysis, the convective heat transfer coefficient is expressed in terms of the Nusselt number (Nu), which is generally described as a function of the Reynolds (Re), Prandtl (Pr), and Grashof (Gr) numbers:

$$Nu = f(Re, Pr, Gr) \quad (7.1)$$

Heat transfer coefficients associated with pure forced convection is generally evaluated

from the expression:

$$Nu = C + D(Re)^n (Pr)^p \quad (7.2)$$

where C, D, n and p are constants. The constant p varies between 0.3 and 0.4 with the lower value being commonly used (Morgan, 1975). For infinite cylinders, Žhukauskas (1972) found 0.37 to be more suitable. For flow past a single spherical particle, the average heat transfer coefficient can be estimated from the following relationship (Geankoplis, 1978), which is valid for Reynolds and Prandtl numbers between 1 and 70,000 and 0.6 to 400 respectively:

$$Nu = 2.0 + 0.60 Re^{0.5} Pr^{1/3} \quad (7.3)$$

Whitaker (1972), presented a more general correlation for flow of gases and liquids across a single sphere in the form:

$$Nu = 2.0 + (0.4 Re^{0.5} + 0.06 Re^{2/3}) Pr^{0.4} \left(\frac{\mu_\infty}{\mu_w} \right)^{0.25} \quad (7.4)$$

Eq. (7.4) is valid for Re between 3.5 and 80000, Pr between 0.7 and 380, and μ_∞/μ_w between 1 and 3.2. For free convection on an isothermal horizontal cylinder, Churchill and Chu (1975) proposed a relationship, valid for Rayleigh number (Ra) between 10^{-4} and 10^{12} :

$$Nu^{1/2} = 0.60 + \frac{0.387 Ra^{1/6}}{[1 + (0.559/Pr)^{9/19}]^{8/27}} \quad (7.5)$$

For flow of gases and liquids over a single cylinder, Whitaker (1972) proposed the relationship:

$$Nu = [0.4 Re^{0.5} + 0.06 Re^{2/3}]^{0.4} \left(\frac{\mu_{\infty}}{\mu_w} \right)^{0.25} \quad (7.6)$$

which is valid for Re between 40 and 10^5 ; Pr between 0.67 and 300; and μ_{∞}/μ_w between 0.25 and 5.2. Churchill and Bernstein (1977) correlated experimental data from several fluids including air, water, and liquid sodium to derive an expression for a cylinder, which is valid for Re between 100 and 10^7 and Peclet number (Re.Pr) greater than 0.2 for forced convection:

$$Nu = 0.3 + \frac{0.62 Re^{1/2} Pr^{1/3}}{[1 + (0.4/Pr)^{2/3}]^{1/4}} \left[1 + \left(\frac{Re}{282,000} \right)^{5/8} \right]^{4/5} \quad (7.7)$$

The magnitude of the dimensionless group Gr/Re^2 , describes the ratio of buoyant to inertia forces and governs the relative importance of free to forced convection. Again, it delineates free, forced, and mixed convection regimes (Ozisik, 1985; Sucec, 1985; Chapman, 1989). Yuge (1960), indicated that forced convection dominates for flow over a sphere when the condition $Gr/Re^2 < 0.01$ is satisfied. According to Johnson *et al.* (1988), mixed convection occurs when the ratio Gr/Re^2 falls between 0.08 and 5.10. The

authors performed numerical evaluation of the Navier-Stokes momentum equations and the energy equations using a finite difference procedure, and verified their analysis with experimental data obtained from an isothermal sphere submerged in a wind tunnel with air flowing vertically upward. For a horizontal cylinder in cross flow, Fand and Keswani (1973) found forced convection to dominate when $Gr/Re^2 < 0.5$, whereas natural convection dominated when the ratio exceeded 40. Between 0.5 and 2, natural convection contributed 10% to the overall heat transfer. According to the authors, both forced and natural convection are of the same order of magnitude when the ratio falls between 2 and 40 for a cylinder. For the same order of magnitude the two mechanisms should be analyzed simultaneously (Ozisik, 1985).

To make the significance of Gr/Re^2 plausible, the ratio of buoyant to inertial forces is often considered in mixed convection models. For air flow normal to a long horizontal cylinder, Oosthuizen and Madan (1970) recommended for $100 < Re < 3000$ and $2.5 \times 10^4 < Gr < 3 \times 10^5$, the relationship:

$$\frac{Nu}{Nu_{forced}} = 1 + 0.18 \frac{Gr}{Re^2} - 0.011 \left(\frac{Gr}{Re^2} \right)^2 \quad (7.8)$$

where $Nu_{forced} = 0.464Re^{1/2} + 0.0004Re$. Churchill (1977) in a critical survey on mixed convection, suggested the relationship:

$$Nu_{combined}^3 = Nu_{forced}^3 + Nu_{natural}^3 \quad (7.9)$$

In order to correlate data for the region $0.5 < Gr/Re^2 < 2.0$ where forced convection

contributed over 90%, Fand and Keswani (1973) considered natural convection as an additive term, but proportional to Gr/Re^2 raised to a power (m) which depends on the orientation of the fluid velocity relative to the gravitational field:

$$Nu = \left[0.255 + 0.699 Re^{0.5} + C \left(\frac{Gr}{Re^2} \right)^m \cdot Gr^{0.25} \right] Pr^{0.29} \quad (7.10)$$

where C and m are constants ranging from -0.0240 to 0.0330 and 0.15 to 0.30 respectively.

MATERIALS AND METHODS

Materials and Experimental Conditions

Spherical Teflon, cylindrical potato and Teflon samples were prepared as detailed in Chapters III and IV, and heated under simulated flow rates at temperatures between 90 and 110°C using either Newtonian or non-Newtonian fluids (0 - 1.0% CMC solutions) in two pipes of internal diameters 5.08 and 7.62 cm. High temperature rheological data, obtained in the form of power law model parameters m, and n are listed in Table 7.1 (Abdelrahim, 1994). Physical properties for Teflon and potato are as detailed in Chapters III and IV. Physical properties for water were obtained from Chapman (1989). Heat transfer coefficients were estimated with the rate method and the Nusselt numbers were calculated from the relationship $Nu = h_{fp} d_{cd} / k_f$, where d_{cd} and k_f are the characteristic dimension of the particle and thermal conductivity of the fluid respectively.

Table 7.1 Power law parameters^a for CMC solution rheology at various temperatures and concentrations

Concentration (%)	Temperature (°C)	Consistency Coefficient (Pas ⁿ)	Flow behaviour index
0.5	90	0.046	1.012
0.5	100	0.029	1.041
0.5	110	0.021	1.042
1.0	90	0.199	0.751
1.0	100	0.078	0.820
1.0	110	0.062	0.989

^aAbdelrahim (1994)

Characteristic Dimension

Zuritz *et al.* (1990) used the projected cap perimeter of a mushroom-shaped particle to develop dimensionless relationships. For an infinite cylinder in cross flow, the diameter is generally used as the characteristic dimension, whereas the length is used for axial flows (ASHRAE, 1981; Žukauskas and Žiugžda, 1985). For a finite cylinder, both diameter (d) and length (L) can be expected to influence heat transfer. King (1932) recommended the ratio of the product of d and L to the sum of d and L as the characteristic dimension. Sparrow and Ansari (1983) refuted King's approach on the basis that it overpredicted heat transfer coefficients by 40 to 50% for a finite cylinder with diameter-to-length ratio equal to unity. The authors suggested particle diameter as the appropriate dimension. Since the diameter-to-length ratio used in the present study varied between 0.63 and 1.0, two characteristic dimensions were investigated in addition to those reported in the literature. Firstly, a correlation which incorporates the length of the cylinder was adopted. This was defined as the diameter of a sphere having the same volume as a finite cylinder, giving a simplified relationship $d_s = 1.15d_c$, where d_s and d_c represents the diameters of a sphere and cylinder respectively when the diameter-to-length ratio of the cylinder is unity. The 15% increase was redefined to include particle length as follows:

$$d_{cd} = d \left(1 + \frac{0.15d}{L} \right) \quad (7.11)$$

where d_{cd} and L are the characteristic dimension and length of a cylinder respectively. The

second characteristic dimension was defined as the volume-to-total surface area ratio of a cylinder, giving a simplified relationship:

$$d_{cd} = \frac{0.5L}{\left(1 + \frac{2L}{d}\right)} \quad (7.12)$$

Characteristic dimensions defined above were individually tested for appropriateness in correlating experimental data.

Data Analysis

The criteria suggested by Fand and Keswani (1973), Yuge (1960), and Johnson *et al.* (1988) for a cylinder and sphere were individually considered in establishing the appropriate regimes prior to data analysis. However, in view of the fact that simulated relative velocities were obtained through pumping, forced convection was considered as a first approximation, neglecting natural convection and using a modified relationship which takes particle and tube dimensions into consideration:

$$Nu = A + B Re^n Pr^m \left(\frac{d_p}{D_t}\right)^r \left(\frac{d_p}{L_p}\right)^s \quad (7.13)$$

To account for natural convection the generalized Grashof and Gr/Re^2 were simultaneously introduced and investigated as follows:

$$Nu = A + B Re^n Pr^m Gr^q \left(\frac{d_p}{D_t}\right)^r \left(\frac{Gr}{Re^2}\right)^s \left(\frac{d_p}{L_p}\right)^t \quad (7.14)$$

where A, B, n, m, q, r, s and t are constants. Multiple regression was performed after logarithmic linearization of each model. The criteria used to evaluate accuracy of fit for each model were the coefficient of determination (R^2), the percentage average error (PAE), the percentage deviation modulus (PDM) and percentage standard deviation (PSD) defined respectively as follows:

$$PAE = \frac{1}{n} \sum_{i=1}^n M_i \quad (7.15)$$

$$PDM = \frac{1}{n} \sum_{i=1}^n |M_i| \quad (7.16)$$

$$PSD^2 = \frac{1}{n-1} \left[\sum_{i=1}^n M_i^2 - \frac{1}{n} \left(\sum_{i=1}^n M_i \right)^2 \right] \quad (7.17)$$

where n represents the total number of data points, with Nu_{cal} and Nu_{exp} representing the predicted and experimental Nusselt numbers in the relationship $M_i = (N_{cal} - N_{exp}) * 100 / N_{exp}$. The generalized Reynolds (GRe), Prandtl (GPr), and Grashof (GGr) were used as defined in Chapter IV.

RESULTS AND DISCUSSION

Characteristic Dimension

The determination coefficient (R^2), the percentage average error (PAE), the

percentage deviation modulus (PDM), and the percentage standard deviation (PSD) varied from 0.976 to 0.986, -3.24 to 2.52%, 18.14 to 19.65%, and 22.35 to 24.59% respectively as presented in Table 7.2 depending on the characteristic dimension used in developing the correlation. The optimum characteristic dimension was defined as the dimension which yielded the highest R^2 , the least PAE, PDM and PSD using a common model. Apparently, all characteristic dimensions fitted the experimental data well, with marginal differences between predicted and experimental data. Since characteristic dimensions affect dimensionless groups to different orders of magnitude, care should be taken in selecting the appropriate one if comparison is to be made with published correlations. In this study, characteristic dimension "d" was chosen so that calculated GGr/GRe^2 will have the same criteria as published (Fand and Keswani, 1973) for comparison of flow regimes.

Traditionally, fluid physical properties are estimated at film temperatures, defined as the average of the bulk fluid and the surface temperature under steady state conditions. However, particles suspended in carrier fluids experience a transient temperature profile which becomes asymptotic to the medium temperature with time. Therefore, the bulk fluid temperature was adopted for calculating fluid physical properties. Two reference temperatures were hypothesized for calculating, in particular, the temperature difference (ΔT) associated with the generalized Grashof number. These were defined as (1) the arithmetic mean of the bulk fluid and initial temperature of the particle, and (2) the difference between the bulk fluid and the initial temperature of the particle. The validity of these temperature differences were tested with experimental data using the same model and characteristic dimension. Surprisingly, only marginal differences in R^2 (0.9796 and

Table 7.2 Errors associated with various characteristic dimensions

Dimension (m)	PAE (%)	PDM (%)	PSD (%)	R ²
$d_{cd} = d$	-3.243	18.119	22.346	0.978
$d_{cd} = 0.5 L/(1+(2L/d))$	2.369	19.648	24.594	0.986
$d_{cd} = d (1+ 0.1447d/L)$	2.368	18.141	23.142	0.976
$d_{cd} = d L/(d + L)$	2.521	19.184	24.002	0.981

0.9790), PAE (1.923 and 2.066), PDM (16.15 and 17.0381) and PSD (20.485 and 21.444) resulted from using the arithmetic mean and the difference between the bulk and sample initial temperatures respectively. The difference between the bulk fluid and particle initial temperatures was adopted in this study to conform with relationships used by Alhamdan and Sastry (1990) for studies on natural convection.

Although all the characteristic dimensions discussed above fitted the experimental data covering diameter-to-length ratios ranging from 0.625 to 1.0, it is important to recognize the fact that the magnitude of estimated dimensionless group would strongly be influenced by the magnitude of the characteristic dimension used. To be consistent with established criterion (i.e., GGr/GRe^2 for both spherical and finite cylindrical particles) for differentiating flow regimes, the diameter of the particle was adopted. To accommodate different sample lengths, the diameter-to-particle length ratio was introduced as an additional factor in all models prior to data analysis.

The generalized particle Reynolds (GRe), Grashof (GGr), and Prandtl (GPr) numbers ranged from 4.3 to 8750; 216 to 1.6×10^8 ; and 1.6 to 800 respectively for finite cylindrical particles. The corresponding Nusselt number and GGr/GRe^2 ratio ranged from 2.1 to 24 and 0.88 to 31 respectively. The GGr/GRe^2 ratio obtained in the study indicates that two flow regimes can be established for a finite cylinder: the region where free convection contributes about 10% (i.e., $0.88 < GGr/GRe^2 < 2.0$) to the overall heat transfer and the region where both free and forced contribute significantly ($2 < GGr/GRe^2 < 31$).

Limiting Nusselt Number for Finite Cylinder

The limiting Nusselt number was determined using Eq. (7.14) as the reference model and Eqs. (7.15), (7.16) and (7.17) as the criteria for accuracy. Predicted data compared well with experimental data when the constant A (Eq. 7.14) varied between 0.31 and 0.6. The optimum value found was 0.36. This value falls as expected, between 0.3 and 2.0 for an infinite cylinder and a sphere respectively.

Forced Convection to Finite Cylinders

Since free convection contributes 10% to the overall heat transfer for $0.5 < GGr/GrRe^2 < 2.0$, pure forced convection was considered, resulting in the following relationship with finite teflon cylinder data:

$$Nu - 0.36 = 0.008 GrRe^{1.8} \left(\frac{GPr}{900}\right)^{1.66} \left(\frac{d}{D}\right)^{-2.04} \left(\frac{d}{L}\right)^{-2.0} \quad (7.18)$$

Although a higher R^2 (0.993) was obtained, the associated PSD (32.798%), PDM (27.31%), and PAE (4.843) were quite high. Introducing the Grashof number and Gr/Re^2 ratio resulted in the relationship:

$$\frac{Nu - 0.36}{GrRe^{1.8} \left(\frac{GPr}{900}\right)^{3.03}} = 10^{-2.87} GGr^{0.69} \left(\frac{GGr}{GrRe^2}\right)^{0.83} \left(\frac{d}{D}\right)^2 \left(\frac{d}{L}\right)^{-8.6} \quad (7.19)$$

with R^2 , PSD, PDM, and PAE changing to 0.996, 25.67%, 20.715%, and 2.939% respectively. Eq. 7.19 is valid for $GGr/GrRe^2$ between 0.88 and 13; $GrRe$ between 14 and

8038 and GPr between 1.8 and 558, each dimensionless group including the particle-to-tube diameter and the particle diameter-to-length ratios contributing significantly ($p < 0.05$) to the model. The marked improvement in the model confirms observations made by Fand and Keswani (1973) with regards to the effect of free convection even in situations where forced convection predominates the mechanism of heat transfer. Figure 7.1 shows a rearranged form of Eq. (7.19) and illustrates an excellent fit between predicted and experimental data for teflon. However, the model underpredicted data for potato, giving a percentage average error (PAE) of -24%, although the percentage standard deviation (PSD) was (13.4%).

Two streams of data distribution can be identified with Figure 7.1. The upper stream represents high Reynolds and Grashof numbers, whilst the lower stream represents the opposite, each distribution satisfying the GGr/GRe^2 criterion between 0.88 and 2.0 for finite cylinders. The reason for this observation is that, as the fluid temperature increases, the fluid apparent viscosity decreases while the temperature difference (ΔT) between the bulk fluid and the particle increases, hence causing a simultaneous increase in both the generalized Reynolds and Grashof numbers. The reverse trend occurs at lower temperatures. Figure 7.1 also shows that the Nusselt number increases with increase in the generalized Reynolds as well as the generalized Grashof numbers.

Mixed Convection to Finite Cylinders

Experimental data for cylindrical Teflon particles with GGr/GRe^2 greater than 2.0 was used in modelling mixed convection heat transfer and verified with data obtained for

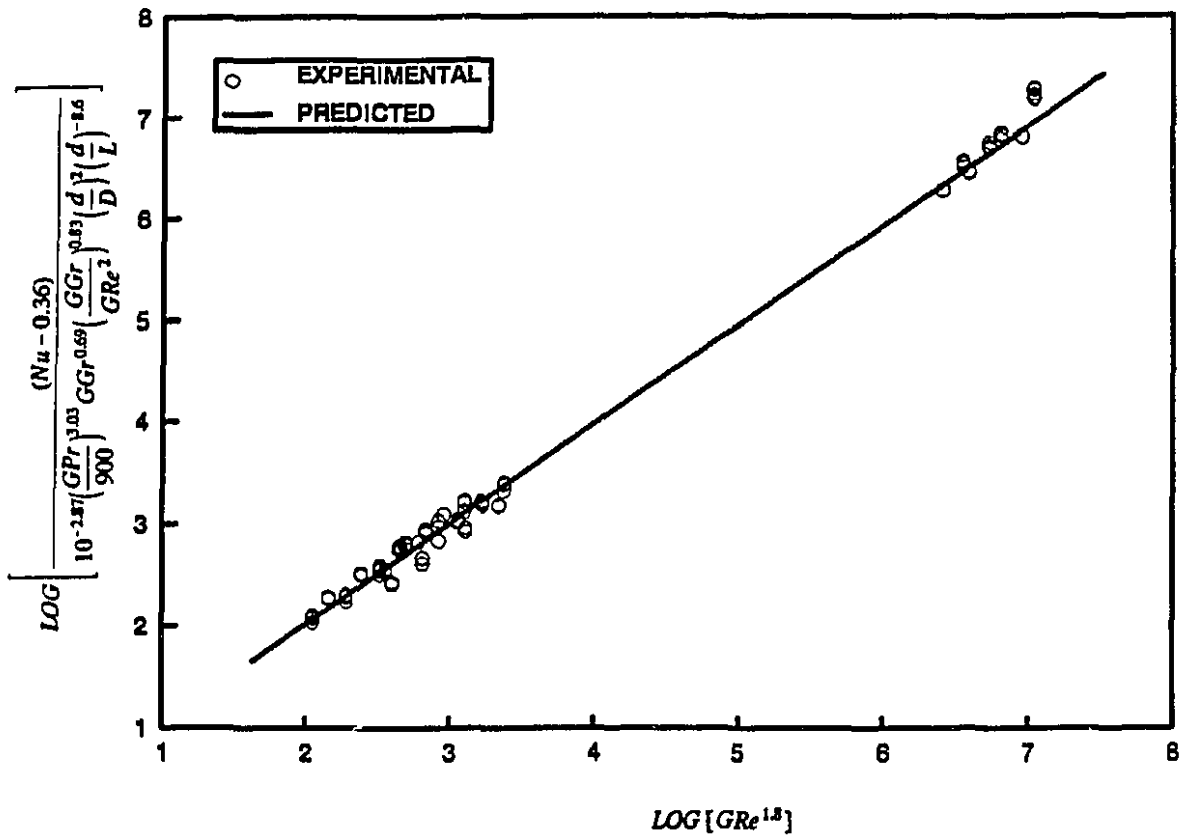


Figure 7.1 Correlation between predicted and Observed Nusselt number (Eq. 7.19).

potato. A stepwise regression was performed, relating the Nusselt number to other dimensionless groups. The optimum correlation, which is valid for GGr/Gr^2 between 2 and 31; GGr between 216 and 1.6×10^8 ; Gr between 4.3 and 8751; and GPr between 1.6 and 800:

$$\frac{Nu - 0.36}{\left(\frac{d}{D}\right)^{0.31} \left(\frac{100d}{L}\right)^{-4.49}} = 18.24 Gr^{0.8} GPr^{2.0} GGr^{0.66} \quad (7.20)$$

The R^2 , PAE, PDM and PSD were 0.98, 0.93%, 16.81% and 21.18% respectively. With the exception of the GGr/Gr^2 ratio which had less impact ($p > 0.05$), all dimensionless parameters had significant influence ($p < 0.05$) on Eq. (7.20). Increasing particle diameter for a given length (Eq. 7.20), decreases the Nusselt number. This is evident from the negative index associated with the diameter-to-length ratio in Eq. (7.20). Figure 7.2 shows a uniform distribution of the 560 experimental data points used in developing Eq. (7.20). Similar trends were observed for plots of Nusselt number as a function of either the generalized Reynolds, Prandtl or the Grashof number.

The fluid-to-particle convective heat transfer coefficient is a boundary layer property and independent of the type of material used. However, correlations developed with data obtained for Teflon underpredicted results for potato, giving a total percentage average error (PAE) and percentage modulus (PDM) as high as -88.64%. The reason for this behaviour is due, probably to the fact that different materials absorb or relinquish heat at different rates as a result of their different heat capacities. In addition, mass transfer may have probably occurred between potato particles and the carrier fluid whereas

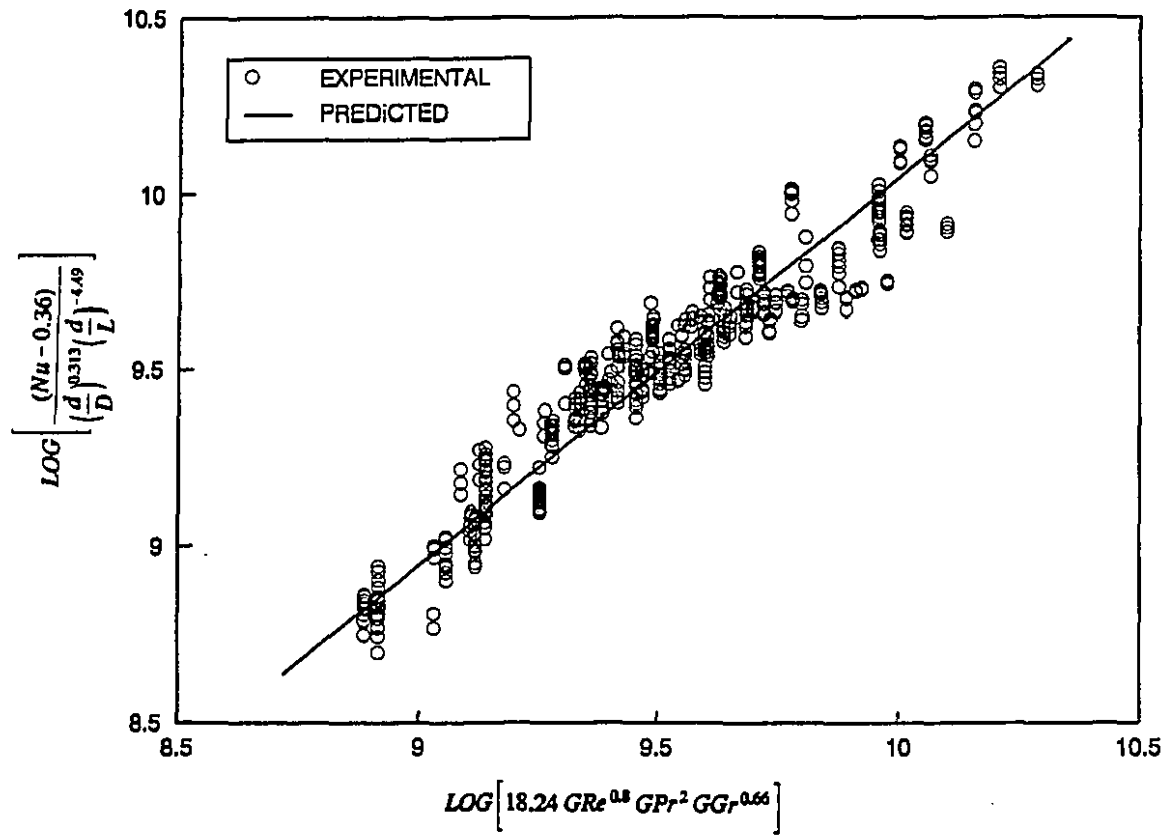


Figure 7.2. Correlation between predicted and observed Nusselt number for cylindrical particles satisfying GGr/GRe^2 ratio between 2.0 and 31 (Eq. 7.20).

nothing of that nature happens with the inert Teflon particle. Since natural convection contributes significantly to the overall heat transfer for mixed mode regimes, it may be necessary to consider the type of material in developing heat transfer correlations.

To account for the above differences, data for both potato and Teflon were combined, sorted by the GGr/Re^2 criterion and analyzed using a stepwise multiple regression to identify the significant parameters. An additional factor called "Thermal diffusivity ratio" which is defined as the ratio of particle-to-fluid thermal diffusivities (α_p/α_f) was introduced prior to data analysis and investigated. The reason for introducing this factor is due to the fact that thermal diffusivity indicates how fast heat propagates into a material as a function of moisture content, temperature, composition and porosity. The diffusivity ratio was consistently found to have significant impact on the Nusselt number and also decreased the PAE, PDM and PSD associated with developed models. For GGr/GRe^2 between 0.88 and 1.8, the model which best fitted experimental data was:

$$\frac{Nu - 0.36}{GRe^{2.5} \left(\frac{d}{D}\right)^2 \left(\frac{\alpha_p}{\alpha_f}\right)^{4.09}} = 10^{-3.53} GGr^{0.76} \left(\frac{d}{L}\right)^{-8.99} \left(\frac{GPr}{800}\right)^{3.86} \quad (7.21)$$

The PAE, PDM, PSD, and R^2 associated with Eq. (7.21) were 4.37, 25.70, 30.77 and 99.7% respectively. Eq. (7.21) is valid for GGr , GRe , GPr , d/L , d/D , and α_p/α_f from 265 to 1.1×10^8 , 14 to 8038, 1.6 to 564, 0.625 to 1.0, 0.313 to 0.5, and 0.8 and 1.0 respectively. Apparently, the GGr/Re^2 ratio did not have any influence on the model due possibly to the introduction of α_p/α_f . However, ignoring both α_p/α_f ratio and the

generalized Grashof number increased the PAE, PDM, and PSD to 9, 35 and 49% respectively. Figure 7.3 shows an excellent fit between observed and predicted data for the left hand side of Eq. (7.21) using experimental data for both Teflon and potato.

A similar correlation as well as excellent fit between observed and predicted data (Figure 7.4) were obtained for GGr/Gr^2 between 2.0 and 31.3 using data for both Teflon and potato particles with GGr , Gr , GPr , d/L , d/D , and α_p/α_f ranging from 216 to 1.6×10^8 , 4.3 to 8750, 1.6 to 800, 0.625 to 1.0, 0.197 to 0.5, and 0.8 to 1.0 respectively. The best correlation which showed a marked improvement in R^2 (99.2%), PAE (7.9%), PDM (29.9%) and PSD (41.8%) was:

$$\frac{Nu - 0.36}{Gr^{2.12} \left(\frac{d}{D}\right)^{-1.05} \left(\frac{\alpha_p}{\alpha_f}\right)^3} = 10^{-2.06} GGr^{0.19} \left(\frac{d}{L}\right)^{-3.1} \left(\frac{GPr}{800}\right)^{2.39} \quad (7.22)$$

Comparison of the present models with published relationships is impossible due to lack of information on heat transfer to finite cylinders submerged in carrier fluids.

Spherical Particles

The GGr/Gr^2 for spherical particles ranged from 1.3 to 23.5, exceeding the limit proposed by Yuge (1960) for pure forced convection. Although the GGr/Gr^2 range obtained falls within the limits suggested by Johnson *et al.* (1988) for mixed convection, it did not conform with the general relationship between the Nusselt and generalized Grashof numbers for pure natural convection. A modified form of Eq. (7.2) and (7.4) were

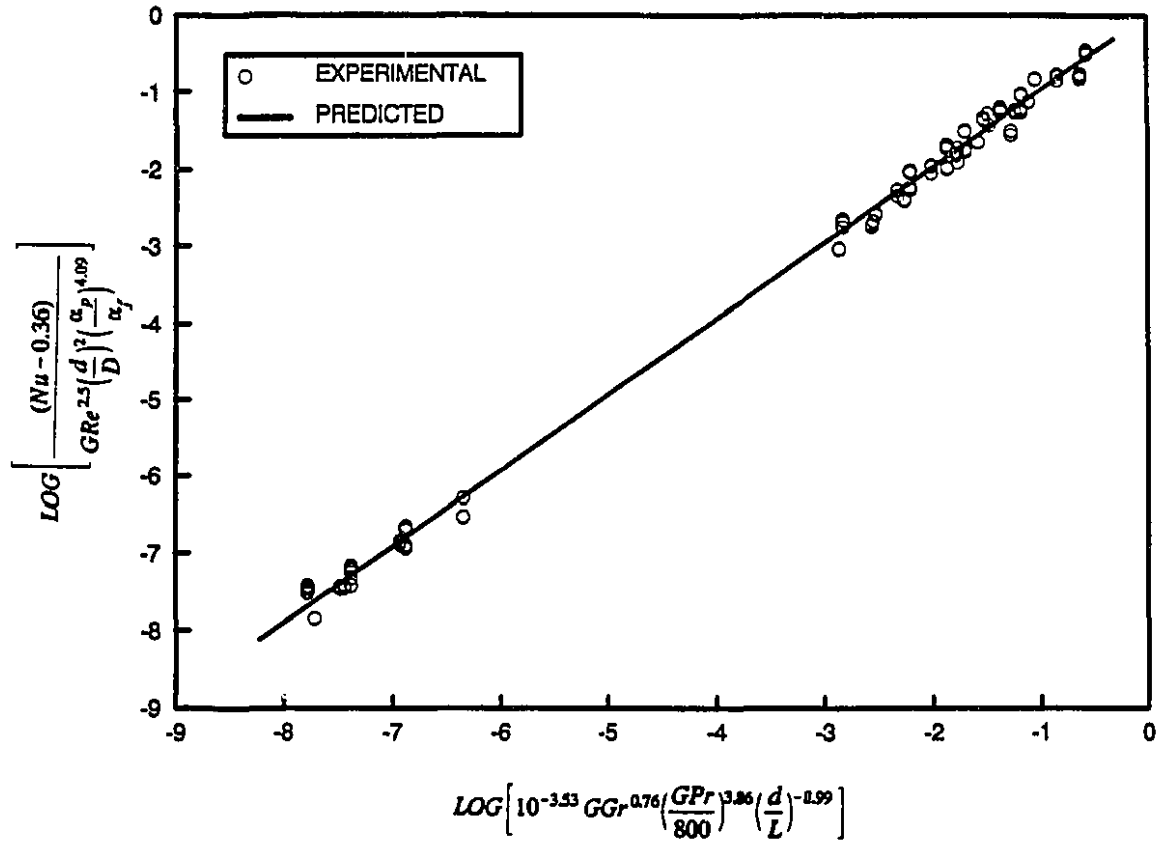


Figure 7.3 Correlation for observed and predicted Nusselt numbers after introducing the diffusivity ratio in Eq. (7.21) for GGr/Gr^2 between 0.88 and 2.0.

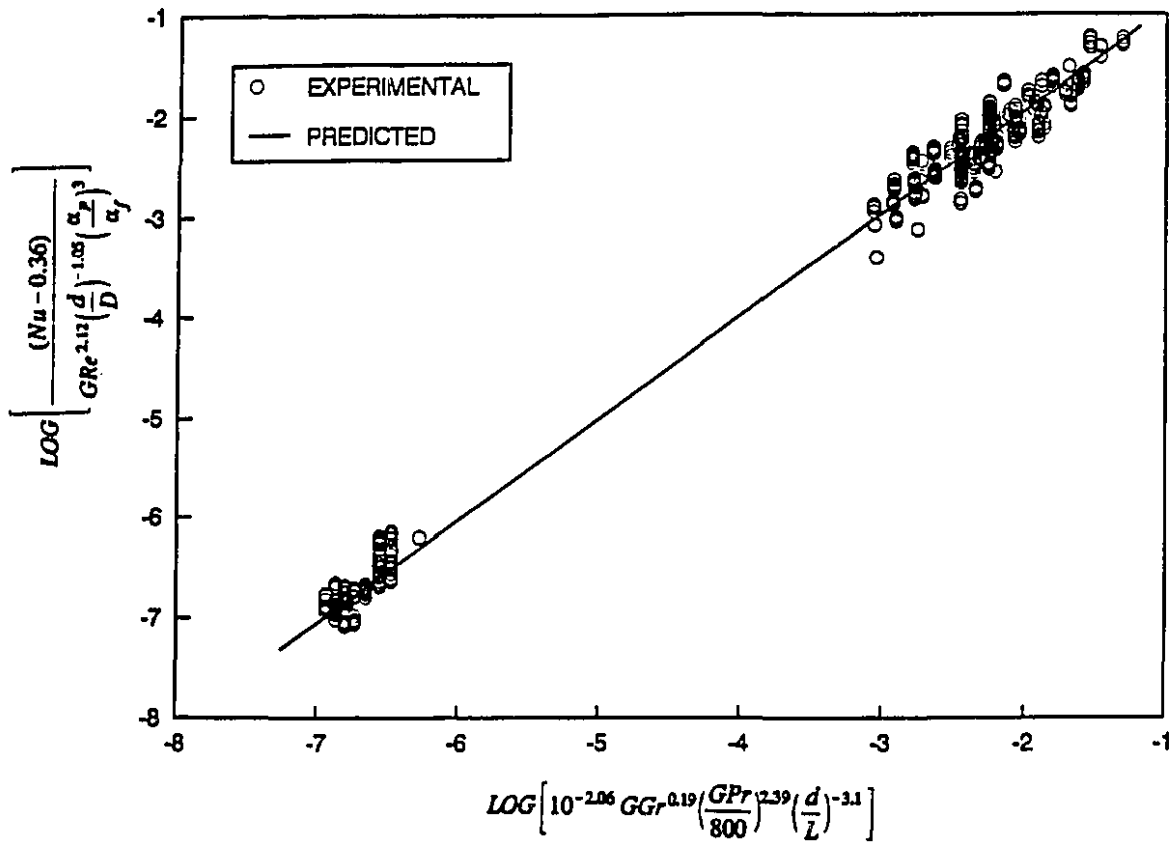


Figure 7.4. Correlation for observed and predicted Nusselt numbers after introducing the diffusivity ratio for GGr/Gr^2 ratio between 2.0 and 31 (Eq. 7.22).

used as initial approximations to model pure force convection alone, giving the relationships:

$$Nu = 2.0 + 0.07 GRe^{0.62} GPr^{0.53} \left(\frac{d}{D}\right)^{0.16} \quad (7.23)$$

$$Nu = 2.0 + 0.36(0.4 GRe^{0.5} + 0.06 GPr^{0.67}) GPr^{0.46} \left(\frac{d}{D}\right)^{0.33} \quad (7.24)$$

The PAE, PDM, PSD, and R^2 for Eq. 7.23 and 7.24 were 0.34, 7.78, 9.38, 84 %, and 0.28, 7.714, 9.40, and 98.8% respectively. Contributions from natural convection were accounted for by introducing both GGr and GGr/GRe^2 ratios in Eq. (7.24) and investigating, resulting in the relationship:

$$Nu = 2.0 + 0.32(0.4 GRe^{0.5} + 0.06 GPr^{0.67}) GPr^{0.46} \left(\frac{d}{D}\right)^{0.17} \left(\frac{GGr}{GRe^2}\right)^{-0.04} \quad (7.25)$$

The PAE, PDM, PSD, and R^2 calculated with Eq. 7.25 were 0.315, 7.59, 9.17 and 98.8% respectively. Although Eq. (7.24) and (7.25) have the same R^2 , the PDM and PSD associated with Eq. (7.25) are lower than Eq. (7.24). The range of applicability of Eq. (7.23), (7.24), and (7.25) are as follows: $1380 < GGr < 4.7 \times 10^7$; $7.7 < GRe < 2693$; $1.8 < GPr < 332$; and $0.25 < d/D < 0.38$. Again, comparison of the present models with published correlations is difficult because of the lack of information on mixed convection to submerged particles. In addition, attempts made to compare the above models with well-known correlations of Geankoplis (1978), and Whitaker (1972) for forced

convection failed because they overpredicted the Nusselt number. This discrepancy can be expected because the relationships derived from the literature are for unbounded flow around a sphere. It is invalid to compare the present results with correlations presented by Sastry *et al.* (1989) and Zuritz *et al.* (1990) for forced convection about submerged particles because of differences in experimental procedures, and most importantly differences in the range of particle Reynolds and fluid Prandtl numbers.

CONCLUSIONS

Dimensionless correlations for mixed and forced convection to finite cylindrical and spherical particles submerged in both Newtonian and non-Newtonian fluids at temperatures between 90 to 110°C are presented. The suitability of four characteristic dimensions were investigated in relation to developing predictive models for estimating the Nusselt number. Although each dimension gave excellent fit between experimental data and predicted values, extreme care is required if comparison is to be made with published correlations. Correlations developed with experimental data from Teflon was generally found to underestimate data for potatoes. This discrepancy was attributed to differences in heat capacities and the possibility of mass transfer across potato particles and the carrier fluid. Evidently, heat capacity and for that matter, the type of particle material, affects the Nusselt number by influencing operating buoyant forces. Introducing the diffusivity ratio was found to improve correlations developed with data obtained from both particles. In general, excellent correlations were obtained between predicted and observed data with coefficients of determination (R^2) ranging between 0.97 to 0.998.

CHAPTER VIII

THERMAL INACTIVATION KINETICS OF TRYPSIN AT ASEPTIC PROCESSING TEMPERATURES

ABSTRACT

Kinetics of thermal inactivation of trypsin (bovine pancreas) were evaluated in the temperature range, 90 - 130 °C, common to aseptic processing of high/low acid foods. Aliquots of trypsin in buffer, at three pH values, 3.8, 5.1 and 6.0, were subjected to selected heat treatments at various temperatures. Kinetic parameters were evaluated from the residual enzyme activity. Reference k and D values (at 121.1°C) ranged from 0.0719 to 0.349 min⁻¹ and 32.0 to 6.6 min, and E_a and z values ranged from 84.9 to 69.9 kJ/mole and 33.1 to 39.9 C°, respectively, in the pH range 3.8 - 6.0. The thermal inactivation resistance of trypsin in the acid and low acid pH range makes it a potential bio-indicator for high temperature thermal processes.

INTRODUCTION

Thermal processing is an important technique for shelf life extension of both low and high acid foods. The primary purpose is to produce a commercially sterile product by destroying pathogenic microorganisms while creating an environment to suppress the growth of others. Quality improvements in thermally processed products have been made possible through adaptation of HTST/UHT, thin profile, rotational as well as aseptic

processing principles. Since temperature measurement of moving particles is a serious problem, aseptic processing of particulate foods rely on microbiological/biological validations (Dignan *et al.*, 1989). Problems associated with the use of microorganisms as bio-indicators have been detailed in several studies (Pflug and Odlaug, 1978; Sastry *et al.*, 1988; Berry *et al.*, 1989a,b; Weng *et al.*, 1991a,b).

Process optimization has been traditionally attempted through studies on the destruction of nutrients/enzymes. Mulley *et al.* (1975a) used thiamine hydrochloride as a chemical index to evaluate sterilization efficacy. Textural changes in meat was used as a heating index by Tennigen and Olstad (1979). Berry *et al.* (1989a) studied the destruction kinetics of methyl methionine sulfonium (MMS) in buffer solutions and found it to be suitable for indexing microbial lethality. They recommended MMS as a substitute for microorganisms in thermal process evaluation.

The activation energy associated with microorganisms is higher than for nutrients and enzymes. Therefore, the rate of destruction of microorganisms proceeds more rapidly as temperature increases in comparison to destruction of enzymes and nutrients (Schwartz, 1992). For high-temperature short-time processing, it might be necessary to use enzymes as indicators rather than microbial spores and nutrients. For vegetable processing, peroxidase inactivation is often used as indicator due to its reported heat stability.

Trypsins are a family of enzymes that catalyze preferentially the hydrolysis of ester and peptide bonds involving the carboxyl groups of L-lysine and L-arginine with serine and a histidine residue participating in the mechanism of catalysis (Keil, 1971; Richardson and Hyslop, 1985). Trypsin has been isolated from several sources of food

including cow, sheep, turkey, fish and pigs (Simpson and Haard, 1984; Northrop *et al.*, 1948; Travis 1968).

Thermal inactivation studies related to trypsin have often been carried out with respect to its inhibitors which are usually inactivated at pasteurization temperatures (Soetrisno *et al.*, 1982; Rao *et al.*, 1989; van der Poel *et al.*, 1990). According to Keil (1971), trypsin is most stable at pH 3.0. Northrop (1932) indicated that solutions of crystalline trypsin exhibit a remarkable property quite different from other enzymes: in dilute acid solutions (pH 1.0 to 7.0), trypsin can be heated to boiling with little or no loss in activity, and without apparent formation of any denatured protein. Simpson and Haard (1984) found that bovine trypsin retained virtually all its activity after 30 minutes heating at 80°C. Activation energy ranged from 46.5 to 56.1 kJ/mole depending on the substrate and concentration of calcium ions used. A search of the literature indicates that there is lack of data on effect of heat on trypsin at different pH in the thermal processing temperature range (90 - 130°C).

The objectives of this work were to study (1) the thermal inactivation kinetics of trypsin in the pH range covering both low and high acid foods, and (2) to evaluate the possibility of using trypsin as a bio-indicator for aseptic processes.

MATERIALS AND METHODS

Enzyme and Chemicals

Bovine pancreas trypsin (type III) and benzoyl-DL-arginine p-nitroanilide (BAPA) were obtained from Sigma Chemical Co. (St. Louis, MO). Tris (hydroxy-methyl-amino-

methane) was obtained from ICN Biochemicals (Cleveland, MO). Calcium chloride and dimethyl sulfoxide (DMS) were obtained from Anachemia Science (Montreal, Canada).

Enzyme Assay

The amidase activity of trypsin was assayed using the method of Erlanger *et al.* (1961). BAPA served as the substrate. The reaction mixture consisted of 0.2 mL of enzyme solution and 2.8 mL of BAPA substrate (dissolved in DMS) in 0.05 M Tris-HCl buffer (pH 8.2) containing 0.02 M $\text{CaCl}_2 \cdot 2\text{H}_2\text{O}$. The increase in light absorption was measured with a Beckman DU 7500 diorray spectrophotometer at 410 nm and 25°C. Control experiments were run using 0.2 mL 1 mM HCl or citrate buffer, instead of enzyme, and 2.8 ml of the substrate.

Heat Treatment

Trypsin dissolved in dilute 1 mM HCl (pH 3.8) or citrate buffer (pH 5.1, and 6.0) was appropriately adjusted to give similar activity on the substrate. Aliquots of trypsin were sealed in 2 mL glass ampoules (Canlab Canada, Montreal, PQ) using a gas flame and immediately submerged in ice/water mixture. Initial studies showed that the sealing process had no effect on the initial enzyme activity. Heating was done in a well-agitated constant temperature oil bath. Temperatures studied were 90, 100, 110, 120, and 130°C. For a given temperature, samples were taken from the oil bath at 5 min intervals for pH 3.8 and 5.1 and 1 min intervals at pH 6.0 and cooled immediately in an ice/water mixture. Prior to enzyme assay for residual activity, the sample temperature was equilibrated to

25°C. Needle type copper-constantan thermocouples (Ecklund-Harrison Technologies, Cape Coral, FL) were inserted into ampoules and sealed with silicone glue. Time-temperature data were gathered during the come-up period and heating times were corrected for the lag period prior to kinetic data analyses.

Kinetic Data Analysis

Thermal inactivation of trypsin was assumed to follow a first order kinetic process expressed as:

$$\log_e \left[\frac{A}{A_0} \right] = -kt \quad (8.1)$$

where A = enzyme activity (change in optical density/min), t = time (min), A₀ = initial enzyme activity and k = reaction rate constant (min⁻¹). k values were obtained as negative slopes of log_e [A/A₀] vs t regression. The decimal reduction time (D-value, time needed to reduce 90% of the activity) was calculated from:

$$D = \frac{2.303}{k} \quad (8.2)$$

The half-life (t_{1/2}) was calculated from the expression:

$$t_{1/2} = \frac{0.693}{k} \quad (8.3)$$

The temperature dependence of rate constants were analyzed by both Arrhenius and thermal death time (TDT) concepts. For the Arrhenius model, the activation energy E_a (kJ/mole) was obtained from the slope of the semi-logarithmic plot of Eq. (8.4):

$$k = s e^{E_a/RT} \quad (8.4)$$

where s = frequency factor, k = reaction rate constant (min^{-1}), T = absolute temperature (K), and R = universal gas constant (8.314×10^{-3} kJ/mole K). From the D value curve, z-value (temperature range required to change D by 90%) was calculated from the relationship:

$$\log \left[\frac{D_1}{D_2} \right] = \frac{T_2 - T_1}{z} \quad (8.5)$$

where T_2 and T_1 are temperatures corresponding to D_2 and D_1 . Heating times (t_{actual}) were corrected based on the duration (t_{CUT}) and effectiveness fraction (E) of come-up period using the procedure adopted by Nath and Ranganna (1977):

$$t_{\text{corrected}} = t_{\text{actual}} - t_{\text{CUT}} * (1 - E) \quad (8.6)$$

Briefly, the following procedure was adopted: For a given pH with its associated uncorrected D and z-values, enzyme inactivation contributed during the come-up period was evaluated from the gathered time-temperature data. Come-up effectiveness was calculated as the fraction of accumulated inactivation during come-up period divided by the theoretical inactivation that would have been contributed by instantaneous exposure

at bath temperature for the same period. Heating times were corrected using Eq (8.6), and D-values and z values were recalculated. Based on corrected D and z-values, the effectiveness was again recalculated and the entire procedure was repeated until the difference between the previous and recent D and z values were less than 0.5%.

Trypsin versus Microbial and other Enzyme Kinetics

Two approaches were used to compare the destruction kinetics of trypsin with other indicators, as well to demonstrate its utility in aseptic processing applications. First, the decimal reduction time equivalencies (1D) of various indicators and *Bacillus stearothermophilus* were compared at various temperatures with respect to equivalent heating times (EHT) at 121.1°C using a $z = 10\text{ C}^\circ$ (which is the same as process lethality or F_0 value as commonly employed in thermal processing). In order to do this, first the decimal reduction times of enzyme activity or microbial population were calculated at various temperatures based on their respective D_0 and z values:

$$D_T = D_0 * 10^{[(121.1 - T)/z]} \quad (8.7)$$

The corresponding equivalent heating times (EHT) at the reference temperature of 121.1°C were then calculated assuming the traditional reference z value of 10 C°:

$$EHT = D_T * 10^{[(T - 121.1)/10]} \quad (8.8)$$

The second approach was to compare residual activities of various bioindicators

following a standard heat process. An F_0 value (process lethality) of 10 min (commonly employed in several thermal processing applications) was chosen for this purpose. The percentage residual activity (RA) of the bioindicator was evaluated using a reverse approach to Eq. (8.7) and (8.8). The heating time (F_T , $z = 10\text{ C}^\circ$) at various temperatures equivalent to an F_0 of 10 min were first calculated:

$$F_T = 10 * 10^{[(121.1 - T)/10]} \quad (8.9)$$

This was then coupled with the corresponding decimal reduction time (D_T) obtained from Eq. (8.7) to compute the percentage residual activity:

$$RA(\%) = 10^{(2.0 - F_T/D_T)} \quad (8.10)$$

Data on kinetic parameters for the different indicators were obtained from literature. D_0 and z values were, respectively, for peroxidase: 12.94 min and 31.39 C° (Adams, 1978); MMS at pH 6.0: 7.53 min and 20.0 C° (Berry *et al.*, 1989a); *Bacillus stearothermophilus* at pH 5.0: 4.0 min and $z = 7.8\text{ C}^\circ$ and at pH 6.0: 5.0 min and 12.2 C° (Stumbo, 1973; Berry *et al.*, 1989a).

RESULTS AND DISCUSSION

Figures 8.1 - 8.3 show the first order plots of percent residual activity of trypsin at various pH as a function of time at five inactivation temperatures. With the exception of data at 90°C for pH 5.1, the associated R^2 were higher than 80% (Table 8.1). Lenz and

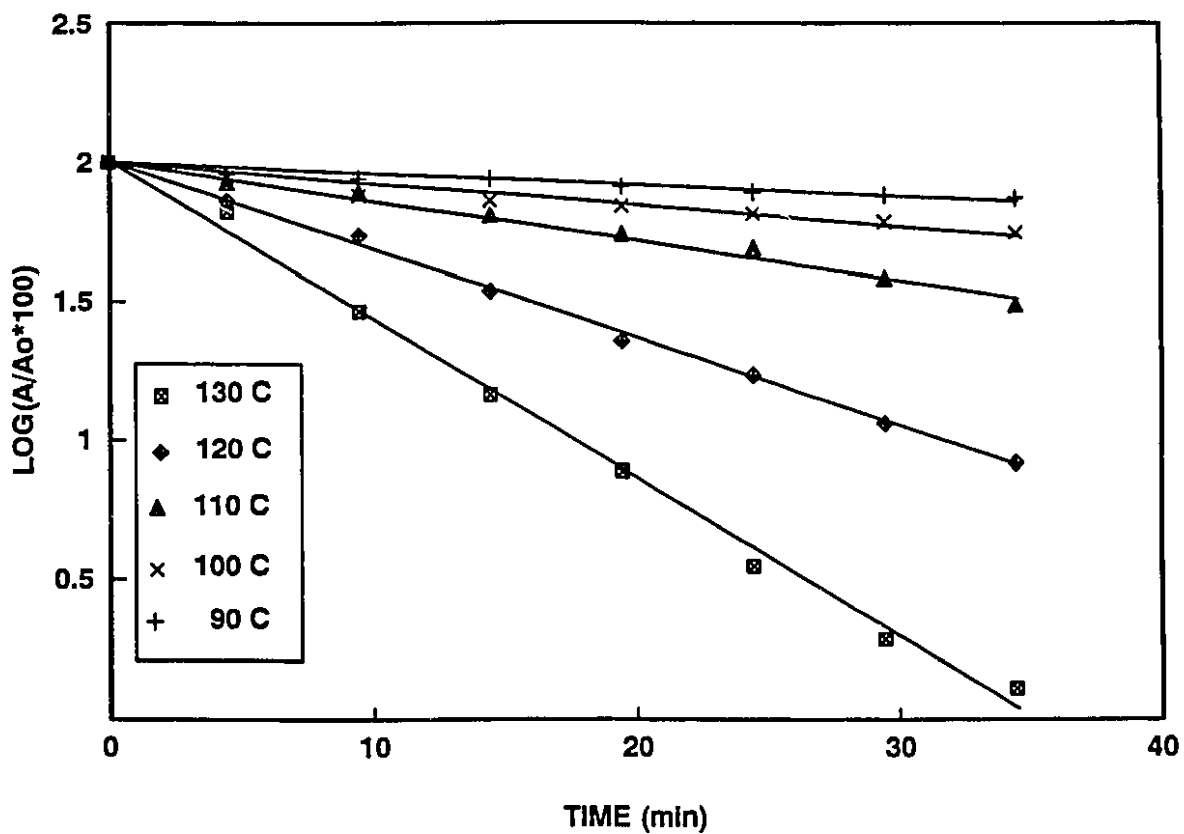


Figure 8.1. Residual activity as a function of heating time at various temperatures for trypsin in dilute HCl (pH = 3.8).

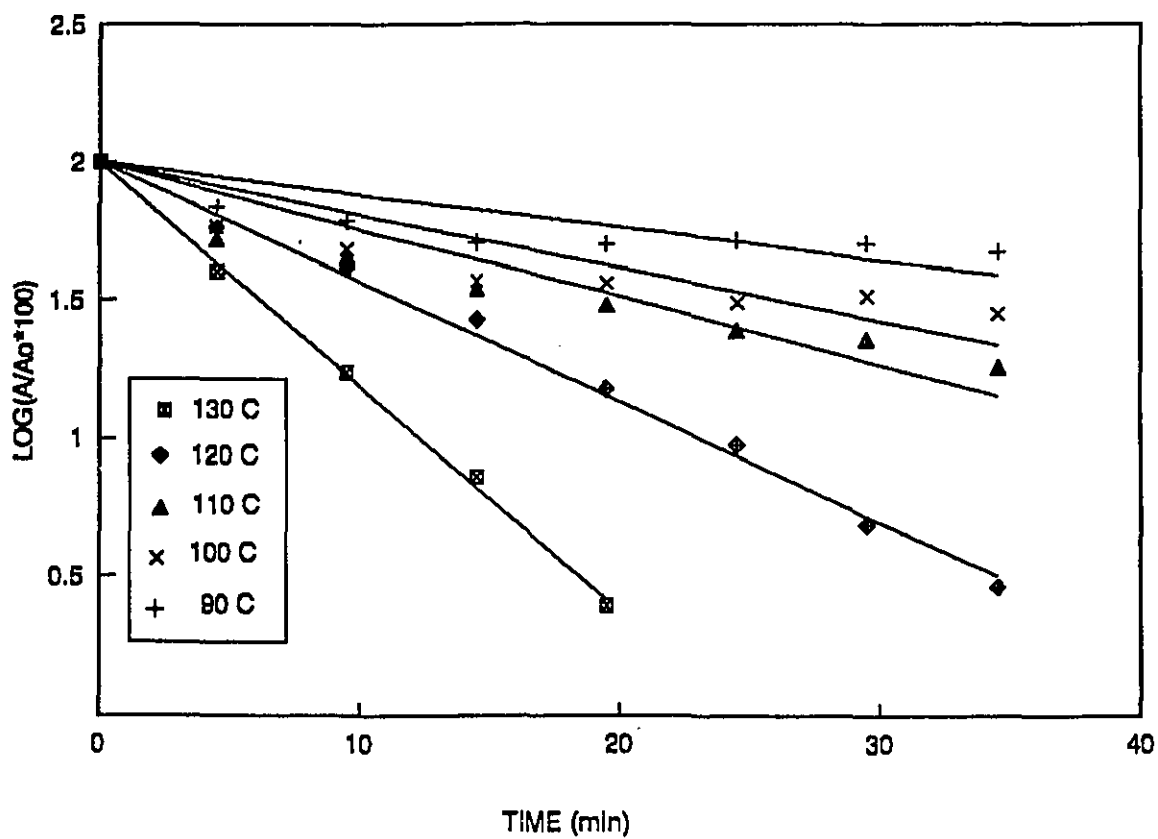


Figure 8.2. Residual activity as a function of heating time at various temperatures for trypsin in citrate buffer solution (pH = 5.1).

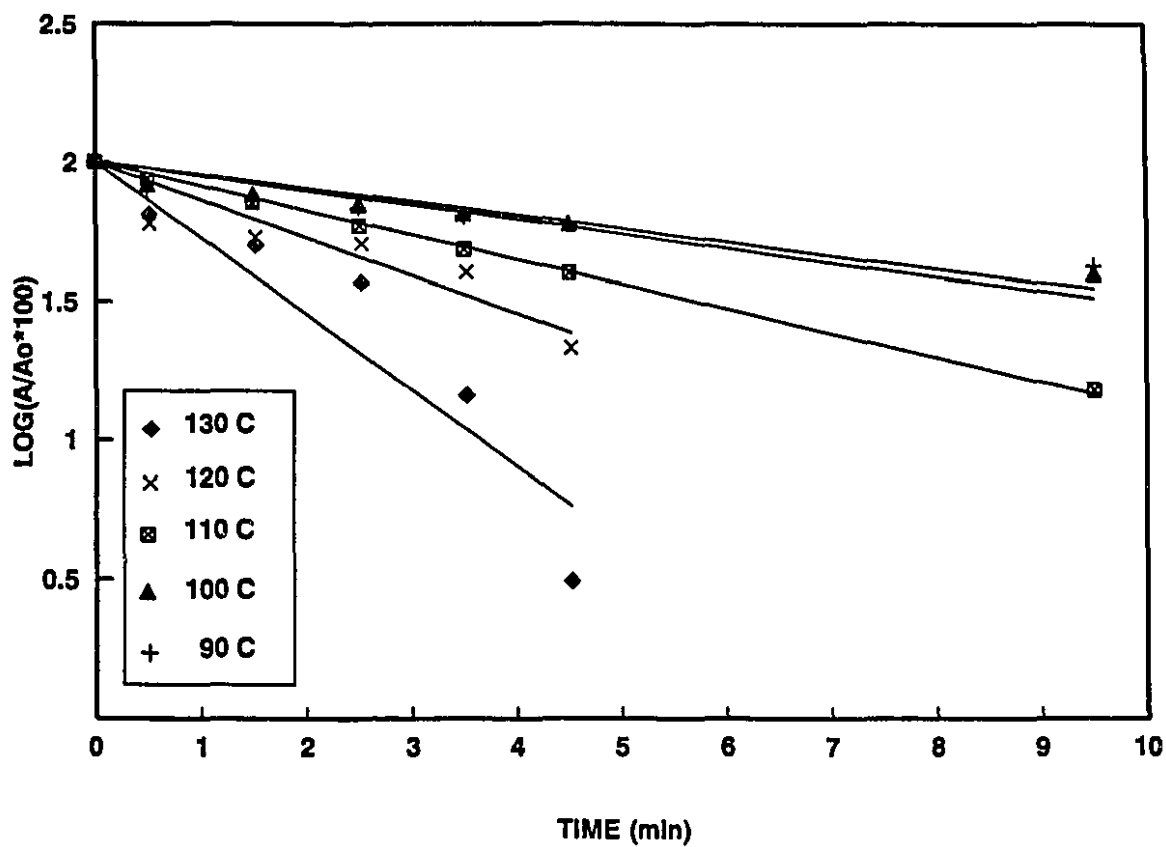


Figure 8.3. Residual activity as a function of heating time at various temperatures for trypsin in citrate buffer solution (pH = 6.0).

Table 8.1. Kinetic parameters for trypsin in dilute HCl and citrate buffer.

pH	Temperature (°C)	D-value (min)	k-value (min ⁻¹)	t _{1/2} (min)	R ²
3.8	90	279.7	0.008233	84.17	0.96
	100	144.0	0.015998	43.32	0.97
	110	68.9	0.033413	20.74	0.99
	120	31.5	0.073153	9.47	0.99
	130	18.4	0.125396	5.53	0.99
5.1	90	132.0	0.017449	39.72	0.71
	100	72.8	0.031643	21.90	0.83
	110	50.8	0.045099	15.37	0.96
	120	22.8	0.101223	6.85	0.99
	130	11.7	0.196330	3.53	0.99
6.0	90	33.3	0.069271	10.00	0.79
	100	27.9	0.082585	8.39	0.90
	110	11.8	0.194773	3.56	0.99
	120	8.5	0.270479	2.56	0.87
	130	3.4	0.687139	1.01	0.90

Lund (1980) reported that when the half-life (time needed to destroy 50% of initial activity) of an enzyme is ≤ 20 min, significant inactivation of enzyme occurs during the lag or come-up period. The half-life of trypsin was generally lower than 20 min under most experimental situations (Table 8.1). Therefore, correction to the come-up (lag) period was necessary. The come-up times were approximately 95 sec and come-up period effectiveness varied from 0.65 to 0.68. Generally, D-values decreased with increasing pH and temperature. For example, as the pH increased from 3.8 to 6.0, the D-value decreased by 5.5 times at 130°C. Figure 8.4 shows TDT curves for the pH range studied. The Arrhenius plots (not shown) gave somewhat similar fit. The R^2 values obtained for z and E_a values (Table 8.2) indicate that the Arrhenius and TDT models are comparable in spite of their contradictory nature with respect to describing the temperature dependence of kinetic parameters (in Arrhenius model, kinetic parameters on logarithmic scale is inversely proportional to temperature, while in TDT approach the proportionality is direct). This observation supports that made by Ramaswamy *et al.* (1989) with regard to the models providing similar results. Simpson and Haard (1984) reported lower E_a values for trypsin than found in this study, possibly due to the low temperature range (5 - 35°C) and high pH (8.2 - 9.5) conditions employed in their study.

The z-values were pH dependent and increased by approximately 20% between pH 3.8 and 5.1. Thereafter, there was only a marginal increase up to 6.0 (Table 8.2). The marginal differences can be observed from the seemingly similar slopes (Figure 8.4). The activation energy dropped with pH in consistence with its reciprocal relationship with z value (Table 8.2). Again, the difference between activation energy at pH 5.1 and 6.0 was

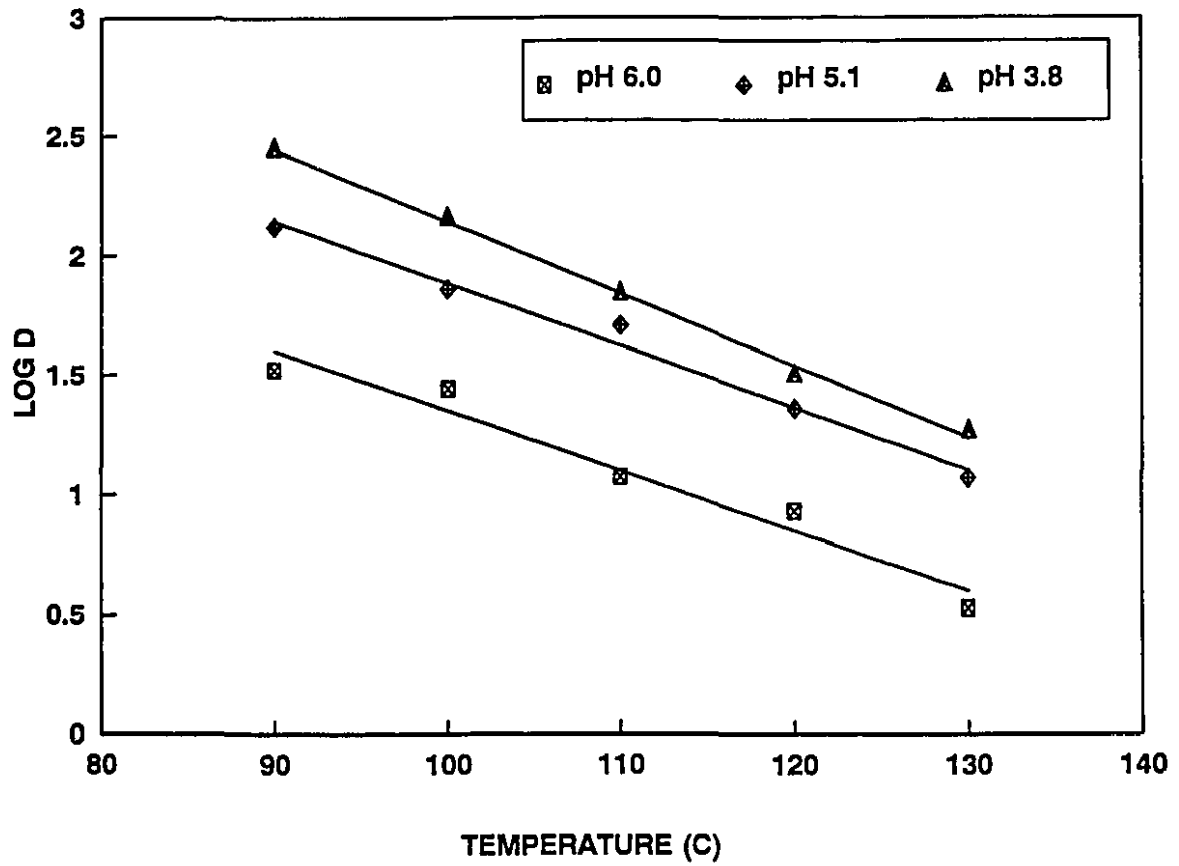


Figure 8.4. Thermal inactivation time curves for trypsin in relation to pH.

Table 8.2. Activation energy (E_a), z values, D_0 , k_0 and their corresponding R^2 values for trypsin in dilute HCl or citrate buffer solutions.

pH	Temperature (°C)	E_a (kJ/mole)	k_0 (min ⁻¹)	R^2	z (C°)	D_0 (min)	R^2
3.8	90 - 130	84.9	0.071969	0.99	33.1	32.0	0.99
5.1	90 - 130	72.8	0.106620	0.98	38.4	21.6	0.99
6.0	90 - 130	69.9	0.348939	0.95	39.9	6.6	0.96

marginal.

Due to lack of published data on trypsin inactivation in the literature, comparative verification of the present results was difficult. The utility of kinetic data were, however, evaluated based on its similarity to other chemical, biochemical and microbiological validators (MMS, peroxidase and *Bacillus stearothermophilus*). Lu and Whitaker (1974) found that thermal inactivation of horseradish peroxidase was pH dependent. At pH 3.5, all activity was lost within 0.5 min at 76°C, and the rate of inactivation decreased eight times when the pH was increased from 4.0 to 7.0. For peroxidase inactivation of low-acid fruits and vegetables (Schwimmer, 1981), z values range from 8.8 to 71.9°C. For acid foods, values range from 10F° (~5.6C°) to 34 F° (~18.9C°). Adams (1978) reported z, E_a, and D₀ values for horseradish peroxidase (RZ = 3.2) to be 31.4C°, 29.6 kcal/mole, and 12.94 min, respectively (in acetate buffer at pH 5.6 and temperatures ranging from 70 to 150°C). The z-values for trypsin fell in the range reported for peroxidase in low-acid fruits and vegetables. The D₀ value reported by Adams (1978) falls in the range found for trypsin in citrate buffer at pH 5.1 and 6.0 (Table 8.2).

Figure 8.5 shows variations in EHT values representing one decimal reduction in the activity of trypsin, *Bacillus stearothermophilus*, peroxidase and MMS, plotted as a function of temperature. The decimal reduction EHTs at 130°C of the various indicators in the increasing order of resistance were as follows: 2.24 min (*Bacillus stearothermophilus*); 21 min (MMS); 30.7 min (trypsin at pH 6); 52.3 min (peroxidase); 98.3 min (trypsin at pH 3.8). EHT values represent the equivalent heating times at the reference temperature of 121.1°C, which should be differentiated from the decimal

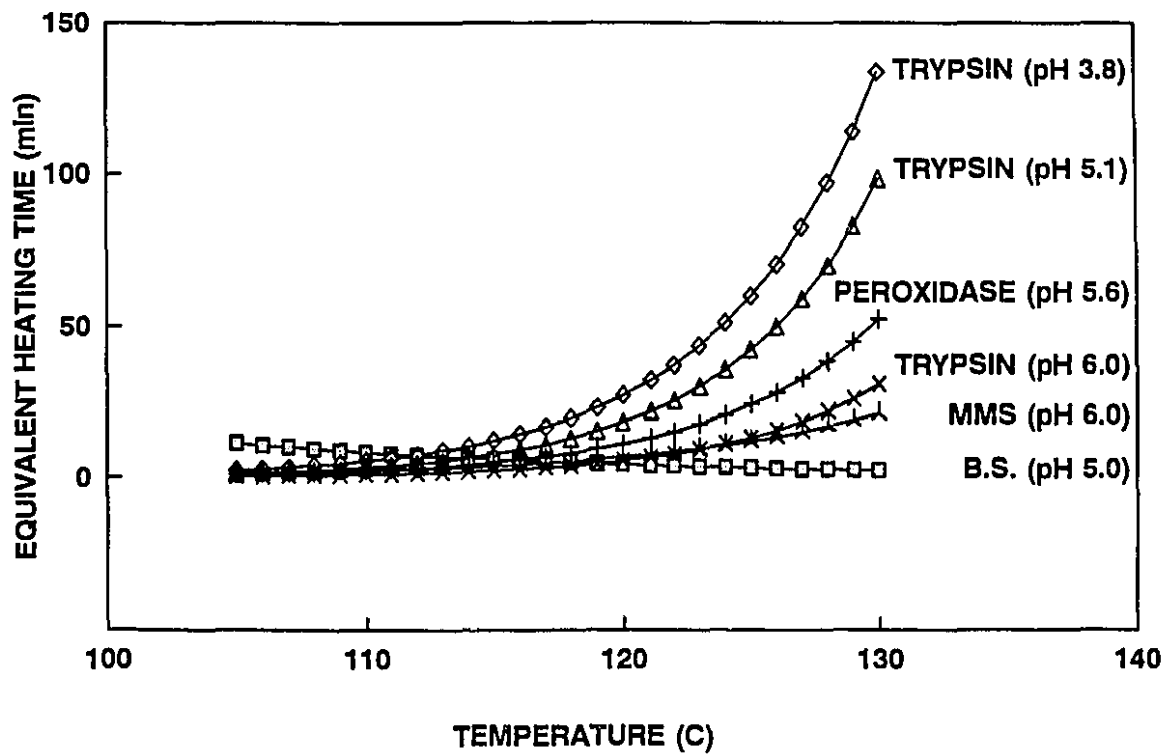


Figure 8.5. Process lethality (F_0) achieved by a decimal reduction in activity of trypsin and selected bio-indicators at various temperatures.

reduction times at the condition in question. In the above example the real D values were: 0.29, 2.7, 3.95, 6.7, 12.7, and 17.2 min. EHT concept has been used in the analysis to get a more realistic comparison of the inactivation behaviour of various enzymes at different temperatures because the process times are based on F_0 calculated using a z value of 10°C while the enzyme inactivation is characterised by its own characteristic D_0 and z values. As is evident from Figure 8.5, the order of resistance to thermal destruction of different bioindicators are not the same at different temperatures. At lower temperatures, *Bacillus stearothermophilus* has a higher thermal resistance than all other indicators with an EHT value of 11.4 min as compared to 0.4 - 2.4 min for the others, while the trend reverses as processing temperatures exceed 120°C . At the high temperatures employed for aseptic processing, therefore, enzymes serve as better indicators for verification of the process.

In Figure 8.6, the extent of inactivation/destruction of various indicators in a process with equivalent F_0 of 10 min are compared. The residual activity/concentration of all the enzymes as well as MMS were higher than *Bacillus stearothermophilus*. At the aseptic processing temperature of 130°C , approximately 47% of the original trypsin activity was retained at pH 6.0 while at pH 3.8 the residual trypsin activity was as high as 84%. Percentage retention of MMS and peroxidase at 130°C were 33 and 64% respectively with the corresponding pH values of 6.0 and 5.6. Accurate measurement of residual activities of all these enzymes in the range mentioned above is possible. These results indicate that trypsin, especially at pH 6.0, with its associated thermal resistance characteristics approximately between those of MMS and peroxidase, can be a good candidate for biovalidation purposes. Although microbiological verification and validation are the final

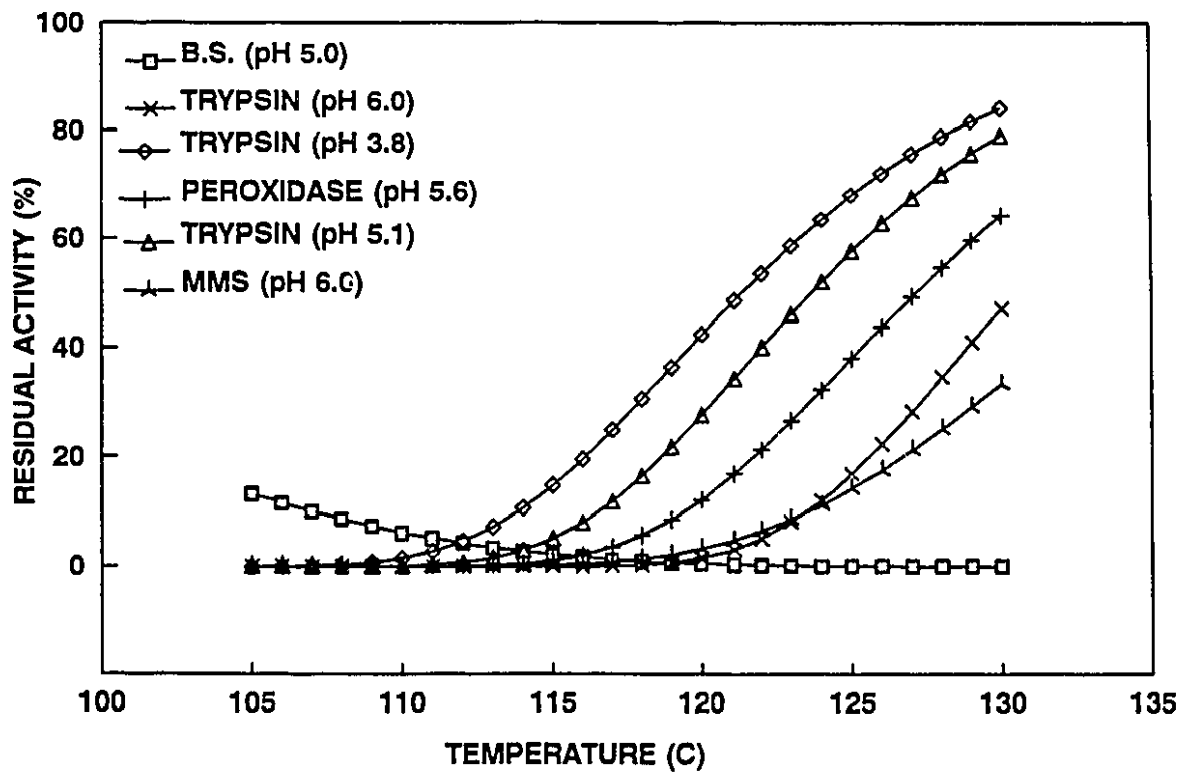


Figure 8.6. Residual activity (%) of trypsin and selected bio-indicators as a function of temperature resulting in F_0 of 10 min.

criteria in aseptic processes, it may be prudent to consider enzymes as process indicators because of their convenience in handling and evaluation.

CONCLUSIONS

Thermal inactivation of trypsin has been shown to follow a first order reaction over the pH range studied. Data obtained could be described by both the TDT and Arrhenius models. Results indicate that trypsin is heat resistant, with pH dependent thermal kinetics. The thermal resistance of trypsin especially at pH 6, is somewhat comparable to that of peroxidase and MMS. This makes trypsin a potential bio-indicator for low acid foods.

CHAPTER IX

BIOLOGICAL VERIFICATION OF FLUID-TO-PARTICLE INTERFACIAL HEAT TRANSFER COEFFICIENTS IN A PILOT SCALE HOLDING TUBE SIMULATOR

ABSTRACT

Immobilized bovine pancreas trypsin (type III) was used in conjunction with a finite difference model to verify fluid-to-particle heat transfer coefficients to particulates in a holding tube of a pilot scale aseptic simulator operated at temperatures ranging from 90 and 110°C. The enzyme was sealed in a stainless steel capsule and embedded at the centre of a finite cylindrical particle, which was pretested to be suitable for HTST applications. The percentage retention of the enzyme was calculated using transient temperatures and their respective D-values in a finite difference program. Heat transfer coefficients estimated for the potato particles under similar experimental conditions were used as input data. Excellent comparison was observed between predicted and measured percentage retention.

INTRODUCTION

Recent industrial motivation to adopt continuous high-temperature short-time (HTST) concepts to products containing suspended particles is to achieve higher quality as compared to conventional alternatives. However, if success is to be achieved without undue constraints as realized with high acid foods, then microbiological assurance should be proven for all portions of the product. Commercial sterility related to particulate laden

products in continuous flow is calculated on two premises: (1) the use of an accurate time-temperature history, gathered from the coldest spot of the fastest moving particle or (2) biological quantification of lethality (F_0 -value) delivered to the coldest spot (Dignan *et al.*, 1989). In view of technological challenges associated with measuring particle centre temperature in a continuous flowing media, and recognizing its implications/influence on particle hydrodynamics, conservative estimate of the F_0 -value can be made and verified with biological measurement techniques (Dignan *et al.*, 1989; Bernard *et al.*, 1990).

Potential solution to this problem is to use appropriate mathematical models (Ramaswamy and Ghazala, 1990; Sastry, 1992; Maesmans *et al.*, 1994) to predict the time-temperature history for estimating both sterility and nutrient degradation, if one is not to be traded off for the other. The other alternative (Dignan *et al.*, 1989) is to measure the temperature profile in a stationary particle immobilized in a system designed to simulate actual processing conditions. According to the authors, such procedures present relevant estimates of the actual F_0 values needed to impact definitive microbiological destruction. Since particles are heated indirectly by the surrounding carrier fluid, heat penetration is dictated primarily by the heat transfer coefficient at the fluid/particle interface, which as mentioned in earlier chapters, is the most difficult parameter to estimate under aseptic conditions.

An immobilized bioindicator is one technique which is readily adoptable to high temperature verification of processing parameters. These indicators are time-temperature dependent devices which undergo irreversible, yet measurable changes in response to temperature variations (Maesmans *et al.*, 1994; Taoukis and Labuza, 1989). Spores of

Bacillus stearothermophilus, a thermophilic bacterium, has been used by several researchers to evaluate sterilization efficacy (Bean *et al.*, 1979; Pflug *et al.*, 1980; Sastry *et al.*, 1988; Ronner, 1990). Hunter (1972) immobilized spores of *Bacillus anthracis* in 0.31 cm diameter polymethylmethacrylate beads, and injected them into an aseptic simulator at 100°C for heat transfer studies. The author used Heisler's chart in solving the unsteady state heating of spherical particles iteratively, till the experimental F_0 value equalled theoretical value. Hunter (1972) obtained higher h_p values (2800 W/m²C) for lower flow rate (53 cm/s) than for higher flow rate (1760 W/m²C at 60 cm/s). Heppel (1985) used a similar approach but with *Bacillus stearothermophilus* spores immobilized in 3.1 mm diameter alginate beads. Survival spore concentration was enumerated after subjecting the beads to a continuous heat-hold-cool system containing water. The average heat transfer coefficient was obtained by comparing experimental results with data generated from a mathematical model. Values obtained were 1850 and 7300 W/m²C for Reynolds numbers of 5300 and 50,000 respectively. Recently, Gratzek and Toledo (1994) used Heppel's approach but with spore of *Bacillus stearothermophilus* immobilized in Gellan cubes for heat transfer studies in a 2.54 cm diameter holding tube at temperatures ranging from 129 to 131°C. The heat transfer coefficient ranged from 2000 to 4500 W/m²C with pipe Reynolds number ranging from 3000 to 9000.

The Food and Drug Administration (FDA) stipulates the use of microorganisms for validating process efficacy. However, the use of microorganisms for routine estimation of the interfacial fluid-to-particle heat transfer coefficient can be time consuming. Furthermore, there could be lack of reproducibility in estimated values due to sample-to-

sample variations (Sastry, 1992). Chemical and enzymatic indicators have been proposed as alternatives for estimating heat transfer coefficients as well as process validation purposes (Berry *et al.*, 1989,1990; Weng *et al.*, 1991a,b, 1992; Kim and Taub, 1993); however, limited studies have been conducted with particulates under aseptic conditions. Accuracies associated with enzymatic indicators gives them significant advantages over classical microbiological procedures (Jason, 1983; Maesmans *et al.*, 1992).

Weng *et al.* (1991b) used horseradish peroxidase covalently immobilized on glass beads in a dodecane medium to estimate heat transfer coefficients. The indicator was imbedded in 25 mm diameter polyacetal particles held stationary at the centre of a can which was processed at 85 °C. Heat transfer coefficients, ranging from 123.12 to 233.71 W/m² C, were obtained using the Least Absolute Lethality Approach.

Different property materials including metals (Rodriguez and Teixeira, 1988), plastics (Hunter, 1972; Pflug *et al.*, 1980; Weng *et al.*, 1991b; Hendrickx *et al.*, 1992a), and model food systems fabricated with alginate (Brown *et al.*, 1984; Hinton *et al.*, 1989; Gaze *et al.*, 1990; Abdelrahim, 1994) have been used as carrier particles for biological indicators. The sensitivity of metals in particular to temperature, limits its use for estimating heat transfer coefficients (Maesmans *et al.*, 1994) since changes in h_p due to different environmental conditions may not be reflected by the indicator. According to the authors, it is most convenient for practical purposes, to homogenize the bioindicator with the carrier material or, to infuse it at the centre of the particle, notwithstanding the fact that the most obvious location would have been the particle's surface. However, a small indicator embedded in a solid as a measuring point would be more sensitive to changes

at convective interfaces than an indicator totally homogenized over the entire carrier material. It is important to note that the magnitude of estimated heat transfer coefficients can be influenced if leakage and the formation of chemical complexes occur between enzymatic or chemical markers and other indigenous compounds at elevated temperatures.

The objectives of this study were to (1) develop a method for rapid verification of heat transfer coefficients under aseptic conditions using a bioindicator and (2) verify h_p estimates calculated from heat penetration data for heating finite cylindrical particles using a mathematical model and established kinetic data for the bioindicator.

MATERIALS AND METHODS

Sample Preparation

Cylindrical potato particles were used in this study. Finite cylindrical samples were obtained using a 21 mm internal diameter cork borer, and the required length (24 mm) was cut with a knife. The dimensions of each particle was verified with a calliper. A cylindrical cavity (Figure 9A) of approximately 7.56 mm diameter and 13.4 mm deep was drilled in the axial direction of the cylinder to facilitate placement of the bioindicator as demonstrated in Figures 9.1A and 9.1B.

Preparation and Immobilization of Bioindicator

Bovine pancreas trypsin (type III), dissolved in 1 mM citrate buffer (pH 5.1) was used as the bioindicator. 60 μ l of the enzyme stock was transfer into a stainless steel differential scanning calorimeter (DSC) capsule (Perkin-Elmer Corp., Norwalk, CT),

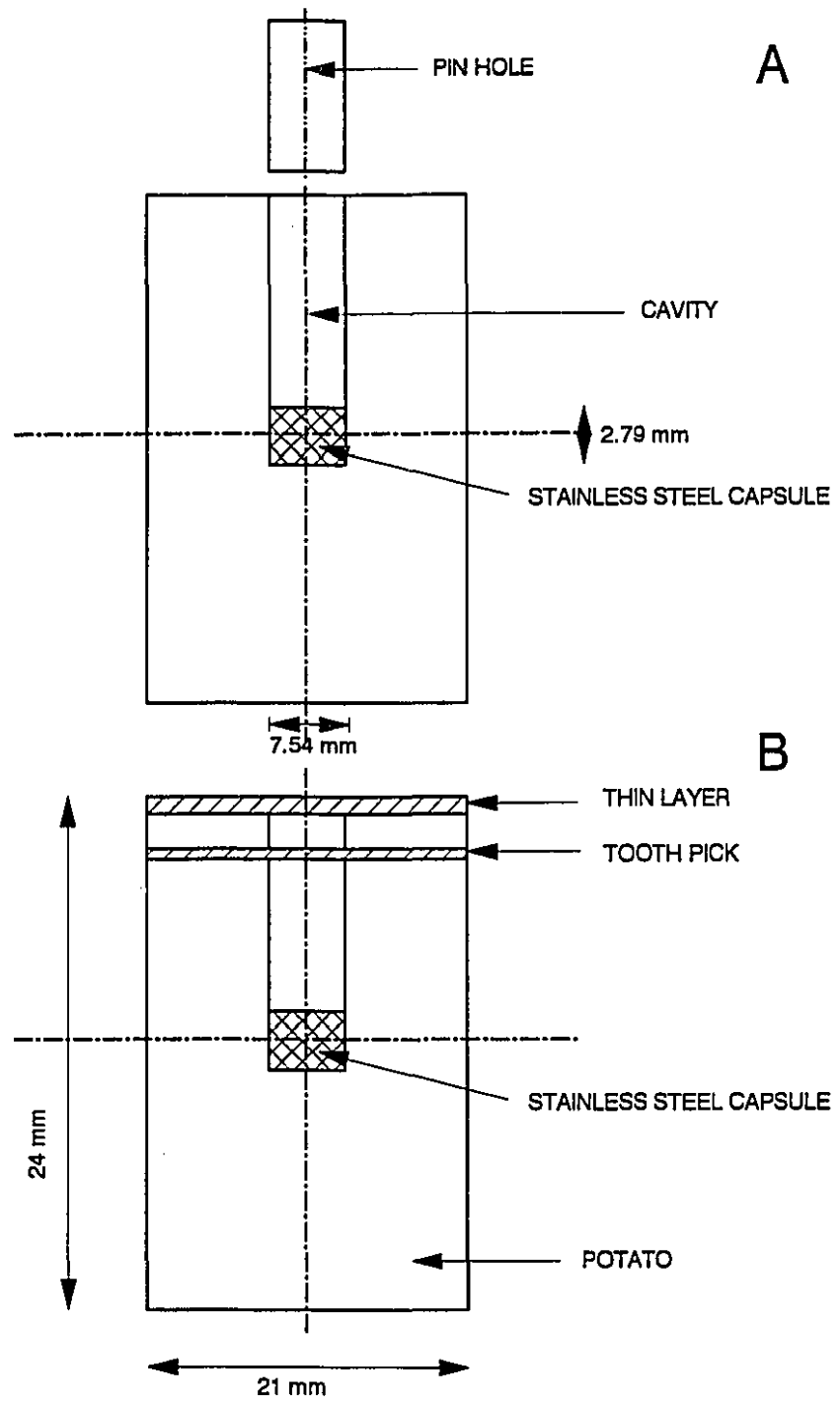


Figure 9.1 A schematic of sample preparation for verification studies.

equipped with an O-ring for high pressure (~350 psi) and temperature (~225°C) applications. The diameter, height and weight of the capsule were 7.54 mm, 2.79 mm, and 0.33 grams respectively. Dye (potassium permanganate) filled capsules were tested in boiling water for leakages using two approaches. Firstly, the heating medium was monitored for traces of the dye during heating, and secondly, by the total weight loss approach which confirmed no leakages. A filled and properly sealed capsule was placed in the cavity created in the finite potato sample (Figure 9.1A). Approximately two to three drops of industrial adhesive (Loctite Canada Inc., Mississauga, ON) was added on top of the capsule to fill possible gaps between the capsule and potato. A 7.6 mm diameter potato cylinder having a pinhole through its axial direction was used to close the cavity (Figure 9.1A). The pinhole facilitated the removal of air from the cavity as the smaller cylindrical piece was pushed into place, while the adhesive helped in sealing off the pinhole as well as the interface between the wall of the cavity and smaller cylindrical piece. A "tooth pick" was used to secure the capsule/small-cylinder combination in place as shown in Figure 9.1B. A thin potato disc (Figure 9.1B) having the same diameter as the test sample was glued onto the sample to prevent channelling of fluid into the test particle.

The procedure described above was tested in relation to particle integrity and disintegration and found to be adequate for temperatures up to 113°C. Again, the possibility of the bioindicator leaking out of a test particle was eliminated with the introduction of the capsule which isolated it from the particle material.

Experimental Setup and Conditions

Prior to using the stainless steel capsule technique, kinetic studies at selected conditions were carried out in a constant temperature oil bath for comparison with data established with the ampoule method (Chapter VIII). The pilot scale aseptic holding tube simulator was used for this study with samples held stationary in the test chamber as detailed in Chapter V. Test particles were heat treated at selected conditions of time duration (2-8 min), temperature (90-110°C), concentration (0 and 0.5% w/w CMC) at a fluid/particle relative velocity of $1.5 \times 10^{-4} \text{ m}^3/\text{s}$ in a 5.08 cm diameter tube. The particles were recovered from the test chamber after cooling for times ranging from 2 to 5 minutes. A minimum of three replicates were performed for each experimental condition.

Enzyme Recovery and Assay

Recovered capsules were thoroughly washed by dipping in a detergent solution and rinsed in distilled water. A small hole was punched in the capsule and the enzyme was recovered using a micro-syringe. 30 μL of the recovered enzyme was transferred to a test tube and the volume adjusted to 230 μL . The amidase activity of trypsin was assayed using the method of Erlanger *et al.* (1961). The reaction mixture consisted of 0.1 mL of the enzyme solution and 2.9 mL of BAPA (substrate dissolved in DMS) in 0.05 M Tris-HCl buffer (pH 8.2) containing 0.02 M $\text{CaCl}_2 \cdot 2\text{H}_2\text{O}$. The increase in light absorption was measured with a spectrophotometer as detailed in Chapter VIII. The percentage retention of the enzyme was calculated for comparison with data obtained using a mathematical model.

Mathematical Formulation of Heat Conduction to a Finite Cylinders

The governing partial differential equation for a finite, isotropic, homogeneous cylinder of radius r and half-length L is:

$$\frac{1}{\alpha} \frac{\partial T}{\partial t} = \frac{\partial^2 T}{\partial r^2} + \frac{1}{r} \frac{\partial T}{\partial r} + \frac{\partial^2 T}{\partial z^2} \quad (9.1)$$

with the initial condition:

$$T = T_o \begin{cases} t = 0 \\ 0 \leq r \leq R \\ -L \leq z \leq +L \end{cases} \quad (9.2)$$

The convective boundary condition is:

$$k \frac{\partial T}{\partial n} = h_{fp} [T_s - T_w] \begin{cases} 0 < t \leq X_T \\ r = R \\ z = \pm L \end{cases} \quad (9.3)$$

and the symmetry conditions are as follows:

$$\frac{\partial T}{\partial r} = 0 \begin{cases} r = 0 \\ 0 \leq t \leq X_T \end{cases} \quad (9.4)$$

$$\frac{\partial T}{\partial z} = 0 \begin{cases} z = 0 \\ 0 \leq t \leq X_T \end{cases} \quad (9.5)$$

where $\partial T/\partial n$, and X_T are the outward normal gradient of temperature, and total time respectively.

Considering a single point temperature history within the capsule was found inadequate, because the capsule was considered to occupy a significant portion of the test sample which was far bigger for a single point profile to be considered. A finite difference option was considered because analytical solutions though accurate, are complex and cumbersome to handle mathematically especially for a finite cylinder. To solve the above equations numerically, the cross section of the finite cylinder was divided into four quadrants (Figure 9.2), each having concentric rings and rectangular grids. Finite difference approximations were developed for the boundaries and internal nodal points (Figure 9.2) using the implicit Crank-Nicolson finite difference algorithm. Spatial derivatives were evaluated at the next time step and the time derivative by forward difference. The advantage of this scheme is that there is no restriction on the maximum time step required to effect stability. The finite difference approximation for the internal nodal points is given by the following relationship:

$$\begin{aligned} & \frac{1}{2\Delta r^2} \left[T_{i-1,j}^{n+1} - 2T_{i,j}^{n+1} + T_{i+1,j}^{n+1} + T_{i-1,j}^n - 2T_{i,j}^n + T_{i+1,j}^n \right] + \\ & \frac{1}{4(i-1)\Delta r^2} \left[T_{i+1,j}^{n+1} - T_{i-1,j}^{n+1} + T_{i+1,j}^n - T_{i-1,j}^n \right] + \\ & \frac{1}{2\Delta z^2} \left[T_{i,j+1}^{n+1} - 2T_{i,j}^{n+1} + T_{i,j-1}^{n+1} + T_{i,j+1}^n - 2T_{i,j}^n + T_{i,j-1}^n \right] = \\ & \frac{1}{\alpha \Delta t} \left[T_{i,j}^{n+1} - T_{i,j}^n \right] \end{aligned} \quad (9.6)$$

where T_{ij}^n and T_{ij}^{n+1} , for instance represents temperatures at the previous and current times respectively. The finite difference approximations derived for boundaries labelled 1-9 (Figure 9.2) were solved using the Successive Over-Relaxation (SOR) method and coded in a set of Fortran 77 subroutines (Appendix 2). The computer programme was pretested to agree with the simplified equations developed by Ramaswamy *et al.* (1982).

Data Analysis

Temperatures at different nodal locations (6 in the i direction and 10 in the j direction) occupied by the capsule (Figure 9.2, centre rectangle) were gathered from the finite difference program using h_p values previously estimated for potatoes under similar experimental conditions. Using this representative temperature and established D -values at specific temperatures (Chapter VIII), the D -values corresponding to all intermediate temperatures (i.e mass average temperature of all nodal points within the capsule at each time step) were calculated by interpolation on a logarithmic scale of D vs temperature. Using the estimated D -values, the percentage retention was calculated by numerical integration as follows:

$$RA(\%) = \int_0^t 10^{(2-t/D)} dt \quad (9.7)$$

where t represents the total (i.e. heating and cooling) time in minutes.

RESULTS AND DISCUSSION

Experimental and Simulated Temperature Profiles

Figure 9.3 shows measured and simulated time-temperature profiles for heating potato in 90°C water flowing at 1.5×10^{-4} m³/s in 5.08 cm diameter tube, followed by cooling with water at 20°C. Heat transfer coefficients used were those established for heating (458 W/m²C) and cooling (252 W/m²C) under similar experimental condition. Figure 9.3 shows a good fit between predicted and measured time-temperature data, however, two anomalies can be observed at the beginning of the heating and cooling stages. This observation is not surprising due to instantaneous exposure of the test chamber and particle (Chapter V) to a dynamic fluid medium which caused some form of turbulence to be generated within the first 80-90 sec of heating (Figure 9.3). This phenomenon enhanced heat transfer to the particle as indicated by higher particle initial temperature till a smooth fluid flow profile was established. Such initial discrepancies are irrelevant in process evaluations since low temperatures contribute insignificantly to overall lethality. The other anomaly which occurred during the transition from heating to cooling, can have serious implications on derived percentage retention due primarily to overshoot in temperature predicted with the mathematical model. Under such circumstances, the mathematical model will overpredict imparted lethality.

Comparison of Kinetic Data obtained with Ampoule and Capsule Methods

Inactivation kinetic data for trypsin (pH 5.1) was evaluated using capsules at 100°C for heating times ranging from 10 to 30 mins. The associate D-value, k-value and

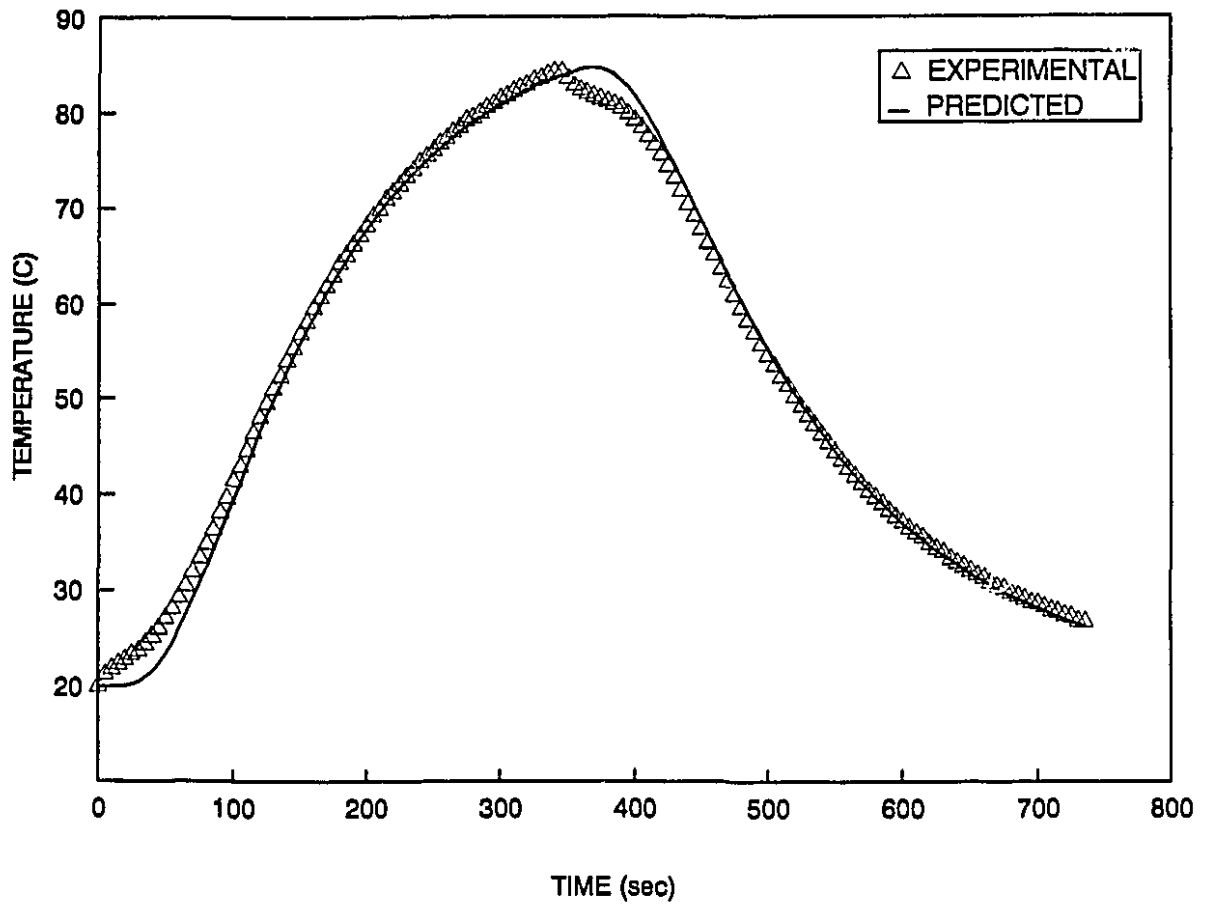


Figure 9.3. Measured and predicted heat penetration curves for heating potato in water at 90°C.

half life were 77.3 min, $0.029789 \text{ min}^{-1}$, and 23 min respectively. The coefficient of determination (R^2) was 0.98. Although these values were found to be higher compared to their counterparts obtained with the ampoule method (Chapter VIII), they compared favourably well.

Low Temperature Kinetics for Trypsin (pH = 5.1)

Initial attempts to match predicted and observed percentage retention failed, because observed retention values were extremely lower (up to 90%) than predicted values depending on heating times. To verify the above discrepancies, additional experiments were carried out under two heating conditions. Firstly, a beaker was filled with approximately 150 mL of water and heated with sealed capsules alone from 20 to 90°C. The time-temperature data of the heating medium was continuously gathered while the enzymes was recovered at specific temperatures, cooled immediately in ice/water mixture and assayed for residual activity. Secondly, the beaker was filled with water and heated to a predetermined constant temperature before the capsules were dropped in. The capsules were recovered at selected time intervals, cooled immediately and assayed for residual activity. It is important to note the differences between the two procedures. With the first method, the capsules were taken out immediately when the desired temperature was reached. This implies that the capsule goes through a transient heating profile exhibited by conductive heating objects. For the second approach, the capsule establishes a constant temperature rapidly and stays at that operating temperature for predetermined times. Approximately 57, 78, and 80% loss in residual activity at 60, 80, and 90°C

respectively was found with the first approach. The corresponding heating times were 4.4, 6.2 and 7.22 mins. For 6 and 10 mins heating at 80°C with the second approach, the loss in activity were 56 and 65% respectively. However, with the second approach at 60°C for 6 and 10 min heating, the loss in activity were 80 and 88% respectively. The comparatively higher loss in activity at temperatures between 60 to 80°C prompted the establishment of kinetic data at lower temperatures.

Figure 9.4 illustrates that trypsin (pH 5.1) is susceptible to thermal inactivation as temperature increases from 50 to 70°C. Beyond 70°C the enzyme gained stability with temperature (Figure 9.4). Comparison of the present data with those established at higher temperatures (Chapter VIII) indicate the enzyme to be stable at higher than lower temperatures. In addition, instantaneous exposure to temperature appeared to have minimal degradation effect on the enzyme. This is evident from the relatively higher D-values associated with the capsule method compared with the ampoule method. These complications are difficult to explain theoretically. Price and Stevens (1989), indicated that complications can arise with enzymes which exhibit two interconvertible forms, which causes discontinuity in the Arrhenius plot around the temperature where such changes occur. For purposes of the present study, the kinetic data for the low temperature range was established for heating times up to 4 mins (Table 9.1). This is based on the assumption that the enzyme does not encounter a particular temperature for more than 4 mins. A z-value of 22C° was obtained for temperatures between 50-70°C, with a corresponding R² of 0.98.

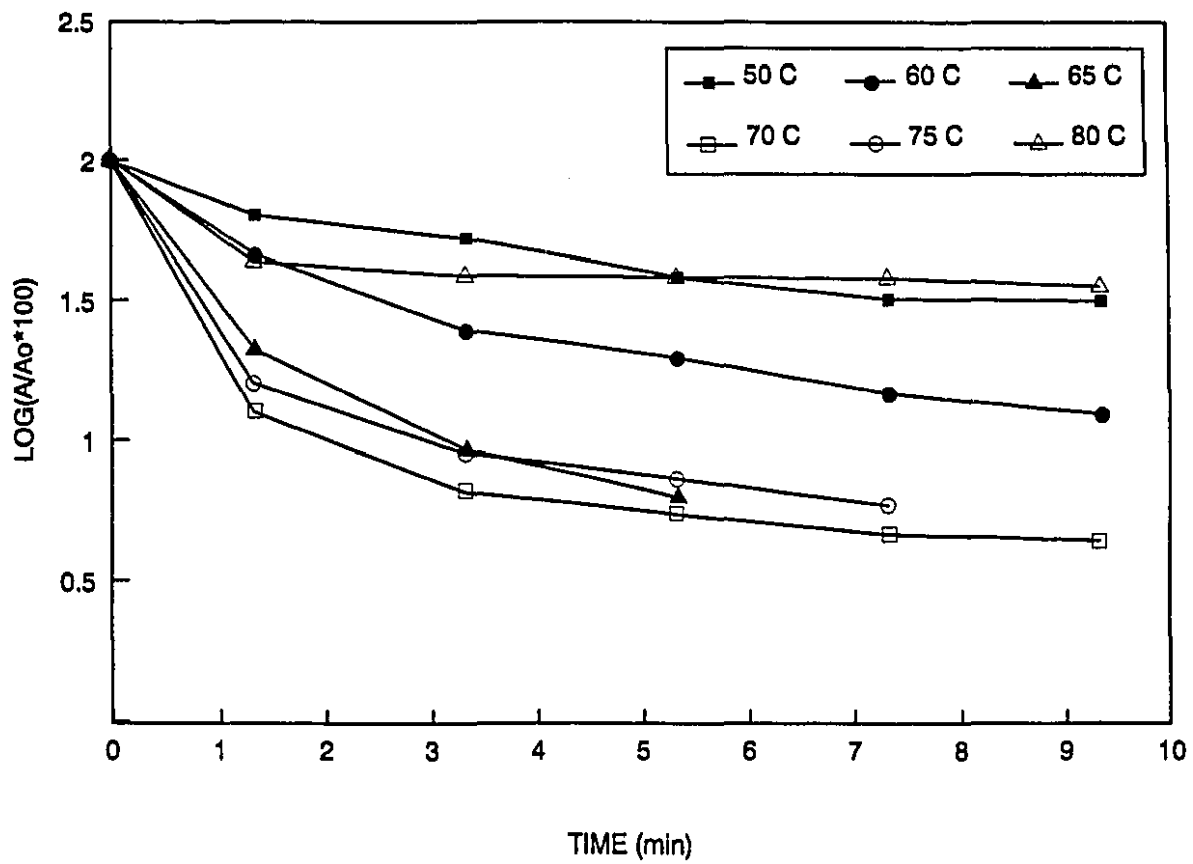


Figure 9.4 Residual activity as a function of heating time at temperatures (50-80°C) for trypsin in citrate buffer (pH = 5.1).

Table 9.1. Low temperature kinetic data for trypsin in citrate buffer (pH = 5.1) .

Temperature (°C)	D-value (min)	k-value (min ⁻¹)	t _{1/2} (min)	R ²
50	12.6	0.18336	3.77945	0.90
60	5.6	0.40980	1.69110	0.97
65	2.8	0.81090	0.85461	0.93
70	1.6	1.48580	0.04664	0.98
75	6.9	0.33158	2.08998	0.97
80	14.7	0.15645	4.42942	0.62

Biological Verification of Heat Transfer Coefficients

The behaviour exhibited by trypsin at relatively low temperatures (i.e., a "zigzag" nature in activity between 50 to 90°C) made it impossible to establish a common z-value for estimating percentage retention with the Formula method. The exact retention of the enzyme was calculated on the basis of the transient temperatures and inactivation rate appropriate at these temperatures. Table 9.2 shows a comparison between h_p values predicted with the mathematical model and those obtained by heating immobilized enzymes in the pilot scale aseptic simulator. In general, the predicted and observed values compared well, resulting in standard deviations ranging from 0.01 to 0.57%. The corresponding percentage coefficient of variation (CV) ranged from 0.05 to 9.07%. The minimal differences between observed and predicted values indicate that input h_p values are representative of conditions under which experiments were performed. Again the results confirm the behaviour exhibited by trypsin as it goes through a transient temperature profile. However, with the exception of heating in water for 3 minutes at 90°C (Table 9.2), predicted values were generally found to be higher than observed ones. This is not surprising because (1) there was always the need to depressurize the simulator prior to the beginning of cooling and (2) the unpredictable time lapse between heating and cooling in relation to closing and opening appropriate valves manually to initiate cooling. Aside from the above factors, minor discrepancies between observed and predicted data can be attributed to the overshoot in predicted temperature profile as demonstrated in figure 9.3.

The results also shows that the capsule approach can be used for h_p verification

Table 9.2 A comparison of experimental and predicted percentage retention of immobilized trypsin at selected heating conditions.

HT ¹ (°C)	Heating Time (min)	Conc ² (% CMC)	h _{fp} (W/m ² C)	Retention	
				Exp ³ (%)	Pred ⁴ (%)
90	3	0.5	302 ± 9	12.06 (0.46)	12.57 (0.45)
90	5	0.5	302 ± 9	6.26 (0.57)	7.53 (0.14)
90	3	0	458 ± 15	8.15 (0.49)	7.48 (0.57)
90	5	0	458 ± 15	6.46 (0.08)	6.65 (0.07)
90	8	0	458 ± 15	6.26 (0.08)	6.49 (0.29)
100	3.2	0.5	346 ± 17	8.99 (0.14)	9.29 (0.39)
100	8	0.5	346 ± 17	8.67 (0.42)	8.89 (0.16)
110	5	0.5	493 ± 26	10.95 (0.43)	12.53 (0.25)
110	2	0	518 ± 38	11.20 (0.27)	11.71 (0.01)

¹ Heating medium temperature.

² Fluid concentration.

³ Average and standard deviation of percentage retention obtained from experiments (n = 3 - 4). ⁴ Average and standard deviation of percentage retention predicted with the mathematical model (n = 3 - 4).

purposes without loss in accuracy, assuming an infinite heat transfer coefficient at the interface between the particle and capsule. The method allows rapid recovery and assay of residual activity without the need to worry about efficient procedures for isolating the indicator for assay after heat treatment. It is important to emphasize that irrespective of how precisely mathematical models are, the accuracy of this method, as with all biological indicators will depend on how accurate input kinetic data are determined in relation to their responses to transient temperature profiles. Therefore, in situations where the TDT concept breaks down for lack of continuity in the z-value as the product temperature rises from its initial temperature to that of the heating medium, the D-value at specific temperatures becomes handy and could be used in conjunction with the mass average effect of all lethal temperatures for calculating the percentage retention.

CONCLUSIONS

The capsule method for immobilizing enzymes was used to verify fluid-to-particle convective heat transfer coefficient data established for particulates in a dynamic system at temperatures ranging from 90 to 110°C. Using potato particles, the method was pretested to be suitable for high-temperature short-time applications without particle fragmentation. The method was found adequate since it isolated the bioindicator from the particle material. A finite difference program was developed for solving heat transfer from a carrier fluid at constant temperature to a finite cylinder, and subsequently, was validated with an analytical solution. Trypsin was found to exhibit a zigzag behaviour at lower temperatures between 50 to 90°C as opposed to its first order decay trend previously

observed at relatively higher temperatures. Verification studies were carried out using the capsule method and the finite difference program with previously established heat transfer coefficient as input data. Excellent results were obtained between predicted and measured percentage retention values.

CHAPTER X

GENERAL CONCLUSIONS

1. For routine estimation of heat transfer coefficients, mathematical models should be simple to handle and not overly sensitive to minor errors in parametric values. Two analytical routines for calculating heat transfer coefficients were identified and tested in relation to sensitivity to errors in input parametric data, using inert materials in regular shapes under different environmental conditions. Heat transfer coefficient ranged from 15 to 420 W/m²C depending on the method used, the type of sample, shape and ambient conditions. The two routines, namely the Ratio and Rate methods compared favourably well especially when the associated heat transfer coefficients were low (Biot number, Bi, less than 10); however, both methods were found to be sensitive to minor variations in reference input data when the associated Bi exceeded 20. The ratio method generally overestimated heat transfer coefficients. The rate method which is independent of thermocouple placement was found to predict more conservative and consistent estimates compared to the ratio method.
2. Carrier fluid temperature and concentration of CMC influenced its power law parameters and, hence, increased h_{fp} as fluid temperature increased for heating both carrot and potato samples under mild temperatures and low flow conditions. CMC concentration had the largest impact on estimated h_{fp} values with an increase

in concentration decreasing h_{fp} . Fluid velocity, sample size and the direction of fluid flow had only marginal effects on h_{fp} values. Probably due to structural and textural differences, carrots generally had higher heat transfer coefficients than potatoes. Fluid flow regime indicated the possibility of laminar flow natural convection. Therefore, the Nusselt number was modeled as a function of Rayleigh number.

3. A cost effective pilot scale holding tube simulator was designed and fabricated for rapid gathering of heat penetration data for h_{fp} calculations under aseptic processing conditions. A constraint posed by the "soft" components of the on-line sine pump limited its operation to 115 °C. The simulator was calibrated to give flow conditions comparable to real processing situations and pretested to give constant medium temperature by manual regulation of the steam inlet value. To avoid fluid distortions due to pipe bends, adequate pipe lengths were provided before and after the test chamber. Fluid medium temperature could be established in either a time dependent or time independent modes for studying temperature histories for suspended particle and carrier fluids.
4. Fluid-to-particle heat transfer coefficient was investigated under aseptic processing conditions in relation to fluid temperature, concentration, particle size, shape, tube diameter and particle orientation. With the exception of particle length and orientation, all the above parameters had significant impact ($p < 0.05$) on heat

transfer coefficients evaluated with both Teflon and potato particles. Increasing particle diameter decreased heat transfer coefficients evaluated in both 5.05 and 7.62 cm diameter pipes. Depending on experimental conditions, up to 72% drop in h_{fp} was found when particle diameter was changed from 19.05 to 25.4 mm. Higher h_{fp} values were generally found to be associated with potato compared to Teflon, with both materials exhibiting different responses to processing conditions. The trends exhibited by both materials suggested the dependence of h_{fp} on material property. A 7 to 29% difference was found between spherical and finite cylindrical particles having length equal to diameter. A 36% drop in h_{fp} was found between heating and cooling potato particles. Further studies are needed using other methodologies to address the inconsistencies in published data in relation to presented effects of particle size and particle-to-tube relationships on the heat transfer coefficient.

5. Dimensionless correlations describing Nusselt number as a function of the generalized Reynolds, Prandtl, Grashof numbers were developed for forced and mixed heat transfer to spherical and finite cylindrical particles under aseptic processing conditions. The type of sample material was found to have significant impact on the Nusselt number. To accommodate such situations, a thermal diffusivity ratio was introduced which was found to improve developed correlations. Contributions from natural convection should probably be accounted for even in situations where forced convection is anticipated to be the dominant

mechanism of heat transfer. Excellent correlations were generally obtained with coefficient of determinations generally greater than 0.97.

- 6 Sealed glass ampoules were used to establish thermal inactivation kinetic data for trypsin (bovine pancreas type III) in both low and high pH media at temperatures ranging from 90 to 130°C. The enzyme inactivation was modelled based on first order and found to be adequately stable for thermal processing studies especially in the low pH range. Temperature dependent kinetic parameters were analyzed using both the Arrhenius and TDT concepts. Comparative studies with other bioindicators suggested trypsin to be a potential bioindicator for verification purposes.

7. Center point nutrient degradation of trypsin in a finite cylindrical potato particle was used in conjunction with a mathematical model to verify evaluated heat transfer coefficients under simulated aseptic processing conditions. Initial attempts to use established kinetic data for predicting percentage retention of trypsin after processing failed because the enzyme was surprisingly found to be more susceptible to inactivation at lower temperatures, thus prompting the establishment of additional kinetic data. A stainless steel capsule was used for holding the enzyme, and was pretested to be capable of withstanding aseptic processing temperatures without leakages. The percentage retention of the enzyme after processing was calculated as the mass average of all temperatures within the

capsule. Excellent comparison was made between predicted and measured percentage retentions.

8. The present study illustrates the importance of the fluid-to-particle heat transfer coefficient in relation to both product and system parameters at aseptic temperatures. Particle size, fluid/particle relative velocity, pipe diameter and fluid concentration appeared to be key parameters likely to limit the rate of heat penetration to the coldest spot of particles suspended in dynamic systems by influencing the associated fluid-to-particle heat transfer coefficient. Although heat transfer coefficient theoretically should be independent of test sample used, the type of particle material was found to have an impact on h_{fp} due probably to the presence of buoyancy forces and mass transfer across the boundary of the carrier fluid and particle.

REFERENCES

- Abdelrahim, K. A., Ramaswamy, H. S. and Awuah, G. B. 1991. Rheological properties of carboxyl-methyl-cellulose (CMC) as influenced by concentration. Paper Presented at the 34th Annual Meeting of the CIFST. Montreal. June 16-19.
- Abdelrahim, K. A. 1994. Residence time distribution of food particles and rheological properties of carrier fluids under aseptic processing conditions. Ph.D Thesis, Mcdonald Campus, McGill University, Montreal.
- Adams, J. B. 1978. The inactivation and regeneration of peroxidase in relation to the high temperature-short time processing of vegetables. *J. Food Technol.* 13(4):281-297.
- Adams, J.P., Simunovic, J. and Smith, K. L. 1984. Temperature histories in a UHT indirect heat exchanger. *J. Food Sci.* 49:273-277.
- Alhamdan, A. and Sastry, S. K. 1990. Natural convection heat transfer coefficient between non-Newtonian fluid and an irregular shaped particle. *J. Food Proc. Eng.* 13:113-124.
- Alhamdan, A., Sastry, S. K. and Blaisdell, J. L. 1990. Natural convection heat transfer between water and an irregular shaped particle. *Trans. ASAE.* 33:620-624.
- ASHRAE. 1981. *ASHRAE Handbook*. 1981 Fundamentals. American Society for Heating Refrigerating and Air Conditioning Engineers, New York.
- Astrom, F. A., Ohlsson, T., Skjoldebrand, C. and Falk, C. 1988. Prediction of food quality during continuous heat treatment of particulate products. *Proc. of Intl. Symp. on Progress in Food Preservation Processes*, Ceria, Brussels, Belgium, April 12-14, Vol. 2, pp. 29-38.
- Astrom, A. and Bark G. 1994. Heat transfer between fluid particles in aseptic processing. *J. Food Eng.* 21:97-125.
- Awuah, G. B., Ramaswamy, H. S. and Simpson, B. K. 1993. Surface heat transfer coefficient associated with heating of food particles in CMC solutions. *J. Food Proc. Eng.* 16:39-57.
- Balasubramaniam, S. K. and Sastry, S. K. 1994. Noninvasive estimation of heat transfer between fluid and particle in continuous tube flow using a remote temperature sensor. Presented at the Annual Meeting of the Institute of Food Technologists. Atlanta, GA. USA. June 25-29.

- Ball, C. O. 1923. Thermal process times for canned foods. Bull. 37. National Research council, Washington, DC.
- Ball, C. O. and Olson, F. C. W. 1957. Sterilization in Food Technology, McGraw Hill Book. Co. , New York.
- Banga, J. R., Perez-Martin, R. I., Gallardo, J. M. and Casares, J. J. 1991. Optimization of thermal processing of conduction-heated canned foods: study of several objective functions. J. Food Eng. 14:25-51.
- Bateson, R. N. 1969. Effect of age distribution on aseptic processing. Presented at the 66th National meeting of the American Institute of Chemical Engineers. Portland Oregon. August 24-27.
- Bean, P. G., Dallyn, H. and Ranjith, H. M. P. 1979. The use of alginate spore beads in the investigation of ultra-high temperature processing. *In* "Food Microbiology and Technology". B. Javis, J. H. B. Christian and H. D. Michener (eds.). Proceedings of the Int. Meeting of Food Microbiology and Technology. Medicina Viva Servizio Congressi S. r. I. Parma, Italy.
- Bernard, D. T., Gavin, A. III., Scott, V. N., Shafer, B. D. Stevenson, K. E. Unverferth, J. A. and Chandarana, D. I. 1990. Validation of aseptic processing and packaging. Food Technol. 44(12):119-122.
- Berry, M. F., Singh, R. K. and Nelson, P. E. 1989b. Kinetics of methylmethionine sulfonium salt destruction in a model particulate system. J. Food Sci. 55:502-505.
- Berry, M. R. 1989. Predicting fastest particle residence time. Proceedings of the First International Congress on Aseptic Processing Technologies, Indianapolis, IN, March 19-21. pp 6-17.
- Berry, M. F., Singh, R. K. and Nelson, P. E. 1989a. Kinetics of methylmethionine sulfonium in buffer solutions for estimating thermal treatment of liquid foods. J. Food Proc. and Preserv. 13:475-488.
- Berry, M. F., Singh, R. K. and Nelson, P. E. 1990. Kinetics of methylmethionine sulfonium in buffer solutions for estimating thermal treatment of liquid foods. J. Food Proc. Preserv. 13:475-488.
- Bhowmik S. R. and Hayakawa, K-I. 1979. A new method for determining the apparent thermal diffusivity of thermally conductive food. J. Food Sci. 44:469-474.

- Bourne, M. C. 1982. Food Texture and Viscosity: concept and measurement. Academic Press. New York.
- Brown, K. L. 1991. Principle of heat preservation. In "Processing and packaging of heat preserved foods. J. A. G. Rees and J. Bettison (eds.). Van Nostrand Reinhold. New York. p.72-91
- Brown, K. L. Ayres, C. A., Gaze, J. E. and Newman, M. E. 1984. Thermal destruction of bacterial spores immobilized in food/alginate particles. Food Microbiol. 1:187-198.
- Brown, L. F. and Fogler, H. S. 1986. Distributions of residence times for chemical reactors. In "Elements of chemical reaction engineering". Fogler, H. S. (ed.). Prentice-Hall, Inc., Englewood Cliffs, NJ. pp. 629.
- Bucher, N. 1993. Aseptic processing and packaging and packaging of particulates. "In "Aseptic Processing and Packaging of Particulate Foods". E. M. A. Willhoft (ed.). Blackie Academic and Professionals. London. pp. 1-21.
- Burfoot, D. James, S. J., Foster, A. M., Self, K. P. and Wilkins, T. J. 1990. Temperature uniformity after reheating in domestic microwave ovens. *In* "Process engineering in the food industry". R. W. Field and J. A. Howell (eds.). Elsevier Applied Sci. New York. pp. 1-14.
- Burfoot, D. and James, S.J. 1988. The effect of spatial variations of heat transfer coefficient on meat processing times. J. Food Eng. 7:41-61.
- Burfoot, D. and Self, K. P. 1988. Prediction of heating times for cubes of beef during water cooking. Int. J. Food Sci. and Technol. 23:247-257.
- Burmeister, L. C. 1983. Convective Heat Transfer. John Wiley & Sons. New York.
- Carslaw, H. S. and Jaeger, J. C. 1959. Conduction of Heat in Solids. 2nd ed. Oxford Univ. Press. London. England.
- Chandarana, D. I., Gavin, A. and Heldman, D. R. 1990a. Modelling and heat transfer in aseptic processing of heterogeneous foods. *In* " Engineering and Food . Vol 2: preservation processes and related techniques. W. E. L. Spiess, and H. Schubert (eds.). Elsevier Applied Science. pp 31-49.
- Chandarana, D. I., Gavin, A. and Wheaton, F. W. 1990b. Particle/fluid interface heat transfer under UHT conditions at low particle/fluid relative velocities. J. Food Proc. Eng. 13:191-206.

- Chandarana, D. I., Unverferth, J. A., Stoforos, N. G., Gavin, A. and Cashed, K. A. 1991. Particle residence time distribution of aseptically processed low-acid foods. Cited in Chandarana, D. I. 1992. Acceptance procedures for aseptically processed particulate foods. *In* "Advances in Aseptic Processing Technologies". R. K. Singh and P. E. Nelson. (eds). Elsevier Applied Science. London & New York. pp. 261-278.
- Chandarana, D. I. 1992. Acceptance procedure for aseptically processed particulate foods. *In* "Advances in Aseptic Processing Technologies". R. K. Singh and P. E. Nelson (eds.). Elsevier Applied Science. London. pp 261-278.
- Chandarana, D. I. and Gavin, A. III. 1989a. Modelling and heat transfer studies of heterogeneous foods processed aseptically. *In* "Innovations in aseptic processing of particulates". J. V. Chambers. (ed.). 1st Intl. congress on aseptic processing technologies. Indianapolis, IN. USA. March 19-21.
- Chandarana, D. I. 1992. Acceptance procedures for aseptically processed particulate foods. *In* "Advances in Aseptic Processing Technologies". R. K. Singh and P. E. Nelson (eds.). Elsevier Applied Science. London & New York. pp. 261-278.
- Chandarana, D. I., Gavin, A. and Wheaton, F. W. 1989. Simulation of parameters for modelling aseptic processing of food containing particulates. *Food Technol.* 43(3):137-143.
- Chandarana, D. I., Gavin, A. III. and Wheaton, F. W. 1988. Particle/fluid interface heat transfer during aseptic processing of foods. ASAE Paper No. 88-6599. American Society of Agricultural Engineers, St. Joseph, MI.
- Chandarana, D. I. and Gavin, A. III. 1989b. Establishing thermal processes for heterogenous foods to be processed aseptically: a theoretical comparison of process development methods. *J. Food Sci.* 54:198-204.
- Chang, S. Y. and Toledo, R. T. 1990. Simultaneous determination of thermal diffusivity and heat transfer coefficient during sterilization of carrot dices in a packed bed. *J. Food Sci.* 55:199-205.
- Chang, S. K. and Toledo, R. T. 1989. Heat transfer and simulated sterilization of particulate solids in a continuously flowing system. *J. Food Sci.* 54:1017-1023,1030.
- Chapman, A. J. 1989. *Heat Transfer*. 4th ed. Macmillan Publishing Co. New York. NY.
- Charm, S. E. 1962. The nature and role of fluid consistency in food engineering applications. *In* "Advances in Food Research". Academic Press, New York.

- Charm, S. E. 1966. On the margin of food safety in canned foods. *Food Technol.* 20(5):97-99.
- Charm, S. E. 1978. *Fundamental of Food Engineering*. 3rd Edn. Van Nostrand Reinhold./AVI, New York.
- Chau, K. V. and Synder, G. V. 1988 Mathematical model for temperature distribution of thermally processed shrimp. *Trans. ASAE.* 31:608- 612.
- Chen, C. J. and Thomsen, D. M. 1975. On transient cylindrical surface heat flux predicted from interior temperature response. *J. AIAA.* 13:697-699.
- Churchill, S. W. and Chu, H. H. S. 1975. Correlating equations for laminar and turbulent free convection from a horizontal cylinder. *Int. J. Heat Mass Transfer.* 18:1049-1053.
- Churchill, S. W. 1977. A comprehensive correlating equation for laminar, assisted forced and free convection. *J. AIChE* 23:10-16.
- Churchill, S. W. and Bernstein, M. 1977. A correlating equation for forced convection from gases and liquids to a circular cylinder in cross flow. *J. Heat Transfer.* 99:300-306.
- Churchill, S. W. 1983. Combined free and forced convection around immersed bodies. In "Heat Exchanger Design Handbook". Hemisphere Pub. Co. New York. pp. 2.5.9-1-2.5.9-7.
- Clark, P. J. 1978. Mathematical modelling in sterilization processes. *Food Technol.* 32(3): 73-75.
- Cuevas, R., Cheryan, M. and Porter, V. L. 1982. Heat transfer and thermal process design in scraped surface heat exchangers. *AIChE. Symp. Ser.*, 78:49-57.
- Dail, R. 1985. Calculation of required hold time of aseptically processed low-acid food containing particulates utilizing the Ball method. *J. Food Sci.* 50:1703-1706.
- Danckwerts, P. V. 1953. Continuous flow system (distribution of residence times). *Chem. Eng. Sci.* 2:1-3.
- de Ruyter, P. W. and Brunet, R. (1973). Estimation of process conditions for continuous sterilization of food containing particulates. *Food Technol.* 27(7):44-51.
- Deniston, M. F., Hassan, B. H. and Merson, R. 1987. Heat transfer coefficients to liquids with food particles in axially rotating cans. *J. Food Sci.* 52:962-966.

- Dennis, C. 1990. HTST processing-Scientific situation and perspective of the industry. *In* "Processing an quality of foods. Vol 1. High temperature/short time (HTST) processing: quarantee for high quality food with long shelflife" P. Zeuthen, J.C. Cheftel, C. Eriksson, T.R. Gormley, P. Linko. and K. Paulus. (eds.). Elsevier Applied Science. pp. 1.36-1.49.
- Dickerson, Jr., R. W., Scalzo, A. M., Reed, Jr., R. B. and Parker, P. W. 1968. Residence time of milk products in holding tubes of high-temperature short-time pasteurizers. *J. Dairy Sci.* 51:1731-1736.
- Dignan, D.M., Berry, M.R., Pflug, I.J. and Gardine, T.D. 1989. Safety considerations in establishing aseptic processes for low-acid foods containing particulates. *Food Technol.* 43(3):118-121,131.
- Dutta, B. and Sastry, S. K. 1990b. Velocity distribution of food particle suspensions in holding tube flow: distribution characteristics of and fastest-particle velocities. *J. Food Sci.* 55:1703-1710.
- Dutta, B. and Sastry, S. K. 1990a. Velocity distributions of food particle suspensions in holding tube: Experimental and modelling studies on average particle velocities. *J. Food Sci.* 55:1448-1453.
- Erlanger, B. F., Kokowsky, N. and Cohen, W. 1961. The preparation and properties of two new chromogenic substrates of trypsin. *Arch. Biochem. Biophys.* 95:271-278.
- Evans, L. B. 1982. Optimization theory and its application in food processing. *Food Technol.*, 36(7):88-93.
- Fand, R. M. and Keswani, K. K. 1973. Combined natural and forced convection heat transfer from horizontal cylinders to water. *Int. J. Heat and Mass Transfer.* 16:1175-1191.
- Fellows, P. 1988. *Food Processing Technology: Principles and Practices.* Ellis Horwood Ltd., Chichester, England.
- Flambert, F. and Deltour, J. 1972b. Exact lethality calculation for sterilizing process. I. Principles of the method. *Lebensm-Wiss u. Technol.* 5:72.
- Frank, H. P. 1968. *Polypropylene.* Gordon and Breach Science Publishers, New York.
- Gaffney, J. J., Baird, C. D. and Eshleman, W. D. 1980. Review and analysis of the transient method for determining thermal diffusivity of fruits and vegetables. *ASHRAE Trans.* 86:261-280.

- Gavin, A. 1985. Thermal process establishment for low-acid aseptic products containing large particulates. Proc. Natl Food Assoc. Conf. Capitalizing on aseptic II. The Food Processors Institute, Washington, DC, pp 13-14.
- Gaze, J. E., Spence, L. E. Brown, C. D. and Holdsworth, S. D. 1990. Microbiological assessment of process lethality using food/alginate particles. Tech. Memo. No. 580. Campden Food and Drink Research Assoc. Chipping Campden. pp. 1-47.
- Geankoplis, C. J. 1978. Transport Processes and Unit Operations. Allyn and Bacon, Boston, MA.
- Gillespy, T. G. 1953. Estimation of sterilization values of processes as applied to canned foods. II. Packs heating by conduction: Complex processing conditions and value of coming-up time of retort. J. Sci Food Agric. 4:553-565.
- Gnielinski, V. 1983. Forced convection around immersed bodies. In "Heat Exchanger Design Handbook, Fluid Mechanics and Heat Transfer". Schlunder *et al.* (eds.). Hemisphere Pub. Co. New York.
- Gordon, C. and Thome, S. 1990. Determination of the thermal diffusivity of foods from temperature measurements during cooling. J. Food Eng. 11:133-145.
- Gratzek, J. P. and Toledo, R. T. 1994. Fluid to particle heat transfer coefficients in two-phase continuous flow sterilization determined from spore inactivation. Presented at the Annual Meeting of the Institute of Food Technologists. Atlanta, GA. June 25-29.
- Grigull, U. and Sandner, H. 1984. Heat Conduction. Hemisphere Publishing Co. New York.
- Gunn, D. J. and Narayanan, P. V. 1981. Particle-fluid heat transfer and dispersion in fluidised beds. Chem. Eng. Sci. 36:1985-1995.
- Hallstrom, B., Skjoldebrand, C. and Tragardh, C. 1988. Heat Transfer & Food Products. Elsevier Applied Science. New York.
- Hassan, B. H. 1984. Heat Transfer Coefficients for Particles in Axially Rotating Cans. Ph.D thesis. Dept. of Agricultural Engineering. Univ. of California, Davis, CA.
- Hayakawa, K-I. 1974b. Response charts for estimating temperatures in cylindrical cans of solid food subjected to time variable processing temperatures. J. Food Sci. 39:1090-1098.

- Hayakawa, K-I. 1977. Mathematical methods for estimating proper thermal processes and their computer implementation. *In* "Advances in Food Research. Vol. 23". C. O. Chichester, E. M. Mrak, and G. F. Stewart (eds.). Academic Press. New York. pp 75-141.
- Hayakawa, K-I. and Bakal, A. 1973. New computational procedure for determining the apparent thermal diffusivity of a solid body approximated with an infinite slab. *J. Food Sci.* 38:623-629.
- Hayakawa, K-I. 1974a. Improved procedures for mathematical evaluation of heat processes. *J. Food Sci.* 39:849-850.
- Hayakawa, K-I. 1968. A procedure for calculating sterilization value of a thermal process. *Food Technol.* 22(7):905-907.
- Hayes, J. B. 1988. Scraped surface heat transfer in the food industry. *AIChE Symp. Ser.* 84:251.
- Heisler, M. P. 1947. Temperature charts for induction and constant temperature heating. *Trans ASME* 69:227-236.
- Heldman, D. R. and Singh, R. P. 1981. *Food Process Engineering*, Van Nostrand Reinhold/AVI, New York.
- Heldman, D. R. 1992. Innovative concepts in equipment design for aseptic processing. *In* "Advances in Food Engineering." R. P. Singh and M. A. Wirakartakusumah (eds.). CRC Press, Boca Raton, FL. pp. 309-318.
- Heldman, D. R. 1989. Establishing aseptic processing for low-acid foods containing particulates. *Food Technol.* 43(3):122-123.
- Hendrickx, M., Weng, Z., Maesmans, G. and Tobback, P. 1992a. Validation of a time-temperature-integrator for thermal processing of foods under pasteurization conditions. *Intl. J. Food Sci. Technol.* 27:21-31.
- Hendrickx, M. E., Silva, C. L., Oliveira, F. A. and Tobback, P. 1992b. Optimization of heat transfer in thermal processing of conduction heated foods. *In* "Advances in Food Engineering" R. K. Singh and M. A. Wirakartakusumah (eds.). CRC Press Boca Raton.
- Heppel, N. J. 1985. Measurement of the liquid-solid heat transfer coefficient during continuous sterilization of foodstuffs containing particles. Presented at the 4th Congress on Engineering and Foods, Edmonton, AB, Canada. July 7-10.

- Hermans, W. F. 1988. In-flow fraction specific thermal processing (FSTP) of liquid containing particulates. Int. Fachtagung 'Sterile Prozeßtechnik', Frankfurt. M 7-8 November. pp. 54-61.
- Hersom, A. C. and Shore, D. T. 1981. Aseptic processing of foods comprising sauce and solids. *Food Technol.* 35(5):53-62.
- Hersom, A. C. 1984. "Asepticpack 84 Proceedings". Schotland Business Research Inc., Princeton, NJ. p.247.
- Hinton, Jr., Driver, A., Silverman, M. G. and Taub, I. A. 1989. Validation of the thermal sterilization of particulates processed at elevated temperatures. Activities Report of the R&D Associates. 41(1):39-49.
- Holdsworth, S. D. 1969. Processing on non-Newtonian foods. *Process Biochem.* 4:15
- Holdsworth, S. D. 1992. *Aseptic Processing and Packaging of Food Products*. Elsevier Applied Science. London & New York.
- Holdsworth, S. D. and Richardson, P. S. 1989a. Continuous sterilization operation for aseptic packaging: An overview. *In "Process Engineering in the Food Industry"* R. W. and Howell, J. A. (eds.). Elsevier Applied Science. London & New York. pp. 3.
- Holdsworth, S. S. 1971. Applicability of rheological models to the interpretation of flow and processing behaviour of fluid food products. *J. Texture Studies.* 2:393.
- Holdsworth, S. D. 1985. Optimization of thermal processing: A review. *J. Food Eng.* 4:89-116.
- Holdsworth, S. D. and Richardson, P. S. 1989b. Mathematical modelling and control of sterilization process. *In "Process Engineering in the Food Industry"*. R. W. and Howell, J. A. (eds.). Elsevier Applied Science. London & New York. pp. 169.
- Holman, J. P. 1986. "Heat Transfer", 6th ed. McGraw-Hill Book Co., New York.
- Hunter, G. M. 1972. Continuous sterilization of liquid media containing suspended particles. *Food Technol. Aust.* 24:158-165.
- IFT staff Report. 1989. Top 10 Food Science Innovations: 1939-1989. *Food Technol.* 43(9):309.
- Incropera, F. P. and de Witt, D. P. 1985. *Introduction to Heat Transfer*. John Wiley and Sons, New York. NY.

- Jairus, R. D. D and Merson, R. L. 1990. Kinetic parameters for inactivation of *Bacillus steroothermophilus* at high temperatures. *J. Food Sci.* 55:488-493.
- Jairus, R. D. D. 1992. Aseptic processing of foods: Market advantages and microbiological risks. *In* "Advances in Aseptic Processing Technologies" R. K. Singh and P. E. Nelson (eds.). Elsevier Applied Science. New York. p. 189.
- Jason, A. C. 1983. A deterministic model for monophasic growth of batch cultures of bacteria. *Antonie van Leeuwenhoek. J. Microbiol. Serol.* 49:513-536.
- Johnson, H. F., Pigford, R. L. and Chapin, J. H. 1941. Heat transfer to clouds of falling particles. *Trans. Am. Inst. Chem. Engr.* 37:95.
- Johnson, A. G., Kirk, G. and Shin, T. 1988. Numerical and experimental analysis of mixed forced and natural convection about a sphere. *Trans. ASAE* 31:293-299,304.
- Joyce, D. A. 1993. Microbiological aspects of aseptic processing and packaging. *In* "Aseptic Processing and Packaging of Particulate Foods". E. M. A. Willhoft (ed.). Blackie Academic and Professionals. London. pp. 155-180.
- Keil, B. 1971. Trypsin. *In* "The Enzymes" Vol III P. D. Boyer ed. Academic Press. New York. pp. 249-275.
- Kessler, H. G. and Fink, R. 1986. Changes in heating and stored milk with an interpretation by reaction kinetics. *J. Food Sci.* 51:1105-1111,1155.
- Kim, H. -J. and Taub, I. A. 1993. Intrinsic chemical markers for aseptic processing of particulate foods. *Food Technol.* 47(1):91-99.
- King, W. J. 1932. The Basic Laws And Data of Heat Transmission - III. Free convection. *Mech. Eng.* 54:347-353.
- Klyachko, L. S. 1963. Heat transfer between a gas and a spherical surface with the combined action of free and forced convection. *J. Heat Transfer.* 85:355-357.
- Kopelman, I. J. and Pflug, I. J. 1968. The relationship of the surface, mass average and geometric centre temperatures in transient conduction heat flow. *Food Technol.* 22(6):141-146.
- Kostaropoulos, A. E., Spiess, W. E. L., and Wolf, W. 1975. Reference values for thermal diffusivity of foodstuffs. *Lebensm Wiss. u. Technol.* 8(3):108.

- Kramers, H. 1946. Heat transfer from spheres to flowing media. *Physica*. 12:61. Cited *In* "Fluidization and Fluid Particle Systems". F.A Zenz and D.F Othmer (eds.). Reinhold Pub. Corp., New York., 1960.
- Kreith, F. 1973. *Principles of Heat Transfer*, 3rd Ed., Harper and Row, New York.
- Kwessler, H. G., Fink, R., and Horak, F. P. 1984. The analysis and assessment of heat induced changes in food contents with the aid of reaction kinetics. *Zeit. Lebensmitteltechnol. und Verfahrenstechnik*. 5:372.
- Labuza, T. P. 1982b. Application of chemical kinetics to deterioration of foods. *J. Chem. Ed.* 61:348.
- Labuza, T. P. 1982a. *Open Shelf Life Dating of Foods*. Food and Nutrition Press. Westport, CT.
- Lamberg, I. and Hallstrom, B. 1986. Thermal properties of potatoes and a computer simulation model of a blanching process. *J. Food Technol.* 21:577.
- Larkin, J. W. and Steffe, J. F. 1983. Error analysis in estimating thermal diffusivity from heat penetration data. *J. Food Proc. Eng.* 6:135-158.
- Larkin, J. W. 1990. Mathematical analysis of critical parameters in aseptic particulate processing systems. *J. Food Proc. Eng.* 13:155-167.
- Larkin, J. N. 1989. Use of a modified Ball's formula method to evaluate aseptic processing of foods containing particulates. *Food Technol.* 43(3):124-131.
- Lee, J. H., Singh, R. K. and Larkin, J. W. 1990a. Determination of lethality and process time in continuous sterilization system containing particulates. *J. Food Eng.* 11:67-92.
- Lee, J. H., Singh, R. K. and Chandarana, D. I. 1990b. Sensitivity analysis of aseptic process simulations for foods containing particulates. *J. Food Proc. Eng.* 12:295-321.
- Lee, J. H. and Singh, R. K. 1991. Particle residence time distribution in a model horizontal scraped surface heat exchanger. *J. Food Proc. Eng.* 14:125-146.
- Lee, J. H. and Singh, R. K. 1993. Residence time distribution characteristics of particle flow in a vertical scraped surface heat exchanger. *J. Food Eng.* 18:413-424.

- Lenz, M. K. and Lund, D. B. 1978. The lethality-Fourier number method. Heating rate variations and lethality confidence intervals for forced-convection heated foods in containers. *J. Food Proc. Eng.* 2:227-271.
- Lenz, M. K. and Lund, D. B. 1977. The lethality-Fourier number method: Experimental verification of a model for calculating average quality factor retention in conduction- heating canned foods. *J. Food Sci.* 42:997-1001.
- Lenz, M. K. and Lund, D. B. 1980. Experimental procedure for determining destruction kinetics of food components. *Food Technol.* 34(2):51-55.
- Lenz, M. K. and Lund, D. B. 1973. Temperature distribution during heat/hold processing of food. *J. Food Sci.* 38:630-632.
- Levenspiel, O. 1972. Non-ideal flow. *In* "Chemical Reaction Engineering". 2nd ed. John Wiley & Sons, New York, NY.
- Lin, S. H. 1980. Continuous sterilization of non-Newtonian liquid foods in a tubular sterilizer. *Lebensm.-Wiss.u.-Technol.* 13:138-142.
- Loire, P. 1976. Aseptic packaging of food products in drums. IAPRI Conference, Munich 9-11 June.
- Lopez, A. 1987. A complete course in canning: Book II. Canning Trade Inc. Baltimore, MD. USA.
- Lu, A. T. and Whitaker, J. R. 1974. Some factors affecting rates of heat inactivation and reactivation of horseradish peroxidase. *J. Food Sci.* 39:1173-1178.
- Luikov, A. V. 1968. Analytical Heat Diffusion Theory. Academic Press, New York.
- Lund, D. B. and Singh, R. K. 1993. The system and its elements. *In* "Principles of Aseptic processing and packaging". J. V. Chambers and P. E. Nelson (eds.). pp 3-30.
- Lund, D. B. 1977. Design of thermal processes for maximizing nutrient retention. *Food Technol.* 31(2):71-78.
- Lund, D. B. 1975. Effects of blanching, pasteurization and sterilization on nutrients. *In* Nutritional Evaluation of Food Processing. Harris, R. S and Karmas, E. (ed.). AVI Publication, Westport, CT, pp. 205-240.

- Lund, D. B. 1975. Heat processing. *In* " Principles of Food Science, Part II. Physical principles of food preservation". M. Karel, O. R. Fennema, and D. B. Lund (eds.). Marcel Dekker Inc. New York.
- Maesmans, G. J., Hendrickx, M. E. De Cordt, S. V. and Tobback, P. 1994. Feasibility of the use of a time-temperature integrator and a mathematical model to determine fluid-to-particle heat transfer coefficients. *Food Res. Int.* 27:39-51.
- Maesmans, G., Hendrickx, M., DeCordt, S., Fransis, A. and Tobback, P. 1992. Fluid-to-particle heat transfer coefficient determination of heterogeneous foods: A review. *J. Food Proc. and Preserv.* 16:29-39.
- Mansfield, T. 1974. A brief study of cooking. Quoted in Lund, D. B. 1975. *In* "Principles of Food Science. Part II. Physical Principles of Food Preservation". Fennema, O. R. (ed.). Marcel Dekker. NY. Chap 2.
- Mansfield, T. 1962. High temperature short time sterilization. *Proc. 1st Intl. Cong. Food Sci and Technol.* vol 4. Gordon and Breach, London. pp. 311-316.
- Manson, J. E. and Cullen, J. F. 1974. Thermal process simulation for aseptic processing of foods containing discrete particulate matter. *J. Food Sci.* 39:1084-1089.
- Martens, T. 1980. Mathematical model of heat processing in flat containers. Ph.D Thesis, Katholieke Universiteit Leuven.
- Mauri, L. M., Alzamora, S. M., Chirife, J. and Tomio, M. J. 1989. Review: kinetic parameters for thiamine degradation in foods and model solutions of high water activity. *Int. J. Food Sci. and Technol.*, 24:1-9.
- McCoy, S. C., Zuritz, C. A. and Sastry, S. K. 1987. Residence time distribution of simulated food particles in a holding tube. ASAE Paper No. 87-6536. American Society of Agricultural Engineers. St. Joseph, MI.
- Mckenna, A. B. and Tucker, G. S. 1990. Computer modelling for the control of particulate sterilization under dynamic flow. Tech. Memo. No. 587, Campden Food and Drink Assoc., Chipping Campden, GBR.
- Merson, R. L, Singh, R. P. and Carroad, P. A. 1978. An evaluation of Ball's formula method of thermal process calculations. *Food Technol.* 32(3):66-78.
- Metzner, A. B. and Gluck, D. F. 1960. Heat transfer to non-Newtonian fluids under laminar flow conditions. *Chem. Eng. Sci.* 12:185-190.

- Moffat, R. J. 1990. Some experimental methods for heat transfer studies. *Experimental Thermal and Fluid Science*. 3:14-32.
- Morgan, V. T. 1975. The overall convective heat transfer from smooth circular cylinders. In "Advances In Heat Transfer" T. F. Irvine and J. P. Hartnett (eds.). Academic Press. New York.
- Mulley, E. A., Stumbo, C. R. and Hunting, W. A. 1975a. Thiamine: A chemical index of the sterilization efficacy of thermal processing. *J. Food Sci.* 40:993-996.
- Mulley, E. A., Stumbo, C. R. and Hunting, W. A. 1975b. Kinetics of thiamine degradation by heat: a new method for studying the reaction rates in model systems and food products at high temperatures. *J. Food Sci.* 40:985-988.
- Murakami, E. G., Choi, Y., and Okos, M. R. 1985. An interactive computer program for predicting thermal properties. Paper No. 85-6511, American Society of Engineers, St. Joseph, MI.
- Murakami, E. G. and Okos, M. R. 1987. Heat transfer property studies of composite food. Paper 87-6541, American Society of Engineers, St. Joseph, MI.
- Mwangi, J. M., Rizvi, S. S. H. and Datta, A. K. 1993. Heat transfer to particles in shear flow: application in aseptic processing. *J. Food Eng.* 19:55-74.
- Mwangi, J. M., Datta, A. K. and Rizvi, S. S. 1992. Heat transfer in aseptic processing of particulate foods. In "Advances in Aseptic Processing Technologies". R. K. Singh and P. E. Nelson (eds.). Elsevier Applied Science. London & New York. pp. 73-102.
- Nath, S. and Ranganna, S. 1977. Evaluation of thermal process for acidified canned muskmelon (*Cucumis melo L.*) *J. Food Sci.* 42:1306-1310,1318.
- Norback, J. P. 1980. Techniques for optimization of food processes. *Food Technol.*, 34(2):86-88
- Northrop, J. H. 1932. Crystalline trypsin IV. Reversibility of the inactivation and denaturation of trypsin by heat. *J. Gen. Physiol.* 16:323.
- Northrop, J. H., Kunitz, M. and Herriot, R. 1948. In "Crystalline Enzymes" 2nd Ed. Columbia University Press. New York. pp.125-167.
- Nunes, R. V. and Swartzel, K. R. 1990. Modelling thermal processes using the equivalent point method. *J. Food Eng.* 11:103-117.

- Ohlsson, T. 1989. Heat transfer and flow consideration for control of aseptic processing of particulate food in high viscous liquids. Presented at the 1st Intl. Congress on aseptic processing Technologies. Indianapolis, Indiana, U.S.A. March 19-21.
- Ohlsson, T. 1980b. Optimal sterilization temperature for sensory quality in cylindrical containers. *J. Food Sci.* 45:1517-1521.
- Ohlsson, T. 1980a. Temperature dependence of sensory quality changes during thermal processing. *J. Food Sci.* 45:836-839.
- Olivares, M., Guzman, J. A. and Solar, I. 1986. Thermal diffusivity of nonhomogeneous food. *J. Food Proc Preservation.* 10:57-67.
- Oosthuizen, P. H and Madan, S 1970. Combined convective heat transfer from horizontal cylinders in air. *Trans. ASME, J. Heat Transfer.* 92:194-196.
- Ozisik, M. N. 1985. *Heat Transfer: A Basic Approach*, McGraw-Hill Book Co., New York.
- Patankar, S. V. 1980. *Numerical Heat Transfer and fluid flow*. Hemisphere Publishing Co. New York, NY.
- Patashnik, M. 1953. A simplified procedure for thermal process evaluation *Food Technol.* 7(1):1
- Pflug, I. J., Blaisdell, J. L and Kopelman, I. J. 1965. Developing temperature-time curves for objects that can be approximated by a sphere, infinite plate or infinite cylinder. *ASHRAE Transaction.* 71:238.
- Pflug, I. J. and Odlaug, T. E. 1978. A review of z and F values used to ensure safety of low-acid canned food. *Food Technol.* 32(6):63-70.
- Pflug, I. J. and Berrero, C. 1967. Heating media for processing food in flexible packages. Phase 2. Tech Rep. 67-47-GP. U.S. Army Natick Laboratories, Natick, MA.
- Pflug, I. J. and Christensen, R. 1980. Converting an F-value determined on the basis of one z-value to the F-value determined on the basis of a second z-value. *J. Food Sci.* 45:35-40.
- Pflug, I. J., Smith, G., Holcomb, R. and Blanchett, R. R. 1980. Measuring sterilizing values in containers of food using thermocouples and biological indicator units. *J. Food Protect.* 43:119-23.

- Pflug, I. J., Berry, M. R. and Dignan, D. M. 1990. Establishing the heat-preservation process for aseptically-packed low-acid food containing large particulates, sterilized in a continuous heat-hold-cool system. *J. Food Proc.* 53:312-321.
- Pitts, D. R. and Sissom, L. E. 1977. *Theory And Problems Of Heat Transfer*. McGraw Hill Co. New York.
- Polley, S. L., Synder, O. P. and Kotnour, P. 1980. A compilation of thermal properties of foods. *Food Technol.* 34: (11):76-94.
- Price, N. C. and Stevens, L. 1989. *Fundamentals of Enzymology*. 2nd Ed. Oxford Univ., Press. New York.
- Ramaswamy, H. S., Pannu, K., Simpson, B. K. and Smith, J. P. 1992. An apparatus for particle-to-fluid relative velocity measurement in tube flow at various temperatures under nonpressurized flow conditions. *Food Research International.* 25:277-284.
- Ramaswamy, H. S. and Tung, M. A. 1986. Modelling heat transfer in steam/air processing of thin profile packages. *J. Can Inst. Food Sci. Technol.* 19:215-222.
- Ramaswamy, H. S., Lo, K. V. and Tung, M. A. 1982. Simplified equations for transient temperatures in conductive foods with convective heat transfer at the surface. *J. Food Sci.* 47:2042-2047.
- Ramaswamy, H. S. and Ghazala, S. 1990. Centerpoint nutrient degradation in heat processed conduction heating food model. *J. Food Proc. Eng.* 12:159-169.
- Ramaswamy, H. S., van de Voort, F. R. and Ghazala, S. 1989. Analysis of TDT and Arrhenius methods for handling process and kinetic data. *J. Food Sci.* 54:1322-1326.
- Ramaswamy, H. S., Tung, M. A. and Stark, R. 1983. A method to measure surface heat transfer from steam/air mixtures in batch retorts. *J. Food Sci.* 48:900-904.
- Ranz, W. E. and Marshall, W. R. jr. 1952. Evaporation from drop. *Chem. Eng. Progress.* 48 141. Cited *In* "Introduction to Heat Transfer" F. P. Incropera, and D. P DeWitt (eds.). John Wiley and Sons, New York. 1985.
- Rao, M. A. 1992. Aseptic processing of foods. *In* "Biotechnology and Food Process Engineering". H. G. Schwaetzberg, M. A. Rao (eds.). Marcel Dekker, Inc. New York. pp.247.

- Rao, M. A., Lee, C. Y., Katz, J. and Cooley, H. J. 1981. A kinetic study of loss of vitamin C, color, and firmness during thermal processing of canned peas. *J. Food Sci.* 46:636-637.
- Rao, M. A. 1977. Rheology of liquid foods- A review. *J. Texture Studies.* 8:135.
- Rao, V., Destefano, M. V., Perez, C. R. and Barreiro, J. A. 1989. Kinetics of thermal inactivation of protease (trypsin and Chymotrypsin) inhibitors in Black Beans (*Phaseolus vulgaris*) flour. *J. Food Eng.* 9:35-46.
- Rha, C. 1978. Rheology of fluid foods. *Food Technol.* 32(7):77-81.
- Rice, P., Selman, J. D. and Abdul-Rezzak, R. K. 1988. Effect of temperature on thermal properties of "Record" potato. *Intl J. Food Sci and Technol.* 23:281-286.
- Richardson, P. S. and Bows, J. R. 1990. Product design for microwave reheating. *In "Process engineering in the food industry"*. R. W. Field and J. A. Howell (eds.). Elsevier Applied Sci. New York. pp. 15-32.
- Richardson, T. and Hyslop, D. B. 1985. Enzymes. *In "Food Chemistry"* 2nd edn. O. R. Fennema ed. Marcel Dekker Inc. New York. p.455.
- Richardson, P. S. and Selman, J. D. 1991. Heat processing equipments. *In "Processing and Packaging of Heat Preserved Foods"*. J. A. G. Rees and J. Bettison (eds.). Van Nostrand Reinhold. New York. p.50-71.
- Rodriguez, A., Teixeira, A. A. and Senerage, G. H. 1987. Kinetic modelling of heat-induced reactions affecting bacterial spores. Presented at the 47th Annual Meeting. *Inst. Food Technol., Las Vegas, NV, June 16-19.*
- Rodriguez, L. G., Segurajauregui, J. S., Torres, J. and Brito, E. 1987. Heat transfer to non-Newtonian fluid foods under laminar flow conditions in horizontal tubes. *J. Food Sci.* 52:975-979.
- Rodriguez, A. C., Senerage, G. H., Teixeira, A. A. and Busta, F. F. 1988. Kinetic effects of lethal temperatures on population dynamics of bacterial spores. *Trans. ASAE:31: 1594-1601,1606.*
- Rodriguez, A. C. and Teixeira, A. A. 1988. Heat transfer in hollow cylindrical rods used as bioindicator units for thermal process validation. *Trans. ASAE.* 31:1233-1236.
- Ronner, U. 1990. A new biological indicator for aseptic sterilization. *Food Technology International Europe* 90:43-46.

- Sadler, G. D. 1987. Aseptic chemistry. *In* " Principles of aseptic processing and packaging" P. E. Nelson, J. V. Chambers and J. H. Rodriguez (eds.). The Food Processors Institute, Washington, DC. p. 45-57.
- Saguy, I. 1988. Constraints to quality optimization in aseptic processing. *J. Food Sci.* 53:306-307.
- Saguy, I. and Karel, M. 1979. Optimal retort temperature profile in optimising thiamine retention in conduction type heating of canned foods. *J. Foods Sci.* 44:1485-1490.
- Saguy, I., Levine, L., Symes, S. and Rotstein, E. 1992. Integration of computers in food processing. *In* "Biotechnology and food process engineering". H. G. Schwaetzberg, and M. A. Rao (eds.). Marcel Dekker, Inc. New York. p. 415.
- Sastry, S. K. 1988. Food properties and modelling approaches of importance in the continuous sterilization of liquid-particle mixtures. *In* "Food properties and computer-aided engineering of food processing systems. R. P. Singh and A. G. Medina (eds.). p. 117-119.
- Sastry, S. K. and Zuritz, C. A. 1987. A model for particle suspension flow in a tube. ASAE Paper No. 87-6537. American Society of Agricultural Engineers. St. Joseph, MI.
- Sastry, S. K. 1992. Liquid-to-particle heat transfer coefficient in aseptic processing. *In* "Advances in aseptic processing technologies". R. K. Singh and P. E. Nelson (eds.). Elsevier Applied Science. New York. p 63.
- Sastry, S. K. 1992b. Modelling the continuous sterilization of particulate foods. *In* "Mathematical Modelling of Food Processing Operations". S. Thorne (ed.). Elsevier Applied Science. London & New York. pp. 233-270.
- Sastry, S.K. 1989b. Aseptic Technology for particulate foods: Problems, issues and some potential solutions. Presented at the 1st Intl. Congress on Aseptic Processing Technologists. Indianapolis, IN, USA. March 19-21.
- Sastry, S. K. 1989a. Process evaluation in aseptic processing. *In* " Developments in Food Preservation - 5" S. Thorne (ed.). Elsevier Applied Science. New York. pp 179-206.
- Sastry, S. K., Lima, M., Brim, J., Brun, T. and Heskitt, B. R. 1990. Liquid-to-particle heat transfer during continuous tube flow: Influence of flow rate and particle to tube diameter ratio. *J. Food Process Eng.* 13:239-253.

- Sastry, S. K., Heskitt, B. F. and Blaisdell, J. L. 1989. Experimental and modelling studies on convective heat transfer at particle-liquid interface in aseptic processing systems. *Food Technol.* 43(3):132-136,143.
- Sastry, S. K. 1992a. Liquid-to-particle heat transfer coefficient in aseptic processing. *In* "Advances in Aseptic Processing Technologies". pp. 63-72. P. E. Nelson and R. K. Singh (eds.). Elsevier Applied Science. London and New York.
- Sastry, S. K. Li, S. F., Patel, M., Konanayakam, M. Bafna, P., Doores, S. and Beelman, R. B. 1988. A bioindicator for validation of thermal processes for particulate foods. *J. Food Sci.* 53:1528-1536.
- Sastry, S. K. and Zuritz, C. A. 1987. A model for particle suspension flow in a tube. ASAE Paper No. 87-6537. American Society of Agricultural Engineers. St. Joseph, MI.
- Sastry, S. K. 1986. Mathematical evaluation of process schedules for aseptic processing of low-acid foods containing discrete particulate matter. *J. Food Sci.* 51:1323-1328.
- Schwartz, S. J. 1992. Quality Consideration During Aseptic Processing of foods. *In* "Advances in Aseptic Processing Technologies" R. K. Singh and P. E. Nelson (eds.). Elsevier Applied Science. New York. p 245.
- Schwimmer, S. 1981. Source Book of Food Enzymology. Avi Pub. Co. Inc. Westport, CT. p. 206.
- Scott, V. N. 1985. Aseptic processing and packaging of particulates commercially sterilized and enzymatic considerations. Proc. of National Food Processors Association Conf., Washington, DC. April 11-12. pp. 47.
- Self, K. P., Burfoot, D., Wilkins T. J. and James, S. J. 1990. Microwave pasteurization of pre-packed sliced ham. *In* "Process engineering in the food industry". R. W. Field and J. A. Howell (eds.). Elsevier Applied Sci. New York. pp. 33-44.
- Shih, T. M. 1984. Numerical Heat Transfer. Hemisphere Publishing Co. New York. NY.
- Shin, S. and Bhowmik, S. R. 1990. Computer simulation to evaluate thermal processing of food in cylindrical plastic cans. *J. Food Eng.* 12:117-131.
- Silva, C., Hendrickx, M., Oliveira, F. and Tobback, P. 1992. Critical evaluation of commonly used objective functions to optimize overall quality and nutrient retention of heat-preserved foods. *J. Food Eng.* 17:241-258.

- Simpson, S. G. and Williams, M. C. 1974. An analysis of high temperature short time sterilization during laminar flow. *J. Food Sci.* 39:1047-1054.
- Simpson, B. K. and Haard, H. F. 1984. Trypsin from Greenland Cod, *Gadus Ogac*. Isolation and comparative properties. *Comp. Biochem. Physiol.* 79B:613-622.
- Singh, R. P. 1982. Thermal diffusivity food processing. *Food Technol.* 36(2):87-91.
- Singh, R. K. and Heldman, D. R. 1993. Introduction to Food Engineering, 2nd Edn. Academic Press Inc. New York.
- Singh, R. K. and Lee, J. H. 1992. Residence time distributions of foods with/without particulates in aseptic processing systems. *In "Advances in Aseptic Processing Technologies"*. R. K. Singh and P. E. Nelson (eds.). Elsevier Applied Science. London & New York.
- Singleton, P. and Sainbury, D. 1987. Dictionary of microbiology and molecular biology. 2nd ed. Wiley Interscience Pub. John Wiley, Chichester, GBR.
- Skelland, A. H. P. 1967. Non-Newtonian Flow And Heat Transfer. John Wiley and Sons. New York.
- Skjoldebrand, C. and Ohlsson, T. 1993a. A computer simulation program for evaluation of the continuous heat treatment of particulate food products. Part 2: design. *J. Food Eng.* 20:149-165.
- Skjoldebrand, C. and Ohlsson, T. 1993b. A computer simulation program for evaluation of the continuous heat treatment of particulate food products. Part 2: Utilisation. *J. Food Eng.* 20:167-181.
- Skudder, P. J. 1990. Recent development in the heat processing of high-added-value food products. *In "Foods for the 90's"*. G. G. Birch, G. C. Campbell, and M. G. Lindley (eds.). Elsevier Applied Science. London & New York. pp. 13-23.
- Smith, R. E., Nelson, G. L., and Hendrickson, R. L. 1967. Analysis of transient heat transfer from anomalous shapes. *Trans. ASAE* 10:236-245.
- Soetrisno, U., Holmes, Z. A. and Miller, L. T. 1982. Effect of heating time of soybean on vitamin B6 and folacin retention, trypsin inhibitor activity, and microstructure changes. *J. Food Sci.* 47:530-534,537.
- Sparrow, E. M. and Ansari, M. A. 1983. A refutation of King's rule for multidimensional external natural convection. *Int. J. Heat Mass Transfer.* 26:1357-1364.

- Steel, R. G. D. and Torrie, J. H. 1960. Principles And Procedures Of Statistics. McGraw Hill. New York.
- Stevenson, K. E. and Ito, K. A. 1991. Aseptic processing and packaging of heat preserved foods. *In* "Processing and Packaging of Heat Preserved Foods. J. A. G. Rees and J. Bettison (eds.). Van Nostrand Reinhold. New York. p.72-91
- Stoforos, N. G. 1988. Heat Transfer in Axially Rotating Canned Liquid/particulate food Systems. Ph.D thesis. Dept. of Agricultural Engineering. Univ. of California, Davis, CA.
- Stoforos, N. G., Park, K. L. and Merson, R. L. 1989. Heat transfer in particulate foods during aseptic processing. Presented at the 1989 IFT Annual Meeting, Chicago, IL, USA. June 25-29.
- Stoforos, N. G. and Merson, R. L. 1990. Estimating heat transfer coefficient in liquid/particulate canned foods using only liquid temperature data. *J. Food Sci.* 55:478-483,521.
- Stumbo, C. R. 1953. New procedure for evaluating thermal processes for foods in cylindrical containers. *Food Technol.* 7(8):309-315.
- Stumbo, C. R. 1965. Thermobacteriology in Food Processing. Academic Press. New York.
- Stumbo, C. R. 1973. Thermobacteriology in Food Processing. 2nd ed. Academic Press, New York.
- Sucec, J. 1985. Heat Transfer. W. M. C. Brown Publishers. IA.
- Swartzel, K. R. 1984. A continuous flow procedure for kinetic data generation. *J. Food Sci.* 49:803-806.
- Swartzel, K. R. 1986. Equivalent-point method for thermal evaluation of continuous-flow systems. *J. Agric. Food Chem.* 34:396-401.
- Swartzel, K. R. 1982. Arrhenius kinetics as applied to product constituents losses in ultra high temperature processing. *J. Food Sci.* 47:1886-1891.
- Tadmor, Z. and Klein, I. 1970. Engineering Principles of Plasticating Extrusion. Van Nostrand Reinhold Co. New York.

- Taeymans, D., Roelans, E. and Lenges, J. 1985. Influence of residence time distribution on the sterilization effect in a scraped surface heat exchanger used for processing liquids containing solid particles. *In* "Proceedings of IUFoST Symp. on Aseptic Processing and Packaging of Foods. Tylosand, Sweden. September 9-12.
- Taoukis, P. S. and Labuza, T. P. 1989. Applicability of time-temperature indicators as shelf life monitors of food products. *J. Food Sci.* 54:783-788.
- Teixeira, A. A., Dixon, J. R., Zahradnik, J. W. and Zinsmeister, G. E. 1969. Computer simulation of nutrient retention in thermal processing of conduction heating foods. *Food Technol.* 23(6):137-142.
- Teixeira, A. 1992. Thermal process calculations. *In* "Handbook of food engineering". D. R. Heldman and D. B. Lund (eds.). Marcel Dekker Inc. New York. p 563-619.
- Teixeira, A. A. and Manson, S. E. 1983. Thermal process control for aseptic processing systems. *Food Technol.* 37(4):128-133.
- Tennigen, A. and Olstad, S. 1979. Computer controlled heating of meat with respect to protein denaturation. *In* "Food Process Engineering vol 1. Food processing systems" C.P Linko *et al.* (eds.). Applied Science Publ. London. Ch 15.
- Toledo, R. T. and Chang, S. Y. 1990. Advantages of aseptic processing of fruits and vegetables. *Food Technol.* 44(2):72-76.
- Toledo, R. T. 1986. Postprocessing changes in aseptically packaged beverages. *J. Agric. Food Chem.* 34:405-408.
- Tong, C. H., Sheen, S., Shah, K. K., Huang, V. T. and Lund, D. B. 1993. Reference materials for calibrating probes used for measuring thermal conductivity of frozen foods. *J. Food Sci.* 58: 186-189,192.
- Travis, J. 1968. Studies on the active site of sheep trypsin. *Biochem. Biophys. Res. Commun.* 30:730-734.
- Tucker, G. S. and Clark, P., 1990. Modelling the cooling phase of heat sterilization processes, using heat transfer coefficients. *Int. J. Food Sci. Technol.* 25:668-681.
- Tucker, G. and Holdsworth, S. D. 1990. Optimization of quality factors for foods thermally processed in rectangular containers. *In* "Process Engineering for the Food Industry". 2nd ed. R. W. Field and J. A. Howell (eds.). Elsevier Applied Science. London. pp 59-74.

- Tucker, G. S. and Holdsworth, S. D. 1991. Mathematical modelling of sterilization and cooking processes for heat preserved foods: applications of a new heat transfer model. *Trans. IChemE.* 69:5-12.
- Tung, M. A., Ramaswamy, H. S., Smith, T. and Stark, R. 1984. Surface heat transfer coefficients associated with steam/air mixtures in two pilot scale retorts. *J. Food Sci.* 49:939-943.
- van der Poel, T. F. B., van Zutchem, D. J. and van Oort, M. G. 1990. Thermal inactivation of lecithins and trypsin inhibitor activity during steam processing of dry bean (*Phaseolus vulgaris*) and effects on protein quality. *J. Food Agric.* 53:215-228.
- Warwick, D. 1990. Aseptics: The problems revealed. *Food Manufacture.* 65(6):49.
- Weng, Z. M., Hendrickx, M., Maesmans, G. and Tobback, P. 1992. The use of a time-temperature-integrator in conjunction with mathematical modelling for determining liquid/particle heat transfer coefficients. *J. Food Eng.* 16:197-214.
- Weng, W. M., Hendrickx, M., Maesmans, G. and Tobback, P. 1991a. Immobilized peroxidase: a potential bio-indicator for evaluation of thermal processes. *J. Food Sci.* 56:567-570.
- Weng, W. M., Hendrickx, M., Maesmans, G. and Tobback, P. 1991b. Thermostability of soluble and immobilized horseradish peroxidase. *J. Food Sci.* 56:574-578.
- Whitaker, S. 1972. Forced convection heat transfer calculations for flow in pipes, past flat plates, single cylinders, single spheres, and for flow in packed beds and tube bundles. *J. AIChE.* 18:361-371.
- Williams, G. C. 1942. Ph.D. Thesis, Massachusetts Institute of Technology. Cambridge. Cited in *Fluidization and fluid particle systems.* F. A Zenz and D. F. Othmer, p. 423. Reinhold Pub. Corp. New York. NY.
- Witter, L. D. 1983. Elevated temperature preservation. In "Food Microbiology". A. Rose ed. Academic Press, London. p.48.
- Yamada, T. 1970. The thermal properties of potatoes. *J. Agric Chem. Soc. Jpn.* 44:587-590.
- Yang, B. B., Nunes, R. V. and Swartzel, K. R. 1992. Lethality distribution within particles in the holding section of an aseptic processing system. *J. Food Sci.* 57:1258-1265.

- Yang, B. B. and Swartzel, K. R. 1991. Photo-sensor methodology for determining residence time distributions of particles in continuous flow thermal processing systems. *J. Food Sci.* 56:1076-1081,1086.
- Yuge, T. 1960. Experiments on heat transfer from spheres including combined and forced convection. *J. Heat Transfer.* 82:214-220.
- Zhukauskas, A. A 1972. Heat transfer from a tubes in crossflow. *Advan. Heat Transfer* 8:93-160.
- Žukauskas, A. and Žiugžda, J. 1985. *Heat Transfer of a Cylinder in Crossflow.* Hemisphere Pub. Co. New York.
- Zuritz, C. A., McCoy, S. C. and Sastry, S. K. 1990. Convection heat transfer coefficients for irregular particles immersed in non-Newtonian fluids during tube flow. *J. Food Eng.* 11:159-174.

APPENDIX 1

```
C ITERATIVE PROGRAM FOR CALCULATING FLUID-TO-PARTICLE
C HEAT TRANSFER COEFFICIENT FOR FINITE CYLINDER AND
C SPHERICAL PARTICLE USING THE HEATING RATE INDEX ( $f_h$ ).
C
C WRITTEN BY G. B. AWUAH
C THE PROGRAM IS BASED ON SIMPLIFIED ANALYTICAL
C EQUATIONS DEVELOPED BY RAMASWAMY ET AL.(1982).
C
C DEFINITION OF VARIABLES:
C
C ALENG = PARTICLE LENGTH (mm)
C AMATL = TYPE OF PARTICLE MATERIAL
C BIP,BIC,BIS = FUNCTION OF BIOT NUMBER
C COND = THERMAL CONDUCTIVITY (W/mC)
C DIAM = PARTICLE DIAMETER (mm)
C DIFF = THERMAL DIFFUSIVITY ( $m^2/s$ )
C FH = RATE OF HEAT PENETRATION (EXPERIMENTAL) (min)
C FH1 = RATE OF HEAT PENETRATION (ANALYTICAL) (min)
C HALFT = HALF THICKNESS OF PARTICLE (m)
C HFP = HEAT TRANSFER COEFFICIENT (W/m2C)
C RADS = RADIUS OF PARTICLE (m)
C SHAP = SHAPE OF PARTICLE
C SS,SP,SC = CHARACTERISTIC FUNCTIONS
C VOLU = VOLUME OF PARTICLE (m3)
C
C IMPLICIT REAL *8(A-H, O-Z)
C INTEGER I, J, N, M
C
C OPEN(5,FILE = 'C:\HFP.DAT')
C OPEN(6,FILE = 'C:\HFP.PRN')
C
C PRINT *, 'WHAT IS THE TOTAL NUMBER OF DATA SETS ?'
C READ *, N
C
C PRINT *, 'WHAT IS THE SHAPE OF PARTICLE ?, ENTER 1 FOR
I CYLINDER AND 0 FOR A SPHERE.'
C
C READ *,M
C DO 20 J = 1,N
C
C IF(M.EQ.1)THEN
C READ(5,*)DIAM,ALENG,FH,SHAP,AMATL
```

```

ELSE
READ(5,*)DIAM,FH,SHAP,AMATL
ENDIF
C
PI=22.0D0/7.0D0
RADS = (DIAM/2.0D0)
HALFT = (ALENG/2.0D0)
C
C FOR A CYLINDER, SHAP = 1
C FOR POTATO AMATL = 1
C FOR TEFLON AMATL = 2

IF(AMATL.EQ.1)THEN
    DIFF = 1.59D-07
    COND = 0.556
ELSEIF(AMATL.EQ.2)THEN
    DIFF = 1.35D-07
    COND = 0.29
ELSE
ENDIF
C
IF(SHAP.EQ.1)THEN
    AREA = PI*2.0D0*RADS*ALENG
    VOLU = PI*(RADS**2)*ALENG
ELSE
    AREA = 4.0D0*PI*(RADS**2)
    VOLU = (4.0D0/3.0D0)*PI*(RADS**3)
ENDIF
C
C INITIALIZING PROGRAM WITH HFP CALCULATED WITH
C THE LUMPED CAPACITY APPROACH
C
HFP = (2.303*VOLU*COND)/(FH*60.0D0*AREA*DIFF)
I = 0
25 I = I+1
CALL AUT(SS,SP,SC,HFP,RADS,HALFT,COND,SHAP)
CALL HRATE(SS,SP,SC,RADS,HALFT,DIFF,SHAP,FH,TEST,FH1)
CHECK = 0.005*FH
IF(TEST.GT.CHECK.AND.FH1.GT.FH)THEN
    HFP = HFP+0.050D0
    GOTO 25
ELSEIF(TEST.GT.CHECK.AND.FH1.LT.FH)THEN
    HFP = HFP-0.050D0
    GOTO 25

```

```

ELSE
ENDIF
WRITE(*,101) DIAM,ALENG,SHAP,FH,FH1,HFP
WRITE(6,101) DIAM,ALENG,SHAP,FH,FH1,HFP
101 FORMAT(2X,7F8.2)
20 CONTINUE
STOP
END

C
SUBROUTINE AUT(SS,SP,SC,HFP,RADS,HALFT,COND,SHAP)
IMPLICIT REAL*8(A-H, O-Z)

C
C CHARACTERISTIC EQUATION OF RAMASWAMY ET AL. (1982)
IF(SHAP.EQ.1)THEN
    BIC = (HFP*RADS)/COND
    BIP = (HFP*HALFT)/COND
    SP = (2.0738*(BIP/(BIP+2.0D0)))+(0.2795*ATAN(BIP/3.0D0))-
1      (0.02915*ATAN(5.0*BIP))+0.001171
    SC = (4.1093*(BIC/(BIC+2.0D0)))+(1.2365*ATAN(BIC/3.0D0))-
1      (0.1641*ATAN(2*BIC))-0.007762
ELSE
    BIS = (HFP*RADS)/COND
    SS = ((4.0704*BIS)/(BIS+2.0D0))+(3.556*ATAN(BIS/3.0D0))+
1      (0.1781*ATAN(BIS/8.0D0))-(0.0436*ATAN(7*BIS))+0.002262
ENDIF
RETURN
END

C
SUBROUTINE HRATE(SS,SP,SC,RADS,HALFT,DIFF,SHAP,FH,TEST,FH1)
IMPLICIT REAL*8(A-H, O-Z)

C
IF(SHAP.EQ.1)THEN
    AK1 = SP/(HALFT**2)
    AQ1 = SC/(RADS**2)
    AAW = AK1+AQ1
    FH1 = (2.303/(AAW*DIFF))/60.0D0
ELSE
    Q2 = SS/(RADS**2)
    FH1 = (2.303/(Q2*DIFF))/60.0D0
ENDIF
TEST = ABS(FH1-FH)
RETURN
END

```

APPENDIX 2

C FINITE DIFFERENCE PROGRAM FOR CALCULATING PERCENTAGE
C RETENTION OF ENZYME IN CAPSULE EMBEDDED IN A FINITE
C CYLINDRICAL PARTICLE
C

C PROGRAM JOINTLY WRITTEN BY
C G. B. AWUAH AND S. S. SABLANI
C

C DEFINITION OF VARIABLES:
C

C APP = INTERPOLATED D-VALUE
C ARATE = LETHAL RATE
C ARATE2 = PERCENTAGE RETENTION OF ENZYME
C AZ = Z-VALUE FOR TEMPERATURES BETWEEN 50-70.
C COND = THERMAL CONDUCTIVITY
C COTIME = COOLING TIME
C DIFF = THERMAL DIFFUSIVITY OF PARTICLE
C DTEMP = D-VALUE AT TEMPERATURE T
C D1,T1 = D-VALUE CORRESPONDING TO TEMPERATURE T1
C HETIME = HEATING TIME
C HFP = CONVECTIVE HEAT TRANSFER COEFF. (HEATING)
C HFPCO = CONVECTIVE HEAT TRANSFER COEFF. (COOLING)
C HHCB = HALF THE HEIGHT OF CAPSULE
C HRCB = HALF THE RADIUS OF CAPSULE
C M, N = NUMBER NODAL POINTS
C RAD = RAD OF FINITE CYLINDER IN m
C RES = RESIDUE
C TAVG = MASS AVERAGE TEMPERATURE: WHOLE PARTICLE
C TCAT = TEMPERATURE AT TIME t
C TCAVG = MASS AVERAGE TEMPERATURE WITHIN CAPSULE
C TF = TEMPERATURE OF THE HEATING MEDIUM
C THICK = HALF THICKNESS OF THE CYLINDER
C TI = PARTICLE INITIAL TEMPERATURE
C TNEW = TEMPERATURE AT THE PRESENT TIME
C TOL = TOLERANCE
C TOLD = TEMPERATURE AT PREVIOUS TIME
C TREF = REFERENCE TEMPERATURE FOR INTERPOLATION
C TTIME = TOTAL TIME
C W = RELAXATION FACTOR
C

IMPLICIT REAL*8(A-H, O-Z)
DOUBLE PRECISION TOLD(100,100),TNEW(100,100),CT(100,100)
DOUBLE PRECISION RES(100,100)

```

INTEGER I,J,K,M,N
C OPEN FILES FOR INPUT/OUTPUT OF DATA
OPEN(5,FILE = 'C:\TRYP.DAT')
OPEN(6,FILE = 'A:\TRYM1.PRN')
READ(5,*)RAD,THICK,DIFF,COND,HFP,TF,TI
READ(5,*)DT,W,TOL,TTIME
READ(5,*)N,M
READ(5,*)HETIME,COTIME,HFPCO
C CALCULATING GRID SIZES FOR THE PARTICLE
DR = RAD/(N-1)
DZ = THICK/(M-1)
CUTOF = HETIME+COTIME
TCOOL = TI
C
C CALCULATING GRID SIZE/NODAL POINTS FOR CRUCIBLE IN
C CYLINDER
C
HHCB = 2.79/2000.D0
HRCB = 7.54/2000.D0
IHCB = (HHCB/DZ)
IRCB = (HRCB/DR)
C
C SETTING ALL TEMPERATURE TO AN INITIAL VALUE.
C INITIAL CONDITIONS
C
DO 15 I = 1,N
DO 15 J = 1,M
TOLD(I,J) = TI
15 TNEW(I,J) = TI
C
C PROGRAM INITIATED
C
DO 20 TIME = DT,TTIME,DT
CALL COOL(TF,TIME,HETIME,CUTOF,TCOOL,HFPCO)
C
C CALCULATING TEMPERATURES AT NODAL POINTS
C
K = 0
60 K = K+1
DO 13 J = 1,M
DO 13 I = 1,N
IF(J.EQ.1.AND.I.EQ.1)THEN
CALL EQ1(DR,DZ,DT,DIFF,TOLD,TNEW,I,J)
ELSEIF(J.EQ.1.AND.(I.GT.1.AND.I.LT.N))THEN

```

```

        CALL EQ2(DR,DZ,DT,DIFF,TOLD,TNEW,I,J)
    ELSEIF(I.EQ.N.AND.J.EQ.1)THEN
        CALL EQ3(DR,DZ,DT,DIFF,TOLD,TNEW,COND,HFP,TF,I,J)
    ELSEIF((J.GT.1.AND.J.LT.M).AND.I.EQ.1)THEN
        CALL EQ4(DR,DZ,DT,DIFF,TOLD,TNEW,I,J)
    ELSEIF(I.EQ.1.AND.J.EQ.M)THEN
        CALL EQ5(DR,DZ,DT,DIFF,TOLD,TNEW,COND,HFP,TF,I,J)
    ELSEIF(J.EQ.M.AND.(I.GE.1.AND.I.LT.N))THEN
        CALL EQ6(DR,DZ,DT,DIFF,TOLD,TNEW,COND,HFP,TF,I,J)
    ELSEIF(I.EQ.N.AND.J.EQ.M)THEN
        CALL EQ7(DR,DZ,DT,DIFF,TOLD,TNEW,COND,HFP,TF,I,J)
    ELSEIF(I.EQ.N.AND.(J.GE.1.AND.J.LT.M))THEN
        CALL EQ8(DR,DZ,DT,DIFF,TOLD,TNEW,COND,HFP,TF,I,J)
    ELSE
        CALL EQ9(DR,DZ,DT,DIFF,TOLD,TNEW,I,J)
    ENDIF
    TNEW(I,J) = W*TNEW(I,J)+(1-W)*CT(I,J)
    RES(I,J) = ABS(TNEW(I,J)-CT(I,J))
    CT(I,J) = TNEW(I,J)
13
C
C   CHECKING IF THE TOLERANCE CONDITION HAS BEEN MET
C
    DO 50 I = 1,N
    DO 50 J = 1,M
    IF(RES(I,J).GT.TOL) GO TO 60
50
C   CONTINUE
C
C   CALCULATING MASS AVERAGE TEMPERATURE AT NODAL POINTS
C   FOR BOTH PARTICLE AND POSITION OCCUPIED BY CAPSULE
C
    CALL MAVG(TNEW,TAVG,M,N,DR,DZ,RAD,THICK)
    CALL CRUCI(TNEW,TCAVG,IHCB,IRCB,DR,DZ,HRCB,HHCB)
C
C
C   CALCULATING RETENTION FROM SUBROUTINE LETHA
C
    CALL LETHA(TCAVG,ARATE,TCAT,DTEMP,ARATE2,DT)
C
    WRITE(*,101)TIME,TNEW(1,1),TCAVG,DTEMP,ARATE,ARATE2
    WRITE(6,101)TIME,TNEW(1,1),TCAVG,DTEMP,ARATE,ARATE2
101
C   FORMAT(7F10.4)
C
C   NEW TEMPERATURES REPLACES OLD ONES IN ARRAY
C   PRIOR TO BEGINNING NEXT TIME STEP

```

```

C
DO 55 I = 1,N
DO 55 J = 1,M
55 TOLD(I,J) = TNEW(I,J)
20 CONTINUE
STOP
END

C
C CALCULATING TEMPERATURE AT INTERNAL NODAL POINTS
D
SUBROUTINE EQ9(DR,DZ,DT,DIFF,TOLD,TNEW,I,J)
IMPLICIT REAL*8(A-H, O-Z)
DIMENSION TOLD(100,100),TNEW(100,100)

C
A = (1.0/(2.0*DR**2))
B = (1.0/(4.*(I-1)*DR**2))
C = (1.0/(2.0*DZ**2))
D = (1.0/(DIFF*DT))
E = (A-B)
F = (-2.0*A-2.0*C-D)
G = (A+B)
H = (-A+B)
O = (2.0*A+2.0*C-D)
P = (-A-B)

C
YAW1 = H*TOLD(I-1,J)+O*TOLD(I,J)+P*TOLD(I+1,J)-C*TOLD(I,J-1)-
1 C*TOLD(I,J+1)
YAW2 = E*TNEW(I-1,J)+G*TNEW(I+1,J)+C*TNEW(I,J-1)+C*TNEW(I,J+1)
TNEW(I,J) = (YAW1-YAW2)/F
RETURN
END

C
C CALCULATING TEMPERATURE FOR BOUNDARIES LABELLED 1- 8 IN
C IN CHAPTER IX
C
SUBROUTINE EQ1(DR,DZ,DT,DIFF,TOLD,TNEW,I,J)
IMPLICIT REAL*8(A-H, O-Z)
DIMENSION TOLD(100,100),TNEW(100,100)

C
A = (1.0/(2.0*DR**2))
C = (1.0/(2.0*DZ**2))
D = (1.0/(DIFF*DT))
E = (A)
F = (-2.0*A-2.0*C-D)

```

```

G = (A)
H = (-A)
O = (2.0*A+2.0*C-D)
P = (-A)

```

```

C
YAW1 = (P+H)*TOLD(I+1,J)+O*TOLD(I,J)-(2.0*C)*TOLD(I,J+1)
YAW2 = E*TNEW(I+1,J)+G*TNEW(I+1,J)+C*TNEW(I,J+1)+C*TNEW(I,J+1)
TNEW(I,J) = (YAW1-YAW2)/F
RETURN
END

```

```

C
SUBROUTINE EQ2(DR,DZ,DT,DIFF,TOLD,TNEW,I,J)
IMPLICIT REAL*8(A-H, O-Z)
DIMENSION TOLD(100,100),TNEW(100,100)

```

```

C
A = (1.0/(2.0*DR**2))
B = (1.0/(4.*(I-1)*DR**2))
C = (1.0/(2.0*DZ**2))
D = (1.0/(DIFF*DT))
E = (A-B)
F = (-2.0*A-2.0*C-D)
G = (A+B)
H = (-A+B)
O = (2.0*A+2.0*C-D)
P = (-A-B)

```

```

C
YAW1 = H*TOLD(I-1,J)+O*TOLD(I,J)+P*TOLD(I+1,J)-C*TOLD(I,J+1)-
1 C*TOLD(I,J+1)
YAW2 = E*TNEW(I-1,J)+G*TNEW(I+1,J)+C*TNEW(I,J+1)+C*TNEW(I,J+1)
TNEW(I,J) = (YAW1-YAW2)/F
RETURN
END

```

```

C
SUBROUTINE EQ3(DR,DZ,DT,DIFF,TOLD,TNEW,COND,HFP,TF,I,J)
IMPLICIT REAL*8(A-H, O-Z)
DIMENSION TOLD(100,100),TNEW(100,100)

```

```

C
A = (HFP/(COND*DR))
B = (1.0/(2.0*DZ**2))
C = (1.0/DR**2)
D = (1.0/(2.0*DIFF*DT))

```

```

C
YAW = TNEW(I-1,J)*C+TNEW(I,J+1)*B+TNEW(I,J+1)*B+TOLD(I,J)*D+
1 TF*A

```

```
TNEW(I,J) = YAW/(A+2.0*B+C+D)
RETURN
END
```

C

```
SUBROUTINE EQ4(DR,DZ,DT,DIFF,TOLD,TNEW,I,J)
IMPLICIT REAL*8(A-H, O-Z)
DIMENSION TOLD(100,100),TNEW(100,100)
```

C

```
A = (1.0/(2.0*DR**2))
C = (1.0/(2.0*DZ**2))
D = (1.0/(DIFF*DT))
E = (A)
F = (-2.0*A-2.0*C-D)
G = (A)
H = (-A)
O = (2.0*A+2.0*C-D)
P = (-A)
```

C

```
YAW1 = (P+H)*TOLD(I+1,J)+O*TOLD(I,J)-C*TOLD(I,J-1)-C*TOLD(I,J+1)
YAW2 = (E+G)*TNEW(I+1,J)+C*TNEW(I,J-1)+C*TNEW(I,J+1)
TNEW(I,J) = (YAW1-YAW2)/F
RETURN
END
```

C

```
SUBROUTINE EQ5(DR,DZ,DT,DIFF,TOLD,TNEW,COND,HFP,TF,I,J)
IMPLICIT REAL*8(A-H, O-Z)
DIMENSION TOLD(100,100),TNEW(100,100)
```

C

```
A = (HFP/(COND*DZ))
C = (1.0/DR**2)
D = (1.0/DZ**2)
E = (1.0/(2.0*DIFF*DT))
```

C

```
YAW = TNEW(I+1,J)*C+TNEW(I,J-1)*D+TF*(A)+TOLD(I,J)*E
TNEW(I,J) = YAW/(A+C+D+E)
RETURN
END
```

C

```
SUBROUTINE EQ6(DR,DZ,DT,DIFF,TOLD,TNEW,COND,HFP,TF,I,J)
IMPLICIT REAL*8(A-H, O-Z)
DIMENSION TOLD(100,100),TNEW(100,100)
```

C

```
A = (HFP/(COND*DZ))
B = (1.0-(1.0/(2.0*(I-1))))/(2.0*DR**2)
```

```

C = (1.0+(1.0/(2.0*(I-1))))/(2.0*DR**2)
D = (1.0/DZ**2)
E = (1.0/(2.0*DIFF*DT))
C
1 YAW = TNEW(I-1,J)*B+TNEW(I+1,J)*C+TNEW(I,J-1)*D+TOLD(I,J)*E+
TF*A
TNEW(I,J) = YAW/(A+B+C+D+E)
RETURN
END
C
SUBROUTINE EQ7(DR,DZ,DT,DIFF,TOLD,TNEW,COND,HFP,TF,I,J)
IMPLICIT REAL*8(A-H, O-Z)
DIMENSION TOLD(100,100),TNEW(100,100)
C
A = (HFP/(COND*DZ))
B = (HFP/(COND*DR))
C = (1.0/DR**2)
D = (1.0/DZ**2)
E = (1.0/(2.0*DIFF*DT))
C
YAW = TNEW(I-1,J)*C+TNEW(I,J-1)*D+TF*(A+B)+TOLD(I,J)*E
TNEW(I,J) = YAW/(A+B+C+D+E)
RETURN
END
C
SUBROUTINE EQ8(DR,DZ,DT,DIFF,TOLD,TNEW,COND,HFP,TF,I,J)
IMPLICIT REAL*8(A-H, O-Z)
DIMENSION TOLD(100,100),TNEW(100,100)
C
A = (HFP/(COND*DR))
B = (1.0/(2.0*DZ**2))
C = (1.0/DR**2)
D = (1.0/(2.0*DIFF*DT))
C
1 YAW = TNEW(I-1,J)*C+TNEW(I,J-1)*B+TNEW(I,J+1)*B+TOLD(I,J)*D+
TF*A
TNEW(I,J) = YAW/(A+2.0*B+C+D)
RETURN
END
C
C CALCULATING THE MASS AVERAGE TEMPERATURE FOR ENTIRE
C PARTICLE
C
SUBROUTINE MAVG(TNEW,TAVG,M,N,DR,DZ,RAD,THICK)

```

```

      IMPLICIT REAL*8(A-H, O-Z)
      DIMENSION TNEW(100,100),TV(100,100)
C
      DO 10 J = 1,M-1
      DO 10 I = 1,N-1
10     TV(I,J) = (TNEW(I,J)+TNEW(I+1,J)+TNEW(I,J+1)+TNEW(I+1,J+1))/4.0
      SUM = 0.0
      DO 20 J = 1,M-1
      DO 20 I = 1,N-1
20     SUM = SUM+3.1415*DR**2*DZ*(2.0*I-1)*TV(I,J)
      TAVG = (SUM)/(3.1415*RAD**2*THICK)
      RETURN
      END
C
C     CALCULATING THE MASS AVERAGE TEMPERATURE FOR LOCATION
C     OCCUPIED BY CAPSULE
C
      SUBROUTINE CRUCI(TNEW,TCAVG,IHCB,IRCB,DR,DZ,HRCB,HHCB)
      IMPLICIT REAL*8(A-H, O-Z)
      DIMENSION TNEW(100,100),TV(100,100)
C
      DO 10 J = 1,IHCB-1
      DO 10 I = 1,IRCB-1
10     TV(I,J) = (TNEW(I,J)+TNEW(I+1,J)+TNEW(I,J+1)+TNEW(I+1,J+1))/4.0
      SUM = 0.0
      DO 20 J = 1,IHCB-1
      DO 20 I = 1,IRCB-1
20     SUM = SUM+3.1415*(DR**2)*DZ*(2.0*I-1)*TV(I,J)
      TCAVG = (2.0*SUM)/(3.1415*HRCB**2*HHCB)
      RETURN
      END
C
C     COMPUTING RESPECTIVE D-VALUES AND PERCENTAGE RETENTION
C
      SUBROUTINE LETHA(TCAVG,ARATE, TCAT,DTEMP,ARATE2,DT)
      IMPLICIT REAL*8(A-H, O-Z)
C
      TCAVG1 = TCAVG+0.5D0
      ITCAVG = TCAVG1
C
      IF(ITCAVG.GT.70.0.AND.ITCAVG.LE.75.0)THEN
          D1 = 1.550
          D2 = 6.945
          T1 = 70.0

```

```

        T2 = 75.0
ELSEIF(ITCAVG.GT.75.0.AND.ITCAVG.LE.80.0)THEN
    D1 = 6.945
    D2 = 14.72
    T1 = 75.0
    T2 = 80.0
ELSEIF(ITCAVG.GT.80.0.AND.ITCAVG.LE.90.0)THEN
    D1 = 14.72
    D2 = 132.0
    T1 = 80.0
    T2 = 90.0
ELSEIF(ITCAVG.GT.90.0.AND.ITCAVG.LE.100.0)THEN
    D1 = 132.0
    D2 = 72.8
    T1 = 90.0
    T2 = 100.0
ELSEIF(ITCAVG.GT.100.0.AND.ITCAVG.LE.110.0)THEN
    D1 = 72.8
    D2 = 50.8
    T1 = 100.0
    T2 = 110.0
ELSEIF(ITCAVG.LE.70.0)THEN
    AZ = 22.01
    TREF = 50.00
    D50 = 12.56
ENDIF

```

C

```

IF(ITCAVG.LT.50.0)THEN
    TCAT = ITC AVG
    PAAPS = ((TREF-TCAT)/AZ)+ALOG10(D50)
    DTEMP = 10**(PAAPS)
    ARATE = 1.0D0 / DTEMP
ELSEIF(ITCAVG.GE.50.0.AND.ITCAVG.LE.70.0)THEN
    TCAT = ITC AVG
    PAAPS = ((TREF-TCAT)/AZ)+ALOG10(D70)
    DTEMP = 10**(PAAPS)
    ARATE = 1.0D0 / DTEMP
ELSE
    TCAT = ITC AVG
    DP = (ALOG10(D2)-ALOG10(D1))/(T2-T1)
    APP = DP*(TCAT-T1)+ALOG10(D1)
    DTEMP = 10**(APP)
    ARATE = 1.0D0/DTEMP
ENDIF

```

```

        ARAT = ARAT+ARATE
        ARATE2 = 10**(2.0D0-(ARAT*DT/60.0D0))
RETURN
END
C
SUBROUTINE COOL(TF,TIME,HETIME,CUTOF,TCOOL,HFPCO)
IMPLICIT REAL*8(A-H, O-Z)
C
IF(TIME.GT.CUTOF)THEN
    STOP
ELSEIF(TIME.GT.HETIME)THEN
    TF = TCOOL
    HFP = HFPCO
ELSE
ENDIF
RETURN
END

```